TELEDYNE LECROY
Everywhereyoulook™

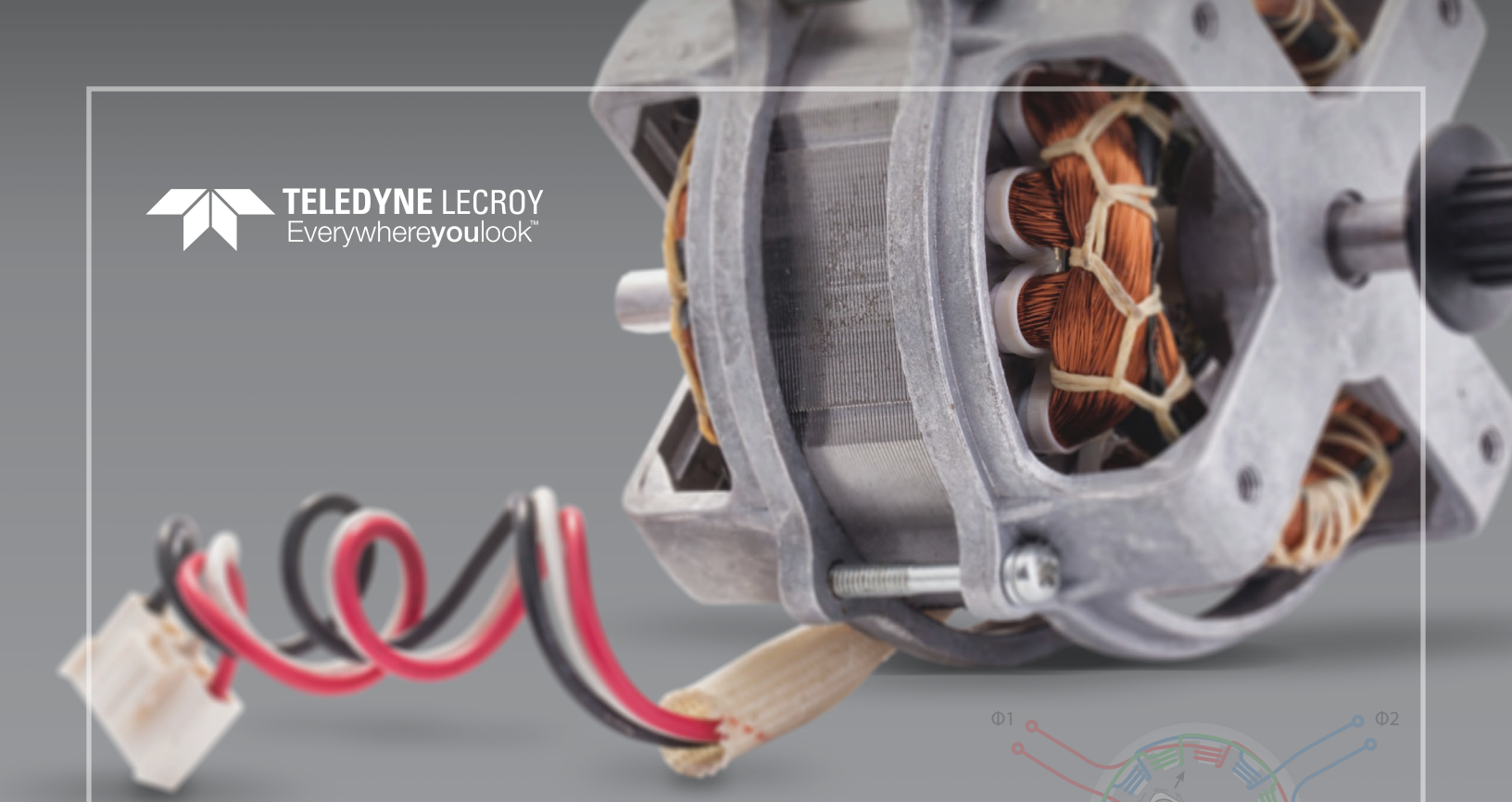

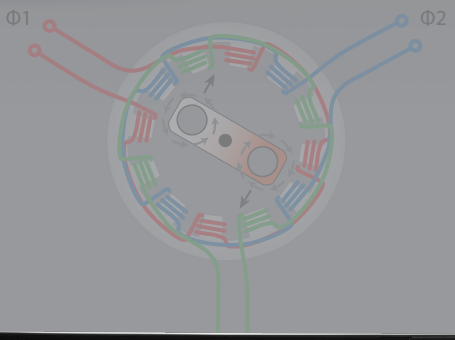


# Motor Drive Technical Primer


A background primer on motor drives, from AC line input to motor mechanical shaft output, including topics on measurement of AC line and drive output (distorted) power values, power conversion devices and topologies, control architectures, motors, and torque and speed sensing.


## Ken Johnson

*Director of Marketing, Product Architect*
Teledyne LeCroy


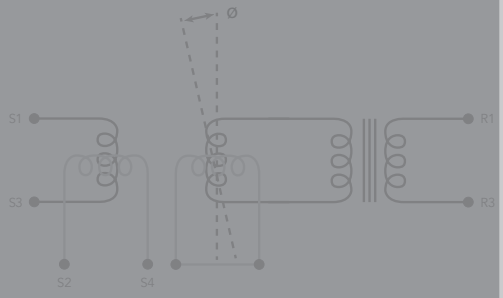


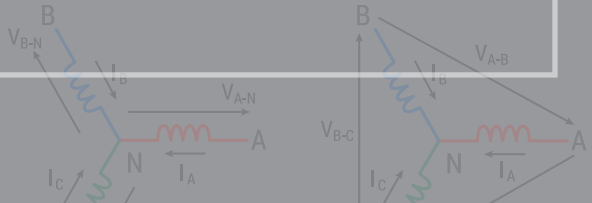

# Table of Contents



 

 

 

 

# Introduction

Many excellent textbooks have been written on the subject of motor drives, but most of these require pre-requisite knowledge and/or are difficult sources of basic understanding for newcomers. While there is also useful information on the internet, such material is typically aimed at narrow applications or specific products and markets. In addition, many of the public domain materials lack “real-world” examples that are vital to gain a full understanding of the topic. Both textbooks and the internet are more useful reference sources given a broad overview.

This technical primer aims to provide such an overview by explaining the basics of a motor drive from the input signals (AC line inputs) through motor shaft sensing (mechanical power) and all relevant areas in between. It targets newcomers to these fields desiring a broad overview before seeking deeper technical information from other sources. Among the newcomers this series targets are:

- Engineering students who are just beginning to learn about the field
- Design engineers new to the field or who wish to learn more about this field. This would include software (control) engineers, inverter subsection engineers, systems engineers, power semiconductor device engineers, and motor engineers.
- Plant or field maintenance personnel who may wish to learn more about this topic, but don't wish to read a detailed textbook(s).

Broadly speaking, this technical primer will address eight main topics:

- AC line voltage and current
- Power semiconductors
- Power conversion systems
- Motors
- Variable frequency motor drives
- Sensing of motor shaft torque, speed, direction, and angle
- Power measurements on sinusoidal (AC line) waveforms
- Power measurements on distorted waveforms, e.g., pulse-width modulated (PWM) outputs from drive systems

Naturally, within each of these topics, there are many subtopics that need to be addressed in order to provide a solid foundation in motor drives.

Persons too numerous to mention have assisted the author by enhancing understanding of these topics or providing editorial assistance. For those who provided time in their labs, during a phone call, or with editing skills, thank you for your time and assistance. This primer would not have been possible without your help.

If you have any feedback or questions, find mistakes, or would like to suggest changes or additions, please do not hesitate to contact the author at ken.johnson@teledynelecroy.com. Information around specific and interesting applications for the use of oscilloscopes in the areas described in this document is especially welcomed.

 

## About The Author

*Kenneth Johnson is a Director of Marketing and Product Architect at Teledyne LeCroy. He began his career in the field of high voltage test and measurement at Hipotronics, with a focus on <69-kV electrical apparatus ac, dc and impulse testing with a particular focus on testing of transformers, induction motors and generators. In 2000, Ken joined Teledyne LeCroy as a product manager and has managed a wide range of oscilloscope, serial data protocol and probe products. He has three patents in the area of simultaneous physical layer and protocol analysis. His current focus is in the fields of power electronics and motor drive test solutions, and he works primarily in a technical marketing role as a product architect for new solution sets in this area. Ken holds a B.S.E.E. from Rensselaer Polytechnic Institute.*

# Alternating Current (AC) Line Systems (Voltage, Current, Power)

## Introduction

For electrical engineers familiar with printed circuit assembly (PCA) design (i.e., designs built on printed circuit boards), their knowledge of AC line power voltages and currents may end with the most basic input ratings of a switching power supply operating from a 120 V or 240 V single-phase wall socket. Unless they are working in the power or power conversion field, many electrical engineers are far more familiar with the very small DC distribution rails and digital logic family operating voltages present in PCAs than with AC line voltages and currents.

However, a basic understanding of AC line voltage and current ratings might give you valuable insight into component or product ratings. Have you ever wondered…

- why HV differential voltage probes commonly have a 1000 $V_{RMS}$ common-mode safety rating?
- why something rated "120 V" could have much higher peak-peak voltages present?
- why rectified AC line voltages result in the DC values that they do?
- why a current probe with a given $A_{RMS}$ rating may not meet your needs if you are trying to measure currents that are not rated in $A_{RMS}$ terms?

Additionally, AC line voltages are much higher than those typically measured with oscilloscopes when probing on a low-voltage PCA. These high voltages present considerable risk to you and the equipment you are using. Thus, education is necessary so that proper cautions can be well understood, and personal and equipment safety can be assured.

## Background

We often refer to AC line power (and AC line voltage and current) as utility, grid, household, power line, or mains power (or voltage and current). This is the typically 50 or 60Hz sinusoidal voltage and current transmitted through current carrying conductors to the home or business through a service drop, and further distributed within the home or business to various other panels, "drops," or sockets for use. While some may consider power conversion (PWM) outputs to be "AC", we are specifically excluding their treatment in this section – voltage, current and power for PWM signals are covered separately and the information in this section does not apply to those PWM signals.

The AC line system can contain a single "phase" or multiple "phases." Independently invented in the late 1880s by separate inventors, three-phase systems were first extensively commercialized by a partnership between Nikola Tesla and the Westinghouse Electric Company. three-phase systems are more efficient and cost-effective than single- or two-phase systems because, for a given level of transmitted power, three-phase systems require less material in the current-carrying inductors.

A single-phase system requires supply and return (neutral) wires both rated for the full current-carrying (power rating) of the system. A three-phase system, to deliver an equivalent amount of power, has three supply wires rated for less current-carrying capability and only requires one neutral wire. Furthermore, the neutral wire in a three-phase system need not be rated for very high current-carrying capability. That's because the neutral wire in a balanced three-phase system (the normal operating

 

condition) conducts zero current since, by definition, the phase return currents will flow through another phase, and the three phase currents therefore sum to zero at the neutral. Thus, for a modest 50% increase in cost (three current-carrying conductors versus two), the three-phase system supplies three times the power, or a 200% increase. For a variety of reasons, it is also less complicated and less expensive to build a three-phase generator and transformer. Further, three-phase power provides better control and power delivery capability for even low-power motors.

We give distinct names to each of the three phases in a three-phase system. For three-phase line systems (i.e., from the utility), they are commonly referred to A, B, and C phases, and less commonly as L1, L2, and L3 phases. There are other even less commonly used designations as well.

An electric utility supply system always contains three phases, but a small residential service load may only have single-phase service from the three-phase transmission and distribution system. Larger commercial loads that need more power will have full three-phase service from the utility. Here are the most common combinations:

- Single-phase, two-wire
- Single-phase, three-wire
- Three-phase, four-wire
- Three-phase, three-wire

More than three phases is uncommon, and is never present in a utility service. However, one may find four, five, or six phases in non-utility supplies or in applications that require high reliability through redundancy, such as vehicle, aircraft or military applications. In such cases where there are more than three phases, they are typically generated with a motor drive and not by the utility supply. We discuss this topic in the Variable Frequency (Motor) Drives section.

> Note: Some other power applications, such as voltage regulator modules (VRMs) and digital power management integrated circuits (PMICs), also use the term “phase” to describe additive DC-DC converters supplying time-interleaved current to a single power rail in an on-board embedded computing system. In such systems, each phase corresponds to an individual DC-DC converter power stage (typically consisting of one or two power MOSFETs and an inductor) with the outputs of multiple power stages summed to generate higher levels of output current. The timing of the turn-on and turn off each power stage is controlled according to the number of power stages or phases employed to achieve the required amount of current on the power rail while maximizing system efficiency. In any event, this usage of "phases" is distinctly different from the “phases” of a three-phase ac system—do not confuse the terminology in this case.

The AC frequency provided by the utility is either 50 or 60 Hz, depending on the geographic location. Synchronization of the supplied frequency occurs across the electric utility’s entire supply grid and is enforced for grid-stability purposes. Historically, utilities have achieved frequency synchronization and stability using generator synchronization and electro-mechanical volt-amperes reactive (VAr) compensation circuitry. However, power conversion systems play an increasing role in this area as

 

semiconductor device voltages increase, power conversion systems costs decrease, and non-traditional generating sources like wind and solar photovoltaics become a larger component of the generated supply.

Some applications, such as shipboard or aircraft applications, may use 400 Hz AC line power supplied by separate generators, but this is not a standard electric utility frequency. In rarer cases, some other applications use different supply frequencies. These non-standard, locally-generated frequencies are not supplied by the electric utilities.

## Cautions

AC systems contain a neutral conductor separate from a ground conductor. The neutral is not ground – always assume that there are voltages on the neutral wire and currents flowing through it even if the normal design case is different. In a single-phase system, the neutral conductor serves to return the current to the supply and complete the circuit. In a balanced, normally operating three-phase system, the neutral should not be carrying current, but it could carry current during a fault condition. Ground is a safety connection from a chassis to earth potential. In a single-phase system, if the neutral connects to the ground as a result of a fault condition, the return current will flow to ground and a protective device, such as a circuit breaker or ground-fault current interrupter (GFCI), will trip and interrupt the current flow. In a three-phase system, the neutral may be connected to ground, but significant currents could flow in the neutral under various fault or other conditions.

An all-inclusive discussion of electrical codes, historically permitted connections, and all safety considerations is beyond the scope of this document. The best practice is to assume the worst and take extra precautions unless you have specific knowledge to the contrary. Furthermore, protective devices could trip in less than a cycle, or may take several cycles. So, if there is voltage potential on the neutral and/or current flow present, a person who is touching the neutral could complete a current-carrying path to ground and sustain serious injury or death.

## AC Line Voltage

### Introduction

AC line voltage values may be expressed in Volts RMS ($V_{RMS}$), but typically they are simply stated as V or $V_{AC}$. Regardless of its expression, it is $V_{RMS}$ – the terms are used interchangeably in this context.

AC line voltages are always sinusoidal, with typical utility requirements that they contain <5% total harmonic distortion (THD) and that customers not disturb the service entrance with >5% THD imposed by “noisy” equipment that generates non-linear current flows and/or results in distorted voltage waveforms on the AC lines (such as PWM motor drives or unfiltered inverters).

In either single-phase or three-phase AC systems, measurements of AC line voltage can be made from a single line (phase) to neutral (line-neutral) or from one line to another line (line-line). In addition, the rated AC voltage is referenced differently for single-phase and three-phase systems. Therefore, the understanding and calculation of the different voltages (peak, peak-peak, RMS, line-neutral or line-line, etc.) in an AC single-phase or three-phase system requires explanation.

 

## Single-Phase AC Line Voltage

A single-phase, two-wire AC system contains a voltage wire, which is 120 V in the United States, and a neutral wire. The ground is supplied at the utility "drop" and within the building – in the United States, this is typically a physically deep-driven earth ground.

A single-phase, three-wire AC system contains two voltage wires, which are both at 120 V in the United States, and a neutral wire. Again, the ground connection comes from within the building. A 120 V potential exists from both wires (lines) to neutral, and 240 V from line to line. The line is "hot" and supplies the current, and the current returns through the neutral line. The building contains a service panel that provides appropriate safety devices (fuses, circuit breakers, etc.) in an enclosure (commonly referred to as a panel or panel board), and the enclosure is connected to earth ground. There is also a physical bond from the utility supply to an earth ground. See Figure 1.

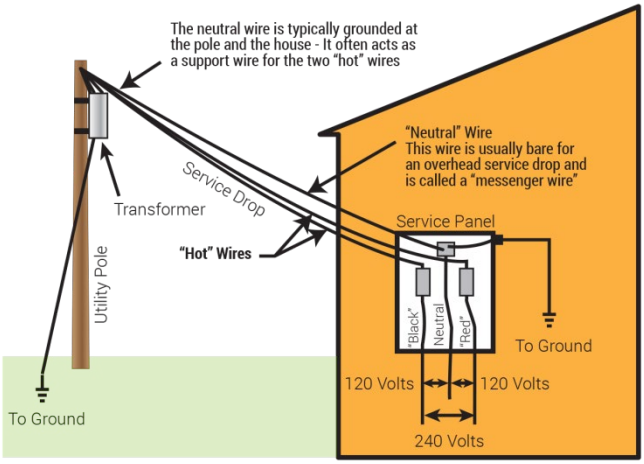


**Figure 1: Typical US residential service drop for a single-phase, three-wire AC supply.**

Note that the neutral wire returns current to the utility line and is connected to the utility ground at the pole and the service ground at the service panel. Earth grounds should be at identical potentials in both locations.

Although we simplify the single-phase AC voltage value to an RMS voltage value, the magnitude varies sinusoidally because the single-phase AC voltage is a rotating vector with a magnitude and an angle. The rotation period is the inverse of the supply frequency. The magnitude of this voltage vector is the instantaneous line-neutral voltage value, with a peak voltage $V_{PEAK}$ equal to √2 * $V_{RMS}$, or 169.7V in the case of a single-phase AC system with a 120 $V_{RMS}$ rating.

The voltage vector completes one revolution at a rate of one period = 1/frequency (50 Hz or 60 Hz). At any given moment in time, the voltage magnitude is equal to $V_{PEAK}$ *sin(α), with α = the angle of rotation in radians. See Figure 2.

 

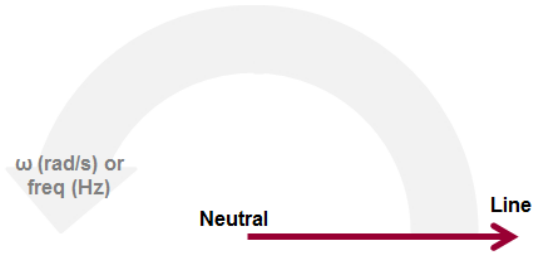


Figure 2: Voltage magnitude.

Figure 3 shows the rotating voltage vector in the time domain as a sinusoidal waveform with a fixed period and frequency.

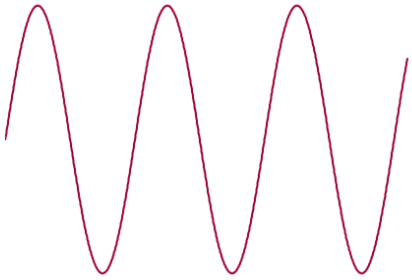

Figure 3: When viewed as a voltage-versus-time waveform, the rotating voltage vector appears as a sine wave.

To further understand the various voltage values (peak, peak-peak, etc.) present on this waveform, let's continue with the example of a sinusoid rated at 120 V or 120 $V_{AC}$; again, what that really means is 120 $V_{RMS}$. Therefore, we can calculate other voltages values, as follows:

$V_{PEAK} = \sqrt{2} * V_{AC}$, or $\sqrt{2} * V_{RMS} = 169.7$ V
$V_{PK\text{-}PK} = 2 * V_{PEAK} = 339.4$ V
$V_{DC} = V_{PEAK} = 169.7$ V (if rectified and filtered)

Figure 4 shows this plotted mathematically.

 

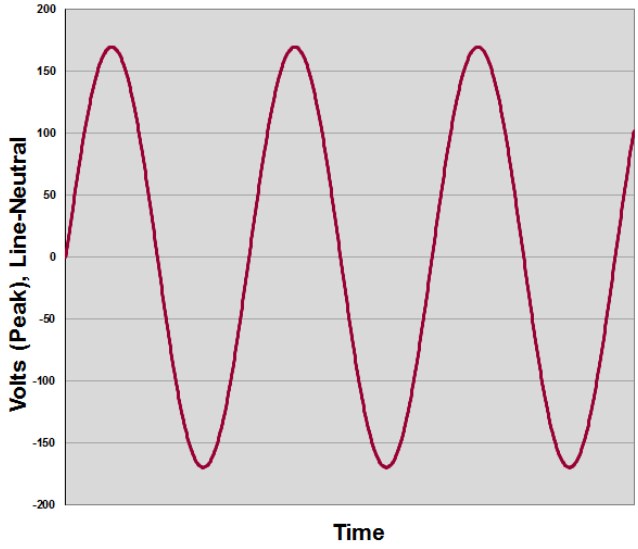


Figure 4: AC single-phase utility voltage, 120 Vac.

Note that the commonly used phrase “true RMS” is a “marketing definition” to describe a mathematically correct RMS calculation as compared to a measurement shortcut taken using inexpensive instruments whereby RMS voltages (or currents) are calculated from $V_{PK-PK}/2$. This measurement shortcut is true only for a pure, single-frequency sinewave, which is rarely present, though the accuracy of the measurement shortcut may be good enough for an inexpensive field measurement instrument.

With an oscilloscope such as Teledyne LeCroy’s 8-channel, 12-bit High Definition Oscilloscopes and Motor Drive Analyzers and a suitably rated voltage probe (e.g., a Teledyne LeCroy HVD3106 HV differential probe), the electric utility’s 120 $V_{AC}$ line can be probed. Then, the built-in oscilloscope measurements are used to measure the various voltage levels.

The screen image shown in Figure 5 is an example of a (nominal) 120 $V_{AC}$ signal captured with a Teledyne LeCroy 8-channel, 12-bit Motor Drive Analyzer with three-phase power analysis measurement capabilities. This particular instrument is model MDA810A:

 

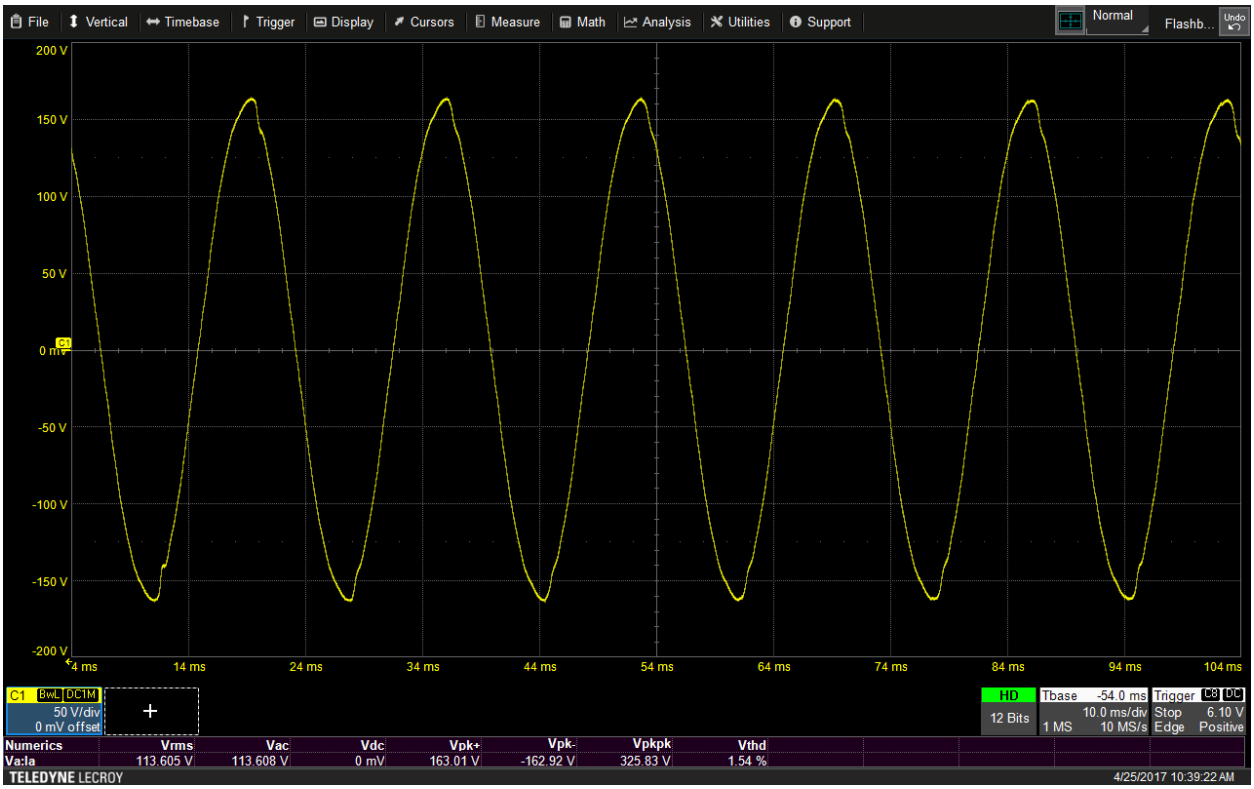


Figure 5: 120 Vac signal captured with a Teledyne LeCroy 8-channel, 12-bit Motor Drive Analyzer.

The Numerics table at the bottom of Figure 5 is shown larger in Figure 6. This table provides the mean measured values for the 120 $V_{AC}$ signal.

| Numerics | Vrms | Vac | Vdc | Vpk+ | Vpk- | Vpkpk | Vthd |
|---|---|---|---|---|---|---|---|
| Va:la | 113.605 V | 113.608 V | 0 mV | 163.01 V | -162.92 V | 325.83 V | 1.54 % |

Figure 6: The Numerics table lists key measurement values from the waveform in Figure 5.

Note that the $V_{RMS}$ and $V_{AC}$ values are the same, $V_{DC}$ is 0 Volts, and the $V_{PK+}$ and $V_{PK-}$ values are roughly equal. While these values differ from the nominal values described earlier, keep in mind that this voltage is measured at the end of a long cable run far from the service drop entrance and is a "load" voltage taken coincident with an ~10A current draw. Such a voltage drop is typical for near full-load conditions in a typical commercial or industrial building. Thus, 120 $V_{AC}$ is also commonly referred to as 115 $V_{AC}$. Note also that while THD is small (1.54%), it is not zero. Pure sinusoids are rare in the real world.

To test the hypothesis that a high current load causes a voltage drop from a nominal 120 $V_{AC}$ line, we can acquire a waveform spanning a longer period of time using the Motor Drive Analyzer and evaluate the performance before, during, and after the application of a load. In this case, the load is a toaster, so applying the load is as simple as "making toast".

 

Figure 7 shows a two-second capture beginning with no load, then a load for approximately one second, then no load again. The full two-second line voltage capture appears in the upper left quadrant of the display, the full two-second line current capture is in the lower left quadrant of the display, and the corresponding zoomed areas are to the right. Because the power calculation software is operating in "Zoom+Gate" mode, the calculations are gated to the zoomed portion of the waveforms where there is no appreciable current delivery (shown to the right of the two-second acquisitions) and the $V_{RMS}$ value is 117.2 V.

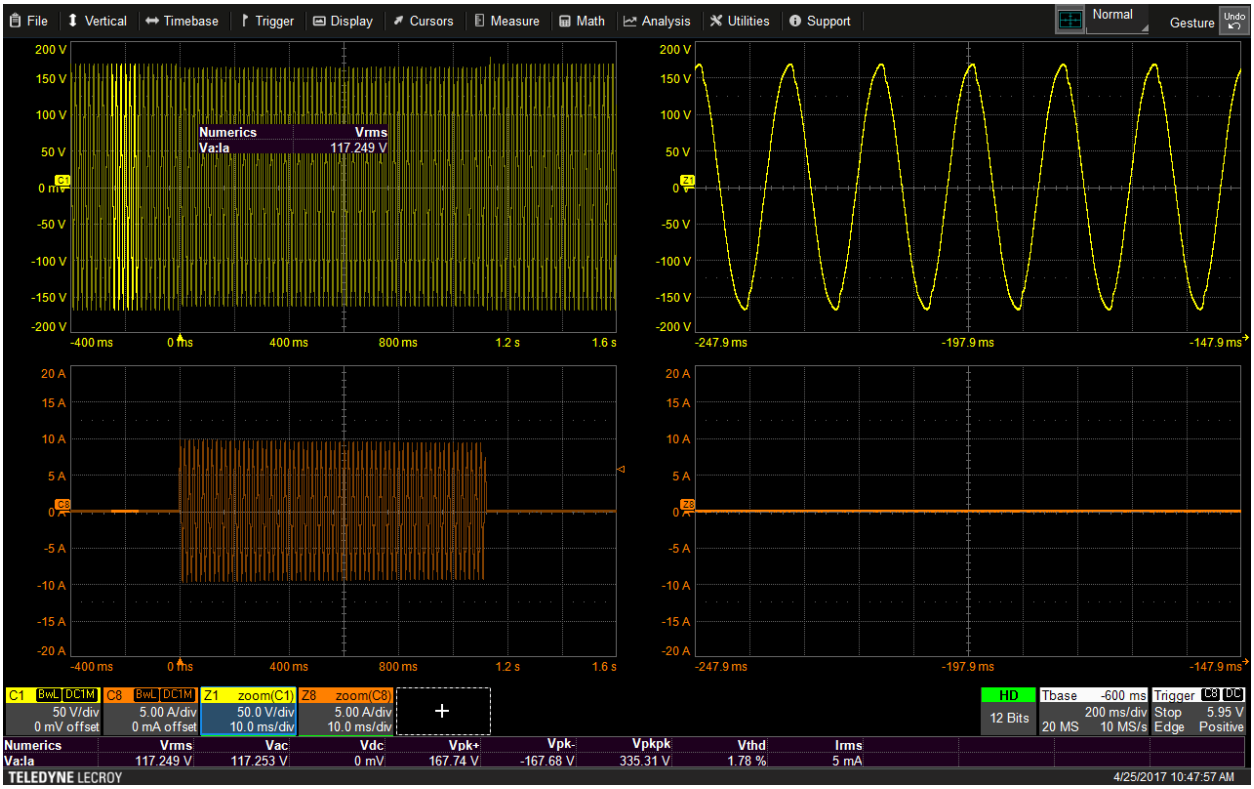


**Figure 7: AC line measurement in the upper left shows a 2-s capture of the line voltage with no load, followed by a toaster load and then no load again. A 2-s capture of the line current is shown in the lower left. Zoomed versions of the voltage and current waveforms are shown on the right.**

 

However, when the toaster is “toasting” (drawing current), the line voltage dips to 113.7 V (shown in Figure 8). The voltage drop appears in the amplitude of the long voltage capture and its calculated value appears in the Numerics table at bottom.

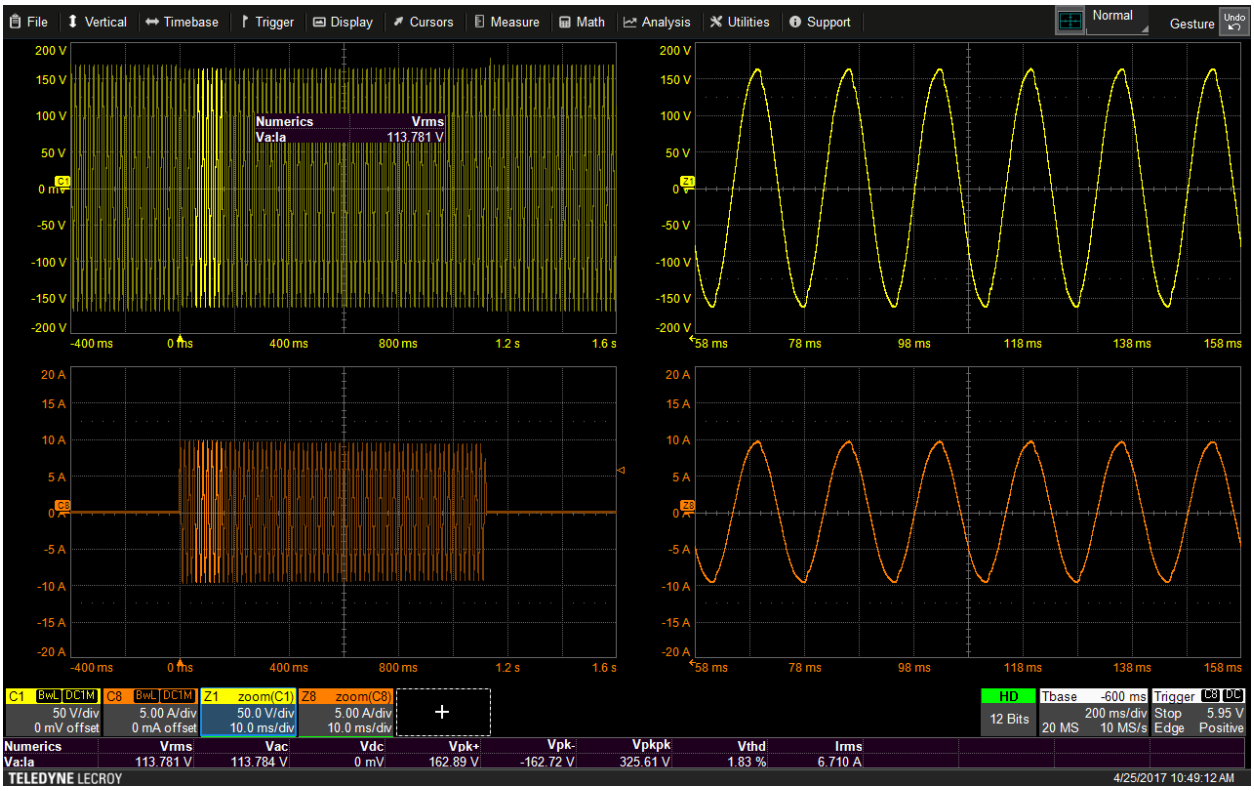


**Figure 8: AC line measurement reveals the voltage drop (117.2 V - 113.7 V) that occurs when the toaster is toasting and drawing current.**

 

Then, when the “toast is done,” the current draw ends and the voltage level returns to its no-load value (Figure 9).

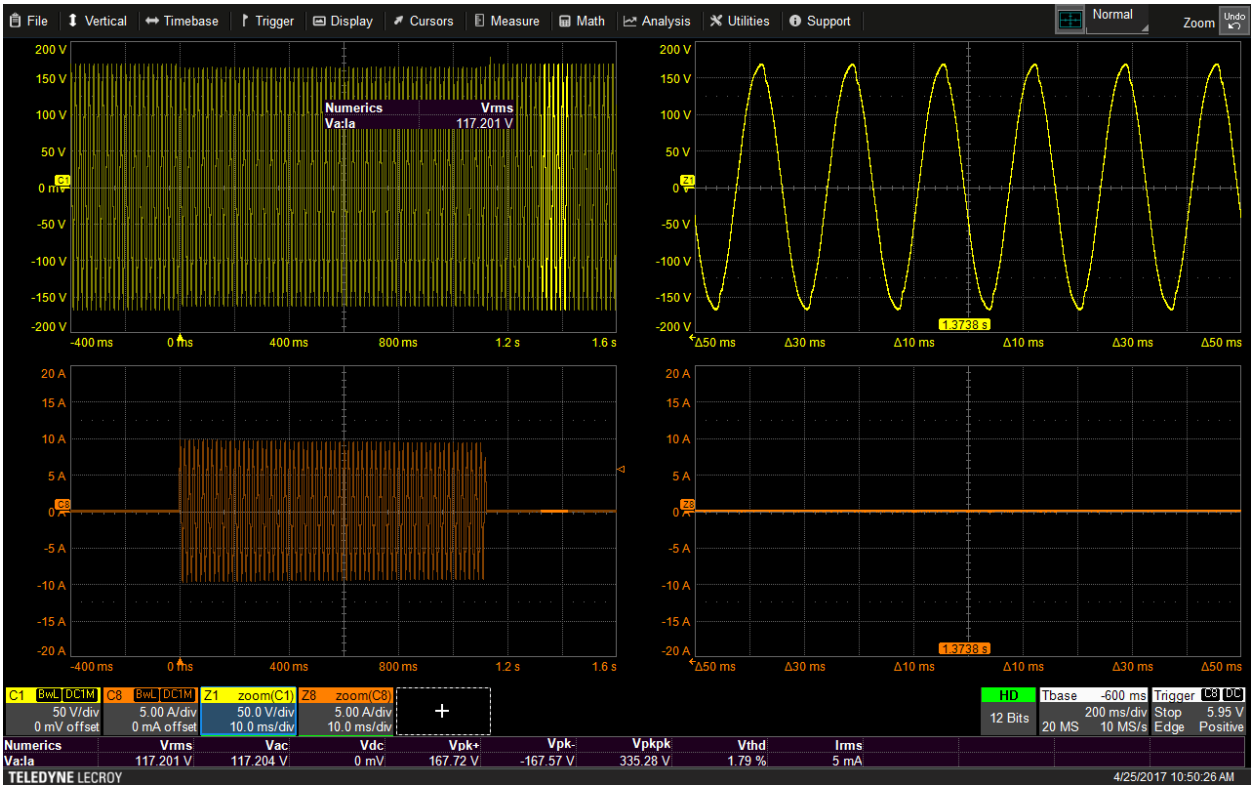


Figure 9: AC line measurements with toaster load off.

Figure 10 shows the setup dialog for the single-phase line voltage (and current) measurements in this example. Note that calculations are made including a harmonic filter (harmonic orders included through the 50th harmonic) and excluding DC measurement offsets (“include DC” checkbox is unchecked) to eliminate the slight (<0.25%) DC offset introduced by the measurement system.

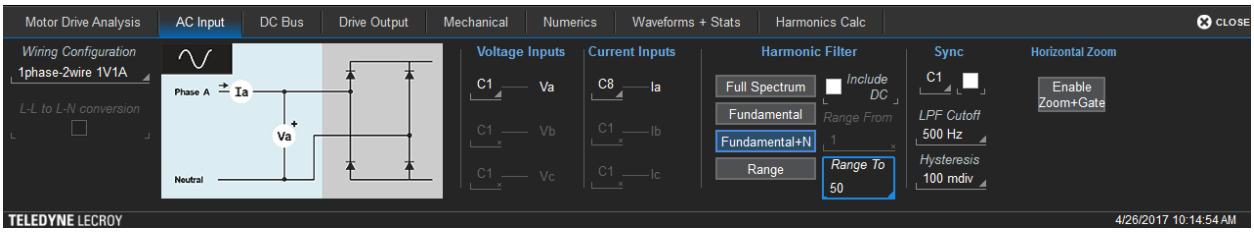


Figure 10: Set-up dialog for single-phase ac line measurements in the toaster load example.

 

## Three-phase AC Line Voltage

Three-phase AC systems are more complicated than single-phase systems when describing voltages. One may distribute three-phase voltages with a variety of different “wye” or “delta” connection configurations. It is beyond the scope of this document to describe all possible permutations, so it will describe only the most common types.

In a three-phase system, there is (by design) “balance,” in that the three-phase voltage vectors have the same voltage magnitude and are separated from the other phases by 120°, or 1/3 of a full sinusoid period. Therefore, the sum of the three voltage vectors in a balanced three-phase system should be zero. Thus, practically speaking, the neutral line is always at zero voltage potential. However, if there is a fault (failure) condition or a leakage of current to ground, the neutral may have a non-zero voltage potential.

As in a single-phase system, the three different phase voltage vectors rotate at a constant rate. This rotation and separation between each phase in a three-phase system makes it possible to produce rotating magnetic fields that can perform work, such as in an electric motor.

Figure 11 shows the three-phase voltage vector system.

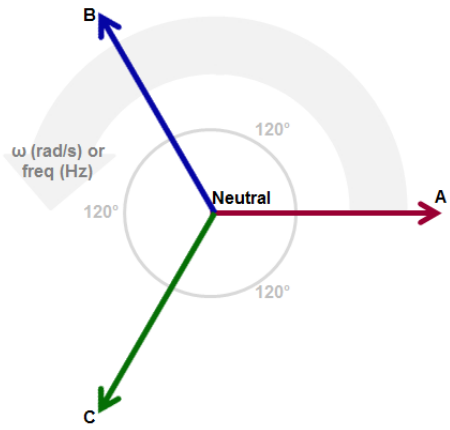


Figure 11: Three-phase voltage vector system.

 

Figure 12 shows the three rotating voltage vectors as three different voltage-vs.-time sinusoidal waveforms. Each have the same fixed frequency but are out of phase with respect to each other by 120°.

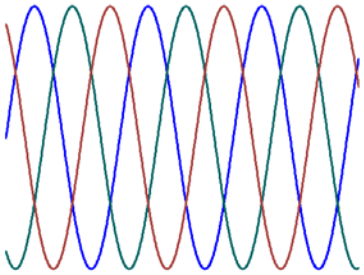

**Figure 12: When viewed in the time domain, the rotating voltage-vector system appears as three sine waves.**

In a three-phase AC system, voltage can be measured either from line-line (phase-phase) or from line-neutral (phase-neutral).

> Note: Line-line may also be referred to as phase-phase. The convention for indicating a line-line measurement is to show the voltage symbol "V" followed by a subscripted "$_{\text{line-line}}$" designation, with the first line shown as the "to" line and the second line shown as the "from" line. Thus, measuring from line A to line B is expressed as $V_{A-B}$ or simply $V_{AB}$. This is different from the vector notation for AB, which defines a vector direction from B to A.

To measure from line-neutral, the neutral must be present and accessible. The neutral is often present in a motor winding but is usually not available as a measurement reference point. Remember that an accessible motor case or chassis ground is ***not*** the same as winding neutral. Thus, it is more common to measure motor voltages from line-line than it is to measure from line-neutral.

> Note: The convention for indicating a line-neutral measurement is to follow the voltage symbol "V" with a subscripted "$_{\text{line-neutral}}$" designation, with the first line shown as the "from" line and the second line shown as the neutral. Thus, measuring from line A to neutral is expressed as $V_{A-N}$ or simply $V_{AN}$.

One may find cases in which line-line voltages may be too high to measure based on the rating of the available voltage measurement device, and the neutral may be inaccessible. In this case, an alternate approach to voltage measurement is on a line-reference basis by connecting the low-voltage side of the measurement devices (e.g., the "ground" of a single-ended probe or the low side of a differential probe; either must carry a sufficient voltage rating) and allowing them to "float" at a voltage other than neutral. This is not a true line-neutral voltage measurement, but it does provide a measurement to a common reference point and is suitable for many measurements.

 

Measurements of line-line RMS voltage magnitudes may be converted to line-neutral RMS voltage magnitudes using the simple formula, $V_{L\text{-}N} = V_{L\text{-}L} / \sqrt{3}$. The peak line-line voltage magnitude will lag the peak line-neutral magnitude by 30°. Figure 13 shows the two different voltage vectors. Note that the voltage vector rotation is counter-clockwise.

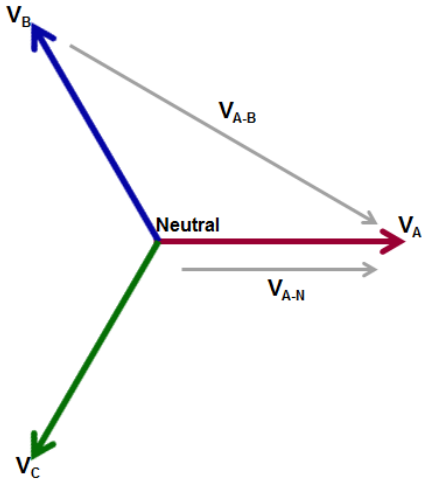


Figure 13: This vector diagram illustrates the conversion of a line-to-neutral voltage to a line-to-line voltage.

In a three-phase system, we express the rated AC voltage in $V_{RMS}$, but the rated voltage value is a line-line voltage value. In a single-phase system, the rated voltage value is a line-neutral value because there may not be a second line to reference a voltage to in a single-phase system. Therefore, if a three-phase system is rated at 480 V or 480 $V_{AC}$, this means that the three-phase system is 480 $V_{RMS}$ *line-line*. Applying that knowledge allows us to calculate other voltage values, as follows:

$V_{PEAK(L\text{-}L)} = \sqrt{2} * V_{AC}$, or $\sqrt{2} * V_{RMS} = 679$ V
$V_{PK\text{-}PK(L\text{-}L)} = 2 * V_{PEAK(L\text{-}L)} = 1358$ V

We show this in Figure 14.

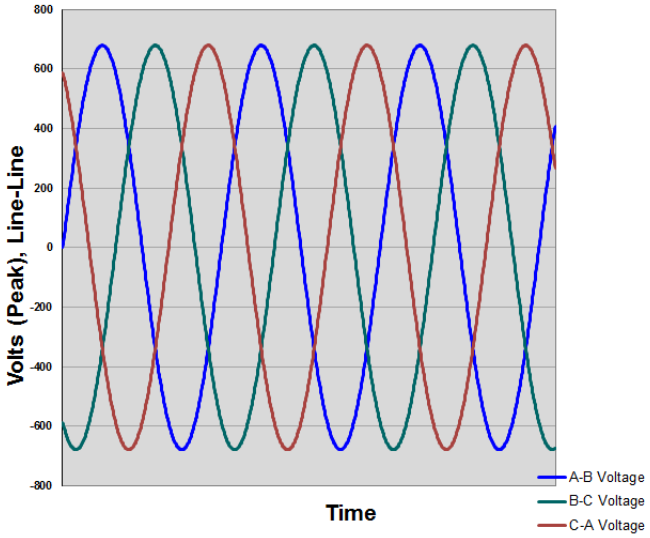


Figure 14: AC three-phase utility voltage, 480 Vac, measured line to line.

 

When using a Motor Drive Analyzer with a suitably rated voltage probe (e.g., a Teledyne LeCroy HVD3106 HV differential probe) to perform line-line probing of a 480 V electric utility AC supply, we may verify these signal levels through use of the cursors and measurement parameters. Note that in this case, a differential voltage probe is required with sufficient isolation to ground (a safe value is the calculated $V_{DC}$ value) and a differential voltage measurement capability equal to the maximum peak-peak voltage expected (in this case 1358 V) plus a sufficient margin (determined by the user). The HVD series of probes is rated 1000 $V_{RMS}$ isolation to ground and up to 2000 $V_{PK-PK}$, making it a suitable choice. Figure 14 is an example of (nominal) 480 $V_{AC}$ three-phase line-line voltage signals acquired and displayed.

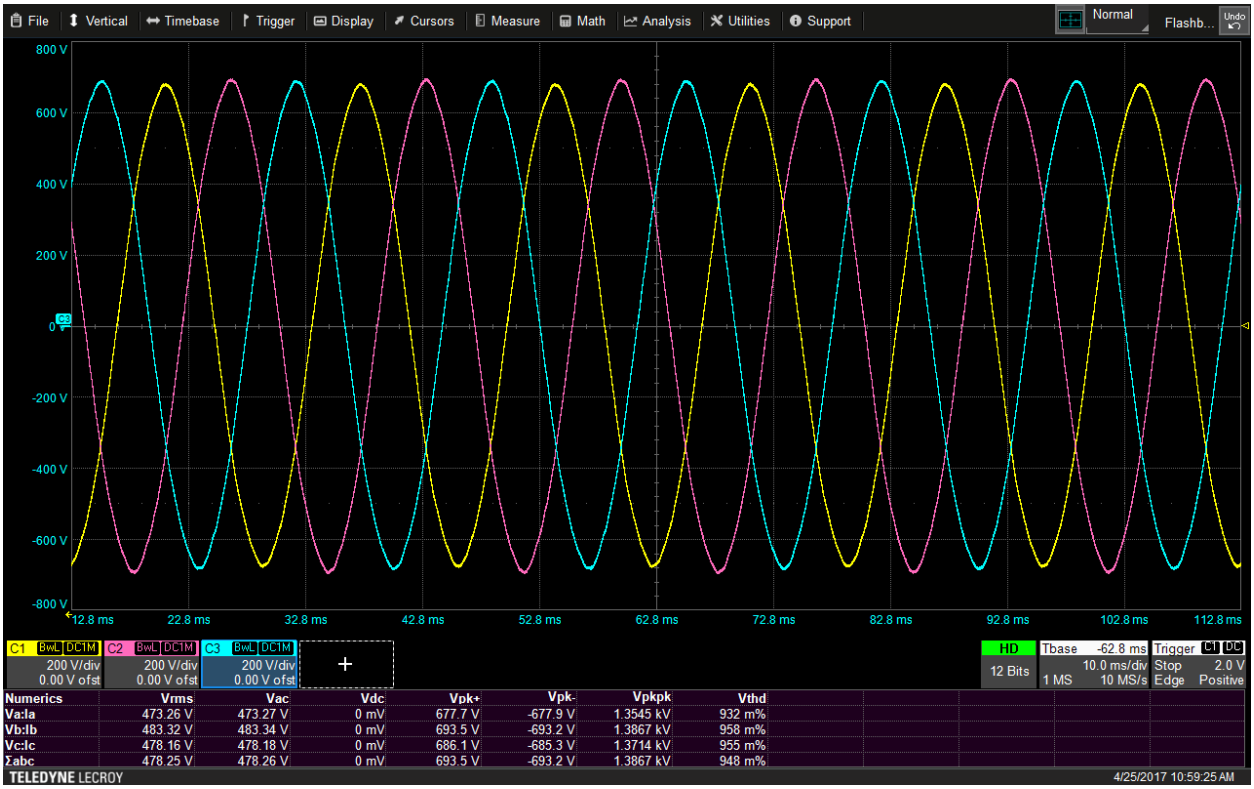


**Figure 15: Waveforms for a 480-Vac three-phase line-line signal as measured by a Motor Drive Analyzer and suitably rated voltage probes.**

Figure 16 shows a larger version of the Numerics table at the bottom of Figure 15. This table provides measurement values for the line-line voltage waveforms:

| Numerics | Vrms | Vac | Vdc | Vpk+ | Vpk- | Vpkpk | Vthd |
|---|---|---|---|---|---|---|---|
| Va:Ia | 473.26 V | 473.27 V | 0 mV | 677.7 V | -677.9 V | 1.3545 kV | 932 m% |
| Vb:Ib | 483.32 V | 483.34 V | 0 mV | 693.5 V | -693.2 V | 1.3867 kV | 958 m% |
| Vc:Ic | 478.16 V | 478.18 V | 0 mV | 686.1 V | -685.3 V | 1.3714 kV | 955 m% |
| Σabc | 478.25 V | 478.26 V | 0 mV | 693.5 V | -693.2 V | 1.3867 kV | 948 m% |

**Figure 16: The voltage readings associated with the 480-Vac waveforms displayed in Figure 15.**

 

Note that the $V_{RMS}$ and $V_{AC}$ values are the same for a given line-line voltage but differ slightly amongst the phases (this is normal). $V_{DC}$ is 0 Volts, and the $V_{PK+}$ and $V_{PK-}$ values are roughly equal. These various voltage values differ only slightly from the nominal values described earlier, most likely because these various voltage values were measured under a no-load condition. Under load, the voltage may be reduced (as with the 120 V example described earlier), and this is why 480 $V_{AC}$ is also commonly referred to as 440 $V_{AC}$ or 460 $V_{AC}$. Note also that the THD is a small percentage (<1%) but is not zero. If a load were present, there would likely be more distortion on this signal.

Figure 17 shows the setup dialog for the measurements shown in Figure 16. Note that calculations are made with a harmonic filter applied (harmonic orders included through the 50th harmonic) and excluding DC measurement offsets ("include DC" checkbox is unchecked) to eliminate the slight (<0.25%) DC offset introduced by the measurement system.

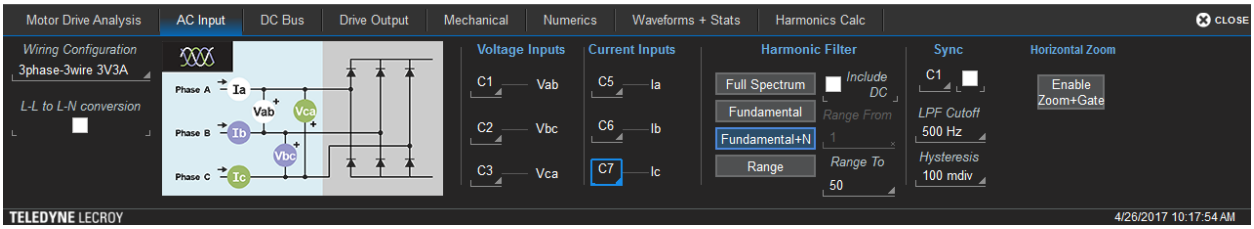


**Figure 17: Setup dialog for 480-Vac three-phase voltage measurements.**

The three-phase voltages may be measured line-neutral if a neutral wire is present. Applying our earlier description allows us to calculate the following:

$V_{L\text{-}N(RMS)} = V_{L\text{-}L(RMS)} / \sqrt{3} = 277$ V (in this case)
$V_{PEAK(L\text{-}N)} = \sqrt{2} * V_{AC(L\text{-}N)}$, or $\sqrt{2} * V_{RMS(L\text{-}N)} = 392$V
$V_{PK\text{-}PK(L\text{-}N)} = 2 * V_{PEAK(L\text{-}N)} = 792$ V
$V_{DC} = \sqrt{2} * V_{AC(L\text{-}N)} * \sqrt{3} = 392$ V $* \sqrt{3} = 679$ $V_{DC}$ (if rectified and filtered)

We show this plotted in Figure 18.

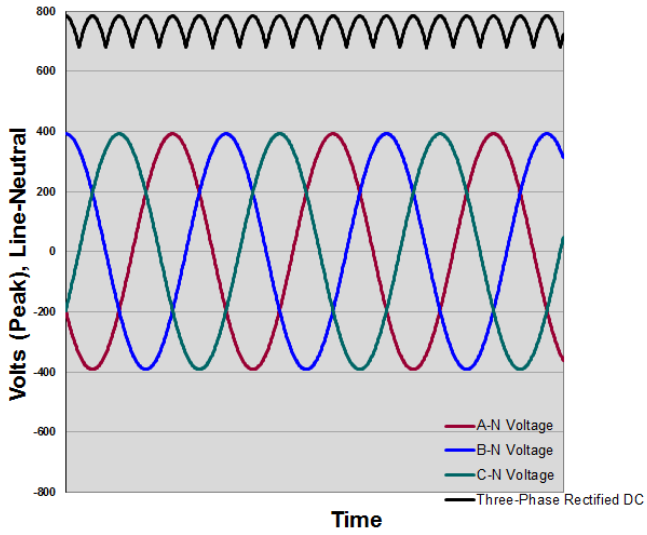


**Figure 18: AC three-phase "utility" voltage 480 Vac, measured line-to-neutral.**

 

A Motor Drive Analyzer with a suitably rated voltage probe (e.g., a Teledyne LeCroy HVD3106 HV differential probe) performs line-neutral probing of a 480 V electric utility AC supply, and we verify these signal levels through use of the cursors and measurement parameters. Figure 19 shows a (nominal) 480 $V_{AC}$ line-neutral signal acquisition with a complete set of voltage measurements.

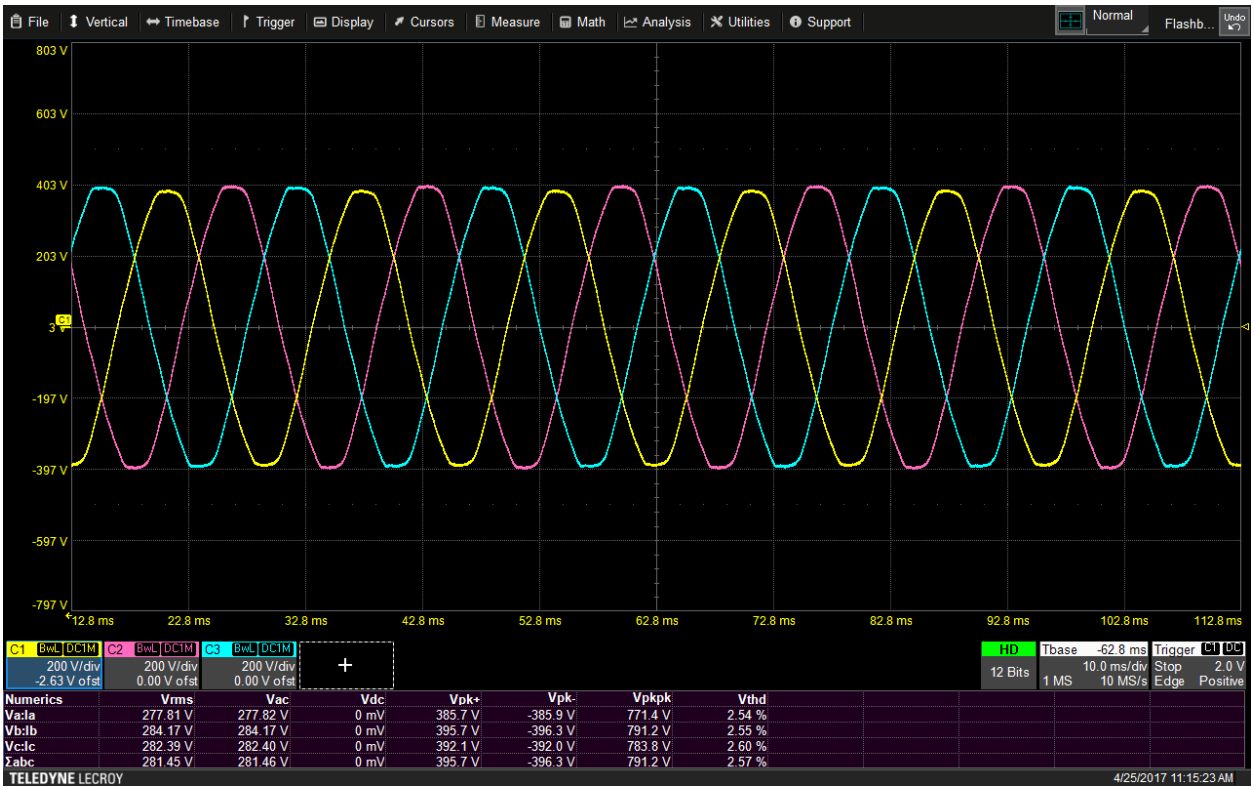


**Figure 19: 480-Vac three-phase voltage waveforms measured line to neutral.**

Figure 20 shows an enlargement of the Numerics table at the bottom Figure 19. This table provides measurement values for the line-neutral voltage waveforms.

| Numerics | Vrms | Vac | Vdc | Vpk+ | Vpk- | Vpkpk | Vthd |
|---|---|---|---|---|---|---|---|
| Va:Ia | 277.81 V | 277.82 V | 0 mV | 385.7 V | -385.9 V | 771.4 V | 2.54 % |
| Vb:Ib | 284.17 V | 284.17 V | 0 mV | 395.7 V | -396.3 V | 791.2 V | 2.55 % |
| Vc:Ic | 282.39 V | 282.40 V | 0 mV | 392.1 V | -392.0 V | 783.8 V | 2.60 % |
| Σabc | 281.45 V | 281.46 V | 0 mV | 395.7 V | -396.3 V | 791.2 V | 2.57 % |

**Figure 20: The voltage readings associated with the 480-Vac waveforms displayed in Fig. 19.**

Note that the $V_{RMS}$ and $V_{AC}$ values are the same, $V_{DC}$ is zero Volts, and the $V_{PK+}$ and $V_{PK-}$ values are roughly equal. The $V_{RMS}$ values are slightly higher than the nominal calculated values described earlier, most likely because these voltages were measured early in the morning before most nearby commercial customers were drawing significant load current from the utility service.

 

When the three line-neutral waveforms are “six-pulse rectified” (using an absolute value math function in the Motor Drive Analyzer (shown as F1, F2, and F3 in the right half of Figure 21) and summed (shown as F4, also in the right half of Figure 21), we see that the rectified voltage value varies from ~700 V to ~790 V.

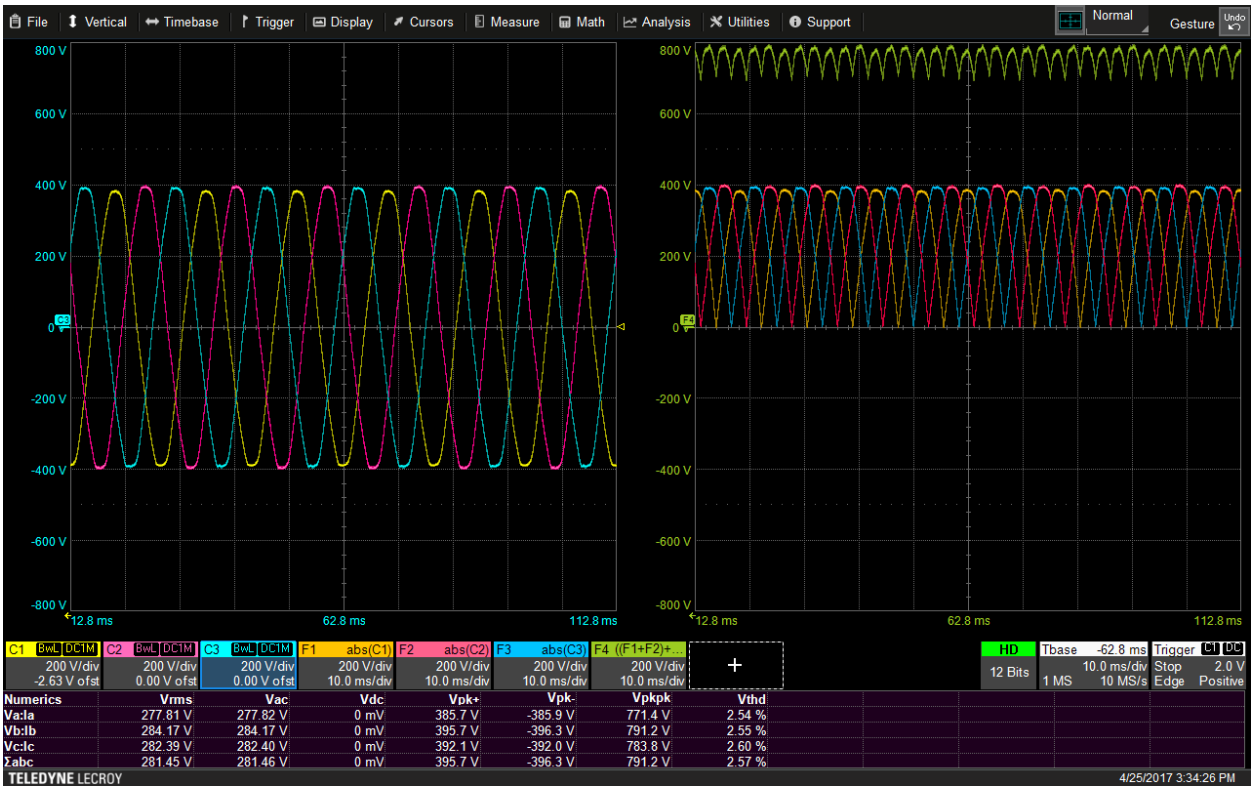


**Figure 21: Motor Drive Analyzer math functions simulating a six-pulse rectifier circuit and resultant waveforms.**

 

When we measure the DC bus voltage using a high-precision (1% accuracy), high-voltage differential probe, and compare the predicted (math) result in Figure 21 to the actual 480 $V_{AC}$ drive DC bus voltage, we see close correlation. The DC bus voltage is Channel 8 (orange trace) in Figure 22, and the actual as-measured value is 693 V after rectification and filtering. This is consistent with a math calculation (√2 * 281.47 * √3 = 689.5 V) and within the 1% accuracy rating of the high-voltage differential probe.

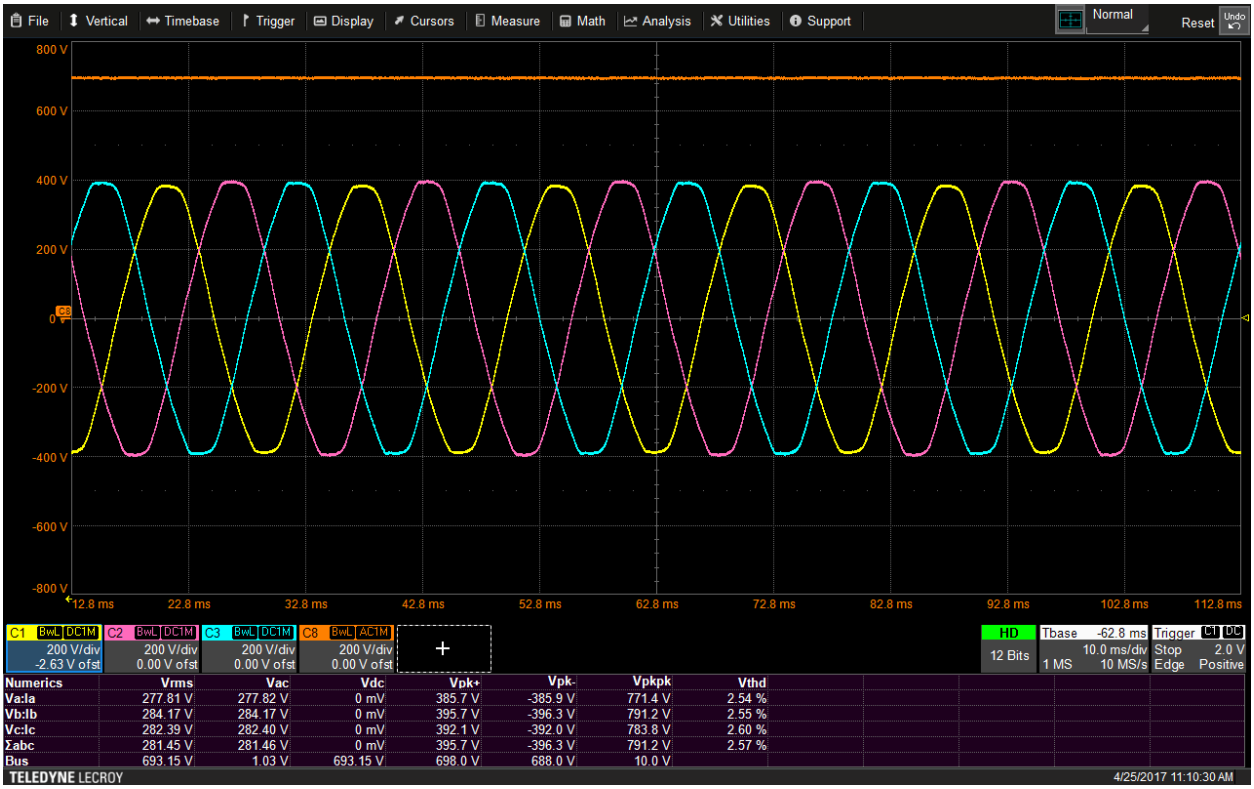


**Figure 22: Applying actual rectification and filtering to the 480-Vac waveforms produces the DC bus voltage measured on channel 8 (orange trace). Its value is 693 V, which is close to the theoretical value calculated by the Motor Drive Analyzer.**

Figure 23 shows the setup dialog for all of the three-phase voltage measurements described. Note that calculations are made with a harmonic filter applied (harmonic orders included through the 50$^{th}$ harmonic) and excluding DC measurement offsets ("include DC" checkbox is unchecked) to eliminate the slight (<0.25%) DC offset introduced by the measurement system.

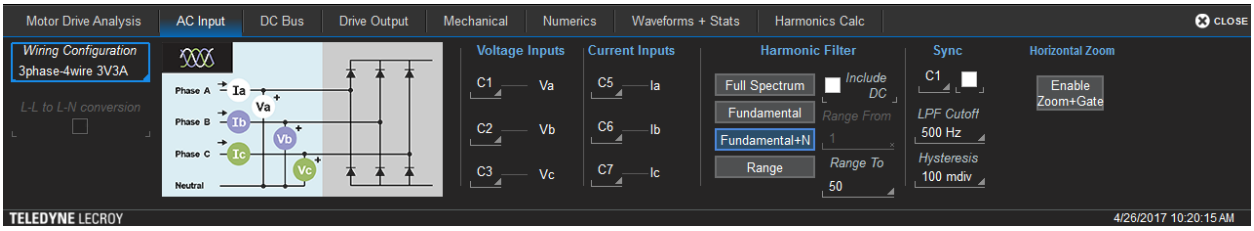


**Figure 23: Setup dialog for 480-Vac three-phase voltage measurements.**

 

## Utility Voltage Classes

Various standards bodies, including the American National Standards Institute (ANSI), Institute of Electrical and Electronics Engineers (IEEE), International Electrotechnical Commission (IEC) and many others, define equipment and testing standards with representatives from the electric utility industry. These standards apply to the various products used to generate, transmit and distribute electricity through an electric utility power system. Standards help to simplify the power system design, equipment purchasing, and manufacture of products within a country or region following the same standards.

A voltage "class" is a grouping of similar voltages or voltage ranges, and it is one of the items that is standardized by ANSI, IEEE, IEC, and others. Below is a listing of the ANSI C84.1-1989 standard describing voltage classes. ANSI is a United States organization but organizations in other countries standardize similarly, and many of the standards cross-reference each other.

- Low Voltage, 600 V Class (Distribution), <1000 Vrms
  - Single-phase (residential and small commercial)
    - 120 V
    - 208 V
    - 240 V
  - Three-phase
    - 400 V
    - 480 V
    - 600 V
- Medium Voltage (Generation, Distribution, Subtransmission)
  - 5 kV (includes 2.4 kV, 3.3 kV, 4.16 kV, etc.)
  - 15 kV (includes 6.6 kV, 6.9 kV, 7.2 kV, 13.8 kV, 14.4 kV, etc.)
  - 25 kV
  - 35 kV
  - 69 kV
- High Voltage and Extra High Voltage Transmission are >69 kV

Note that the definition of "low voltage" is very different from what is present on a typical circuit board.

The voltage class ratings are "nominal." The voltage "classes" may also be known by a slightly lower voltage (e.g., 110 V or 115 V instead of 120 V, 380 V instead of 400 V, 440 V or 460 V instead of 480 V, or 575 V instead of 600 V). The lower voltage simply represents a possible or expected supply voltage reduction through the distribution lines in a home or commercial location. Additionally, standards define, and equipment manufacturers often assume, that the nominal voltage will be 15% higher and test accordingly. Companies may also produce equipment for export at higher voltage rating than would be used in the home market. To wit, Europe is predominantly 400 V, the United States is predominantly 480 V, and Canada is predominantly 600 V. Companies that produce devices likely design, test, and certify them to operate at all of these voltages.

 

Thus, a European company will need to test 600 V-rated products, and likely will want to test them at 600 V + 15% (690 $V_{RMS}$) voltage ratings. If we apply this to earlier calculations of voltage values:

$V_{PEAK(L-L)} = \sqrt{2} * V_{AC}$, or $\sqrt{2} * V_{RMS} = 976$ V
$V_{PK-PK(L-L)} = 2 * V_{PEAK(L-L)} = 1952$ V

The line-neutral measurement case is as follows:

$V_{L-N(RMS)} = V_{L-L(RMS)} / \sqrt{3} = 398$ V (in this case)
$V_{PEAK(L-N)} = \sqrt{2} * V_{AC(L-N)}$, or $\sqrt{2} * V_{RMS(L-N)} = 563$ V
$V_{PK-PK(L-N)} = 2 * V_{PEAK(L-N)} = 1127$ V
$V_{DC} = \sqrt{2} * V_{AC(L-N)} * \sqrt{3} = 392$ V $* \sqrt{3} = 976$ $V_{DC}$ (if rectified and filtered)

Many HV differential probes are rated to 1000 $V_{RMS}$ and the above calculations indicate why this is the case. A voltage of 1000 $V_{RMS}$ is just above the maximum common-mode voltage that could be present in a 600 V class system in the field or under test conditions, as defined by the standards bodies.

If we perform the same calculations on a 4160 V system (a typical 5 kV class voltage), the results would be:

$V_{PEAK(L-L)} = \sqrt{2} * V_{AC}$, or $\sqrt{2} * V_{RMS} = 5883$ V
$V_{PK-PK(L-L)} = 2 * V_{PEAK(L-L)} = 11.766$ kV

The line-neutral measurement case is as follows:

$V_{L-N(RMS)} = V_{L-L(RMS)} / \sqrt{3} = 2402$ V
$V_{PEAK(L-N)} = \sqrt{2} * V_{AC(L-N)}$, or $\sqrt{2} * V_{RMS(L-N)} = 3397$ V
$V_{PK-PK(L-N)} = 2 * V_{PEAK(L-N)} = 6793$ V
$V_{DC} = \sqrt{2} * V_{AC(L-N)} * \sqrt{3} = 392$ V $* \sqrt{3} = 5879$ $V_{DC}$ (if rectified and filtered)

Another widely used, yet unofficial voltage “class,” known as low-voltage 50 V safety, rests on the assumption that contact with 50 V presents little danger to people. Many low-voltage motors driven from batteries, such as power tools, or motors in automobiles, operate at <50 V. Additionally, some power conversion systems that drive motors step down the 120 V or 240 V inputs to a lower voltage to drive a motor at <50 V line-line or line-neutral.

 

# AC Line Current

## Introduction

Formally, we state AC line current values in amperes RMS ($A_{RMS}$), but in practice they are simply stated as A or $A_{AC}$. In this context, the terms A, $A_{AC}$, and $A_{RMS}$ are interchangeable.

Measurements of AC line current are always from a single line (conductor). In the case of a wye (star) three-phase connection, the measurement is a line-neutral measurement, which corresponds to the current flowing through a single winding to neutral (line-neutral). In the case of a three-phase delta connection, the line currents are flowing into a terminal supplying current to two windings. In this case, there is no way to determine how much current is flowing in each of the two windings, unlike the wye (star) case where the line-neutral current is the winding current (more on this later).

In a balanced, three-phase system driving a linear, balanced load, the neutral current should be zero. If not, then the system is not balanced; there are leakage currents, or the current flow measured in the neutral is the uncertainty in the current measurement equipment.

AC line currents supplied from the electric utility are always sinusoidal, with typical utility requirements that they contain <5% total harmonic distortion (THD) and that customers not disturb the service entrance with >5% THD.

 

## Single-phase AC Line Current

A single-phase, two-wire AC system contains a single current-carrying wire and a neutral wire. A single-phase, three-wire AC system contains two current-carrying wires.

As with voltage, the AC current is a rotating vector with a magnitude and an angle. The magnitude varies sinusoidally because the single-phase AC current is a rotating vector with a magnitude and an angle. The rotation period is the inverse of the supply frequency. The magnitude of this current vector is the instantaneous line-neutral current value, with a peak current $I_{PEAK}$ equal to √2 * $I_{RMS}$. The voltage vector completes one revolution at a rate of one period = 1/frequency (50 Hz or 60 Hz). At any given moment in time, the current magnitude is equal to $I_{PEAK}$ *sin(α), with α = the angle of rotation in radians. Reference Figure 24.

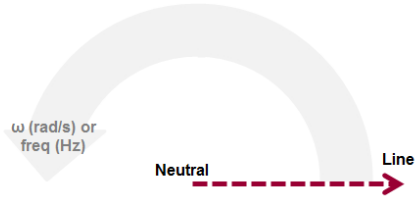


Figure 24: Single-phase current vector system.

Figure 25 shows the rotating current vector in the time domain as a sinusoidal waveform with a fixed period and frequency.

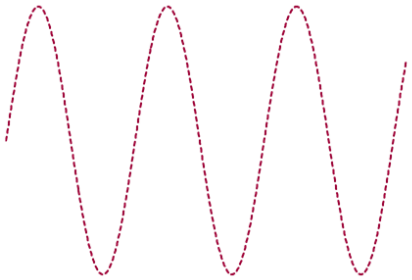

Figure 25: A time-domain view of the single-phase current vector system.

If this sinusoid is 5 A or 5 $A_{AC}$, then by definition it 5 $A_{RMS}$. From that, we can calculate the following:

$A_{PEAK}$ = √2 * $A_{AC}$, or √2 * $A_{RMS}$ = 7.07 A
$A_{PK-PK}$ = 2 * $A_{PEAK}$ = 14.14 A

Figure 26 shows a Motor Drive Analyzer with an appropriate current probe (e.g., Teledyne LeCroy's CP030) probing the line current to verify these signal levels with measurement parameters. In this case, we are using the same toaster as described in the single-phase voltage section and measuring current while the toaster is "toasting." The current signal is on Channel 8 (C8, orange signal).

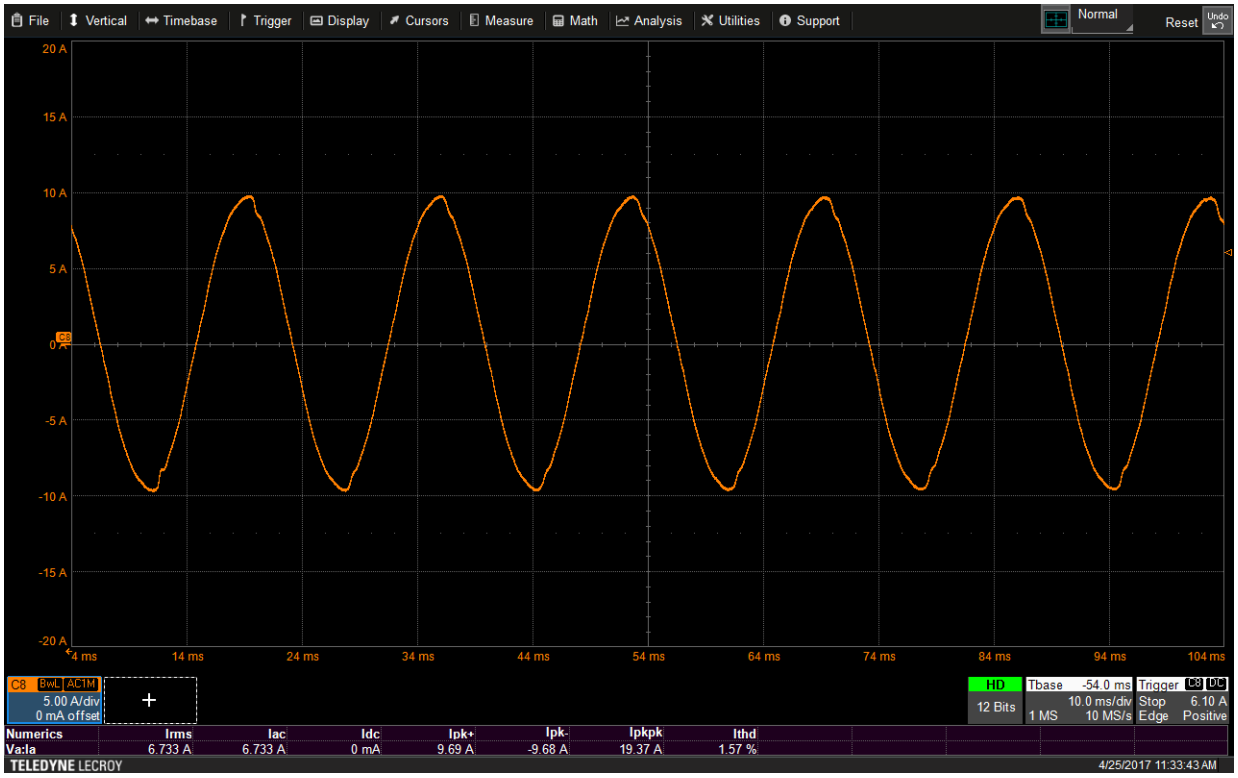


**Figure 26: AC line current signal captured with a Teledyne LeCroy 8-channel, 12-bit Motor Drive Analyzer. This measurement is identical to the voltage measurement of the 120-V ac signal in part 2, except for the use of a current probe in place of a high-voltage probe.**

Figure 27 shows an enlarged version of the Numerics table at bottom of Figure 26. This table provides measurement values for the line-neutral current waveforms:

| Numerics | Irms | Iac | Idc | Ipk+ | Ipk- | Ipkpk | Ithd |
|---|---|---|---|---|---|---|---|
| Va:Ia | 6.733 A | 6.733 A | 0 mA | 9.69 A | -9.68 A | 19.37 A | 1.57 % |

**Figure 27: The Numerics table lists key measurement values from the waveform in Figure 26.**

 

Figure 28 shows both the line current and the 120 VAC voltage waveforms. Note that the line current measured in this example is supplying a resistive load. Therefore, the current waveform and the voltage waveform are in-phase.


**Figure 28: AC line current (orange trace) and 120 Vac voltage (yellow trace) waveforms captured with a Teledyne LeCroy 8-channel, 12-bit Motor Drive Analyzer. The two signals are in phase as expected with a resistive load.**

Additionally, note that the resistive load above is linear – the resistance is constant and the applied voltage results in a current that is linear in relation to the applied voltage. Therefore, the distortion profile ("shape") of the line current closely matches that of the line voltage, which is distinctly sinusoidal. A non-linear load, such as a switch-mode power supply using pulse-width modulation (PWM), consumes current non-linearly, and the line current consists of a series of pulses and is very non-sinusoidal, as shown in Figure 29.

 

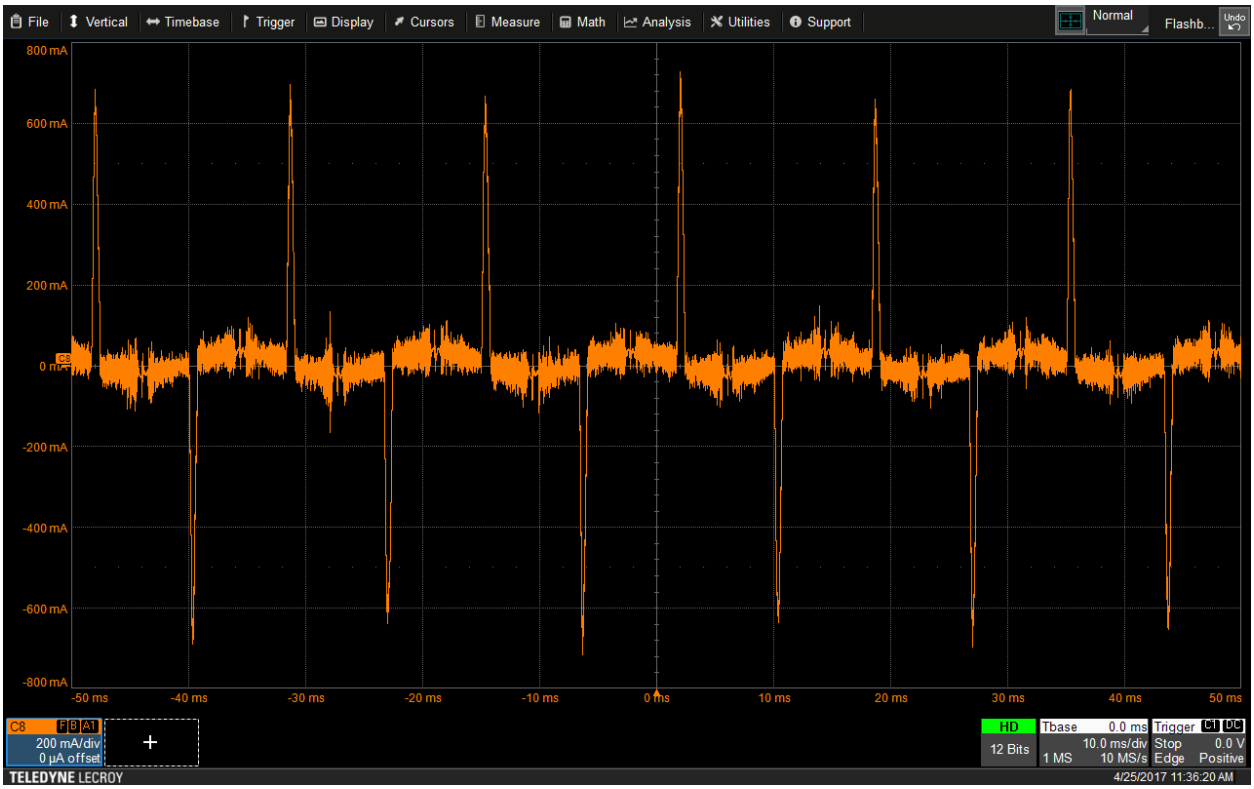


**Figure 29: Line current measurement on the input of a switched-mode power supply. The nonlinear nature of the load produces this non-sinusoidal current waveform.**

## Three-phase AC Line Currents

Three-phase AC systems are more complicated than single-phase systems with regards to describing currents. One may distribute three-phase current with a variety of different wye or delta connection configurations – it is beyond the scope of this document to describe all the various permutations, so this document will only describe the most common types.

In a three-phase system, there is (by design) "balance," meaning that the three-phase current vectors have the same current magnitude and are separated from the other phases by 120°, or 1/3 of a full sinusoid period, and should therefore vector sum to zero. Thus, in a balanced three-phase system, the sum of all the line currents is zero. Practically speaking, this means that the return current for each phase travels in the opposite direction in the other two phases. Contrary to a single-phase system, the three-phase neutral connection carries no current under normal operating conditions. However, if there is a fault (failure) condition or a leakage of current to ground, the neutral may have some voltage potential and carry some current.

As in a single-phase system, the three-phase current vectors rotate at a constant rate. This rotation and phase difference between each phase in a three-phase system makes it possible to produce rotating magnetic fields that can perform work, such as in an electric motor.

 

Figure 30 shows the three-phase current vector system.

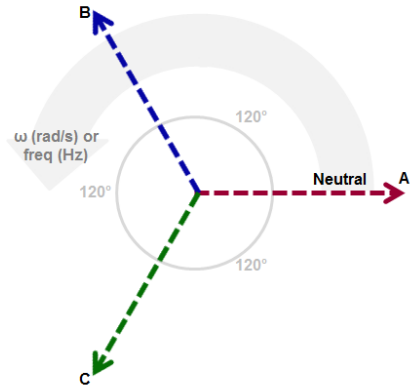


Figure 30: Three-phase current vector system.

Figure 31 shows the three "rotating" current vectors viewed in the time-domain as three sinusoidal waveforms, each with the same fixed frequency, and out of phase with respect to each other by 120°.

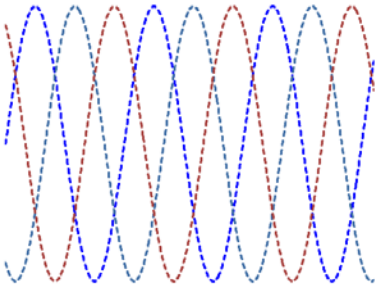

Figure 31: A time-domain view of the three-phase current vector system.

We may also refer to line current as phase current. The convention for indicating a line current measurement is to show the current symbol "I" followed by a subscripted "$_{line}$" designation. Thus, phase A line current would be represented as $I_A$.

Because we measure three-phase line currents to a neutral in a wye (Y or star) configuration and to a terminal in a Delta (or Δ) configuration, the calculation of the various current values is identical to that of the single-phase case.

As described in the single-phase case, the line current could supply a linear or a non-linear load. In the case of a linear load, the three line currents are sinusoidal (within distortion limits). A motor drive provides a non-linear load, and the currents are distorted as in the single-phase case. Figure 32 shows the three-phase current input to a 480 $V_{AC}$ motor drive.

 

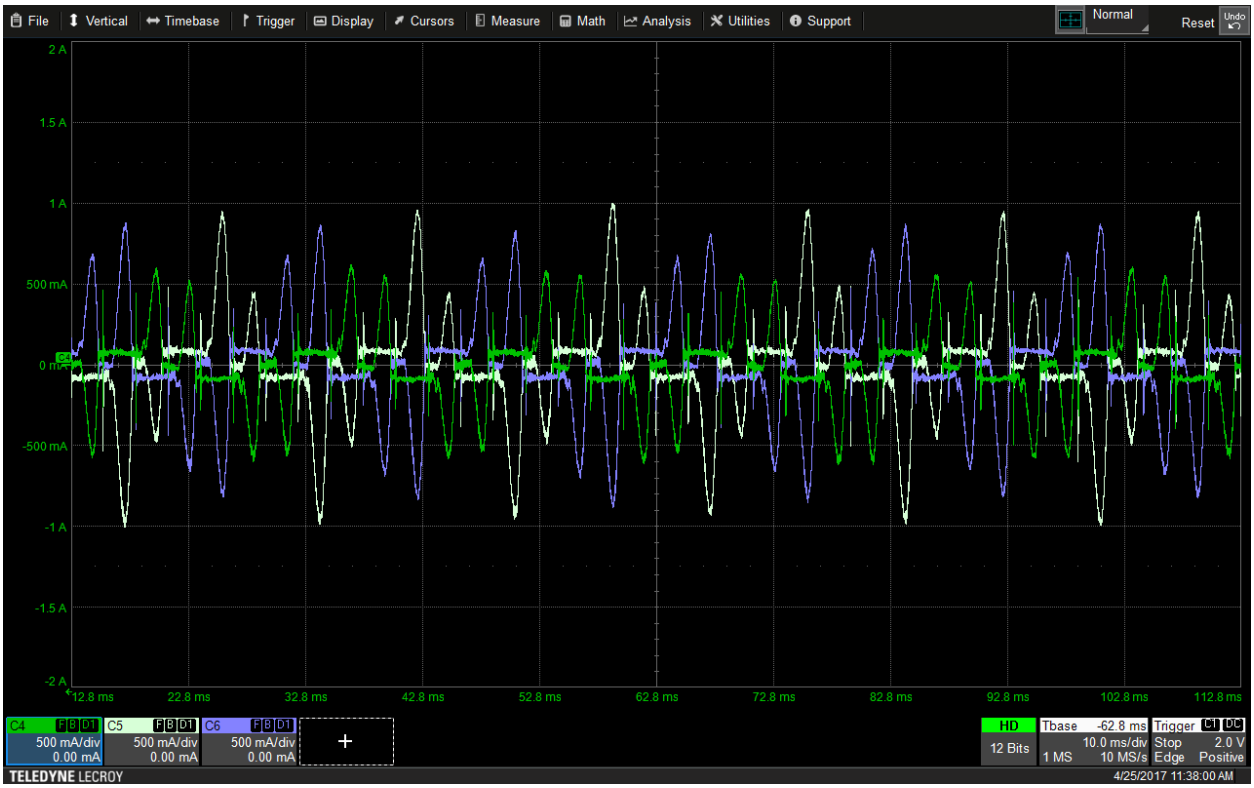


**Figure 32: Three-phase current input to a 480-Vac motor drive captured with a Teledyne LeCroy 8-channel, 12-bit Motor Drive Analyzer.**

 

### *Line-Line to Line-Neutral Voltage Relationships*

As described earlier, one may measure a three-phase system voltage from line-line or from line-neutral. Earlier in this primer, we calculated the expected voltage magnitudes for line-line and line-neutral voltages for a 480 V system (displayed in the previous examples). Figure 33 consolidates this information to better illustrate the relationship. Channel 1 (C1, or Yellow) is the line-line voltage $V_{A\text{-}B}$ and channel 8 (C8, or orange) is the line-neutral voltage $V_{A\text{-}N}$.


**Figure 33: Comparing the magnitude of a line-to-line voltage (VA-B on ch 1) in a 480-V three-phase system with a line-to-neutral voltage (VA-N on ch 8).**

Figure 34 shows a larger view of the measurement parameters at the bottom of Figure 33.

| Measure | P1:rms(C1) | P2:pkpk(C1) | P3:- - - | P4:rms(C8) | P5:pkpk(C8) | P6:- - - | P7:phase(C1,... |
|---|---|---|---|---|---|---|---|
| value | 474.4 V | 1.3608 kV | | 275.2 V | 764.8 V | | 28.95689458 ° |
| status | ✓ | ✓ | | ✓ | ✓ | | ✓ |

**Figure 34: Measure table comparing voltage measurements in Fig. 32.**

The RMS and peak-peak voltage values are as expected, and the nominal 30° phase angle between the two waveforms is also as anticipated.

Figure 35 shows all three line-line voltage waveforms acquired simultaneously (this time displayed on Channel 1, 2, and 3, or the line-line voltages $V_{A\text{-}B}$, $V_{B\text{-}C}$, $V_{C\text{-}A}$, respectively). We measure the phase angle between them and see that the three-phase system has three line-neutral voltage waveforms, each 120° out of phase with each other, with one phase rotation equal to 360°.

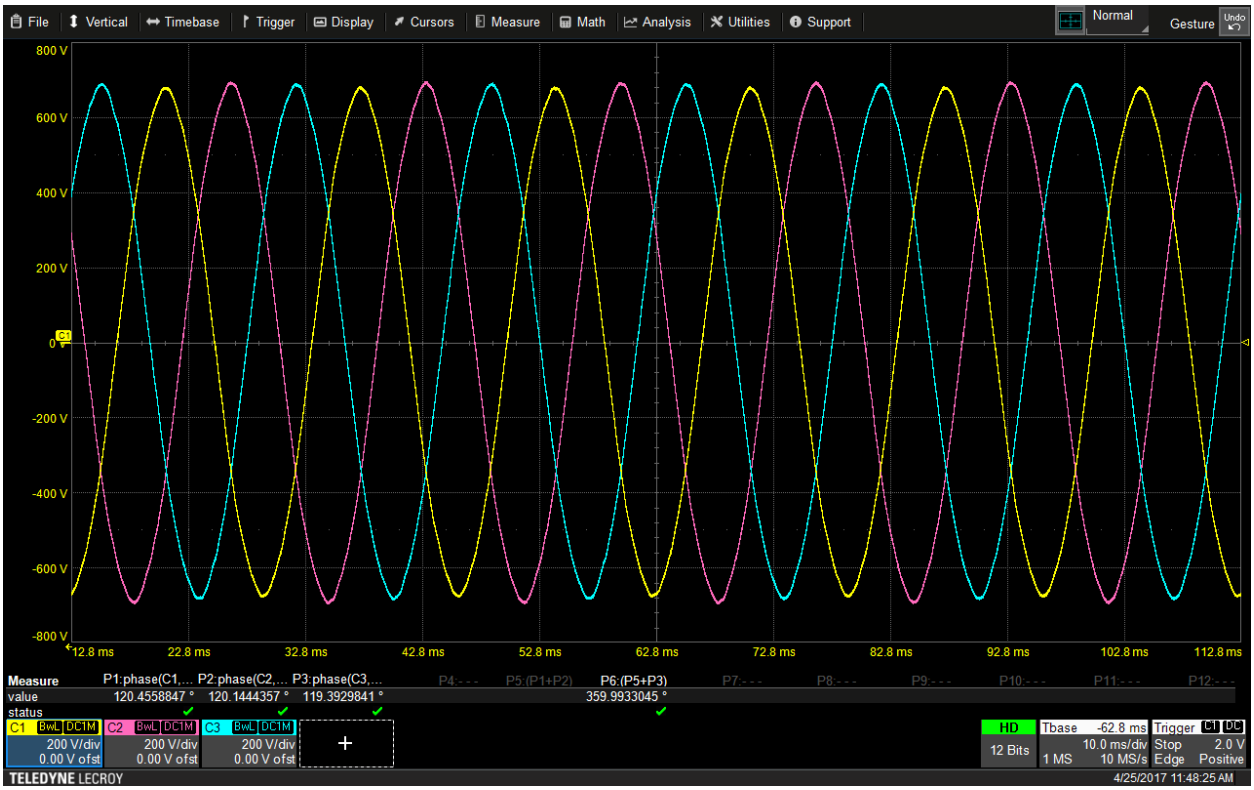


**Figure 35: Acquiring all three line-to-line voltages for a three-phase, three wire ac system simultaneously.**

Figure 36 shows a larger view of the Measure table with the phase calculations.

| Measure | P1:phase(C1,... | P2:phase(C2,... | P3:phase(C3,... | P4:- - - | P5:(P1+P2) | P6:(P5+P3) |
|---|---|---|---|---|---|---|
| value | 120.4558847 ° | 120.1444357 ° | 119.3929841 ° | | | 359.9933045 ° |
| status | ✔ | ✔ | ✔ | | | ✔ |

**Figure 36: Measure table showing the phase separation between each line-line voltage and the total of 360 degrees in one complete phase rotation.**

 

## Three-phase Winding Configurations

Until now, we have discussed only the voltage and current phase vectors. For a single-phase, two-wire system, there is one voltage and one current vector, and for a single-phase three-wire system, there are two voltage and two current vectors. However, for a three-phase system, there are three voltage and three current vectors, and how we produce these voltage vectors and how current flows when voltage is present depends on the three-phase winding configuration.

The neutral wire may or may not be available in a three-phase system, and the three phases may be arranged in a wye (Y or star, shown at left in Figure 37) or delta (or Δ, shown at right in Figure 37) configuration:

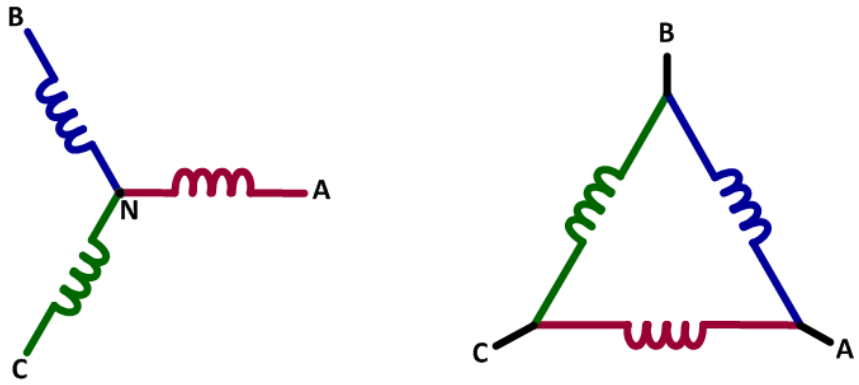


Figure 37: Wye or star (left) and delta (right) three-phase winding configurations.

Wye (Y or Star) configurations always have a neutral in the winding, but it might be inaccessible depending on the physical construction of the winding. In motors, the neutral is typically inaccessible.

Delta (Δ) configurations may or may not have a neutral connection. When they do, it is usually one phase ("leg") of the delta tied to neutral (e.g., phase A), or one winding with a neutral connection at the midway point in the winding. Delta (Δ) configurations with neutral connections are uncommon in motors or drives.

Measuring winding current in a three-phase system can be problematic. In a delta winding, a known current flows into a terminal, but that terminal current is shared by two different windings. In this case, there is no way to measure the current in the winding because the winding rotates as a function of motor operation. Therefore, we may measure power at the terminal, but it is not possible to measure power in a single winding in a delta configuration. For wye (star) windings, it is more straightforward because the winding current is the line current.

## AC Line Power Calculations

### Introduction

Power is the rate at which energy transfers to a circuit. Units of power consumption are in watts, which equal one joule/second. For resistive loads with single-phase or three-phase applied AC voltage and

current, power calculations are relatively straightforward, and power values, stated in watts, reflect "real" consumption.

For inductive or capacitive loads supplied by single-phase or three-phase AC voltages and currents, power calculations are much more complicated and require full understanding to make proper measurements. In this case, "power" is comprised of a "real" and a "reactive" component that are in a quadrature relationship. The quadrature sum of these two components is the "apparent" power. The "apparent" power is what is required to run the device (e.g., a motor), even though the "real" power is all that is consumed during operation. There is no consumption of the "reactive" power, it is merely transferred within the circuit during each power cycle. High levels of reactive power in relation to real power are undesirable as it results in inefficient power delivery to the load.

### Power Consumed by Linear, Resistive Loads

Assume for a purely linear load that a sinewave applied to the load will not be distorted. Furthermore, also assume that the resistive load will consume all the power supplied to it. Here is the formula for calculating power in a resistive circuit for an AC (or a DC) system, with current or voltage expressed in RMS terms:

Power (P) = $I^2R$, or following Ohm's law, = $V^2/R$ or = V*I

In this case, we may compute power consumption for a single cycle in real time on a digitally sampled signal (such as provided by an oscilloscope, power analyzer, or Motor Drive Analyzer) by multiplying the instantaneous voltage and current sampled values over a single sinewave period.

In vector terms, for a purely resistive load the voltage and current vectors for a single-phase system are in phase, and the corresponding line current (I) and line voltage (V) vector magnitudes are simply instantaneously multiplied, as shown in Figure 38.


**Figure 38: Vector representation of instantaneous voltage and current for a purely linear (resistive) load.**

Figure 39 shows the 120 $V_{AC}$ line-neutral waveform captured on Channel 1 (C1, yellow) and the line current waveform captured on Channel 8 (C8, orange) of the Motor Drive Analyzer when using our standard resistive load (the bread toaster). Note that the voltage and current signals are in-phase with each other, as would be expected for a resistive load, and the signals are sinusoidal (with some small amount of distortion present in the AC line supply). As shown earlier, the voltage signal has the same distortion with and without a load, so it appears that this is a linear load. The RMS voltage and current, power (P, in Watts) and power factor (PF) appear at the bottom of the screen image in the Numerics table.

 

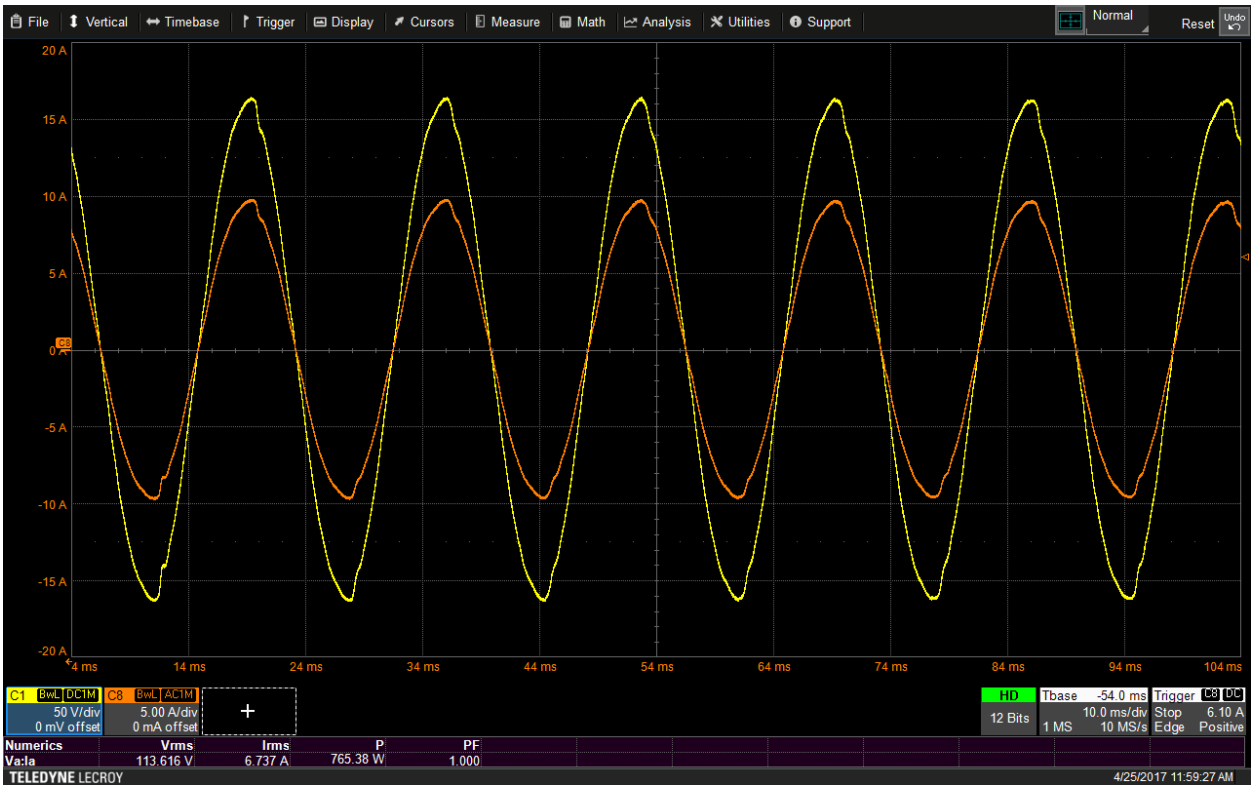


Figure 39: 120Vac line-neutral voltage and line current waveforms supplying a resistive load.

The Numerics table at the bottom of the image in Figure 39 provides measurement values for voltage, current, power and power factor. A larger view of this table is shown in Figure 40.

| Numerics | Vrms | Irms | P | PF |
|---|---|---|---|---|
| Va:Ia | 113.616 V | 6.737 A | 765.38 W | 1.000 |

Figure 40: A larger view of the Numerics table from the previous figure.

Note that the power factor is 1.0, as expected for a purely resistive load, and the real power in watts is simply the multiplication of the RMS voltage and current values, after accounting for round-off errors.

## Power Used (Supplied and Consumed) by Linear, Non-Resistive Loads

If the load is inductive or capacitive, power is supplied but is not consumed, and the expression of power becomes more complex because the inductive or capacitive nature of the load causes the current and voltage vectors to be out of phase with respect to each other. Power therefore consists of a “real” (direct, or resistive) component in watts and referred to as “P”, and a “reactive” (imaginary, or capacitive/inductive) component in volt-amperes reactive (VAr) and referred to as Q. The reactive component of power is in quadrature with the real power. There is no consumption of the reactive power, Q, by the load, but rather it is simply transferred from one part of the circuit to another during a single AC period. It is also referred to as the “imaginary” power. The quadratic sum of these two components is the “apparent” power in volt-amperes (VA), referred to as “S”. The apparent power S represents the total power required from the AC line for the circuit to work. The vector relationship of P, Q, and S is shown in Figure 41.

 

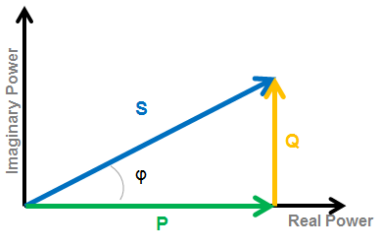


Figure 41: Vector representation of real, imaginary and apparent power for an inductive or capacitive load.

The angle between the real power, P, and the apparent power, S, is the phase angle, φ, expressed in degrees (-90° to +90°) or radians (-π/2 to + π/2 radians), with a zero value representing a purely resistive load.

We also express phase angle as the Power Factor (λ, or PF). Power factor is simply the cos(φ) for sinusoidal waveforms and is a unit-less value from 0 to 1, specified as leading PF (the current vector leads the voltage vector, as in the case of a capacitive load) or lagging PF (current vector lags the voltage vector, as in the case of an inductive load). This is shown in Figure 42.

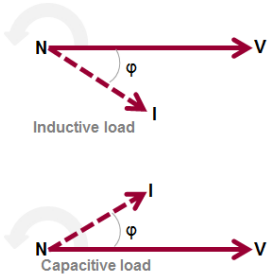


Figure 42: The phase angle (ϕ) between voltage and current for a reactive load is the same as the phase angle between the load's real and apparent power and is used to calculate the power factor.

For a pure, single-frequency, sinusoidal waveform (e.g., a utility-supplied AC line voltage waveform with zero distortion), phase angle is the phase difference between the applied line-neutral voltage sinusoid and the line current sinusoid, as shown in Figure 43.

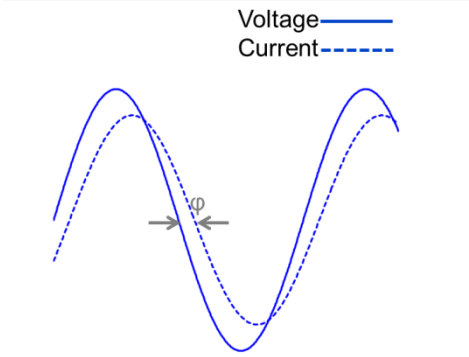


Figure 43: Current leads voltage by a phase angle ϕ, indicating a capacitive load.

 

The phase angle φ shown above leads the voltage signal, indicating a capacitive load. By convention, the phase angle is positive if the voltage is leading the current (it would be negative for the example shown above). If we can accurately measure the phase angle, then we may calculate the real, reactive, and apparent power values as follows for a single power frequency cycle:

- Measure $V_{RMS}$ and $I_{RMS}$
- Measure phase angle
- Calculate Apparent Power (S) using $|S| = Vrms * Irms$
- Calculate Real Power (P) using $P = S * \cos\varphi$
- Calculate Reactive Power (Q) using $Q = \sqrt{S^2 - P^2}$

However, the above is only true for a pure, single-frequency sinusoidal waveform, which is unlikely to be present. However, if the waveform distortion is within normal electric utility guidelines (<5%), it is a reasonable approximation.

### Power Used (Supplied and Consumed) by Non-Linear, Non-Resistive Loads

More often, loads are not purely resistive and may be non-linear. Therefore, the voltage or current waveforms are out-of-phase and distorted. Therefore, the simple calculation technique of measuring phase angle between a single-frequency voltage and current sinewave pair does not apply because the distorted waveform is composed of a complex Fourier series of multiple frequencies, each with a unique phase angle for a given harmonic.

Therefore, we employ a different approach based on digital sampling techniques. This technique is quite common given the pervasiveness of high-resolution analog-to-digital converters with high bandwidth (e.g., digital storage oscilloscopes and power analyzers). After digitally sampling the waveforms, the mathematical calculations are easy. This technique is mathematically correct whether the waveforms are pure sinusoids, distorted sinusoids, pulse-width modulated, or something else. This technique is described in the following steps:

#### *Step 1: Digitally Sample the Waveform*

A digital sampling system should oversample the waveform by 10x (or more) to capture enough detail to be able to re-create the analog waveform from the digital samples. The requisite oversampling depends on the harmonic content of the signal – pure, lower-frequency sinewaves (e.g., an ideal utility supply voltage) require less oversampling than a complex PWM waveform. Figure 44 shows an example of a digitally oversampled analog waveform.

 

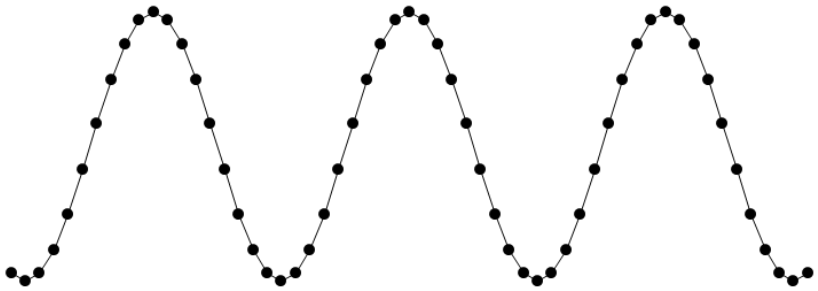

Figure 44: Accurate measurement of voltage and current waveforms using digital techniques, particularly those waveforms associated with nonlinear loads, requires oversampling.

### *Step 2: Determine the Cyclic Period*

Using the digitally sampled data, a complex software algorithm determines a 50% amplitude value for the waveform (the 50% amplitude value equals approximately 0 V for a voltage signal probed line-line, or a line current signal). The algorithm then determines a 50% (or zero) crossing point for each individual cycle, and a time measurement for the start and end of each full cycle present in the acquisition, thereby identifying the exact location of the beginning and end of each cyclic period. A software algorithm determines the 50% (zero) crossing point determination with high precision, typically by combining the following measurement techniques:

- User-settable high-frequency filtering via low pass filter cutoff setting
- Localized interpolation/oversampling at the 50% (zero) crossing point
- Elimination or minimization of the effects of perturbations or non-monotonicities at the 50% (zero) crossing point with a user-defined hysteresis band control

In the case of a pure, single-frequency sinewave (Figure 45), this is a relatively straightforward process and default settings are likely sufficient. For a more complex, distorted PWM waveform, advanced settings may be required to avoid detection of false periods. In both cases, one should visually review the accuracy of the zero-crossing point detection (on the measurement instrument) because the power calculation accuracy depends on it.

Figure 45 shows the detection of two full cyclic periods in this short acquisition:

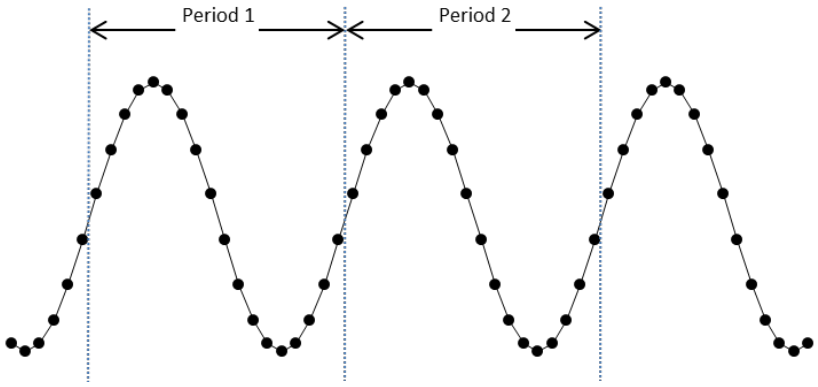


Figure 45: Determining 50% or zero-crossing points is easiest in the case of a pure sinewave.

 

### *Step 3: Determine the Digital Sample Point Set in Each Detected Cyclic Period*

Given the locations of the detected cyclic periods, the sample point set can easily be determined for each cycle. In Figure 46, there are ***N*** periods and ***N*** = 2. For a given cyclic period index ***i***, the digitally sampled waveform is represented as having a set of sample points ***j*** in cyclic period index ***i***, with $M_i$ sample points beginning at $m_i$ and continuing through $m_i+M_i-1$. For example, Period 1 is cyclic period index ***i = 1***. There is a set of sample points ***j*** in cyclic period 1, beginning with point 7 and ending with point 24.

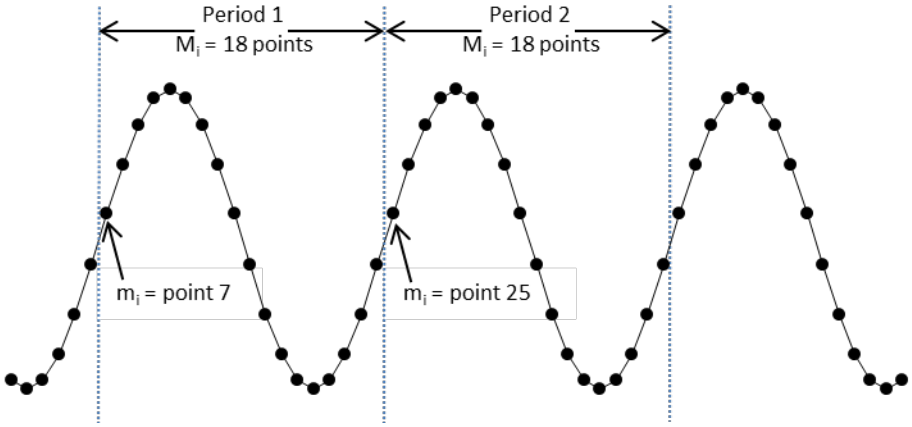


**Figure 46: For a given cyclic period index i, the digitally sampled waveform is represented as having a set of sample points j in cyclic period index i, with Mi sample points.**

 

### *Step 4: Calculations*

Once the sample point sets are determined, we make all cyclic period voltage, current and power calculations with the appropriate set of points using the equations in Table 1.

| | Per-cycle Value Calculations | Mean Value Calculations |
|---|---|---|
| **$V_{RMS}$** | $Vrms_i = \sqrt{\frac{1}{M_i}\sum_{j=m_i}^{m_i+M_i-1} V_j^{\,2}}$ | $Vrms = \frac{1}{N}\sum_{i=1}^{N} Vrms_i$ |
| **$I_{RMS}$** | $Irms_i = \sqrt{\frac{1}{M_i}\sum_{j=m_i}^{m_i+M_i-1} I_j^{\,2}}$ | $Irms = \frac{1}{N}\sum_{i=1}^{N} Irms_i$ |
| **Real Power (P, in Watts)** | $P_i = \frac{1}{M_i}\sum_{j=m_i}^{m_i+M_i-1} V_j * I_j$ | $P = \frac{1}{N}\sum_{i=1}^{N} P_i$ |
| **Apparent Power (S, in VA)** | $S_i = Vrms_i * Irms_i$ | $S = \frac{1}{N}\sum_{i=1}^{N} S_i$ |
| **Reactive Power (Q, in VAr)** | $magnitude\ Q_i = \sqrt{S_i^{\,2} - P_i^{\,2}}$<br>*sign of $Q_i$ is positive if the fundamental voltage vector leads the fundamental current vector* | $Q = \frac{1}{N}\sum_{i=1}^{N} Q_i$ |
| **Power Factor (PF or λ)** | $\lambda_i = \frac{P_i}{S_i}$ | $\lambda = \frac{1}{N}\sum_{i=1}^{N} \lambda_i$ |
| **Phase Angle (φ or ϕ)** | $magnitude\ \phi_i = \cos^{-1}\lambda_i$<br>*sign of $\phi_i$ is positive if the fundamental voltage vector leads the fundamental current vector* | $\phi = \frac{1}{N}\sum_{i=1}^{N} \phi_i$ |

**Table 1: Per-cycle and mean value calculations for voltage, current and power.**

### *Example*

Let's revisit the previous example of the single-phase standard resistive load (the bread toaster).

Figure 47 shows the 120 $V_{AC}$ line-neutral waveform captured on Channel 1 (C1, yellow, top grid) and the line current waveform captured on Channel 8 (C8, orange, top grid) of the Motor Drive Analyzer. The bottom grid shows a 20,000:1 Zoom waveform of Channel 1 (Z1, yellow, bottom grid) and a 20,000:1 Zoom waveform of Channel 8 (Z8, orange, bottom grid). These two zoom traces are time-synchronized with each other.

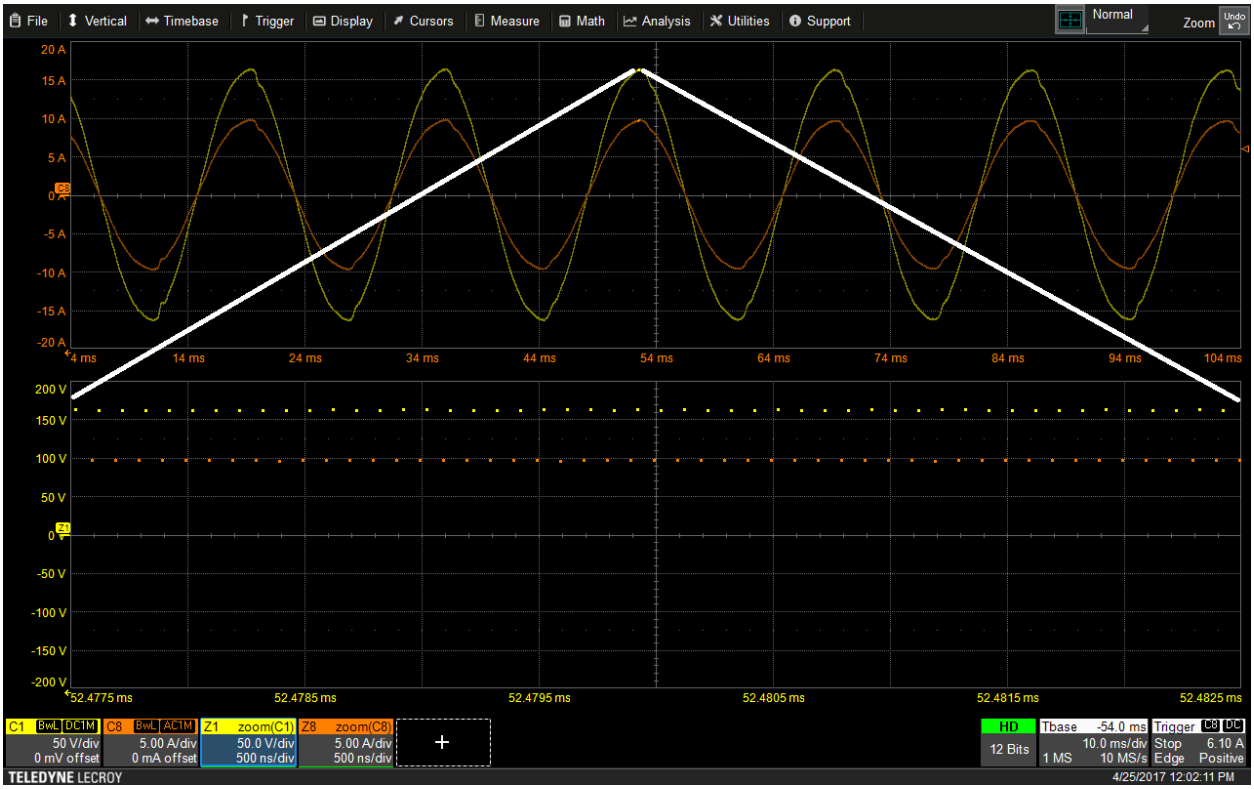


**Figure 47: Line-to-neutral voltage waveform (yellow) and the associated current waveform (orange) for a linear load are shown on channels 1 and 8 at the top of the display. Then, in the bottom of the display, small segments of these waveforms are magnified in the timebase to show the sampled points that comprise the waveforms.**

We add the white lines to the image to draw attention to the small part of the original waveform shown in the zoom traces. Note that in the Motor Drive Analyzer display settings, we have turned "off" the normal line connection between points on the waveforms to make it easier to see the distinct sample points. Also, note that the sample points are spaced 100ns apart – the time scale of the Zx traces is 500 ns/div, and there are 5 points per division. This is to expected given that the sample rate for the full acquisition is 10 MS/s, and therefore the distance between points is 1/(10 MS/s) = 100 ns. This sample rate setting can be changed by the user to be lower (into the kS/s range) or higher (e.g., 2.5 GS/s), depending on the frequency content of the signal and the desired acquisition duration.

 

Figure 48 shows the Zoom traces turned OFF and replaced by the 120 $V_{AC}$ line-neutral waveform (C1) with application of a 500 Hz low-pass filter– this is known as the "Sync" signal. The zero-crossing algorithm has determined the cyclic periods and displayed them with a color-coded annotation on top of the waveform. The annotation indicates a good determination of the cyclic period as well as detection of five full periods. If necessary (as would often be the case with PWM waveforms), the hysteresis setting could be adjusted to aid in the zero-crossing determination.

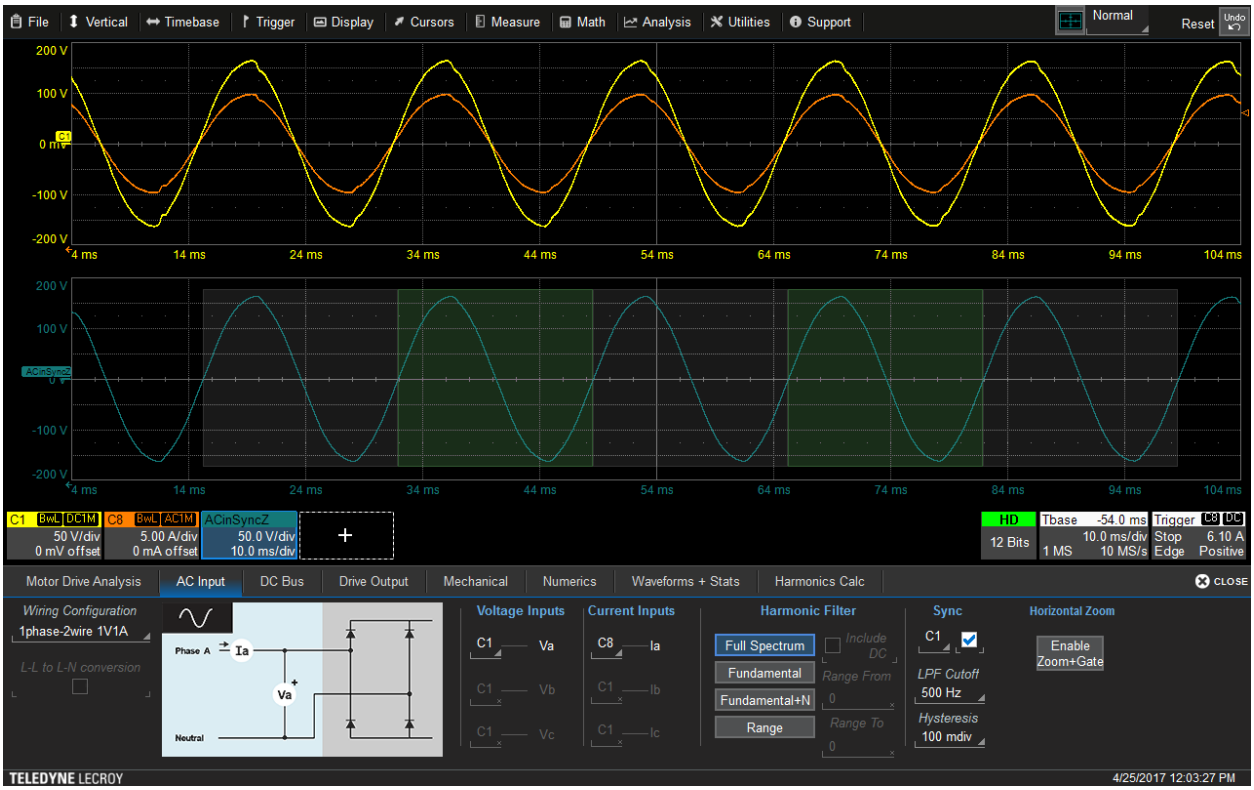


**Figure 48: Line-to-neutral voltage waveform and the associated current waveform for a linear load are again shown on channels 1 and 8 at the top of the display. But the lower waveform is a lowpass filtered version of the voltage waveform, which serves as the sync signal.**

 

In Figure 49 we have turned off the Sync signal and then we again display the Numerics calculation table, this time showing apparent and reactive power and phase angle in addition to real power and power factor.

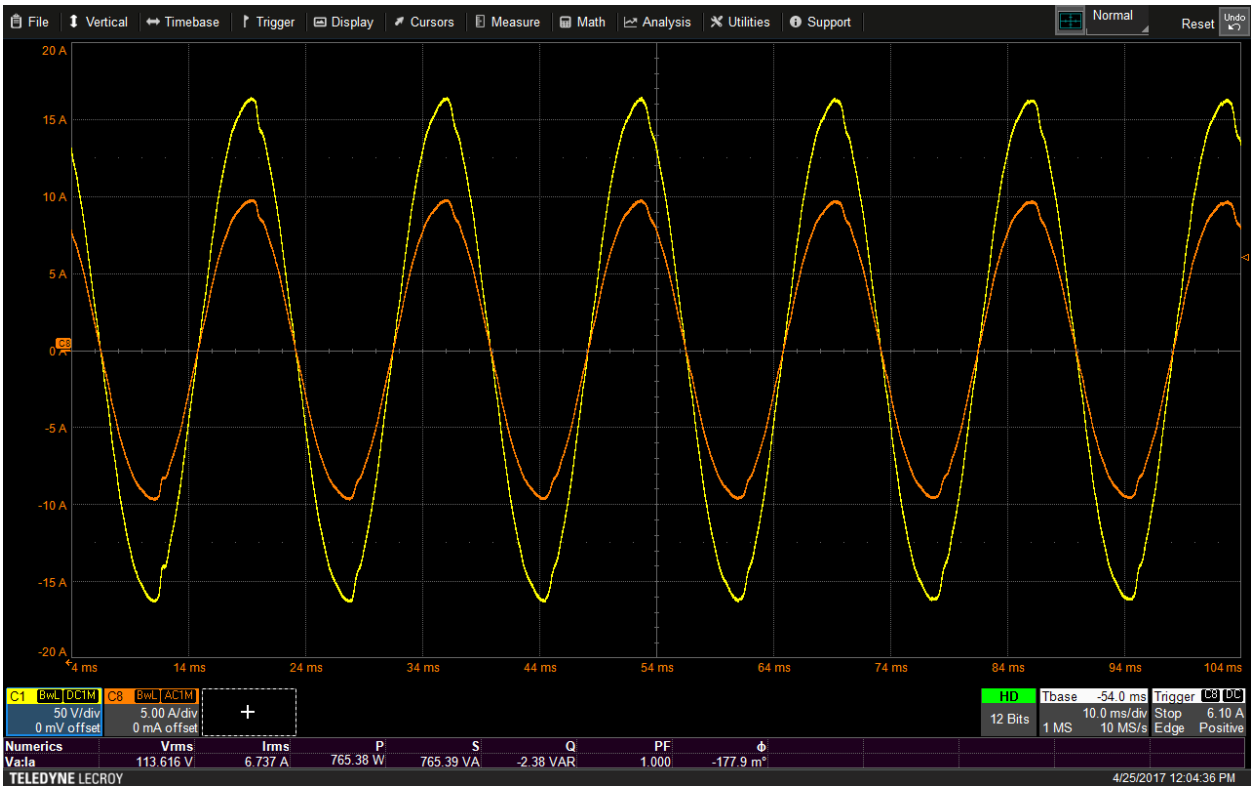


**Figure 49: Line-to-neutral voltage waveform and the associated current waveform for a linear load are shown with the Numerics calculation table, which displays various power-related parameters for these waveforms.**

Figure 50 shows a larger version of the Numerics table that is shown at the bottom of Figure 49.

| Numerics | Vrms | Irms | P | S | Q | PF | ϕ |
|---|---|---|---|---|---|---|---|
| Va:Ia | 113.616 V | 6.737 A | 765.38 W | 765.39 VA | -2.38 VAR | 1.000 | -177.9 m° |

**Figure 50: A larger version of the Numerics table shows the values calculated by the MDA for apparent and reactive power, real power, phase angle and power factor.**

Note that the phase angle is not zero – it is a very small number that is a round-off error in terms of calculating the power factor, but it would seem to indicate that the load is slightly capacitive. We can test this assumption by calculating the power measurements on the fundamental only instead of the full spectrum of the waveform (as set in the Harmonic Filter dialog box in Figure 51). With the Harmonic Filter set to measure power based on the 60 Hz fundamental waveform only, the phase angle is essentially zero and the real power and the apparent power are equal (Figure 51). The visible distortion in the waveforms does have some small measurement impact in this case. The data shows that the bread toaster coils are not purely resistive but have some complex impedance that behaves capacitively at the higher frequencies present in the slightly distorted voltage waveform.

 

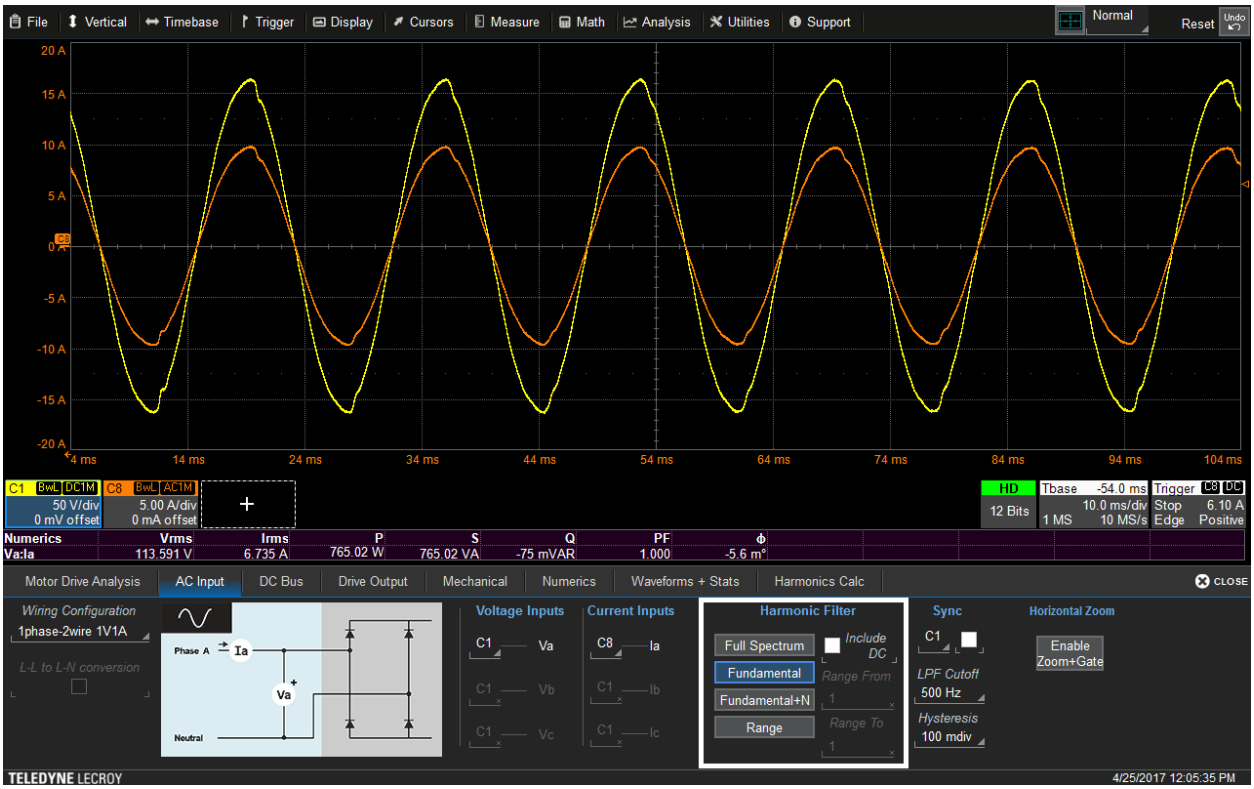


**Figure 51: Voltage and current waveforms with power measured for just the 60-Hz fundamental. Apparent and real power are equal and phase angle is zero. This suggests that the visible distortion in the waveforms is due to some complex impedance in the load at higher frequencies.**

Figure 52 shows a larger version of the Numerics table that is shown at the bottom of Figure 51.

| Numerics | Vrms | Irms | P | S | Q | PF | ϕ |
|---|---|---|---|---|---|---|---|
| Va:Ia | 113.591 V | 6.735 A | 765.02 W | 765.02 VA | -75 mVAR | 1.000 | -5.6 m° |

**Figure 52: A larger version of the Numerics table shown at the bottom of the previous figure.**

 

Further harmonic order analysis reveals significant odd harmonic distortion in the voltage and current signals. Figure 53 shows harmonic order calculations in percentages and spectral displays to the right (because it is always 100%, the fundamental is excluded from the spectral display).


**Figure 53: Harmonic order calculations (as percentages of the fundamental) and spectral displays for the voltage and current waveforms.**

By changing the scaling in the Harmonic Order table to volts and amps (Figure 54), we learn that the value of the fundamental matches the calculated value from Figure 51 and Figure 52.

| Order(ABC) | Va [V] | Ia [A] |
|---|---|---|
| 1 | 113.59 | 6.73 |
| 2 | 0.07 | 0.00 |
| 3 | 0.69 | 0.04 |
| 4 | 0.03 | 0.00 |
| 5 | 0.73 | 0.05 |
| 6 | 0.04 | 0.00 |
| 7 | 0.97 | 0.06 |

**Figure 54: The Motor Drive Analyzer can also display the values of the fundamental and the harmonics in volts and amps.**

## Single-Phase Wiring Configurations

As described above, a single-phase system could contain either two wires (a single current-carrying conductor and a neutral return path, with the voltage referenced to neutral) or three wires (two current-carrying conductors with two voltages, each referenced to the neutral return path). In both cases, voltage is sensed line-neutral.

 

### *One-phase, Two-wire Systems (One Voltage, One Current)*

Figure 55 from Teledyne LeCroy's Motor Drive (Power) Analyzer (MDA) shows the connection schematic diagram indicating the electric utility single-phase AC supply input to a motor drive, represented schematically as a rectifier circuit. The current (Ia) is represented as flowing into the load, and the voltage is probed line-neutral (Va).

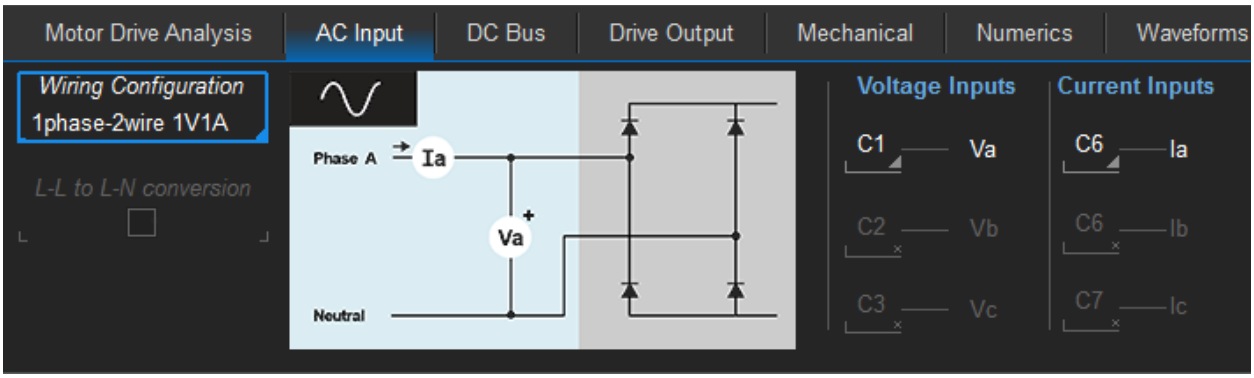


**Figure 55: To aid motor drive analysis, users can designate the connection of the ac supply input to a motor drive, represented schematically as a rectifier circuit. In this case, a single-phase, two wire system feeds power to the motor drive.**

### *One-phase, Three-wire Systems (Two Voltages, Two Currents)*

Figure 56 shows the connection schematic diagram indicating the electric utility single-phase AC supply input to a motor drive, represented schematically as a rectifier circuit. The two currents (Ia and Ib) are represented as flowing into the load, and the two voltages are probed line-neutral (Va and Vb). Note the "+" designation on the Va and Vb elements indicating the polarity of the voltage measurements made at these points (both line-neutral). The total power measurements for the complete system are simply the sum of the separately measured A and B lines.

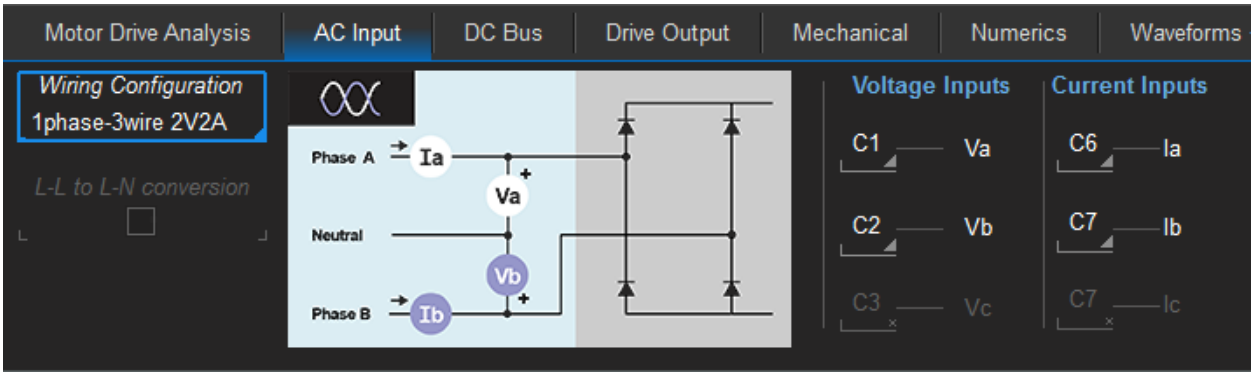


**Figure 56: Here the Motor Drive Analyzer is configured to show the connection of the AC supply input to a motor drive, where a single-phase, three-wire system is used.**

 

## Power Calculations in Three-phase Systems

Extending the power calculations from a single-phase system to a three-phase system is straightforward. In the simplest case for a three-phase AC system, the neutral is present (represented as N in the image below), voltages are sensed line-neutral, and the line currents are measured. If the load is purely resistive, the three-phase line current and voltage vector magnitudes would each be instantaneously multiplied and summed to get the total three-phase power, shown in Figure 57.

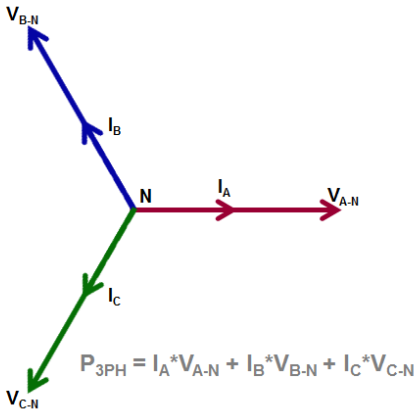


**Figure 57: Vector representation of voltage and current in three-phase system with a purely resistive load. Magnitudes of currents and voltages can be multiplied and summed to calculate three-phase power.**

However, in the case of power consumed by and supplied to non-resistive loads, the phase angle complicates matters. Figure 58 shows an inductive load with current lagging voltage.

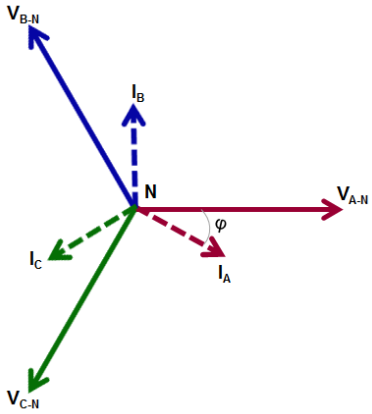


**Figure 58: Vector representation of voltage and current in three-phase system with a non-resistive (inductive) load. In this case, calculation of three-phase power becomes more complex.**

In this case, real (P), reactive (Q), and apparent (S) power must be computed on each phase and summed to get the total three-phase power, as shown in Figure 59.

 

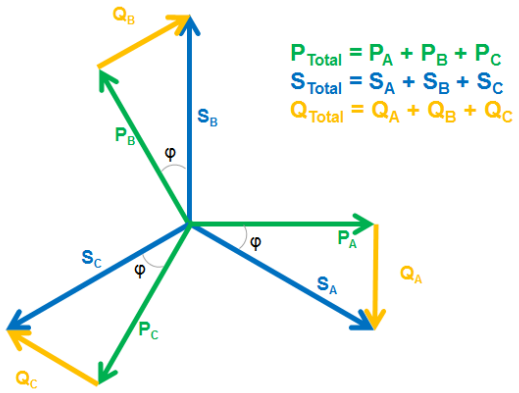


**Figure 59: In a three-phase system with a non-resistive load, the three forms of power (real, reactive and apparent) must be calculated for each phase and then summed.**

The above cases show various power calculations based on an accessible neutral for voltage reference. However, the neutral may not be accessible, requiring line-line voltage sensing, or line-line voltage sensing may be preferred. Line-neutral voltage sensing is not possible on a delta winding because there is no neutral accessible.

Additionally, there are ways to perform total three-phase power calculations by using only two of the three line-line voltages and two of the three line currents (four signals total). Therefore, fewer signals are required, we conserve valuable inputs on measurement instruments, and other measurements may become possible (such as efficiencies or cross-correlation to other system signals).

Thus, there are several different techniques for measuring power in a three-phase system, and it pays to understand them and the results they provide. However, no technique is inherently better or worse or more accurate than others are (with some minor exceptions).

### *Four-wire Wye-connected Systems: Line-Neutral Voltage Sensing*

For a three-phase system in which the neutral is present and voltages can be sensed line-neutral, then the sum of the single-phase calculations for the three-phase system provides the total three-phase power (real, reactive, and apparent).

Figure 60 shows a three-phase Wye-connected coil with an accessible neutral. This is referred to as a three-phase, four-wire system. Note that we are no longer representing current and voltage vectors in the figure, but rather showing a simplified schematic with probe sensing locations and/or the positive polarity of the measured RMS value.

 

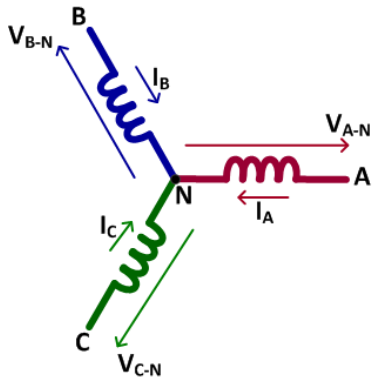


Figure 60: Three-phase Wye-connected coil with an accessible neutral.

Note: The figure above shows the convention of line currents traveling into the coil towards the neutral. This would be typical of a coil within a machine (e.g., a motor) that consumes power. However, at any given time, some of these currents are flowing out of the neutral (in the opposite direction shown), because the currents at neutral must sum to zero. Additionally, even though it would appear from the directions shown that power is negative (because the voltage polarity is opposite that of the current polarity), the power measurement system typically calculates positive power.

In this case, we measure the voltages across the same coil through which the currents are traveling, identically to the vector-based power calculation examples provided above. This is known as a three-wattmeter, four-wire method for power calculations using three voltage and three current signals, and it is an ideal method to use if there is suspicion that the load is unbalanced because per-phase values for power (real, apparent, and reactive) can be calculated from direct voltage and current measurements in each winding.

Figure 61 from Teledyne LeCroy's Motor Drive Analyzer shows the connection schematic diagram indicating the electric utility three-phase AC supply input to a motor drive, represented schematically as a rectifier circuit. . The three currents (Ia, Ib, and Ic) are represented as flowing into the load, and the three voltages are probed line-neutral (Va, Vb, and Vc). Note the "+" designation on the Va, Vb, and Vc elements indicating the polarity of the voltage measurements made at these points (both line-neutral).

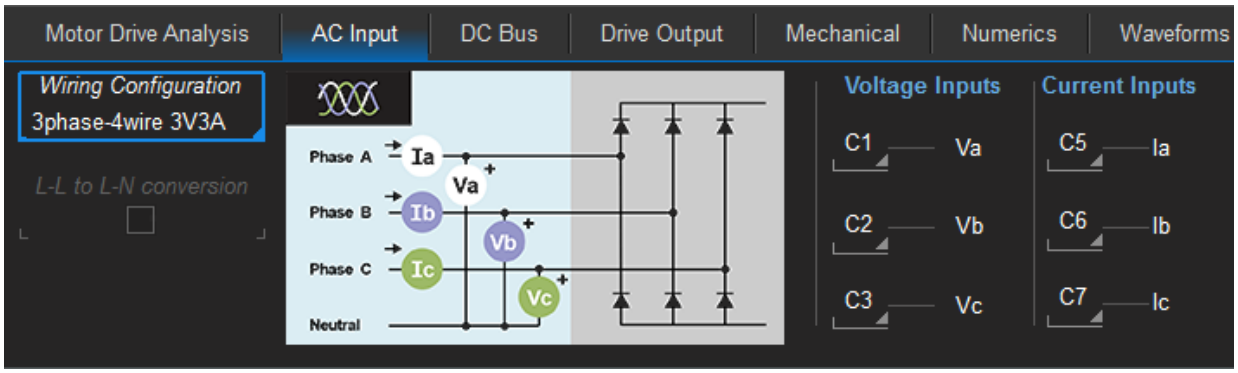


Figure 61: Three-phase, four-wire AC input to a motor drive represented as a rectifier circuit in Teledyne LeCroy's MDA.

 

The eight input channels of the Motor Drive Analyzer facilitate capture of the three voltage and three current signals. Channels 1 (yellow), 2 (magenta), and 3 (cyan, or light blue) on the left side display the $V_{A\text{-}N}$, $V_{B\text{-}N}$, and $V_{C\text{-}N}$ line-neutral voltages respectively, and Channels 5 (light green), 6 (purple) and 7 (red) display the IA, IB, and IC line currents, respectively, shown in Figure 62.


**Figure 62: Measurement of voltage and current signals for a three-phase, four-wire AC input to a motor drive.**

Note that this is a 480 V, three-phase input to a 1990s vintage motor drive and the motor it is powering is not under any load. We observe some distortion in the line current input signals due to the nature of the load, but the sinusoidal nature of these signals is evident.

If the line-neutral voltage signals are placed on the same display grid as the corresponding line current signal, it will be easy to visually observe the phase relationship. At the same time, we may use the built-in three-phase power analysis capabilities in the Motor Drive Analyzer to calculate voltage and current; real, apparent, and reactive power; and power factor and phase angle, as shown in the image below:

 

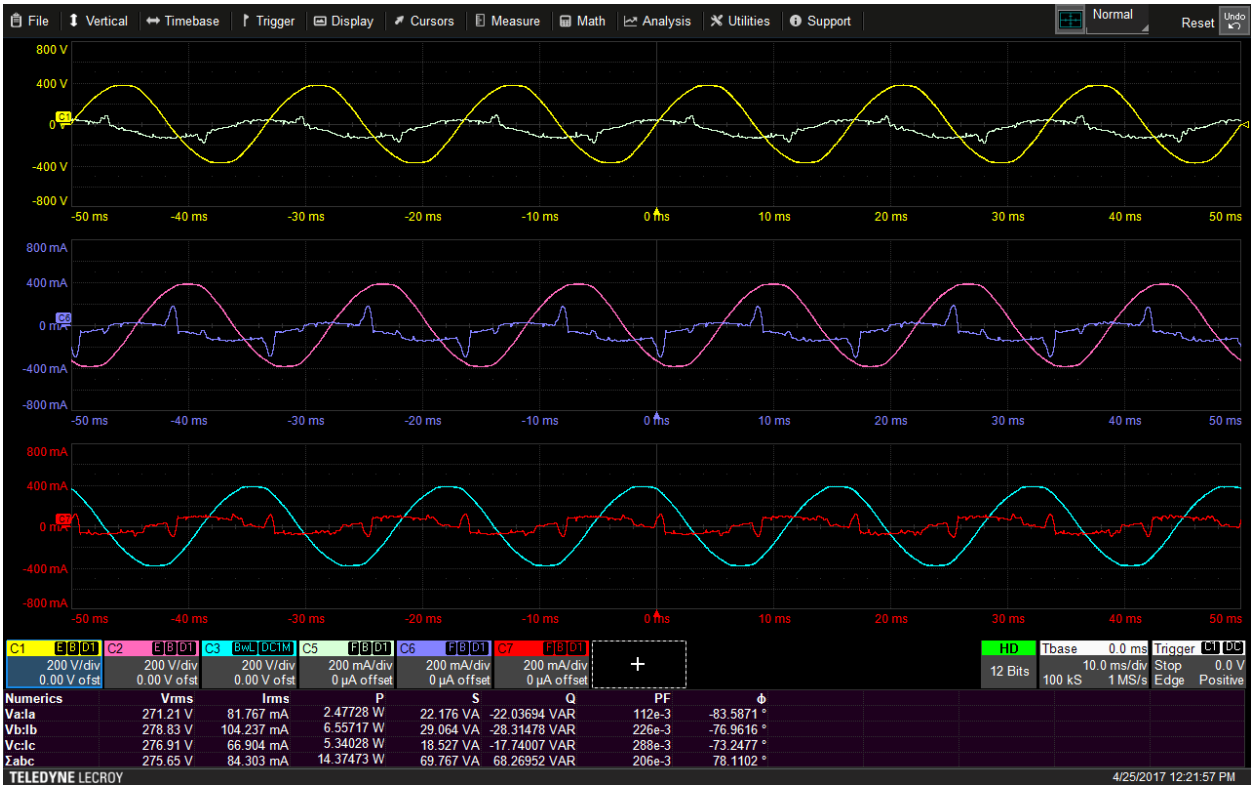


**Figure 63: Displaying voltage and current measurements for each of the three phases concurrently on the same time scale reveals the phase relationships between these signals. These measurements are performed under a no-load condition (the motor drive is off). The associated power parameters calculated by the MDA are shown in the Numerics table in the lower left of the image.**

A larger view of the Numerics table is shown in Figure 64.

| Numerics | Vrms | Irms | P | S | Q | PF | Φ |
|---|---|---|---|---|---|---|---|
| Va:Ia | 271.21 V | 81.767 mA | 2.47728 W | 22.176 VA | -22.03694 VAR | 112e-3 | -83.5871 ° |
| Vb:Ib | 278.83 V | 104.237 mA | 6.55717 W | 29.064 VA | -28.31478 VAR | 226e-3 | -76.9616 ° |
| Vc:Ic | 276.91 V | 66.904 mA | 5.34028 W | 18.527 VA | -17.74007 VAR | 288e-3 | -73.2477 ° |
| Σabc | 275.65 V | 84.303 mA | 14.37473 W | 69.767 VA | 68.26952 VAR | 206e-3 | 78.1102 ° |

**Figure 64: A larger view of the Numerics table from the previous figure.**

Note that the three line-neutral voltages average out to 275.65 V (close to the expected 277 V), and the line-neutral voltages are balanced within a couple of percent. The three-phase power values are not balanced in all three phases because this is a no-load situation with very low levels of current. Therefore, any small imbalance in the motor will be more apparent under a no-load condition.

The total three-phase power values are the sum of the per-phase power values. The load is capacitive, as can be seen in the line-neutral voltage and line current waveform phase relationships (the current is leading the voltage). This is expected, because the input supplies a large DC filter and energy-storage capacitor in this drive. Therefore, we show the per-phase reactive power (Q) values as negative, as is the phase angle (ϕ). The power factor is also fairly low. Again, this is expected because power factors for equipment like this usually increase with load.

 

Figure 65 shows a load applied to the connected motor (in this case, an ~2 N·m load from the dynamometer). With the load, the current consumption on all three phases increases, as does the distortion of the input current waveform (the drive load is very non-linear), the power factor improves (increases) and the phase angle decreases. Note that there is still significant imbalance of current and power across all three phases, even with a load. Note that the applied load is only about 10% of the rated load. If the motor was loaded to 100%, three-phase balance and power factor would likely improve more.

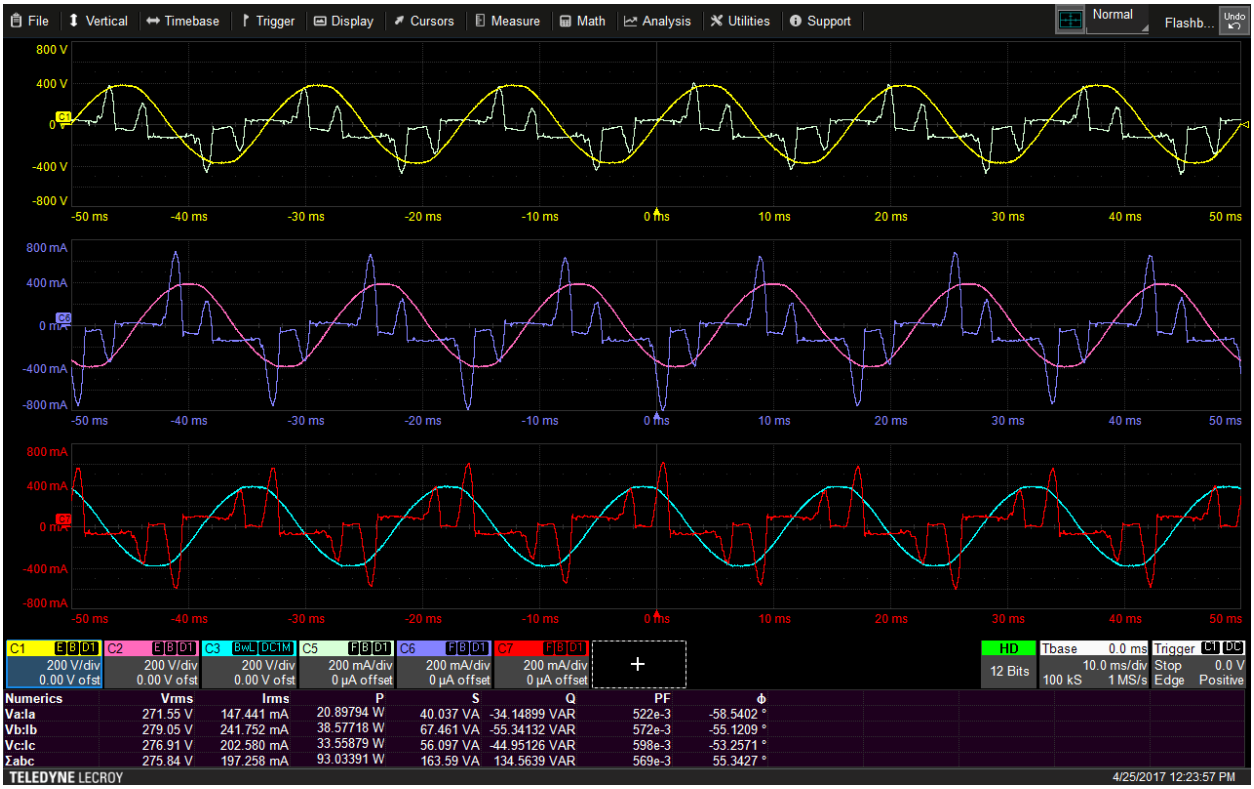


**Figure 65: Voltage and current measurements for the motor drive with the drive energized and the motor loaded at 10%. Compared with the motor drive off measurements, there is greater distortion of input current waveforms, while power factor is higher and phase angle between voltage and current is lower.**

Figure 66 shows a larger view of the Numerics table.

| Numerics | Vrms | Irms | P | S | Q | PF | Φ |
|---|---|---|---|---|---|---|---|
| Va:Ia | 271.55 V | 147.441 mA | 20.89794 W | 40.037 VA | -34.14899 VAR | 522e-3 | -58.5402 ° |
| Vb:Ib | 279.05 V | 241.752 mA | 38.57718 W | 67.461 VA | -55.34132 VAR | 572e-3 | -55.1209 ° |
| Vc:Ic | 276.91 V | 202.580 mA | 33.55879 W | 56.097 VA | -44.95126 VAR | 598e-3 | -53.2571 ° |
| Σabc | 275.84 V | 197.258 mA | 93.03391 W | 163.59 VA | 134.56390 VAR | 569e-3 | 55.3427 ° |

**Figure 66: A larger view of the Numerics table.**

We calculate the same measurement data with the waveforms harmonically filtered to only include the fundamental frequency component (as described in a later section ***Selective Software-based DFT Digital Harmonic Filter***) and show this result in Figure 67. We see essentially the same $V_{RMS}$ calculation, $I_{RMS}$ values reduced by a third, nearly the same real power P, and lower apparent power S. The reactive power Q, the power factor PF, and the phase angle ϕ all substantially change. While this may be

 

counter-intuitive, this is all as expected given the lower levels of harmonic distortion in the voltage signals, the moderate level of distortion in the current signals (despite their visual appearance), and the low impact of the current harmonics on the real power calculation given the low level of voltage harmonics. Likewise, with the lower $I_{RMS}$ calculations, a lower apparent power (S) calculation is expected, and from the lower apparent power, the reactive power (Q), power factor (PF), and phase angle (ϕ) all change significantly. The calculation methods are as described earlier in the section ***Power Used (Supplied and Consumed) by Non-Linear, Non-Resistive Loads.***

| Numerics | Vrms | Irms | P | S | Q | PF | ϕ |
|---|---|---|---|---|---|---|---|
| Va:Ia | 271.38 V | 97.772 mA | 20.78657 W | 26.533 VA | -16.48616 VAR | 783e-3 | -38.4302 ° |
| Vb:Ib | 278.89 V | 157.084 mA | 38.67887 W | 43.809 VA | -20.56694 VAR | 883e-3 | -28.0039 ° |
| Vc:Ic | 276.77 V | 119.428 mA | 32.82864 W | 33.054 VA | -3.85300 VAR | 993e-3 | -6.6924 ° |
| Σabc | 275.68 V | 124.761 mA | 92.29408 W | 103.40 VA | 46.60497 VAR | 893e-3 | 26.7962 ° |

Figure 67: The Numerics table re-calculated based on only the fundamental frequency of the applied data.

### *Three-wire Wye-connected Systems: Line-Line Voltage Sensing (3 Voltages, 3 Currents)*

If the neutral is not accessible for probing, or if voltage is measured line-line and not line-neutral, the measurement becomes more complex. In Figure 68 we show the voltages measured line-line whereas the currents are measured line-neutral.

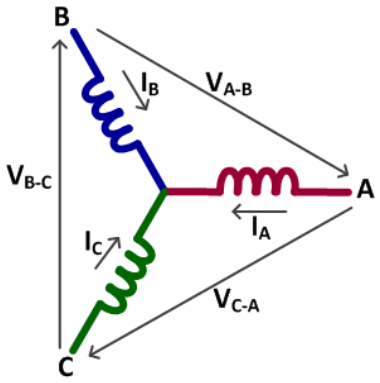


Figure 68: Three-phase Wye-connected coil where the neutral is not accessible.

Figure 69 from Teledyne LeCroy's Motor Drive Analyzer shows the connection schematic diagram indicating the electric utility three-phase AC supply input to a motor drive, represented schematically as a rectifier circuit. The three currents (Ia, Ib, and Ic) are represented as flowing into the load, and the three voltages are probed line-line (Vab, Vbc, and Vca). Note the "+" designation on the Vab, Vbc, and Vca elements indicating the polarity of the voltage measurements made at these points, and note specifically in Figure 68 and Figure 69 that the third line-line voltage is referenced from C to A phase.

 

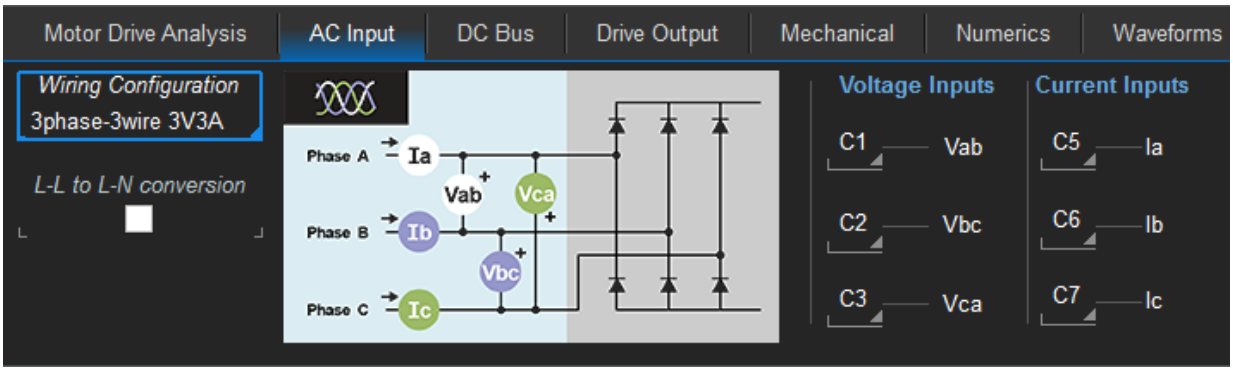


**Figure 69: Three-phase, three-wire AC input to a motor drive represented as a rectifier circuit in Teledyne LeCroy's MDA. In this case voltages are measured line-to-line.**

The eight input channels of the Motor Drive Analyzer facilitate capture of the three voltage and three current signals. Figure 70 shows channels 1 (yellow), 2 (magenta), and 3 (cyan, or light blue) capturing the $V_{A\text{-}B}$, $V_{B\text{-}C}$, and $V_{C\text{-}A}$ line-line voltages, respectively; and Channels 5 (light green), 6 (purple), and 7 (red) display the $I_A$, $I_B$, and $I_C$ line currents, respectively. We again use the built-in three-phase power analysis capabilities in the Motor Drive Analyzer to calculate voltage and current; real, apparent, and reactive power; and power factor and phase angle for the three-phase system as shown at the bottom of Figure 70.

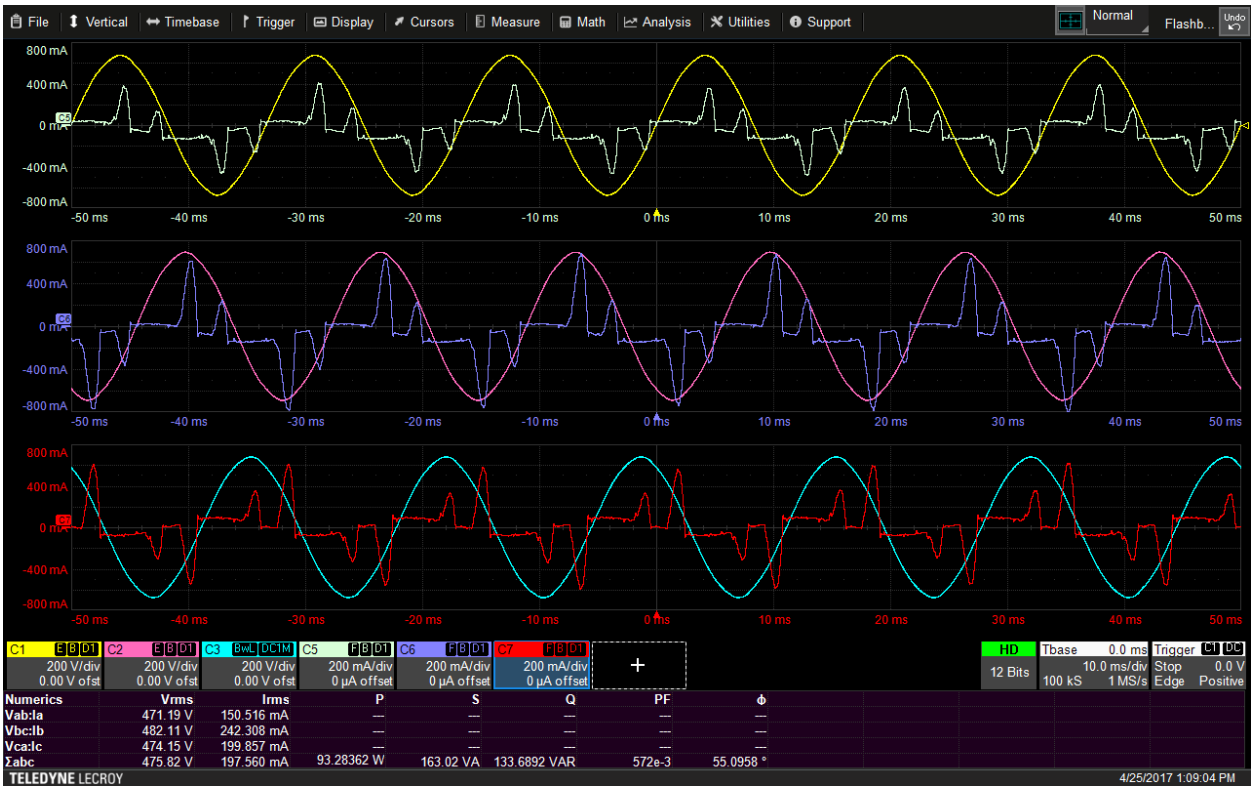


**Figure 70: Voltage and current measurements for the motor drive in with the drive energized and the motor loaded at 10%. The measured line currents are close to those measured in the four-wire case but the line-line voltage signals are larger in magnitude and are phase-shifted by 30°.**

 

Again, this is a 480 V, three-phase input to a 1990s vintage motor drive with a load applied to the connected motor (in this case, an ~2 N·m load from the dynamometer). The measured line currents essentially match those measured in the previous case, but the voltage signals are of higher amplitude and are phase-shifted by 30°.

We show a larger view of the Numerics table in Figure 71.

| Numerics | Vrms | Irms | P | S | Q | PF | ϕ |
|---|---|---|---|---|---|---|---|
| Vab:Ia | 471.19 V | 150.516 mA | --- | --- | --- | --- | --- |
| Vbc:Ib | 482.11 V | 242.308 mA | --- | --- | --- | --- | --- |
| Vca:Ic | 474.15 V | 199.857 mA | --- | --- | --- | --- | --- |
| Σabc | 475.82 V | 197.560 mA | 93.28362 W | 163.02 VA | 133.68920 VAR | 572e-3 | 55.0958 ° |

Figure 71: A larger view of the Numerics table shown in the previous figure.

Note that while voltage and current RMS values can be calculated on all three measurement phases, we display only total three-phase power because the voltage and current vectors are out of phase. Thus, calculation of individual phase power values is impossible. However, given that the three voltages, whether probed line-line or line-neutral, must always vector sum to zero, one may transform both the magnitude and phase to convert the line-line voltages to a line-neutral voltage at a virtual neutral point, as shown in Figure 72.

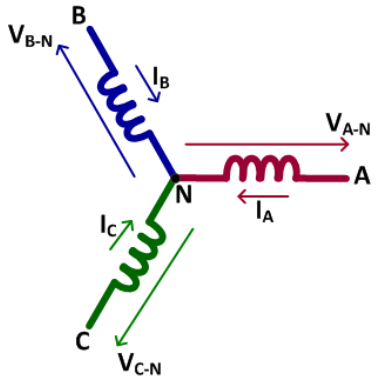


Figure 72: Three-phase Wye-connected coil. Given that the three voltages must always vector sum to zero, line-to-line voltages may be transformed to line-to-neutral voltages at a "virtual" neutral point, which ultimately makes it possible to calculate phase power values.

These transformed line-neutral voltages are then used to calculate power as in the three-phase, four-wire Wye-connected Line-Neutral voltage sensed case above. This is known as "Line-Line to Line-Neutral Conversion." Performed by the Motor Drive Analyzer, this converts both the voltage vector magnitude and phase (as shown in Figure 73 with the "checkbox" selection for L-L to L-N conversion):

 

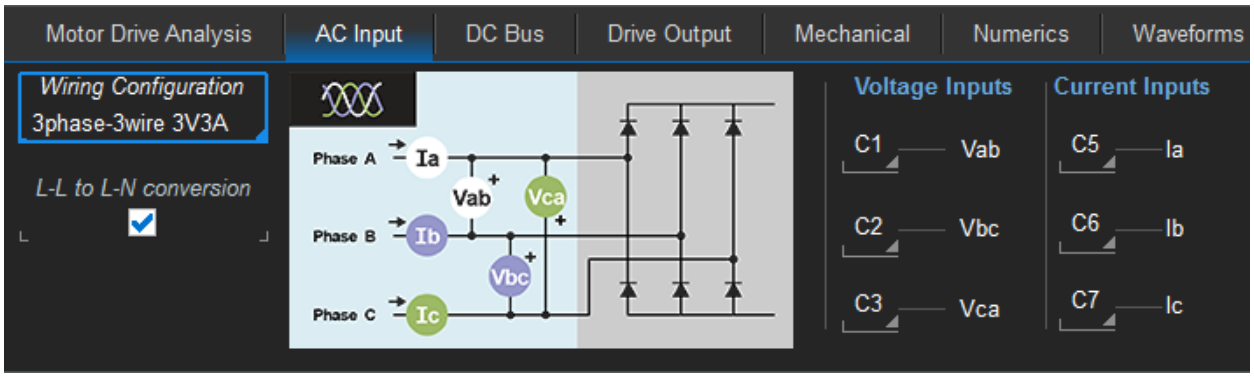


Figure 73: The MDA is configured to convert the sensed line-to-line voltages to their line-to-neutral equivalents.

Then power calculations are made on each individual phase, as in the three-phase, four-wire configuration described earlier, shown in Figure 74.

| Numerics | | Vrms | Irms | P | S | Q | PF | ϕ |
|---|---|---|---|---|---|---|---|---|
| Va:Ia | LL to LN | 270.28 V | 150.516 mA | 21.08219 W | 40.681 VA | -34.79045 VAR | 518e-3 | -58.7911 ° |
| Vb:Ib | LL to LN | 276.08 V | 242.308 mA | 39.16566 W | 66.897 VA | -54.23177 VAR | 585e-3 | -54.1637 ° |
| Vc:Ic | LL to LN | 276.62 V | 235.773 mA | 32.54526 W | 65.220 VA | -56.51842 VAR | 499e-3 | -60.0640 ° |
| Σabc | LL to LN | 274.33 V | 209.532 mA | 92.79311 W | 172.80 VA | 145.76518 VAR | 537e-3 | 57.5207 ° |

Figure 74: The Numerics table showing phase power calculations after the MDA's line-line to line-neutral conversion of the voltages.

Note that to enforce the vector sum to zero, the phase C current values are adjusted — the larger the imbalance (which is considerable in this case), the larger the adjustment of the C phase's current value. While the real power (P) calculation after L-L to L-N conversion for the total three-phase system remains essentially the same, the apparent power (S), reactive power (Q), power factor (PF), and phase angle (ϕ) calculations for the three-phase system differ, primarily due to the system imbalance.

When we then apply a fundamental frequency harmonic filter (as previously described) and display the Numerics table (Figure 75), we can see that the results match very closely with the previous four-wire example. They don't match exactly because this is a different set of acquisition data taken at a later time with a similar but not identical load.

| Numerics | | Vrms | Irms | P | S | Q | PF | ϕ |
|---|---|---|---|---|---|---|---|---|
| Va:Ia | LL to LN | 270.26 V | 99.973 mA | 20.82845 W | 27.019 VA | -17.20585 VAR | 771e-3 | -39.5711 ° |
| Vb:Ib | LL to LN | 276.06 V | 157.590 mA | 38.81214 W | 43.505 VA | -19.64951 VAR | 892e-3 | -26.8556 ° |
| Vc:Ic | LL to LN | 276.60 V | 117.442 mA | 32.19660 W | 32.485 VA | -4.31121 VAR | 991e-3 | -7.6265 ° |
| Σabc | LL to LN | 274.31 V | 125.002 mA | 91.83720 W | 103.01 VA | 46.64648 VAR | 892e-3 | 26.9314 ° |

Figure 75: The Numerics table showing calculated values with the Harmonic filter set to Fundamental frequency only.

### *Three-phase, Three-wire Delta-connected Systems*

In a delta winding, the neutral is not accessible for probing, so voltage must be measured line-line. Again, the three voltages must vector sum to zero, so we may transform the line-line voltages to line-neutral voltages.

However, the line currents into the winding are terminal currents, not coil currents – the terminal currents could flow into either coil adjacent to the terminal connection (Figure 76). While this poses no problem for calculating total three-phase power, we do not directly measure the power in each individual coil because there is no direct measurement of the current flowing through the coil.

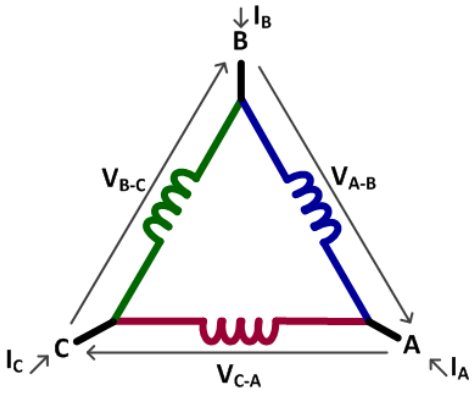


**Figure 76: Three-phase, three-wire delta-connected system. The sensed currents are terminal currents rather than coil currents, so power in individual coils may not be measured directly.**

### *Three-phase, Three-wire Wye- or Delta-connected Systems: Two Wattmeter Method*

In cases where a neutral point is not available (e.g., a delta winding, or an inaccessible neutral in a wye winding), or one wants to conserve input channels for other measurements, the best alternative is the two-wattmeter method. The two-wattmeter method utilizes two line-line voltage measurements to a common line reference (e.g., line C) with two-line current measurements (lines A and B) that do not include the current flowing into the line voltage reference (e.g., phase C).

It can be mathematically proven that this method returns the same calculated total three-phase power (real, apparent, and reactive) value(s) as the three-wattmeter method. However, because there is disassociation of the normal phase relationships between the voltage and current signals, the calculated per-phase power values for the two measured phases will not represent the coil powers, though they will correctly sum to the total three-phase power. Figure 77 shows these measured signals.

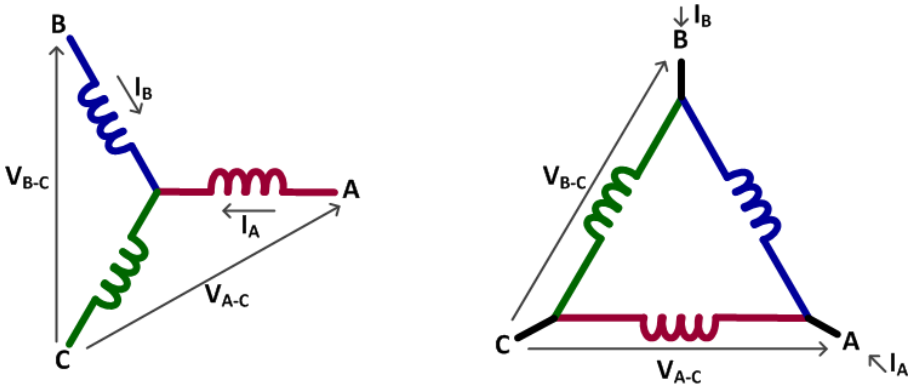


**Figure 77: Three-phase, three-wire wye-connected system (left) and delta connected system (right) showing voltages and currents sensed using the two-wattmeter method.**

 

Figure 78 from Teledyne LeCroy's Motor Drive Analyzer shows the connection schematic diagram indicating the electric utility three-phase AC supply input to a motor drive, represented schematically as a rectifier circuit. The two currents (Ia and Ib) are flowing into the load, and the two voltages are measured line-line (Vac and Vbc). Note the "+" designation on the Vac and Vbc elements, which indicate the polarity of the voltage measurements made at these points. Also, note specifically in Figure 77 and Figure 78 that the first line-line voltage is referenced from A line to C line (which is different from the earlier line-line voltage sensing case in which all three voltages and all three currents were measured).

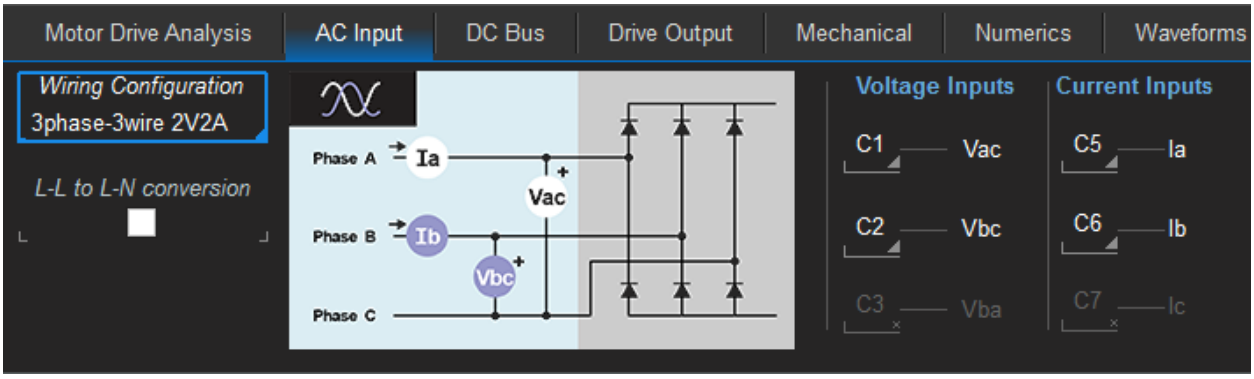


**Figure 78: Three-phase, three-wire AC input to a motor drive represented as a rectifier circuit. In this case two voltages are measured line-to-line and only two currents are measured in keeping with the two-wattmeter method.**

Figure 79 shows the signal capture, motor load, and display of Numerics calculations.


**Figure 79: Voltage and current measurements for the motor drive illustrating the two-wattmeter method.**

 

Figure 80 shows a larger view of the Numerics table.

| Numerics | Vrms | Irms | P | S | Q | PF | ϕ |
|---|---|---|---|---|---|---|---|
| Vac:Ia | 468.84 V | 147.482 mA | 15.98435 W | 69.146 VA | -67.26990 VAR | 231e-3 | -76.6393 ° |
| Vbc:Ib | 482.18 V | 245.540 mA | 77.48008 W | 118.40 VA | 89.52156 VAR | 654e-3 | 49.1250 ° |
| Σabc | 475.51 V | 196.511 mA | 93.46443 W | 162.42 VA | 132.8241 VAR | 575e-3 | 54.8694 ° |

**Figure 80: A larger view of the Numerics table showing voltage and current measurements and the associated power calculations.**

Note that these voltage and current pairs do not represent a phase or coil measurement of power because the voltage and current vectors are not correctly associated. Thus, it is impossible to draw any conclusions from a visual inspection of the voltage and current waveform pair calculations. However, the total three-phase power does sum correctly from these two calculated values.

Figure 81 compares the vector diagrams of the voltage and current associations used in the two-wattmeter method (Figure 81, left) and the three-wattmeter method using line-neutral voltage references (Figure 81, right).

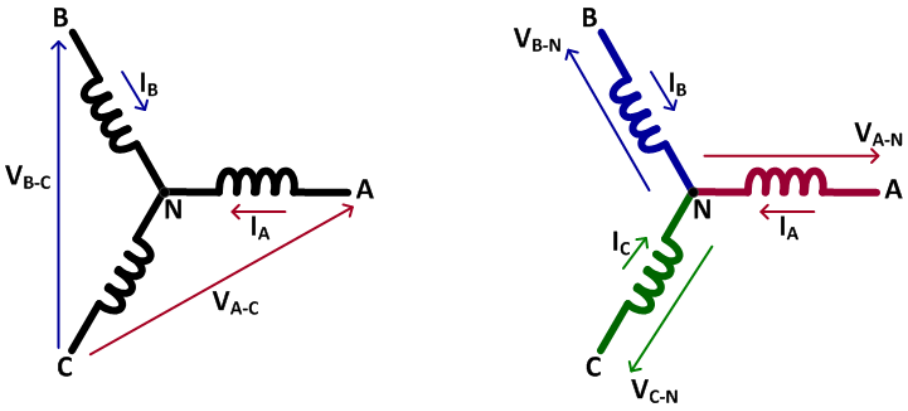


**Figure 81: Vector diagrams for three-phase, Wye-connected systems compare the voltage and current measurements performed using the two-wattmeter method (left) versus the three-wattmeter method (right).**

In the two-wattmeter method, a line-line voltage is associated with a line current in each of the two wattmeters ("blue" and "red" voltage and current pairs). In the three-wattmeter diagram on the right, a line-neutral voltage is associated with a line-neutral current in each of the three wattmeters. If the system is balanced, then the total three-phase wattmeter calculations will be the same in each case.

We may also perform a line-line to line-neutral conversion on the data acquired for the two-wattmeter method. We can then calculate a per-phase value for each of the three phases, again assuming a balanced three-phase system. Figure 82 shows these Numerics table calculations.

| Numerics | | Vrms | Irms | P | S | Q | PF | ϕ |
|---|---|---|---|---|---|---|---|---|
| Va:Ia | LL to LN | 270.22 V | 147.482 mA | 20.85228 W | 39.853 VA | -33.96128 VAR | 523e-3 | -58.4539 ° |
| Vb:Ib | LL to LN | 277.94 V | 245.538 mA | 39.86112 W | 68.245 VA | -55.39257 VAR | 584e-3 | -54.2614 ° |
| Vc:Ic | LL to LN | 274.79 V | 236.366 mA | 32.75037 W | 64.951 VA | -56.08737 VAR | 504e-3 | -59.7185 ° |
| Σabc | LL to LN | 274.32 V | 209.796 mA | 93.46377 W | 173.05 VA | 145.63413 VAR | 540e-3 | 57.3096 ° |

**Figure 82: The Numerics table showing calculated values of current and power produced by the two-wattmeter method with line-line to line-neutral conversion on the data.**

 

When we apply the fundamental frequency harmonic filter, we obtain results similar to that of the four-wire and three-wire three-wattmeter methods, as shown in Figure 83.

| Numerics | | Vrms | Irms | P | S | Q | PF | ϕ |
|---|---|---|---|---|---|---|---|---|
| Va:Ia | LL to LN | 270.20 V | 98.590 mA | 20.64137 W | 26.639 VA | -16.83581 VAR | 775e-3 | -39.2098 ° |
| Vb:Ib | LL to LN | 277.92 V | 159.625 mA | 39.52015 W | 44.363 VA | -20.15379 VAR | 891e-3 | -27.0205 ° |
| Vc:Ic | LL to LN | 274.77 V | 118.866 mA | 32.44737 W | 32.661 VA | -3.70725 VAR | 993e-3 | -6.5288 ° |
| Σabc | LL to LN | 274.30 V | 125.693 mA | 92.60890 W | 103.66 VA | 46.57264 VAR | 893e-3 | 26.7029 ° |

**Figure 83: The Numerics table showing calculated two-wattmeter method values with line-line to line-neutral conversion and fundamental frequency harmonic filtering applied.**

# Power Conversion

## Introduction

The preceding sections have discussed the various winding configurations associated with single-phase and three-phase electrical systems, defined the associated electrical parameters (voltage, current and power) and demonstrated how to measure these parameters using Teledyne LeCroy's Motor Drive Analyzer. These definitions and measurements are essential knowledge for evaluating a motor drive's performance.

Many of the measurements discussed were performed at the input to a motor drive. In this section, we begin to look inside the motor drive to understand its operation by introducing the power semiconductors (also referred to as *power switches*) that control the flow of power to the drive. This section on power semiconductor device physics will be a review for most power electronics engineers. However, for those new to the motor drive field, this section lays the groundwork for a discussion of the power conversion topologies and circuits discussed in subsequent parts of this series.

## Drives and Other Power Converters

Power conversion is the conversion of electric power from one form of power (AC or DC) to another (AC or DC), from one voltage to another, from one frequency to another, or some combination of these conversions. This primer is mainly concerned with one very specific type of power converter – the motor drive.

Typically, the term drive refers to any power converter that transforms one ac or dc line voltage to a different ac voltage or frequency. Motor drives, variable frequency drives, variable speed drives, and inverter drives are all different ways to say the same thing. Drives are sometimes used in non-motor applications such as converting the voltage or frequency produced by a wind turbine.

In addition to drives, there are power converters that perform AC-DC, DC-AC and DC-DC conversions as outlined in Table 2. While these power converter categories are beyond the scope of this primer, there are many design techniques and issues that are common across the different power converter categories. Therefore, much of the material discussed in this primer will be relevant to designers of other power converter types. That includes the discussion that follows on power semiconductors, which are the basic "building blocks" of any power conversion and drive system.

| Type | Function | Examples |
|---|---|---|
| AC-AC | Conversion of AC line voltage to a different ac voltage or frequency. This is commonly referred to as a "drive." | Motor drives, variable frequency drives (VFDs), variable speed drives (VSDs) and inverter drives. |
| AC-DC | Conversion of AC line voltage to a specified dc voltage. Commonly referred to as a "converter," "power supply" or "AC adapter." | Internal and external power supplies for computing and other electronic equipment. |

| | | |
|---|---|---|
| DC-AC | Conversion of DC voltage to a specified AC voltage and frequency. Commonly referred to as an “inverter”. | Inverters used in automotive and other mobile applications as well as solar power inverters. These could also be motor drives (e.g., a battery-powered drill or electric vehicle propulsion motor drive). |
| DC-DC | Conversion of DC voltage to a different specified DC voltage. Commonly referred to as a “DC-DC converter”. | Includes isolated and nonisolated DC-DC converters used in computing, telecom, networking and many other applications. |

Table 2: Power converter types.

For our purposes, power conversion involves use of fast power semiconductor devices as “switching” devices to enable efficient conversion. In most applications, these devices run at typical switching frequencies from 1 to 100 kHz. In this context, we do not consider a 50/60 Hz core/coil device, such as a line frequency step-up or step-down transformer, to be a power conversion device.

## Power Semiconductor Device Operation

One may consider a power semiconductor device, as used in a power conversion system, as a very fast switch with the following characteristics:

- A rated “withstand” (blocking) voltage that is the maximum open-circuit voltage
- A current-carrying capability
- Low losses when carrying current (low forward voltage drop, or low resistance)
- A fast switching capability (kHz)

Figure 84 shows an insulated-gate bipolar transistor (IGBT) with terminal notations. A metal-oxide semiconductor field-effect transistor (MOSFET) is similar, but has different terminal notations, which are shown in Figure 85.

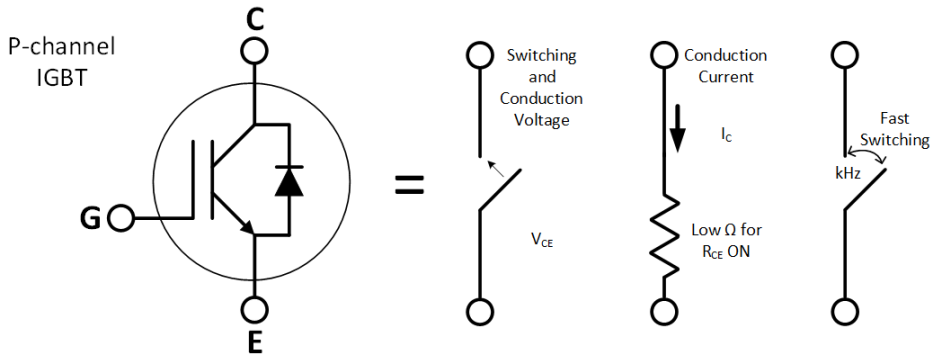


Figure 84: An insulated-gate bipolar transistor (IGBT) with terminal notations.

 

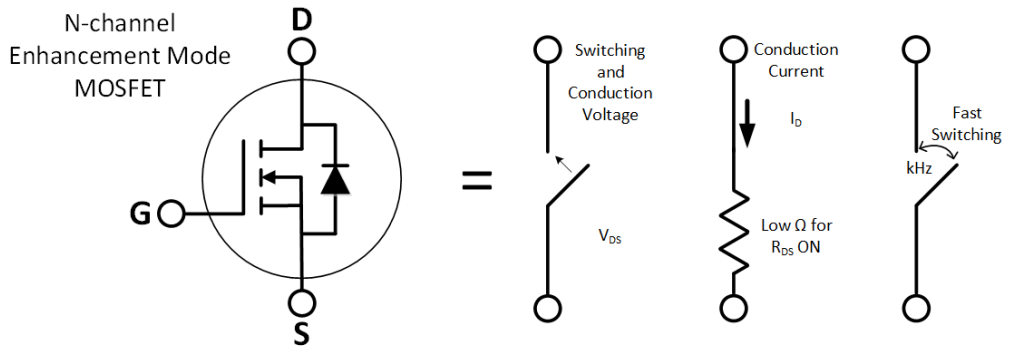


Figure 85: A metal-oxide semiconductor field-effect transistor (MOSFET) with terminal notations.

Applying a voltage from the gate to an IGBT's emitter ($V_{GE}$), or, in a MOSFET, from the gate to the source ($V_{GS}$) controls the device's switching behavior. This voltage is known as the "gate-drive" voltage. Typically, $V_{GE}$ = 0 V (for an IGBT) $V_{GS}$ = 0 V (for a MOSFET) means the power semiconductor is not conducting or is "open".

In power conversion applications, the gate-drive signal is a pulse-width modulated (PWM) unipolar or bipolar signal that switches through a typical 3 to 20 V range, depending on whether it is an IGBT or MOSFET, is Si, SiC, or GaN, and the intended application. When the gate-drive voltage is low, the power semiconductor is "open" from the collector (C) to the emitter (E) (for an IGBT) or from the drain (D) to source (S) (for a MOSFET). When it reaches a switching threshold, it conducts (i.e., the "switch" closes) and conducts a high level of current at the defined biased DC bus voltage.

Figure 86 shows an upper-side gate-drive PWM signal applied at the gate terminal.

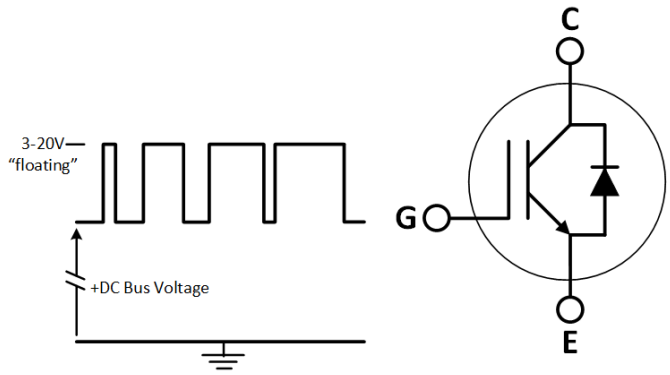


Figure 86: Upper-side gate drive signal for an IGBT.

Note that the power semiconductor device, as implemented in most power-conversion designs, is not referenced to ground potential. The gate-drive signal ($V_{GE}$) and the collector-emitter signal ($V_{CE}$) are therefore "floating" at half or full DC bus voltage (depending on the design), and this could be several hundreds or thousands of volts. Therefore, take care when probing these signals with an oscilloscope and a probe that has a ground reference (e.g., a typical non-isolated oscilloscope and a typical passive probe).

 

For safety's sake, ensure provision of isolation at up to the floating voltage rating in either the oscilloscope or the probe. A high voltage differential probe provides such isolation, though it may not have good enough common-mode rejection ratio (CMRR) to reject in-circuit noise and it may also load the circuit in an undesirable way. A high voltage fiber optically-isolated probe, such as Teledyne LeCroy's HVFO, will provide the best results at high voltages. While some low-voltage power conversion designs (<50 V) with devices referenced to local board ground may be safely probed with an ordinary passive probe and a non-isolated oscilloscope, a high-voltage differential probe may still be desirable for other in-circuit measurements, such as line-line voltage AC input or line-line drive output probing.

When the gate-drive signal is high, current conducts through the power semiconductor. When the gate-drive signal is low, the power semiconductor "switch" opens, blocking current flow.

If the power semiconductor device in this example is supplied with a 170 $V_{DC}$ supply voltage (derived from a 120 Vac single-phase full-wave rectified and filtered line voltage) across $V_{CE}$, then the low-voltage PWM gate-drive signal creates a higher amplitude PWM signal that switches from 0 to 170 $V_{DC}$ at a switching frequency in the kHz range. The gate-drive signal's PWM modulation is determined through a variety of different modulation algorithms programmed into a control system. The PWM gate-drive signal turns the device ON, the device delivers current at the rated DC bus voltage, and then the PWM gate-drive signal turns the device OFF. The device's output voltage is linearly related to the DC bus voltage and the gate-drive pulse width duration (or duty cycle), and the device's output frequency is related to the duty-cycle crossover point (duty cycle reducing to 0%, and then increasing again). If this PWM device output signal were filtered to remove the higher harmonics, the fundamental (rectified) sinewave would be apparent.

Figure 87 shows an example of the output PWM and a representative modulating sinusoid waveform for a single power semiconductor device controlled as described above:

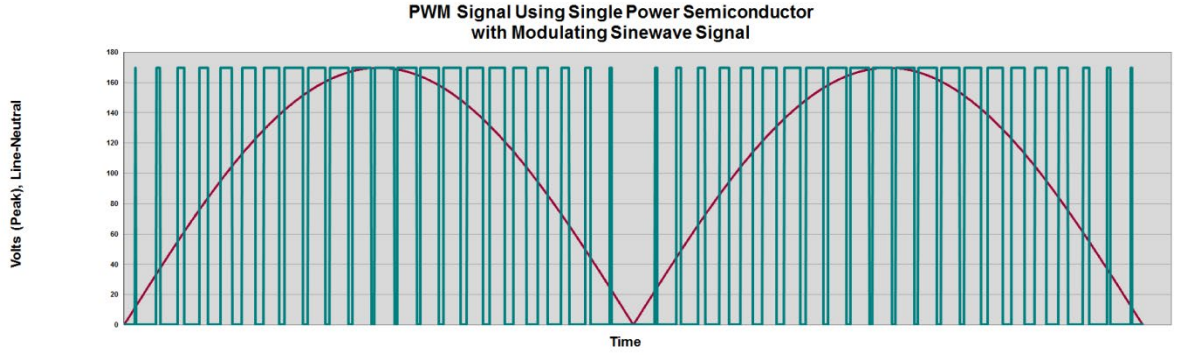


Figure 87: PWM signal using single power semiconductor with modulating (rectified) sinewave signal.

Practically speaking and for various reasons, the output PWM fundamental sinewave's (or rectified fundamental sinewave's) peak voltage never approaches the full DC bus amplitude. For the PWM signal, the peak voltage amplitude is typically 85% (or less) of the DC bus voltage, depending on the modulation and control scheme. For the fundamental AC, the peak amplitude would be much less than shown in the figure above.

 

## N-Channel and P-Channel Devices

Control over the power semiconductor's electrical properties is achieved via addition of dopant impurity materials to the base semiconductor material (e.g., silicon). These additives cause the semiconductor to contain an excess of free current carrying charge carriers. When doped with a material that supplies more free charge-carrying electrons, it is an N-type. When doped with a material that supplies more free charge-carrying holes, it is a P-type. The charge-carrying material defines the "majority carrier" or "channel" of the power semiconductor, and the direction of current flow: thus, we refer to devices as either N-channel or P-channel. However, when we employ MOSFETS in power conversion applications, the lower on-resistance and improved efficiency of N-channel devices makes them a heavy favorite over P-channel devices. For IGBTs, P-channel (minority-carrier) devices are the more efficient of the two. Power -conversion designs are simpler when using a mix of N-channel and P-channel devices, based on circuit location and activity, but it is typically desirable to trade off design complexity for greater overall efficiency by using just one type of device in the entire design.

## Power Semiconductor Device Materials

Power semiconductors are made with silicon (Si), or, more recently, a "wide band-gap" material such as silicon carbide (SiC) or gallium nitride (GaN). Band gap refers to the energy between the conduction and valence bands of the semiconductor material, which is the energy required to generate electron and hole movement. Wider band-gap devices impart useful attributes to a power conversion design, but add cost, design complexity, and EMI/RFI issues. They also may decrease system reliability.

### Silicon (Si)

Traditionally, power semiconductor devices have been based on Si. However, Si has limited blocking voltage when deployed in a (majority-carrier) MOSFET, and $R_{DS\,(ON)}$ increases with blocking voltage, making MOSFETs mostly unsuitable for >500 $V_{DC}$ applications. This generally relegates MOSFETs to 120/240 $V_{AC}$ line-side or lower voltage applications. In (minority-carrier) IGBTs, the blocking voltage is higher (1200 $V_{DC}$ or more) with an approximately constant on-state voltage, but there are significant switching losses and high tail and reverse recovery currents after switching, which reduces the converter's efficiency. This restricts IGBTs mostly to 600 $V_{AC}$ class equipment applications.

### Wide-bandgap Materials

Compared to Si, wide band-gap materials provide higher (breakdown) voltage ratings, faster switching speeds, lower leakage currents at high temperatures, and lower thermal resistance (for SiC). Faster raw device switching speeds translate to rise times in the low-nanosecond range, though deployment in power conversion devices are at much slower speeds to limit harmonics issues and reduce the risk of "shoot-through" (short circuiting, which leads to device failure). The high blocking voltage and higher-temperature performance provides for better reliability and more compact designs and smaller heat sinks. Higher switching frequencies reduce losses during switching and reduce the size of DC bus/link filter components (e.g., capacitors and inductors). Thus, power conversion systems that use wide band-gap power semiconductors have reduced weight, higher power density (due to smaller size) and higher efficiencies.

Design challenges include mitigation of higher manufacturing cost, lack of long-term data on field reliability, a small knowledge base for implementation, and more parasitic and EMI effects in board layout.

SiC and GaN are the two, wide band-gap materials seeing commercial usage in MOSFETs and IGBTs. Compared to Si, SiC has 10X the blocking voltage, lower on-resistance, higher-temperature performance, and greater inherent cooling. We now see more use of SiC in IGBTs, which makes possible 15kV devices for utility applications, opening new applications for solid-state distribution transformers and other utility grid-connected equipment in the 15 kV class. GaN has performance similar to SiC, but breakdown voltages that will likely limit their use to 120/240 $V_{AC}$ line-side and/or <500 $V_{DC}$ applications.

With the advent of wide band-gap materials, rise times are becoming faster and switching losses are falling in power conversion designs. However, faster rise times increase the risk of catastrophic failure and produce more EMI/RFI emissions. In general, the wide band-gap materials' faster rise times impact the switching and conduction-loss measurements for individual devices more than the overall drive system output. While it is helpful to fully understand a power semiconductor device's capabilities, it may often be prudent not to push these devices to their limits in a power conversion system for reasons of cost, reliability, and emissions.

## Power Semiconductor Device Types

One may construct a power conversion circuit using a variety of power semiconductor device types, depending on the input/output voltages, surge power ratings, continuous power ratings, and application.

The main types of power semiconductor devices in use today are:

- Power metal-oxide-semiconductor field-effect transistor (Power MOSFET)
- Insulated-gate bipolar transistor (IGBT)
- High voltage (HV) IGBT
- Integrated gate-commutated thyristor (IGCT) or gate-turn-on thyristor (GTO)
- Silicon-controlled rectifier (SCR, or thyristor)

Figure 88 describes the tradeoffs in switching frequency, breakdown voltage, and current-carrying capability between different silicon power semiconductor devices:

 

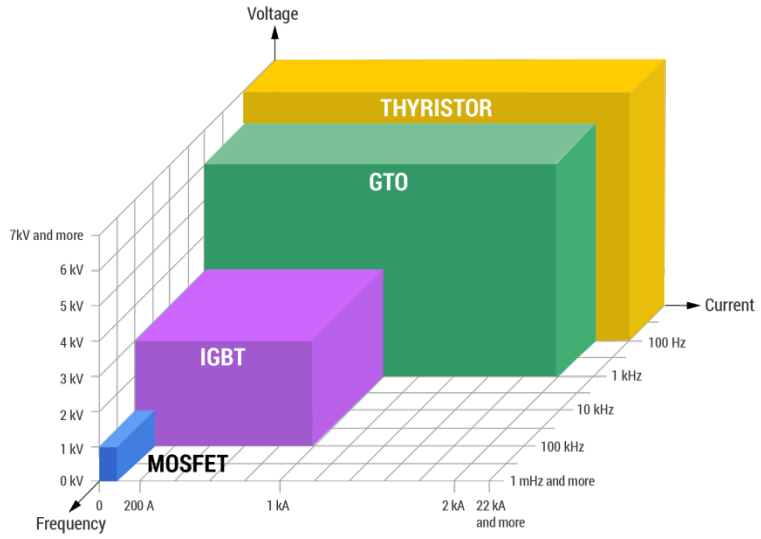


**Figure 88: Comparing breakdown voltage, switching frequency and current-carrying capability of silicon power switches.**

Wide-bandgap materials (SiC and GaN) are attractive because they expand the application range of MOSFETs and IGBTs and incur lower switching losses (if implemented at maximum capabilities). Wide-bandgap devices alter the tradeoffs shown above.

## Power MOSFETs

Power MOSFETs made of Silicon have blocking voltage ratings up to 600 $V_{DC}$ and are used for switching voltages at roughly 500 $V_{DC}$ or less. Although current-carrying capability is in the tens of Amps, paralleling devices makes for higher currents. These devices exhibit high switching frequencies (>100 kHz), high efficiencies (especially at low power levels), and reasonable costs. Typical applications are in 120/240 $V_{AC}$ line-powered switch-mode power supplies, lighting ballasts, DC-DC converters, and low-voltage (<50 V) or low power 120/240 $V_{AC}$ line-powered motor drives.

Power MOSFETs have a source and a drain that are connected to individually and highly doped regions that are separated by the body region. Current flow is across the drain and source when correctly biasing the gate-source voltage ($V_{GS}$). MOSFETs may be N-channel or P-channel. In an N-channel MOSFET, the source and drain are “n+” regions and the body is a “p” region; the opposite is true for a P-channel MOSFET. This defines the direction of current flow when the device is biased. MOSFETs may be either enhancement-mode or depletion-mode types. Enhancement-mode MOSFETs are normally OFF at zero gate-source voltage ($V_{GS}$ = 0 V), whereas depletion-mode MOSFETs are normally ON at $V_{GS}$ = 0 V. Most MOSFETs used in power conversion devices are N-channel (majority carrier) enhancement-mode MOSFETs because N-channel MOSFETs have a third of the on-resistance of P-channel MOSFETs and are thus more efficient.

Figure 89 shows the electrical symbols for N- and P-channel enhancement-mode MOSFETs:

 

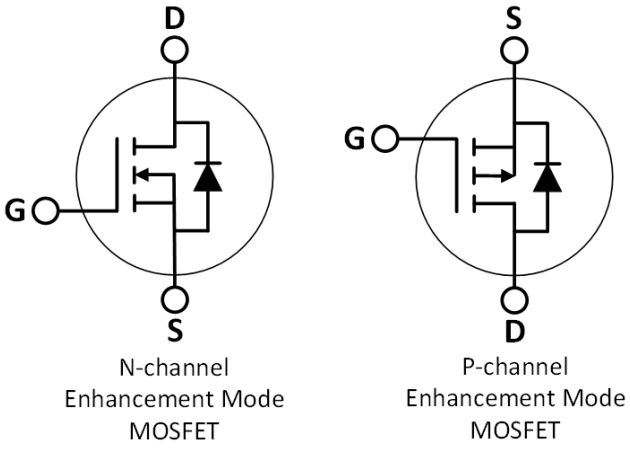


Figure 89: MOSFET Symbols.

## IGBTs

IGBTs have blocking voltage ratings of ~1200 $V_{DC}$ and switching frequencies of 1.5 to 10 kHz (in silicon). High-voltage (HV) IGBTs can reach up to 6000 $V_{DC}$ blocking voltage (typically implemented in designs at half this voltage for reliability reasons). Lower voltage IGBTs can be cascaded to achieve similar ratings (though with higher design complexity). Current-carrying capability is in the hundreds of Amperes. Due to their higher blocking voltage and ruggedness compared to MOSFETs, one often finds IGBTs in 600 $V_{AC}$ class motor drives, propulsion ("traction") motor drives, uninterruptible power supplies (UPS), and welding systems.

In power conversion applications, IGBTs are minority-carrier (P-channel) devices. Figure 90 shows the electrical symbol for a P-channel (minority-carrier) IGBT:

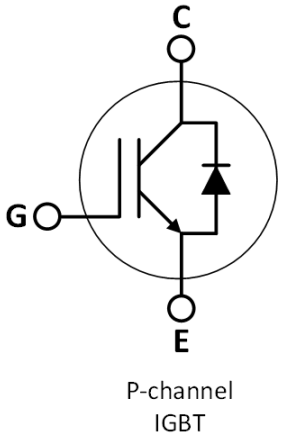


Figure 90: P-Channel IGBT Symbol.

Note that in an IGBT, the source and drain are known as a collector (C) and emitter (E).

 

### IGCTs, GTOs, and SCRs

Historically, IGCTs and GTOs have been the preferred power semiconductor for MV (2.4 $kV_{AC}$ to 7.2 $kV_{AC}$) AC induction motor drives. These devices have blocking voltage ratings up to 6000 $V_{DC}$ (or higher) and a simpler and more efficient architecture for higher power ratings, but a much slower (<1 kHz) switching frequency compared to IGBTs. However, slower switching matches up well with higher voltages because problems often result from attempts to switch high voltages at high speeds. SCRs can switch only once per power cycle — they can switch ON at any point in a cycle but cannot switch OFF until a zero crossing occurs. This makes their switching frequencies very slow, making them suited for very high voltage transmission and distribution applications, but less so for drives and other lower voltage power conversion applications.

## Power Semiconductors as Implemented in Power Conversion Systems

### Introduction

This section does not provide exhaustive technical detail regarding power-electronics designs. Rather, it introduces the common power conversion topologies, explaining in broad terms how they work and the types of outputs they produce.

The topology discussion begins with single-device configurations of buck and boost stages, then moves onto the multi-device topologies—the half-bridge and full bridge (H-bridge). The latter subject covers both the standard (single-phase) and cascaded (three-phase) H-bridges with descriptions of both the sine-modulated and six-step commutated PWM control techniques. Both the half bridge and H-bridges produce two levels of output voltage, albeit with different degrees of control over output voltage and current. For those drive applications requiring even greater control over these parameters or the ability to reach higher output voltages, there are multi-level topologies, which are also introduced here.

Note that in this section's figures, either MOSFET or IGBT symbols may be used. However, all of these topologies can use either MOSFETs or IGBTs depending on voltage, current, and application.

### Single Device

Regardless of type, one may connect a single power semiconductor device in series with the load ("buck") or in parallel with the load ("boost") and may utilize multiple devices paralleled with each other for higher-current operation. Figure 91 shows "buck" and "boost" configurations each with a single device, and Figure 92 shows two devices parallel to each other and in series ("buck") with the load.

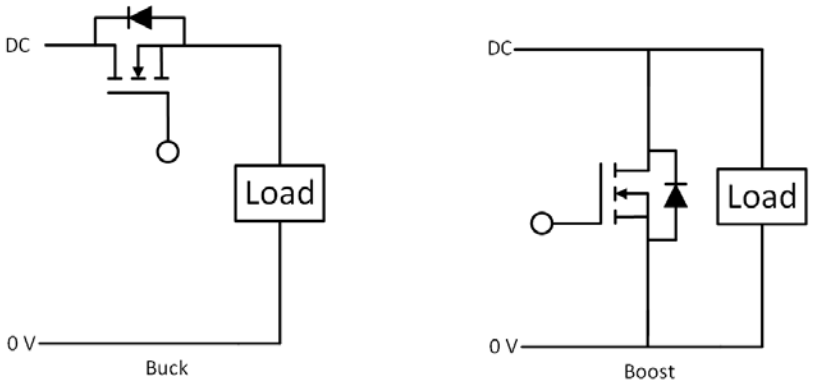


Figure 91: Connecting a power switch in series with the load is referred to as a buck configuration, while connecting a power switch in parallel with the load is known as a boost configuration.

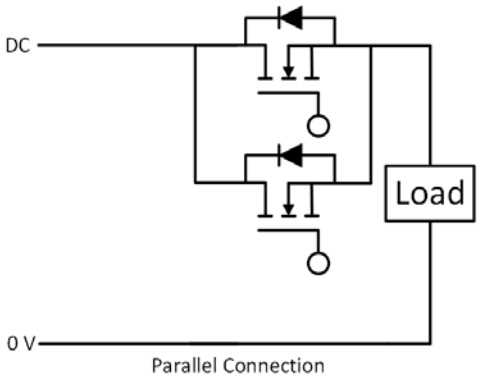


Figure 92: Paralleling multiple power switches allows the power stage to handle higher current levels.

With two devices in parallel, both devices switch identically and together they deliver twice the current of a single device to the load.

Figure 93 shows the PWM and modulating AC voltage for a single device, given a 170 $V_{DC}$ bus voltage.

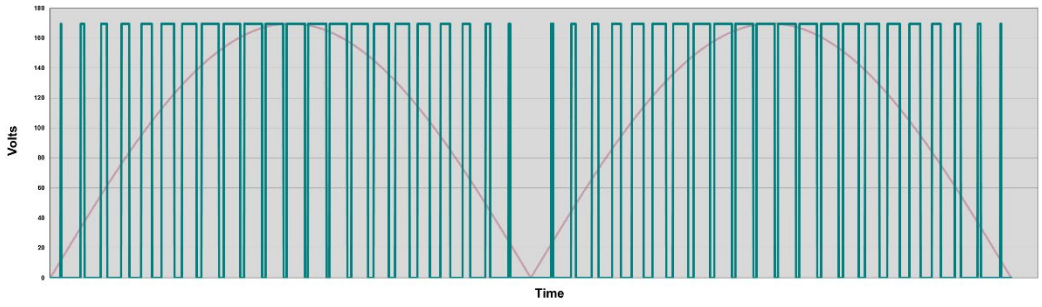


Figure 93: PWM signal for a single power semiconductor shown with modulating sinewave signal.

 

### Series Connection (Half-bridge)

One may connect either IGBTs or MOSFETs in series to provide higher voltage operation and/or AC voltage output biased around zero. This is known as a half-bridge connection. Such circuits serve single-direction control of a load, with the direction of power flow depending on whether we connect the load to the upper rail (DC) or the lower rail (0 V). Bi-directional control is theoretically possible using some sort of reversing mechanical switch, but doing so mitigates against instantaneous switching of the output polarity to the load without damaging the half-bridge devices, the load (motor), or other parts of the circuit. Thus, bi-directional control with a half-bridge is impractical in most situations.

We cannot close both power semiconductor "switches" (conducting) at the same time because a short circuit will destroy both devices. We ensure "dead-time" safety margins with more complex switching control. During this dead time, both devices are "open" and non-conducting before switching to their next assigned "open" or "closed" state. Figure 94 shows this configuration.

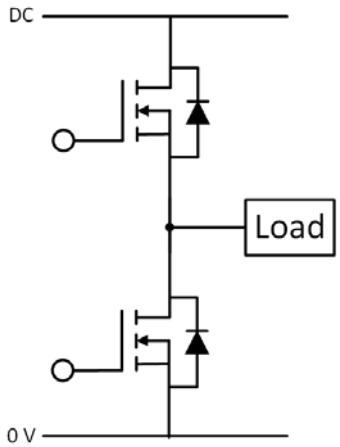


Figure 94: Two series-connected power switches are referred to as a half-bridge.

As in the single-device example (or parallel-device, single-output example), each device is controlled by a gate-drive signal, although in this case the gate-drive signals are different and independent for each device. Again, while the control system manages the gate-drive switching to generate the appropriate output from the devices for voltage and frequency control, each device continues to be driven from (in this example) 0 to 170 $V_{DC}$ derived from the 120 V rectified AC. To achieve a sinusoid-like output, switching commences in a "complementary" fashion with one device "off" while the other is "on". The output to the load is the difference between the two IGBT waveforms at any given time.

Figure 95 shows the switching (green trace) of the upper device (top), the lower device (middle), and the difference between the upper and lower devices (bottom, note the overlay in red of the modulating AC sinewave). The load sees the difference between the upper and lower signals with the polarity determined by termination of the load (at the DC bus or the 0 V rail).

 

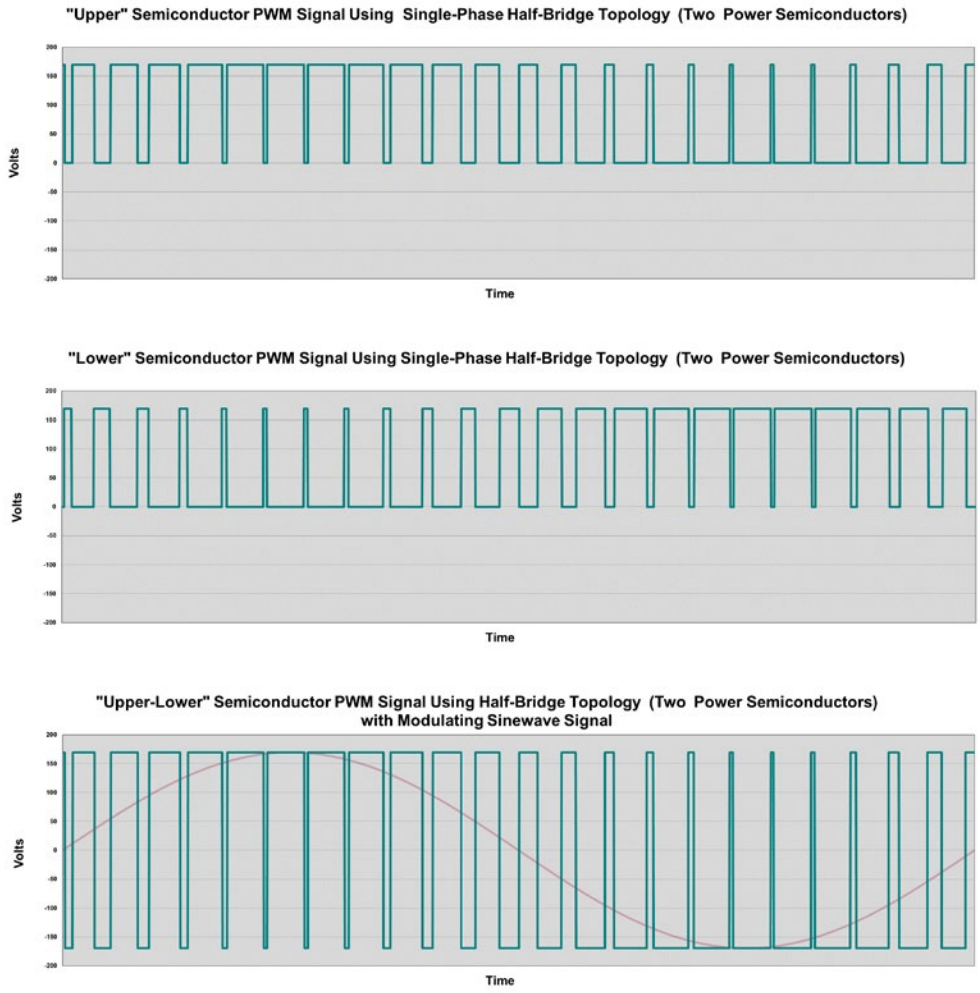


**Figure 95: PWM signals for a single-phase half-bridge power stage. The PWM signal for the "upper" semiconductor is shown at top, the PWM signal for the "lower" semiconductor is shown in the middle, and the combined "upper - lower" semiconductor PWM signal with the modulating sinewave is shown at bottom.**

In the "upper-lower" device output signal, a 50% duty cycle represents a 0 V condition. Note that even though the input was only 120 $V_{AC}$, the power conversion circuit's output is 340 $V_{PK-PK}$.

 

## H-Bridge (Full-bridge) Topology

Power semiconductor devices can also be connected in an H-bridge topology to achieve exactly what the half-bridge (series connection) does, but with built-in bi-directional power flow control and the ability to completely interrupt power flow (e.g., stop a motor) or brake a motor in a controlled fashion. Figure 96 shows a simplified H-bridge topology. Note the connection of the between the series device pairs:

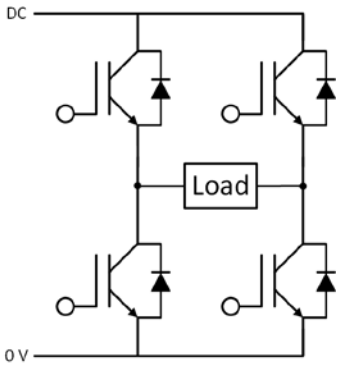


**Figure 96: The H-bridge or full bridge consists of two sets of two power semiconductor devices in series with a load connected across each output.**

As with the half-bridge, we accomplish control using complementary switching of the power semiconductor devices in the circuit. However, the complementary switching is now coordinated amongst series devices that could be in different series device pairs. The “upper” device switches only for positive voltage and the “lower” device switches only for negative voltage. Figure 97 shows the switching (green trace) of the upper device (top), the lower device (middle), and the sum of the upper and lower devices (bottom, note the overlay in red of the modulating AC sinewave). The load sees the sum of the upper and lower device signals.

 

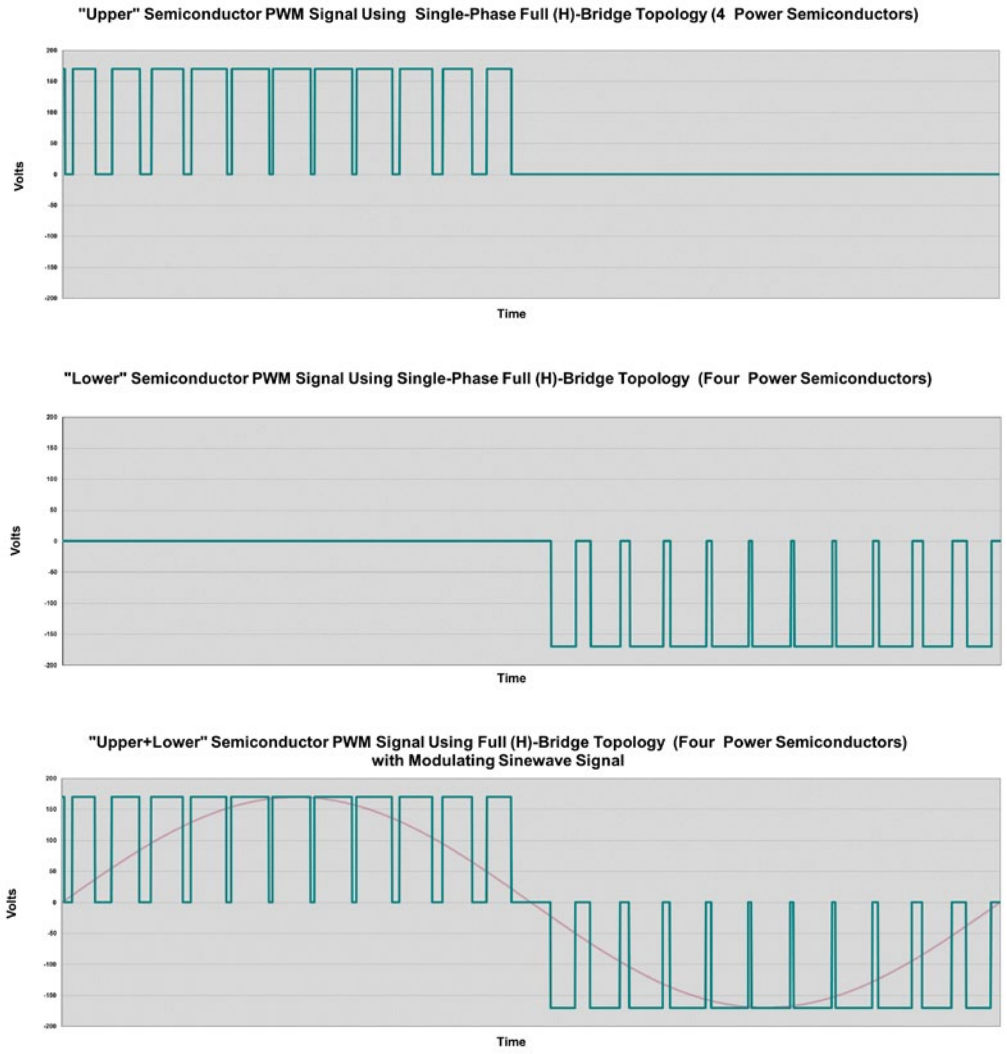


**Figure 97: PWM waveforms for a single-phase H-bridge topology. The PWM signal for the "upper" semiconductor is shown at top, the PWM signal for the "lower" semiconductor is shown in the middle, and the combined "upper + lower" semiconductor PWM signal with the modulating sinewave is shown at bottom.**

 

Figure 98 shows the same type of single-phase signal acquired on Channel 3 of a Teledyne LeCroy 12-bit oscilloscope:


**Figure 98: An output waveform produced by an H-bridge. Because of the +Vdc and –Vdc levels, the H-bridge is also referred to as a two-level inverter or two-level drive.**

Because the digital PWM output from an H-bridge has "two levels" (+$V_{DC}$ and -$V_{DC}$), it is sometimes known as a "two-level inverter" or "two-level drive." The H-bridge design outputs PWM signals from 0 V to +$V_{DC}$ to 0 V and 0 V to -$V_{DC}$ to 0V, with each device switching at the full DC bus voltage.

Figure 99 shows current flow through an H-bridge. For current flow in a positive direction through the load, the upper-left and lower-right devices conduct current while the others are "open." For current flow in the negative direction through the load, the upper-right and lower-left devices conduct current while the others are "open."

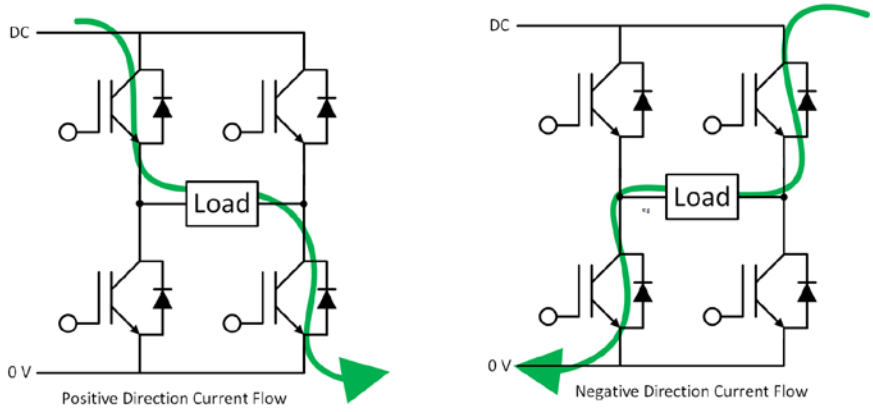


**Figure 99: Current flow in an H-bridge.**

 

To brake a motor in a controlled fashion (i.e., not instantaneously removing power or flipping the polarity) when the motor is moving in a positive direction, one would configure the devices so that both upper devices conduct current while both lower devices stay "open" to block current flow. Thus, both motor terminals are at $V_{DC}$ (avoiding further application of power) while allowing power flow from the motor back into the circuit. To achieve the same result for a motor moving in a negative direction, both lower devices conduct current while both upper devices remain "open." Both motor terminals are thus at ground potential, braking the motor's movement. Figure 100 shows these two cases.

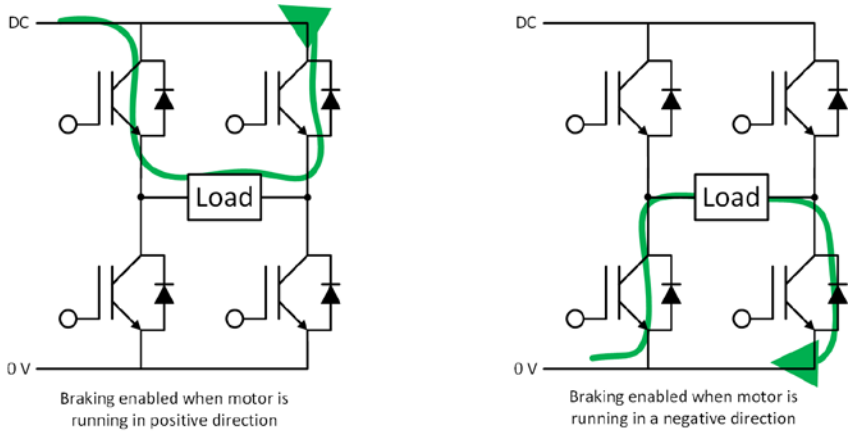


**Figure 100: Current flows within H-bridge during controlled braking of a motor. When the motor is running in a positive direction, the H-bridge is configured so the upper devices conduct while the bottom devices block current. When the motor is moving in a negative direction, it's the lower devices that are conducting.**

To maintain the motor in a "stopped" position, all devices are set to "open."

## Cascaded H-bridge Topology

An H-bridge provides bi-directional control of a single-phase load. To achieve bi-directional control of a three-phase load, the cascaded H-bridge is a popular topology. Figure 101 shows this topology.

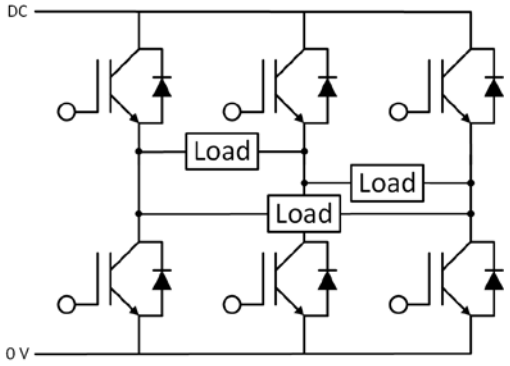


**Figure 101: The cascaded H-bridge provides bidirectional control of a three-phase load.**

Note that increasing the output phases from one to three means only two more devices in the circuit. Thus, users of the cascaded H-bridge accrue all of the benefits of three phases (higher power levels, improved control capabilities, etc.) while only increasing power semiconductor device costs by 50%.

 

The control of the gate-drive signals and the device output operation is very similar to that of an H-bridge with the following exceptions:

- The output voltage now consists of three separate “line-line” voltages (sometimes referred to as U to V, V to W, W to U; or R to S, S to T, T to R). Figure 102 shows a screen capture of these three line-line waveforms taken with a Teledyne LeCroy 12-bit oscilloscope:


**Figure 102: With the load connected as shown in the previous figure, the cascaded H-bridge produces three line-to-line outputs.**

- The device switching behavior remains complementary, but the control is more complicated given the more complicated interactions amongst all the switching devices.
- The device switching control can be either through a three-phase, sine-modulated (carrier-based or space-vector) control scheme or a six-step commutated control scheme. Figure 102 shows a sine-modulated control scheme.

As with the H-bridge topology, some call this a “two-level inverter” or “two-level drive.”

A cascaded H-bridge, built from either MOSFETs or IGBTs, is probably the most common type of inverter topology for creating three-phase output voltages to run 600 $V_{AC}$ class or lower products.

 

### *Sine-modulated Cascaded H-bridge*

As with the H-bridge (single-phase) example, any two devices in series cannot both be "on" at the same time. Otherwise, operation of the complementary gate-drive switching is very similar.

Consider a desired AC waveform shown in Figure 103 with line-neutral voltages $V_{R-N}$, $V_{S-N}$, and $V_{T-N}$ at a time t=0.

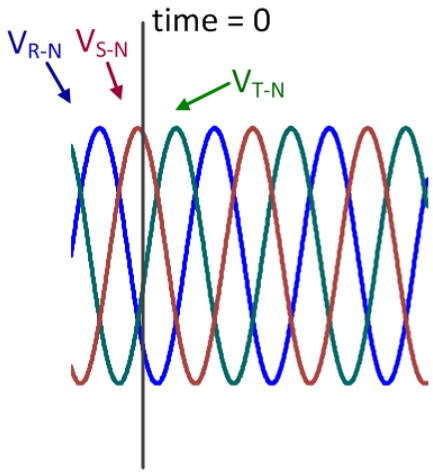


**Figure 103: Three-phase line-neutral voltage waveform example showing a reference time = 0 at which each voltage has a specific magnitude.**

At a given time for such a set of three-phase voltages, a cascaded H-bridge will generate PWM signals so that the individual phases (the mid-point of each half-bridge in the cascaded H-bridge) are either sinking or delivering current, resulting in a three-phase current flow through the cascaded H-bridge as depicted in Figure 104.

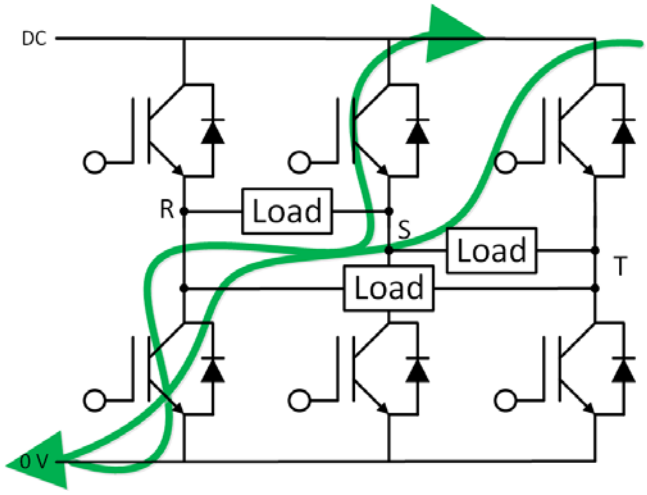


**Figure 104: Current flows in the cascade H-bridge at t = 0.**

 

To achieve the current flow shown in Figure 104 the devices switch as follows:

- Upper R device is “off”
- Lower R device is “on”
- Upper S device is “on”
- Lower S device is “off”
- Upper T device is “on”
- Lower T device is “off”

### *Six-step Commutated Cascaded H-bridge*

In a six-step commutation scheme, we apply voltages across only two of the three phases at any given time, with six “steps” for one complete commutation period. The time intervals for the six steps are typically determined by reading embedded Hall sensors placed in the motor’s rotor but could also be determined virtually using some type of sensorless system. The Hall sensors generate high/low signals that, when read as a three-bit pattern, define a bit pattern (000 and 111 excluded) that dictates when to apply the phase voltages. During this voltage application, the amount of voltage applied is controlled using pulse-width modulation.

For example, Figure 105 shows the six steps labeled across the top. The R, S, and T phase upper and lower devices appear as either ON (high) or OFF (low).

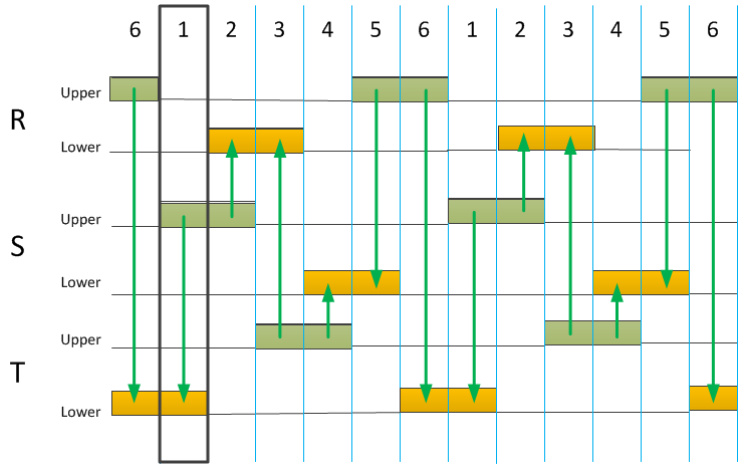


**Figure 105: This diagram shows the conduction states of the six switches in a cascaded H-bridge during implementation of a six-step commutation scheme.**

If you look at commutation step 1 (outlined in Figure 105) phase R is not energized, and phase S and T are energized. According to the Figure 105 switching diagram, the device switching should be as follows:

- Upper R device is “off”
- Lower R device is “off”
- Upper S device is “on”
- Lower S device is “off”
- Upper T device is “off”
- Lower T device is “on”

 

In this particular step of the six-step commutated scheme, current flow will be as shown in Figure 106.

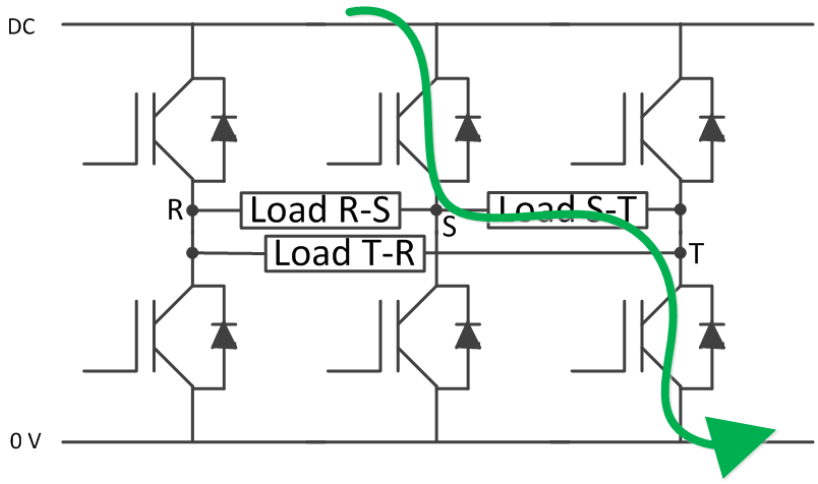


Figure 106: Turning on the upper S switch and lower T switch during step 1 results in the current flow shown here.

Six-step commutation is very common for smaller brushless DC motors as it is less expensive to implement and performs reasonably well but does result in high torque ripple and higher audible noise during operation (compared to sine-modulated methods). Waveforms look very different as well compared with sine-modulated waveforms (as shown later).

## Multi-Level Topologies

As circuits progress from a simple single device (or multiple devices in parallel with a single output), to series device connections (half-bridge) to H-bridge and then to cascaded H-bridge topologies, each succeeding topology offers more voltage control and range, more current-flow control, and multi-phase control. However, there are still only a maximum of two levels for the output voltage for the H-bridge and cascaded H-bridge topologies.

Multi-level topologies provide more output control for the digital PWM voltage levels, achieving more than two levels. Why might one want more than two digital PWM levels?

- To reduce harmonics on the output
- Better and smoother motor control (e.g., less torque ripple)
- Voltage levels are higher than possible when using a cascaded H-bridge

In terms of the last point, we typically use IGBTs (and all power semiconductor devices) well below their breakdown voltage rating for greater field reliability. For instance, a 1200 V IGBT in a cascaded H-bridge with a 480 $V_{AC}$ rectified input would see a maximum voltage of 679 $V_{DC}$ (without overshoot). Developing a drive for a 4160 $V_{AC}$ (nominal voltage) motor is beyond the capability of a single 3300 V device because the DC bus voltage would be 5884 V in this case. However, this is within the capability of two (or more) 6000 V devices.

 

The tradeoff for more voltage levels is higher control complexity of all of the modulation signals, which requires more processing power in the control system. Thus, more than 2-level topologies are very unusual unless one of the above requirements justifies the need.

A common three-level topology is a neutral-point clamped (NPC) topology. The schematic pictured in Figure 107 reveals that the topology consists of two, connected cascaded H-bridges:

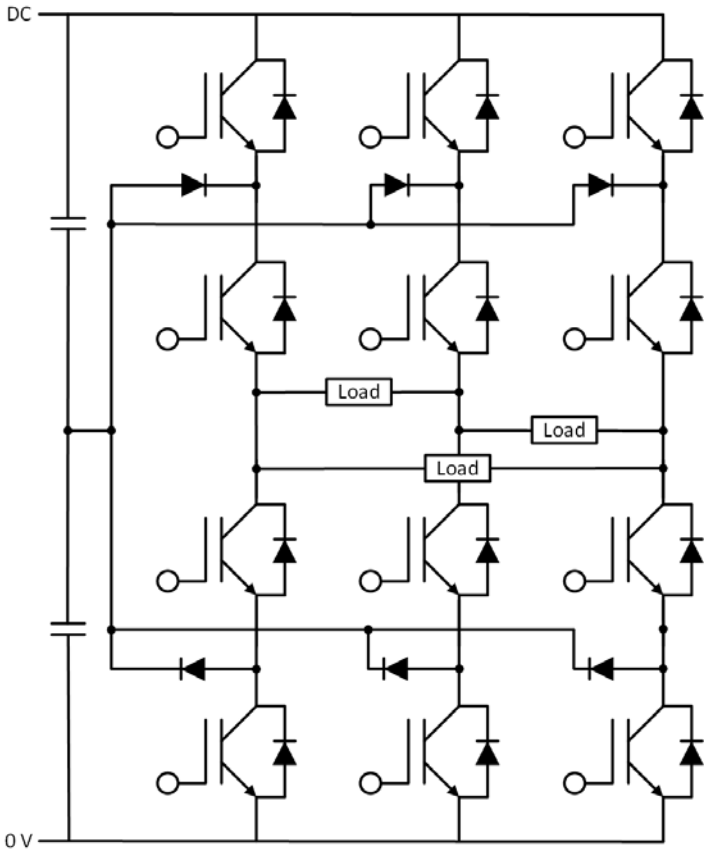


**Figure 107: The neutral point clamped topology is a common three-level topology in which two H-bridges are cascaded.**

 

Figure 108 shows an example of a line-line voltage output signal from an NPC inverter.

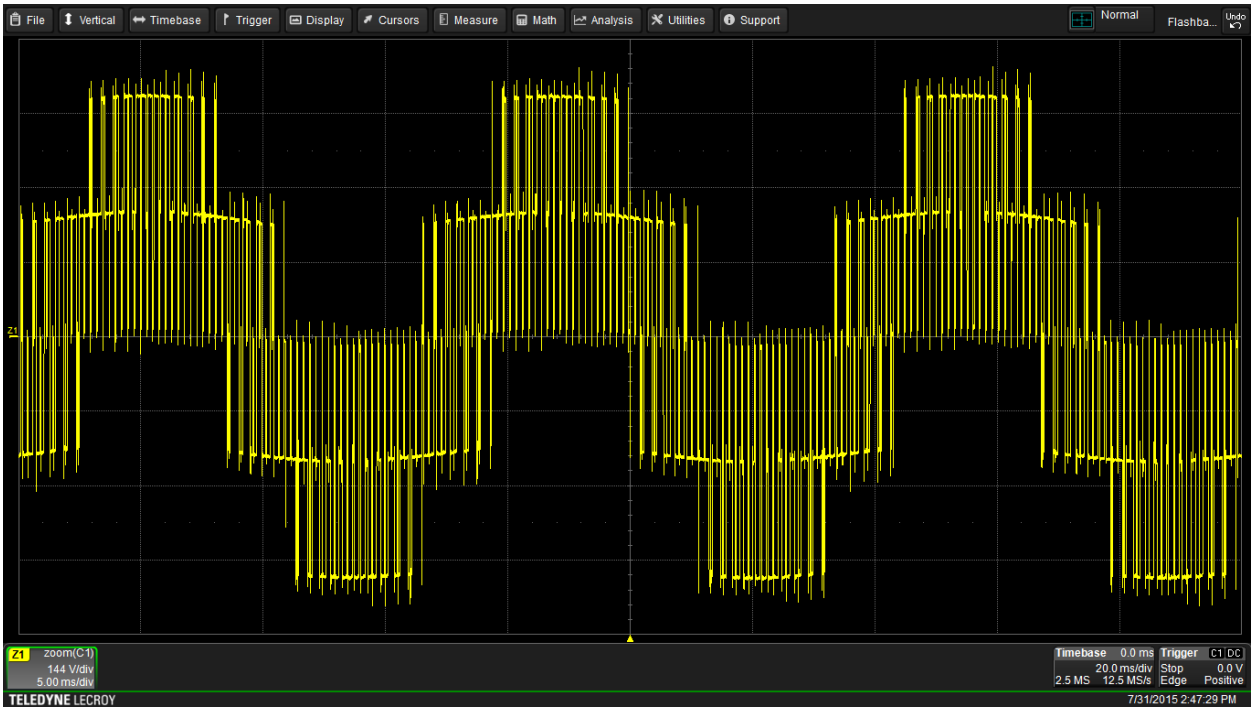


**Figure 108: Output waveform produced by an NPC converter probed line-to-line.**

More than three levels is also possible — the concept scales up to five, seven, or more levels, but at the cost of increasing control complexity. Topologies of more than three levels are unlikely to see as much use as wide-bandgap (i.e., higher voltage) SiC IGBTs become more prevalent. Such devices offer significantly more than 6 kV breakdown (withstand) voltage and make possible 15 kV converters with a three-level, NPC-type topology.

It is possible that such topologies will become more common for >15 $kV_{AC}$ voltage applications (e.g., 35 $kV_{AC}$ distribution voltages, which might be used in a 34.5 $kV_{AC}$ to 480 $V_{AC}$ step-down solid-state distribution transformer).

 

# Motors

## Introduction

Previously, we reviewed power semiconductor devices and power conversion topologies, providing foundational knowledge for understanding how motor drives work and how they are designed. Equally important to understanding motor drives is a knowledge of how the load (i.e. the motor) works. In this section, we begin that discussion, providing an overview of the popular motor types and the basics of how motors work.

## Motor Background

In general, all motors utilize a stator (also referred to as a field or stationary winding) and rotor (or rotating winding) connected to a drive shaft. The stator and rotor have opposing and constantly varying magnetic fields that create angular movement of the rotor. We use various electrical and mechanical constructions for motors depending on the application requirements (e.g., high torque, low speed, precision of movement, low cost, etc.). The vast majority of motors use either single-phase or three-phase windings – those that use more than three phases are found in niche applications where reliability through redundancy is critical (aircraft, military, space), though there is increasing interest in more than three-phase windings in commercial vehicle propulsion applications.

The predominant motors in use today are:

- AC induction motors (ACIM)
- AC (wound-rotor) synchronous motors (ACSM)
- (Brushed) DC motors
- Brushless DC motors (BLDC)
- Permanent-magnet synchronous motors (PMSM)

Conventional “brushed” DC motors are mostly in use today in low-cost applications because more reliable variable frequency (motor) drives and AC motors deliver greater benefits. We typically use AC synchronous motors in industrial applications requiring a fixed output speed. We often see use of AC induction motors, brushless DC motors, and permanent-magnet synchronous motors with drives. There are other types of motors not discussed here (e.g., “stepper” motors or servo motors) that are really special cases of PMSM or BLDC motors as well as other motor types in development that may or may not prove commercially viable.

Worldwide, motors consume ~45% of electrical energy. The largest motors have small unit volume but consume a far larger share of electrical energy. Therefore, there is intense focus on improving the efficiency of the largest motors, either through improvements to motor electro-mechanical design, use of advanced motor drives for higher efficiencies over a range of speeds and loads, or both. Governments around the world have mandated increasingly strict efficiency standards for these motors, beginning in the United States in 1992 and followed in 1998 by the European Union.

 

Essentially, these efficiency standards focus on the larger motors that consume the highest proportion of energy, and fall into four categories:

- Standard (low) efficiency (IEC IE1 level, or US EPAct Below Standard Efficiency)
- High efficiency (IEC IE2 level, or US NEMA Energy Efficiency/EPAct)
- Premium efficiency (IEC IE3 level, or US NEMA Premium level)
- Super Premium efficiency (IEC IE4 level, or US NEMA Super Premium level)

Small motors (less than one horsepower (hp), or equivalent to ~750W) represent 90% of motors by unit volume, but only consume 9% of the total electricity used by all electric motors. These are single-phase or three-phase AC induction motors for general-purpose use; brushless DC (BLDC) / permanent-magnet synchronous (PMSM) or electronically commutated (ECM) motors; and brushed DC motors used in appliances, small pumps, compressors, fans, etc. These motors do not meet efficiency standards, though their design may be very efficient (especially if powered from a battery). Small motors may be paired with motor drives because there is some precision control-related capability that is very important to the proper operation of the motor in its intended use. One may only achieve such precise control with a drive. Examples of high-precision control include the servomotor in a disk drive, a brushless DC motor in a power tool, or the compressor or fan in a mini-split ductless heat pump.

Medium motors (greater than one horsepower/750 W but less than 500 hp/375 kW) represent ~9% of motors by unit volume but consume 68% of the electricity used by all motors. Most of these motors (around 85% market share) are three-phase AC induction motors used in industry, but brushed DC motors (declining share), and permanent-magnet motors (increasing share) are also available in this size range. The IEC and NEMA efficiency standards described above are relevant to motors designed for stand-alone operation in this size range. When we integrate motors into a system in a manner precluding separate testing, they are exempt from these standards. However, we even find many "exempt" motors in this class (e.g., a hybrid vehicle propulsion motor and drive) designed with high levels of efficiency).

Large motors (greater than 500 hp/375 kW) are 0.03% of motors by unit volume but consume about 23% of electricity used by all motors. These motors are three-phase AC induction motors and wound-rotor synchronous motors built-to-order for special-purpose industrial use. While not specifically covered by the efficiency requirements in the standards, the users of these motors are well aware of their high operating costs and efficiency does factor into initial purchase decisions.

Not counted in the totals above are the numerous small motors used in non-utility (grid) connected applications, such as servo-motor drives in hard disk drives, windshield wiper motors, etc.

 

## Basic Motor Operation

All motors contain the same essential elements:

- Stationary winding (typically called the “stator”) that creates a rotating magnetic field. This winding is physically contained in a magnetic “core” material to enhance the generated magnetic field and provide physical support when energized.
- A rotating magnet (typically called the rotor) is alternatively repelled and attracted to the rotating magnetic field generated by the stator. The magnet could be either a permanent magnet, an induced magnetic field (as with an AC induction motor), or a generated magnetic field from a DC power supply (as with a wound-rotor synchronous AC motor).
- A shaft attaches to the rotor with which to extract work.
- Various other mechanical components

We can think of the stator as two fixed permanent magnets arranged across from each other with opposing polarities so that a magnetic field is created between them. We can consider the rotor as another permanent magnet placed between the “stator magnets” and allowed to rotate around its center. If the “rotor magnet” is oriented such that its own magnetic field does not directly align with that of the stator magnets, then it will rotate until it does align, and then stop rotating. Reference Figure 109 below.

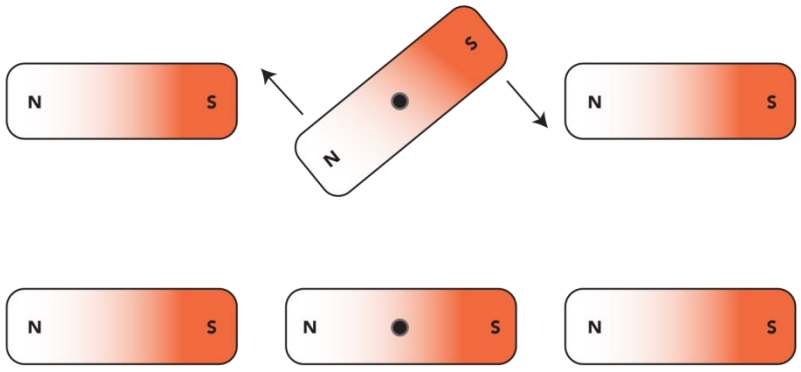


**Figure 109: Basic principle of motor operation. If the rotor magnet is oriented such that its polarities do not align with those of the stator magnets as shown in the top drawing, then the rotor will rotate until its magnet’s polarities do align as shown in the lower drawing.**

To reinitiate “rotor magnet” rotation, we would have to physically switch the polarity of the “stator magnets”, which is impractical. However, it is practical to replace the permanent magnet “stator magnets” with electromagnets energized by an AC waveform that will automatically reverse the magnetic field at the AC frequency. Thus, the rotor magnet rotates as shown in Figure 110, with the top example at time = zero and the bottom example at arbitrary time = one:

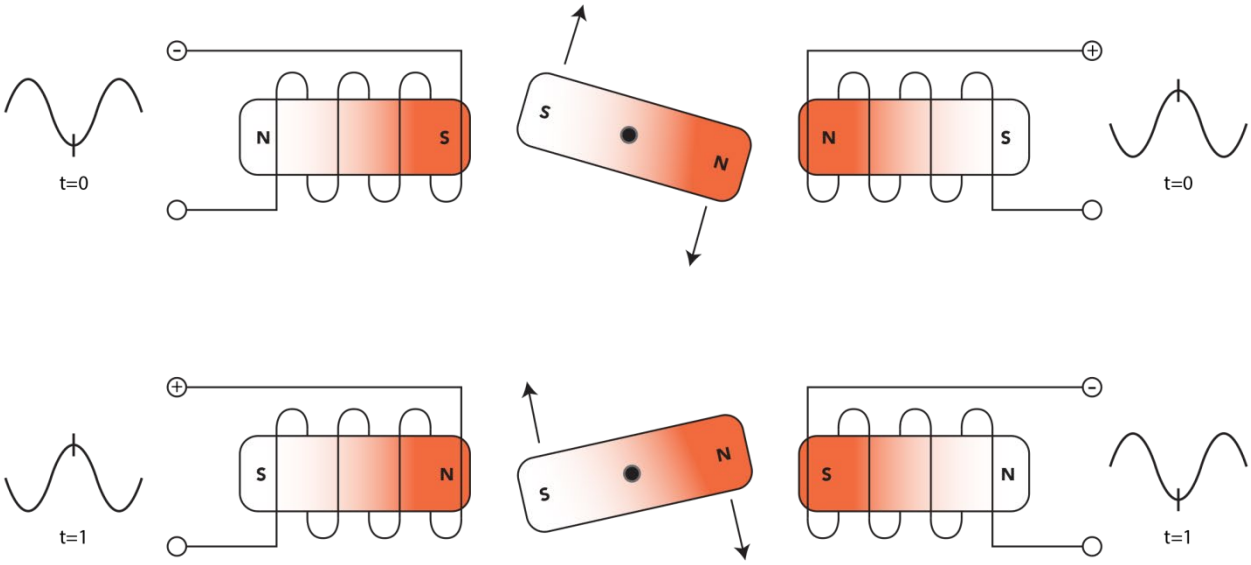


**Figure 110: If electromagnets energized by AC waveforms are used in the stators, the polarities of the stator magnets will continually change, causing the rotor magnet to rotate continually.**

By driving the stator electromagnets from a three-phase AC supply, we create three different magnetic fields, each 120° apart, which create a constantly rotating electromagnetic field (as the voltage and current vectors rotate). Figure 111 illustrates a simplified situation of north and south polarities on the stator electromagnets, and not the actual vector magnitude, and with the left example at time = zero and the right example at arbitrary time = one:

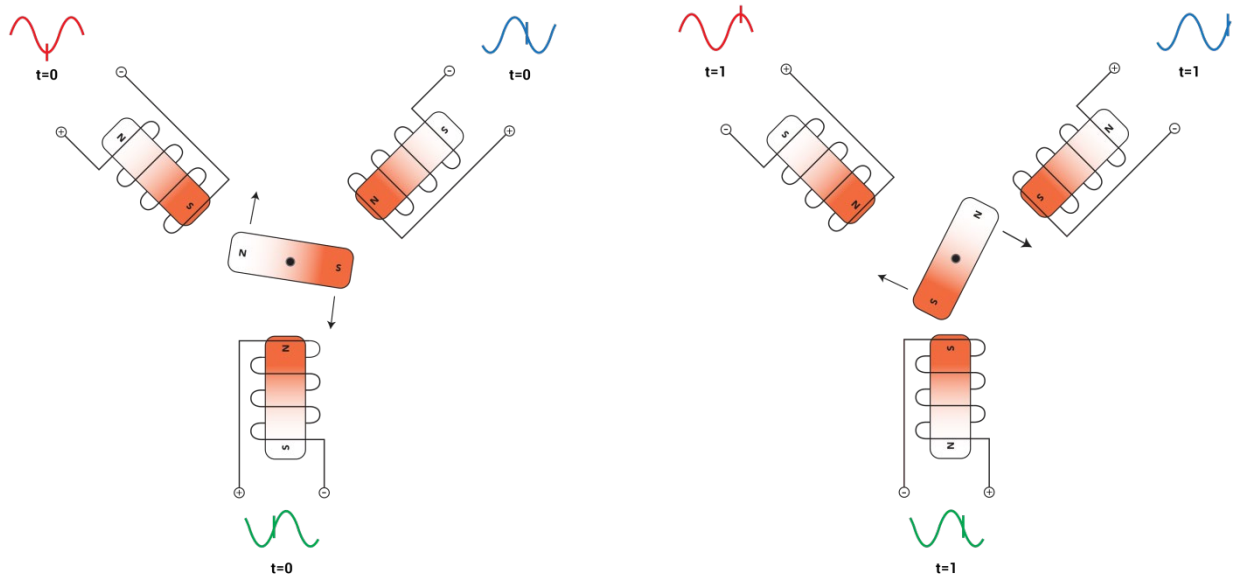


**Figure 111: Adding a third stator electromagnet and driving the three electromagnets with a three-phase AC waveform creates three magnetic fields that are physically 120 degrees apart.**

 

## Motor Stator Poles and Slots

The above simplified examples of basic motor operation showed one (single- or three-phase) rotating-stator magnetic field and one rotor magnetic pole. Such a motor would have considerable variation in the torque it could produce at the output shaft depending on the position of the rotor magnetic field relative to the stator magnetic field. Therefore, most motors have multiple sets of "slots" for the stator winding and may have multiple magnetic "poles" on the rotor.

### Stator Poles and Slots

To provide more magnetic field changes per rotor rotation, we may use "N" poles per phase in the stator winding. For example, a three-phase motor might have three poles, which would mean nine locations in the stator core for a winding. These locations are termed "slots" and there are often multiple slots per pole. By definition, a three-phase motor has a minimum of three slots (one for each phase, which would be a single-pole stator). However, the actual number of slots could be much higher. We design motors for a certain number of stator slots (and poles) to optimize the motor cost and characteristics for its intended application.

Figure 112 shows an example of a three-phase motor that has four poles (per phase) and one slot in the stator core per pole, making 12 slots to hold the stator windings.

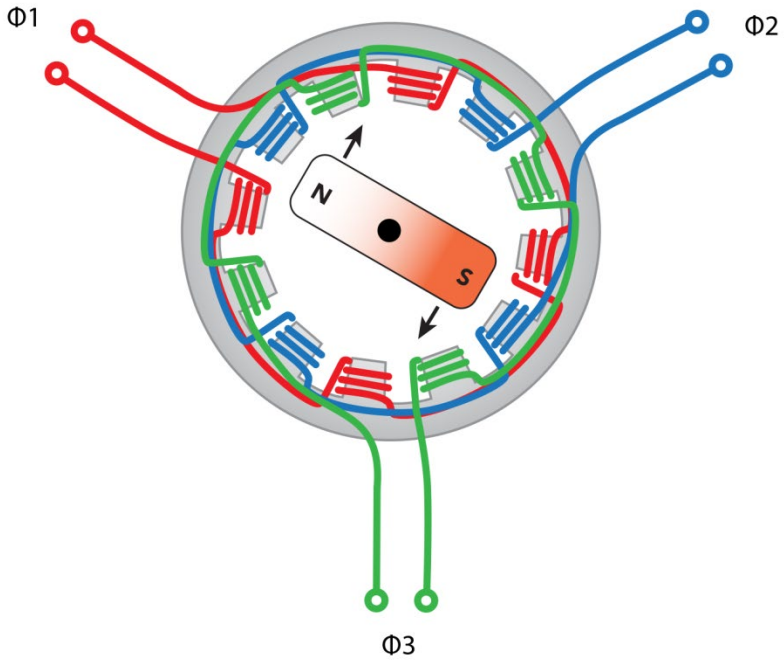


Figure 112: A three-phase motor with four poles (per phase) has twelve "slots" for stator core windings.

 

Figure 113 shows the stator for an AC induction electric motor. This three-phase motor contains a large number of stator slots (what appears to be 39, by count) in the stator core (where insertion of the stator windings takes place). This is certainly far more slots than the number of poles in the stator winding and is likely a 13-pole stator.

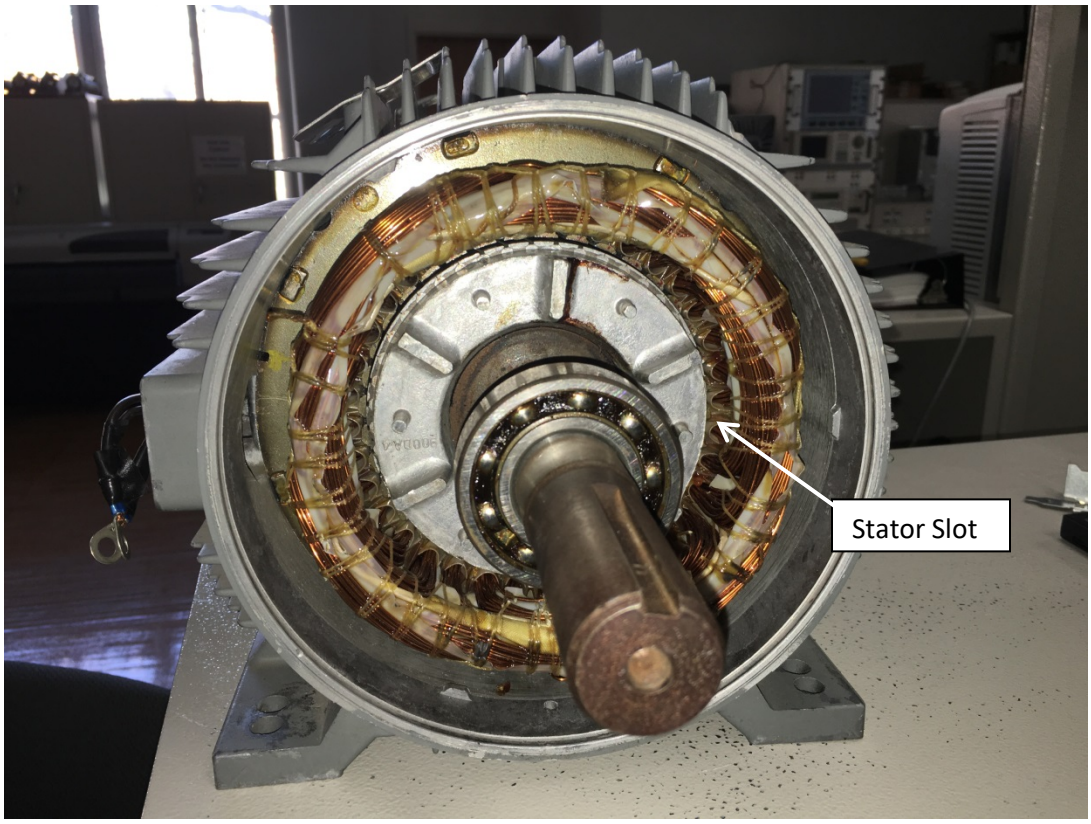


**Figure 113: Stator of a three-phase AC induction motor. This motor has what appears to be 39 stator slots. Photograph courtesy of Wisconsin Electric Machines and Power Electronics Consortium (WEMPEC), University of Wisconsin-Madison. Photograph courtesy of Wisconsin Electric Machines and Power Electronics Consortium (WEMPEC), University of Wisconsin – Madison.**

 

## Rotor Pole Pairs

A rotor "pole" is either a north or south magnetic field on the rotor magnet. We know these as "pole pairs" (a set of one north and one south magnetic field).

The previous example showed a motor with a single rotor pole pair. Figure 114 shows the same example but with a two pole-pair rotor (and again, with four stator poles and a three-phase stator).

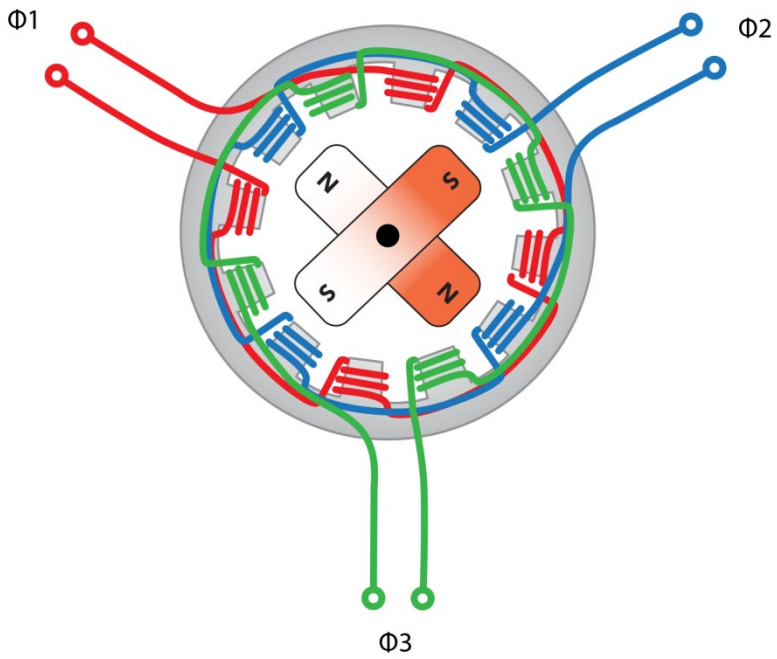


Figure 114: A three-phase motor with four poles (per phase) as in Figure 113, but with a two pole-pair rotor.

As with stator poles, motor engineers design for a given number of rotor pole pairs to optimize the motor cost and characteristics for its intended application.

## Motor Operating Quadrants

Motors have a variety of application requirements and are designed and controlled in so as to behave in specific ways per the application requirements. A motor shaft can rotate and provide torque in either a clockwise or counter-clockwise direction, and it can supply torque to generate power ("motoring") or resist the torque applied to it (i.e., "generating") in either direction as well. The ability to control applied speed and torque in both directions is important for more complex control applications. Additionally, the ability to brake the motor with applied electrical force (instead of a mechanical brake) or re-generate power while braking is attractive for some applications (e.g., elevators, industrial process control, or vehicle propulsion).

One may describe the two rotational directions (clockwise and counter-clockwise) and two torque applications (motoring and generating) in a four-quadrant operating mode diagram, shown in Figure 115.

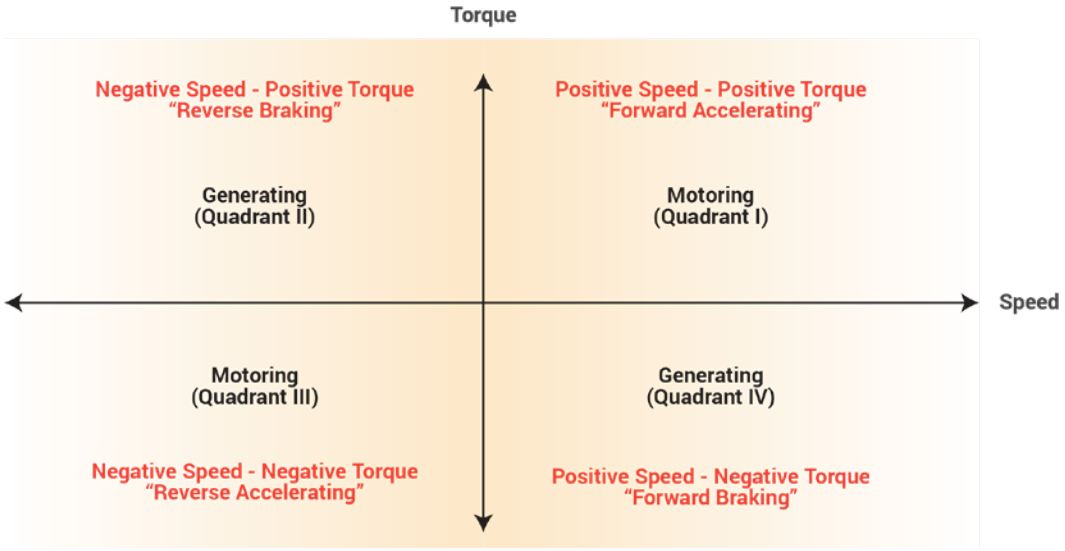


Figure 115: The four quadrants of motor operation.

Straightforward applications, such as small fan or blower motors, operate only in a single direction and provide torque output (motoring) only with no need for electrical braking (i.e., Quadrant 1 operation). A power drill motor might operate in both forward and reverse directions, but with no braking (i.e., Quadrants 1 and 3 only). Vehicle propulsion motors would operate in all four quadrants to provide forward and reverse operation with re-generative braking.

To operate a motor in either direction without requiring a re-connection of supply leads to the stator requires an H-bridge (single-phase) or cascaded H-bridge (three-phase) power conversion and control system. We know such systems as "drives," and they electronically control switching for complex operation in multiple operating quadrants. The most complex four-quadrant operations require use of more complex drive-control architectures and algorithms (e.g., vector field-oriented control, or vector FOC). Such applications call for more informative sensors and more complex control architectures to detect rotation direction and absolute rotor shaft (and therefore rotor magnetic field) position, such as quadrature encoder interfaces (QEIs) or resolvers.

 

## AC Induction Motors (ACIM)

AC induction motors (ACIM) consist of a stationary winding (stator) held inside a stator core, a rotating winding (rotor) connected to a shaft, a mechanical housing, and a bearing/support structure to properly locate the rotor inside the stator and permit rotation. This resembles the "generic" motor we described above but differs in that the rotor magnetic field is induced by the stator magnetic field and is not a supplied or permanent magnet field. The motor "cutaway" in Figure 116 of an AC induction motor shows the different parts.

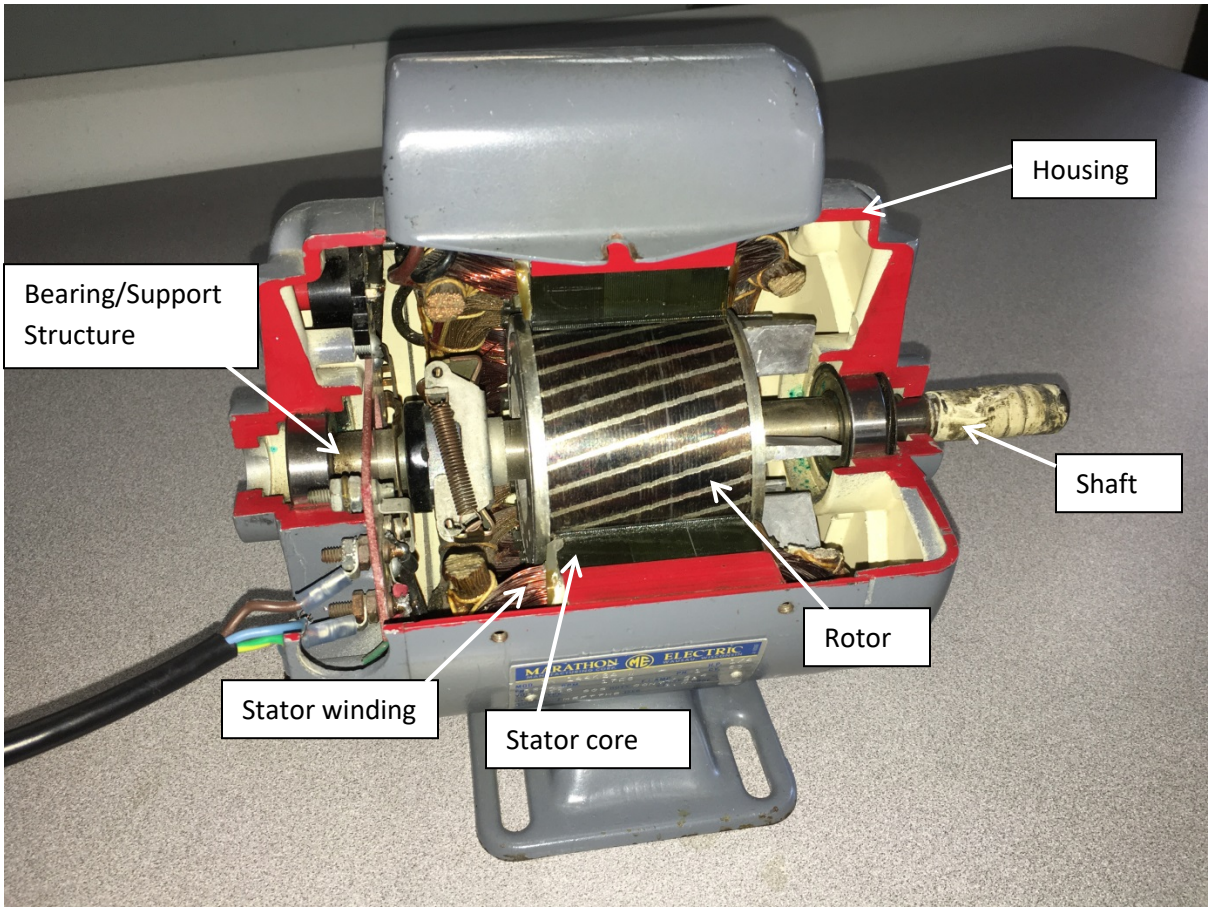


**Figure 116: In an AC induction motor, the rotor magnetic field is induced by the stator magnetic field rather than a supplied or permanent magnet field. Photograph courtesy of Wisconsin Electric Machines and Power Electronics Consortium (WEMPEC), University of Wisconsin-Madison.**

ACIMs have alternating voltage and current (AC) applied to the stator winding. Construction of the stator winding is such that the applied AC voltage rotates around the stator winding, which creates a rotating stator magnetic flux field. This rotating stator magnetic flux field induces a magnetic flux field in the rotor. The two fields have opposing magnetic forces, which compels rotation of the rotor. Because the rotor magnetic field is "induced" by the stator magnetic field, these AC motors are termed "induction motors". Figure 117 depicts how the single-phase stator and rotor magnetic flux fields produce rotation (the currents in the rotor conductor, shown in dark gray, are flowing into and out of the page in this example).

 

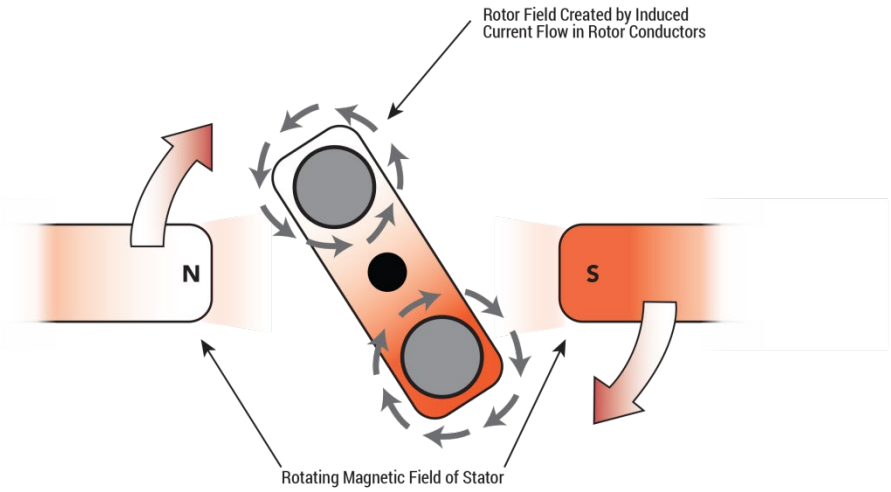


**Figure 117: The applied AC voltage rotates around the stator winding, creating a rotating stator magnetic flux field, which in turn induces a magnetic flux field in the rotor. The two magnetic fields repel each other, causing the rotor to rotate.**

To induce rotor currents with the stator magnetic flux field, the stator magnetic flux field must rotate faster than the rotor's induced magnetic flux field. When the two magnetic flux field angular speeds match, the motor is in a no-load condition and the rotor shaft is rotating at its synchronous speed (100% of its rated speed), but it can generate no torque. Application of a load to the shaft causes the two magnetic flux field angular speeds to diverge and produce torque. Essentially, the angular velocity of the rotor increases or decreases until it reaches the balance point at which the magnitudes of the stator and rotor current and generated rotor torque balances the load applied at the shaft. We call the ratio between the rotor angular speed and stator magnetic flux angular speed slip. Slip, typically expressed in a percentage, is the difference between the synchronous (no-load) speed and the actual speed. Thus, an ACIM never operates at its rated (no-load, or 100%) speed, and is therefore sometimes called an AC asynchronous motor (ACAM).

One may show the relationship of torque to (rotor shaft) speed as a torque-speed curve, and there are optimal points on the curve where maximum torque occurs. The motor stator and rotor construction, and various other factors, determine the shape of the torque-speed curve. Different applications have different torque-to-speed needs. Figure 118 shows a typical ACIM torque-speed curve:

 

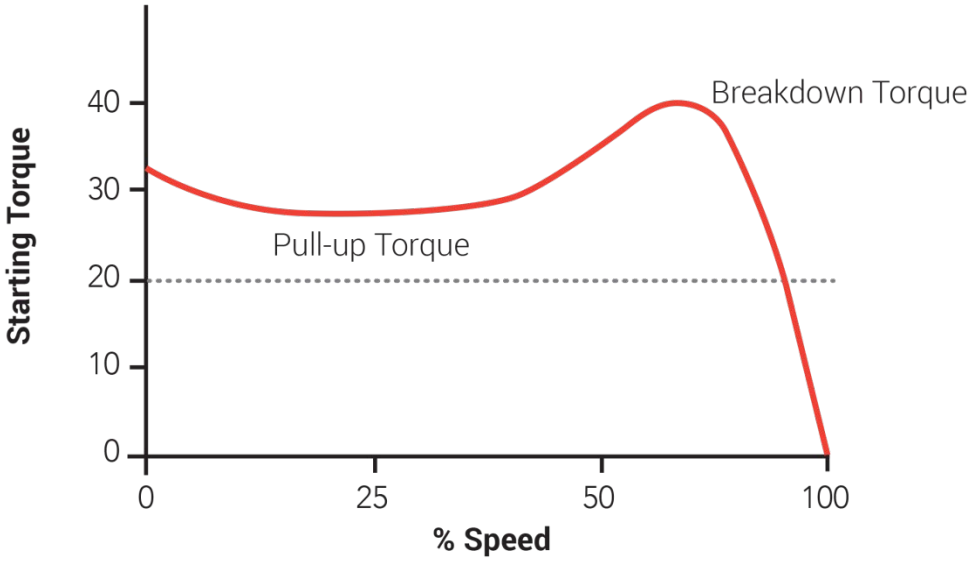


**Figure 118: A typical ACIM torque-speed curve. Looking at a torque-speed curve, users can determine whether torque-speed characteristics of a given ACIM meet their application needs.**

ACIMs can be either single-phase or three-phase types and though their constructions may vary depending on the size of motor, their method of operation is always the same. In general, three-phase motors are more efficient, lend themselves to precision control, and are required for higher power-output levels. At higher power-output levels, three-phase motors are more cost-effective to manufacture and more reliable.

The principal advantage of an ACIM is that there is only one applied power source and no need for an expensive permanent magnet or separate DC power supply for the rotor. It is a simple design that can generate very high levels of power output. The construction is simpler and cost lower than a permanent-magnet motor, and reliability is higher than a similar-sized DC (carbon-brushed) motor. When paired with a variable frequency motor drive, speed and torque control capabilities are at least as good as the carbon-brushed DC motor.

Historically, control of AC induction motor speed or torque had been quite limited — a variable transformer (expensive and limited) provided input voltage adjustment, and output adjustment came by means of a valve (e.g., for a pump motor) or other mechanical device. Usually, motors were oversized and ran well below their rated power with no operator control of their speed or power (torque) output, leading to very inefficient operation. Modern variable frequency motor drives overcame these limitations.

 

### Single-phase ACIM

Single-phase ACIMs are small motors that have a single alternating voltage phase applied to a single stator field winding. Because the single-phase stator magnetic flux field "alternates" and does not "rotate" around the stator, motor rotation could be in either direction at startup depending on the position of the rotor when the single-phase AC voltage is applied. Therefore, single-phase ACIMs often use a second "starting" winding that is 90° out of phase with the stator winding. For this reason, we sometimes describe single-phase ACIMs as two-phase motors. This second winding ensures establishment of the stator rotating magnetic flux field in the correct direction at startup and that the motor shaft spins in the correct direction. Once the motor starts spinning, the second winding is electrically removed from the circuit. We often call these motors capacitor-start or split-phase motors. An example is depicted in Figure 119. They are generally smaller, less expensive motors that often do not use any type of variable frequency motor drive. See the image below:

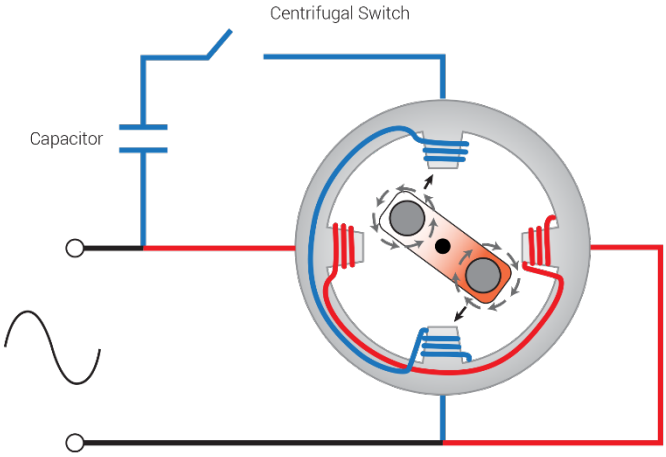


**Figure 119: A capacitor-start or split-phase motor employs a starting winding (blue) that is 90° out of phase with the stator winding to ensure that the rotor begins rotating in the desired direction. But after start-up, this second stator winding is disconnected.**

These motors see application only for simple tasks (fans, blowers), and are limited to 120/240 V inputs with a rating no more than ~1 horsepower or ~1 kW. Small ACIMs controlled by a motor drive may employ a motor drive with a single-phase AC input and a three-phase output to a small three-phase ACIM.

### Three-phase ACIM

three-phase ACIMs range from small to large sizes and have a three-phase AC voltage applied to a three-phase stator field winding. Operation is identical to that of the single-phase ACIM except that the presence of a (naturally) rotating three-phase stator magnetic flux field makes construction and operation simpler and eliminates the need for a starting phase (a three-phase motor will predictably start in the defined direction). The three-phase stator winding creates a natural rotating magnetic field, with the direction and rotational speed of the magnetic field related to the winding and pole construction of the stator. three-phase motors are also more efficient than single-phase motors. Figure 120 shows a three-phase AC induction motor with a single-pole rotor.

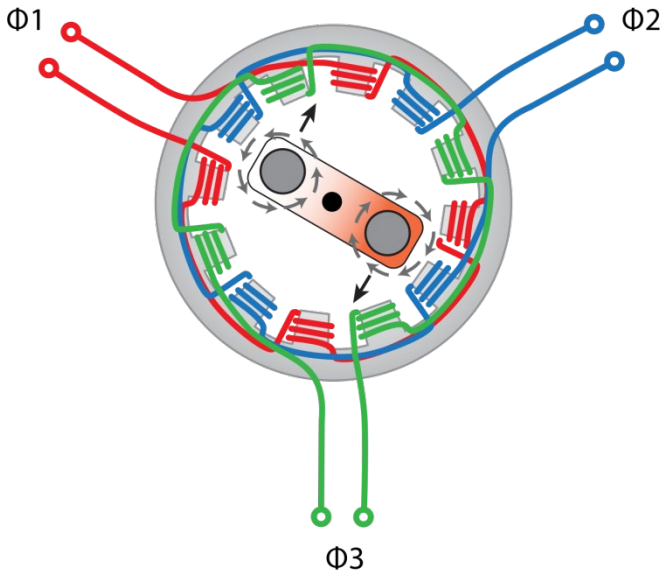


**Figure 120: In this three-phase AC induction motor with a single-pole rotor, the stator's rotating magnetic field induces the rotor magnetic flux field.**

three-phase ACIMs can range from <<1 hp (<750 W) to >1000 hp (>750k W) with voltage ratings from a nominal 120 $V_{AC}$ to 14.4 $kV_{AC}$ , with a majority in the 600 $V_{AC}$ class (120 to 600 $V_{AC}$) running on three-phase power with horsepower ratings <500 hp (375 kW). three-phase ACIMs fall into several broad categories, as follows:

- Small Induction - 120-240 $V_{AC}$, <1 hp (<750 W)
- Medium (Low-Voltage) Induction – 600 $V_{AC}$ class (380 V to 600 $V_{AC}$) typically three-phase except in the lower power ratings, >1 hp (750 W) and up to 500 hp (375 kW)
- Large (Medium- or High-Voltage) Induction – 5 $kV_{AC}$ (2.4$kV_{AC}$ to 7.2 $kV_{AC}$) and 15 $kV_{AC}$ class, three-phase ≥500 hp (375 kW)

 

## AC Permanent-magnet Synchronous Motors (PMSMs)

AC permanent-magnet synchronous motors (PMSMs) have an AC three-phase stator but use a permanent magnet to generate a DC rotor flux field. Do not confuse PMSMs with an AC "wound-rotor" synchronous motor, a different (and much larger) motor type that uses a DC power supply to create a DC magnetic field in a wound coil rotor. Figure 121 shows this motor construction.

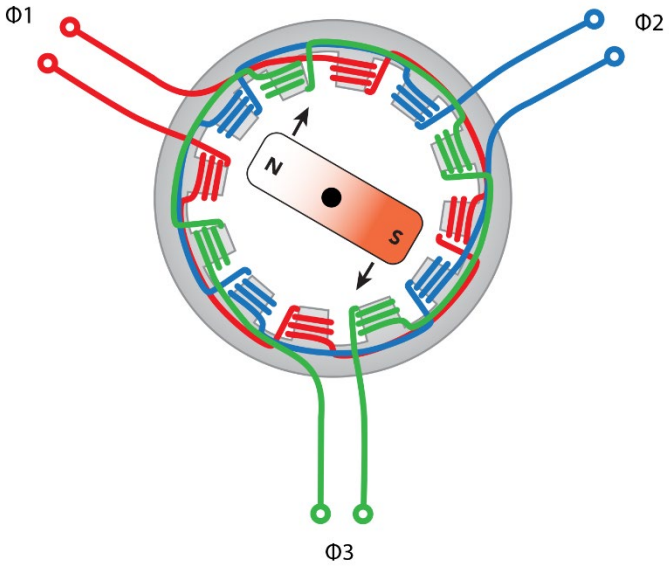


**Figure 121: In this three-phase PMSM motor with a single-pole rotor, the stator's rotating magnetic field interacts with the permanent magnet rotor field to create rotation of the rotor.**

Typically, PMSMs are using some type of motor drive to supply pulse-width modulated (PWM) voltage to the stator. Power ratings can range from <<1 hp (1 kW) to 100 hp (75 kW). In general, these motors have very high power outputs for small size, especially if built with rare-earth permanent magnets (with very high magnetic flux densities).

Some engineers refer to PMSM motors as "brushless DC" (BLDC), "brushless AC" (BLAC), or electronically commutated motors (ECMs). In all these cases, the mechanical design is essentially the same – each contains a permanent magnet rotor, a stator coil, and an inverter circuit that inverts a DC source to create a three-phase PWM output (i.e., "electrical commutation"). However, in general, most engineers would agree that a PMSM motor uses an electrical commutation scheme that applies three-phase voltage to all three windings at any given time, which results in a sinusoidal back-EMF voltage waveform on the stator winding. We know this as "sinewave modulation." This modulation scheme costs more but offers control performance with less audible noise and torque ripple than that described for brushless DC motors.

 

## "Brushless" DC (BLDC) Motors

In reality, "brushless" DC (BLDC) motors are not DC motors at all – the term "brushless" seeks to distinguish them from a "brushed" (conventional carbon-brush) DC motor. We also know BLDC motors as electronically commutated motors (ECMs), Brushless AC (BLAC), or PMSMs. Like PMSMs (described above), they utilize a three-phase electrically commutated AC stator winding with a permanent magnet rotor.

Many use the terms BLDC and PMSM interchangeably because the mechanical and electrical construction of the motor is largely the same for both types. However, in general, most engineers agree that a BLDC motor utilizes a six-step commutation scheme in which rotor position is actively sensed or calculated, and voltage is applied as a PWM waveform to only two of the three stator windings at one time with the switching of the winding voltages based on the sensed or calculated rotor position. Because we apply voltage to only two of the three phases at any given time, the line-neutral back-EMF voltage waveform on each phase is trapezoidal in shape, not sinusoidal. Therefore, we know six-step commutation as "trapezoidal" control. The nature of the applied voltage signal makes BLDC motors noisier during operation (audibly and electrically) than other designs, with higher torque ripple than PMSMs. However, they have reasonable cost and good torque characteristics. They often find use in lower power applications (e.g., small appliances, power tools, small pumps, etc.) where cost is a critical concern.

## "Brushed" DC Motors

Conventional "brushed" DC motors include a field (stator) winding and an armature (rotor) winding. Connection of these two windings may be in series, parallel, or series/parallel. They may be energized from the same DC voltage supply, or the field (stator) winding may be separately excited from the armature (rotor) winding. Different applications require different torque vs. speed performance, or lower or higher levels of control capabilities. Thus, there is a variety of winding constructions and excitation choices.

In all constructions, a DC voltage applied to the field (stator) winding generates a stator magnetic flux field that interacts with the armature (rotor winding). However, rotor rotation requires an alternating or rotating field (stator) magnetic flux field. That field comes from a commutator and carbon brush scheme that periodically reverses the voltage polarity applied to the rotor, which reverses the rotor magnetic field. Figure 122 shows this motor construction.

 

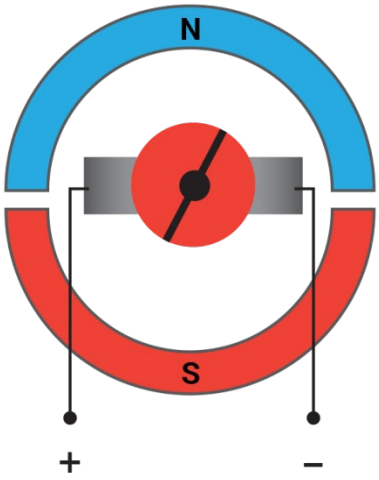


**Figure 122: In a brushed DC motor, a commutator and carbon brush scheme periodically reverses the voltage polarity applied to the rotor, which reverses the rotor magnetic field so that it opposes the stator magnetic field to produce rotation of the rotor.**

In a DC motor, the field (stator) voltage and current control the (fixed direction) magnetic flux density seen by the (armature). By increasing or decreasing the field voltage (and therefore the field current), the field magnetic flux can be increased or decreased (thus controlling the speed). In a DC motor with a separately excited armature (rotor) magnetic flux field (i.e., not a series or shunt-wound design), the armature magnetic flux field can also be varied (thus controlling the torque). The armature magnetic flux field is always (by definition) orthogonal to the field magnetic flux, so the motor is always operating at peak torque for a given armature magnetic flux field (i.e., applied armature voltage).

Lower power brushed DC motors use a permanent magnet to generate the field and armature magnetic flux fields. Higher power brushed DC motors use an applied voltage to generate the field and armature magnetic flux fields.

The drawback of a brushed DC motor is the mechanical complexity, reliability, and cost. The mechanical commutator uses carbon brushes to “commutate” power through an insulated slip ring segment attached to the rotor. Carbon brushes wear over time and require replacement. Additionally, DC voltage is not widely available except from batteries in residential, commercial, or industrial locations, and, for a larger motor, must be supplied by an AC-DC converter, adding cost and complexity.

Despite the mechanical complexity and reliability issues of DC motors, they had very favorable control characteristics. Independent adjustment of voltage in the field and armature windings provides independent and tight control of both speed and torque, a scheme often used in variable-speed applications. Such a scheme always produces peak torque for a given applied voltage, which is a highly desirable situation. Modern AC motor drives replicate these ideal control capabilities using vector field-oriented controls (FOCs) with the mechanically simpler and more reliable ACIMs and PMSMs.

Today, the primary applications for brushed DC motors are as very small and/or low-cost motors used in throwaway devices such as children’s toys, electric toothbrushes, or mobile phone vibrators.

 

## Universal Motors

These motors combine characteristics of ACIMs and brushed DC motors. Given that they employ a carbon-brush commutation scheme, their original market advantage was to offer a better AC motor utilizing an additional DC field coil. With the pervasiveness of motor drives for control of ACIM, PMSM, and BLDC motors, universal motors are not seen as a viable alternative with 50/60 Hz voltage inputs and are not used with motor drives either. Therefore, their usage has declined considerably.

## AC (wound-rotor) Synchronous Motors (ACSM)

ACSMs utilize a three-phase (sinusoidal, utility-supplied) voltage to generate the rotating AC magnetic field in the stator and use a supplied DC voltage from a rectified AC supply (via slip-ring supply) to a rotor winding to generate a DC magnetic flux field. They are sometimes simply known as "synchronous motors." Figure 123 shows this motor construction.

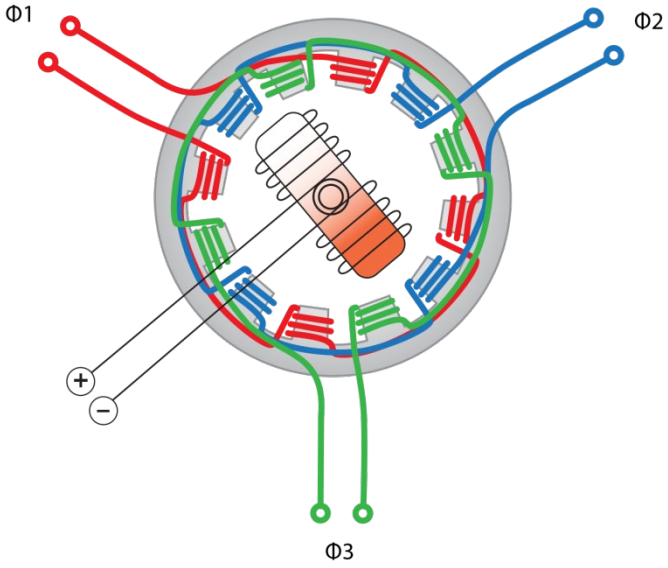


**Figure 123: An AC (wound-rotor) synchronous motor uses a three-phase sinusoidal voltage to generate the rotating AC magnetic field in the stator and uses a rectified AC supply (via slip-ring supply) to generate a supplied DC magnetic flux field in the rotor winding.**

The rotor magnetic flux field rotates at the same rate as the applied AC magnetic flux field. Given a stable applied AC magnetic flux field (as would be supplied by the 50 or 60 Hz from a utility), the rotor spins at a constant, predictable speed related to the AC stator supply frequency and the number of stator and rotor pole pairs as long as the load is not beyond the design rating. The speed is "synchronous" to some multiple of the input frequency up to the rated load of the motor. Unlike an ACIM, there is no slip angle between the stator and rotor magnetic flux fields. Additionally, ACSMs exhibit a power factor of 1.0, to the benefit of larger users of electricity who often pay a penalty to the utility for low power-factor operation. ACSMs are widely used in industrial processes due to their ability to run at a constant speed, despite significant load changes.

ACSMs are also built in small sizes using permanent magnets, but in general, references to an AC synchronous motor today mean a larger (>100 hp) AC motor with an applied DC rotor field run at a

 

constant speed to supply a large industrial load. They do not benefit from use with a variable frequency motor drive given their dedication to constant speed operation.

## Switched Reluctance Motors (SRMs)

Switched reluctance motors became possible with the advent of electronically commutated motor controls. An SRM is essentially a three- or four-phase stator and a rotor that has no magnetic field but possesses magnetizing properties (i.e., laminated steel). As Figure 124 illustrates, the SRM's rotor has no magnetic elements.

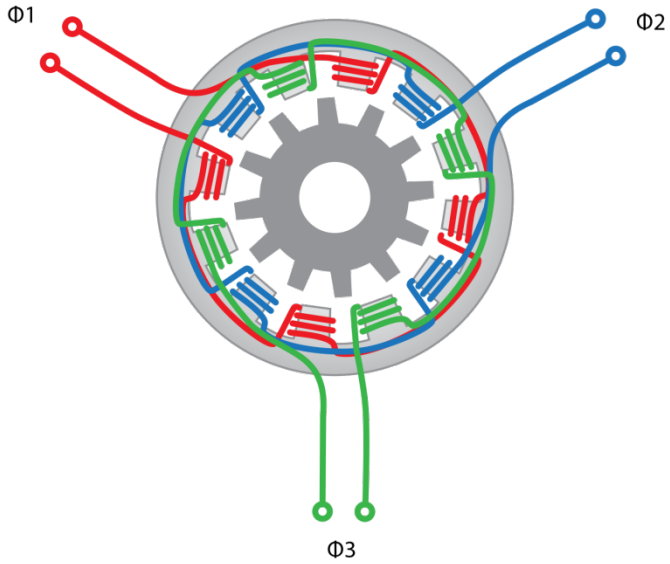


**Figure 124: A switched-reluctance motor (SRM) employs a three- or four-phase stator (three phase is shown here) and a rotor capable of being magnetized by the stator's magnetic field. The misalignment of the rotor magnetic poles with the stator poles creates torque on the rotor.**

As with BLDC motors, sensors determine rotor position, but we apply voltage to only one phase at a time (perhaps two at a time during startup). Application of stator voltage creates a rotating magnetic field, and torque on the rotor comes from the misalignment of the rotor poles with the stator poles. The rotor magnetic flux field follows the path of least magnetic reluctance, hence the name.

SRMs can be very low in cost but have the highest noise and torque ripple of any electronically commutated motor. SRMs are possible only with the advent of motor drives, and there is significant cost savings and reliability improvements associated with their use. However, they carry significant drawbacks (high torque ripple, high noise) and they have only been widely commercialized where these drawbacks aren't commercially penalized. Two application examples are wheel motors for large off-road vehicles and vacuum cleaner motors.

## Servomotors

Servomotors are a sub-class of various types of ACIMs or PMSMs that utilize rotary position sensors to allow movement and setting of an exact rotor position for an industrial application, such as machine tools, valve control, etc. Motors used in servo applications must have well-documented torque vs. speed characteristics, power, mechanical rotor inertia, etc. AC servomotors typically use permanent magnet rotors to minimize motor size and rotor mass. This avoids excessive rotor inertia when positioning the rotor/shaft (we use ACIMs where more power is required). Some type of rotor position feedback with known shaft position is required for detection and control of the exact rotor position.

## Stepper Motors

Stepper motors contain a permanent-magnet rotor with a switchable stator coil operated much like a solenoid coil. By energizing the stator coil to a different pole, the rotor aligns with the stator coil magnetic flux field. As its name implies, a stepper motor does not rotate continuously but merely "steps" from one position to another based on the switching of the stator coil voltage.

# Variable Frequency (Motor) Drives (VFDs)

## Introduction

As described previously, an electric motor operates when an applied rotating magnetic field on the stator causes application of an opposing force to the free-moving rotor that is connected to a rotor shaft that then performs work. Historically, AC induction motors were connected directly to fixed-frequency line voltages, and relatively simple control systems or other mechanical means (a mechanical brake, a valve to adjust fluid flow, etc.) were used to adjust the speed or output. Often, an AC induction motor was oversized, and the output adjustment was very inefficient. This led, in general, to higher initial purchase and operating costs with relatively poor motor speed and torque control. DC brushed motors, with inherent capability for independent speed and torque control, were prized for their control capabilities, but suffered from high mechanical complexity, high cost, and low reliability. Permanent-magnet synchronous motors, when connected to a fixed-frequency line voltage, had the same limitations as AC induction motors.

To combine the reliability of an AC induction motor or permanent-magnet synchronous motor (i.e., no carbon brushes that wear) with the variable speed and precise torque control of a brushed DC motor, we use a complex electronic control. Such a control modulates the duty cycle of a pulse-width "digital" voltage signal applied to the stator winding(s) of the motor and manages the period during which the digital pulse-width's alternate polarity is controlled. By precisely controlling both the pulse width durations and period, we achieve precise control of the applied stator voltage and frequency. The systems that provide these pulse-width-modulated (PWM) outputs and control capabilities are known as variable frequency drives (VFDs), variable-speed drives (VSDs), Inverter drives, or, more commonly, motor drives, and they use power semiconductors to provide the PWM output signals as described previously. We apply the PWM output voltage signals to the motor stator winding, just as a line voltage would be. Note that a PWM signal has quite different harmonic content and signal qualities compared to a sinusoidal line voltage signal, and this must be taken into account when designing a motor to prevent insulation failure in the motor. Thus, we often label motors designed to work with VFDs as such.

After a brief discussion of VFD uses, this section explains VFD operation including a discussion of VFD architecture and topologies. The latter includes a detailed description of the popular dc bus (link) topologies including the voltage-sourced inverter, the current-sourced inverter, the load-commuted inverter and the matrix converter or cyclo-converter. This section also explains the common pulse-width modulation (PWM) techniques—carrier-based and space-vector pulse-width modulation.

## VFD Applications

VFDs can be as simple as a single-phase input/output drive with no sensor inputs ("sensorless") for control of motor speed only. An example is a variable-speed control managing the speed and direction of a ceiling fan. Or, VFDs can be quite complex with three-phase input/output, many precision sensor inputs, and complex algorithmic processing to provide precise speed and torque control in either rotational direction (much like that provided by a brushed DC motor). Such drives handle widely varying loads and may regenerate power back to the source (e.g., a vehicle propulsion application with re-generative braking).

 

By design, ACIMs operate at various speeds using VFDs and thus are a natural fit for many industrial and commercial applications. Often, these motors are oversized and do not need to run at full speed at all times in their intended application. It may also be desirable to control precisely the torque in addition to the speed. Because the power consumption of the motor varies with the cube of the speed, reducing the speed by half reduces the power consumption to one eighth, which is a significant increase in efficiency when a lower rotor speed provides acceptable performance.

In general, we primarily find VFDs paired with larger ACIMs in industrial plants and processes requiring precise speed and/or torque control as well as significant operational efficiencies. VFDs coupled with smaller BLDC or PMSM motors serve complex control capabilities (e.g., washing machine motor, vehicle propulsion motor) where operational efficiency may not be the highest priority. Of course, the lines blur quite often — small mini-split HVAC compressor motor VFDs deliver both control and efficiency optimization while small refrigerator compressor motors are designed primarily for operational efficiencies.

## VFD Operation

All VFDs convert a DC voltage to a pulse-width modulated (PWM) AC signal that is applied to the motor terminals. VFDs operating from a battery input do not require AC rectification, while those that operate from an AC line require rectification and filtering to obtain a stable DC bus.

Figure 125 shows a typical simplified schematic of the complete power conversion section of an AC-AC three-phase VFD. In a preceding section of this primer, we described the cascade H-bridge power conversion topology (shown with IGBTs; MOSFETs may be substituted). We now more appropriately describe it in the simplified schematic as the “Inverter Subsection”. The three-phase AC line input is rectified by a six-pulse (six-diode) rectifier in the “Rectifier Section” and filtered to a low-ripple and stable DC bus voltage in the “DC Bus” or “DC Link” section (the terms are used interchangeably). Also shown are the signals present in the circuit at the AC line input, DC bus, drive output, and gate-drive of the power semiconductor devices. This particular VFD is very representative of most VFD designs and is a class of voltage source inverters (VSIs).

 

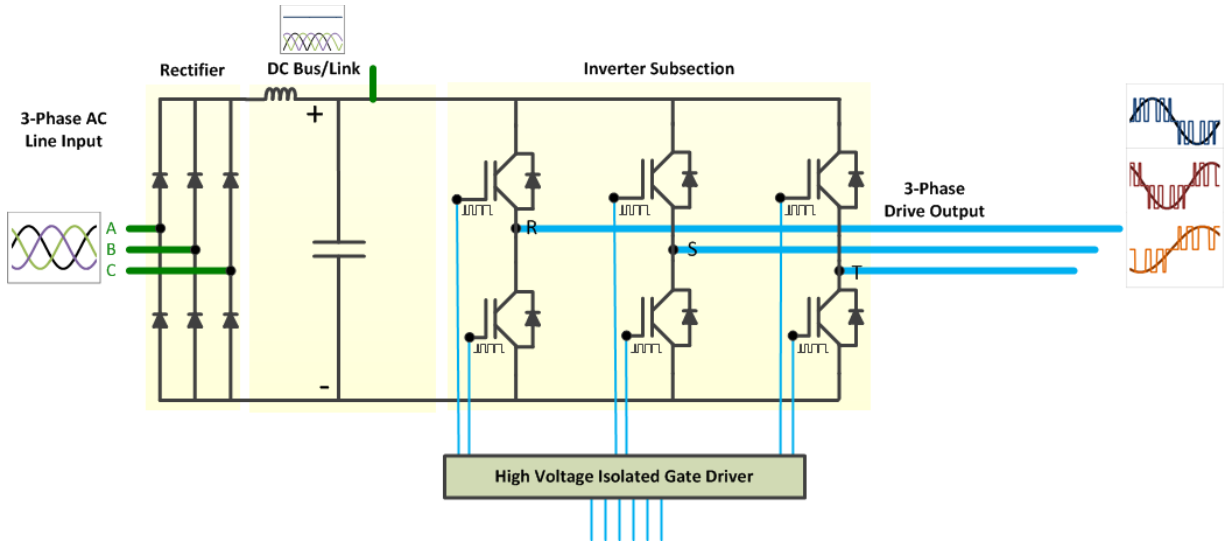


**Figure 125: The power conversion section of an AC-AC three-phase VFD rectifies and filters the AC line input to create a stable DC bus voltage, which then powers the inverter subsection.**

The input to the VFD is typically a 50/60 Hz, single- or three-phase signal (typically referred to as A, B, and C phases). It is supplied at a voltage anywhere from a nominal 120 $V_{AC}$ to a nominal 600 $V_{AC}$. While motor drives with higher voltage inputs or outputs (e.g., 4160 $V_{AC}$) would likely use a multi-level power conversion inverter subsection topology different from that shown above, the concept is the same. When applied to the motor winding, the three-phase PWM motor drive output causes a current to flow in the winding. The characteristics and quality of the PWM voltage output signals relate to the PWM control methodology. Varying the PWM signals' width results in more or less voltage applied to the winding. Varying the period of alternation for the upper and lower gate-drive signals determines the frequency of the alternative positive and negative PWM outputs. Combined, the drive output produces signals resulting in the desired speed, torque, power, and efficiency characteristics from the motor.

A high-voltage, isolated gate driver connects the Control/Logic system to the power semiconductor gate terminal in the Inverter Subsection. The controls take feedback signals from the motor and other parts of the circuit to calculate how to switch the gates of each power transistor on and off to create the appropriate PWM signal at the power semiconductor output. Because the controls connect to the gate of the power semiconductors, there is no ground reference for many of the signals on the controls; thus, the controls are not at ground potential. Operator-exposed control functions are sometimes isolated with optical links or "floated" in an insulated control connection. The control system's complexity depends on the control requirements. Simple scalar V/Hz controls use low-speed microprocessors in the embedded control system, are low in cost, and require few feedback signals from the drive or motor. More complicated vector field-oriented control (FOC) control systems can use very high-speed microprocessors (>500 MHz) with many feedback signals.

Instrumenting the motor shaft provides position, speed, or torque values. One may instrument the motor itself for current inputs, temperature, vibration, or other physical characteristics. Some of these instrumented signals serve as feedback to the VFD control system, and some serve only for design

 

validation or test. More complex control systems require knowledge of absolute rotor/rotor magnetic field position for proper operation, and therefore utilize quadrature encoder interface (QEI) or resolver speed, direction, and positions sensors.

Figure 126 shows a complete drive system with the complete power conversion section (rectifier, DC bus/link, and inverter subsection), control system, motor, sensors, and interface of all components.

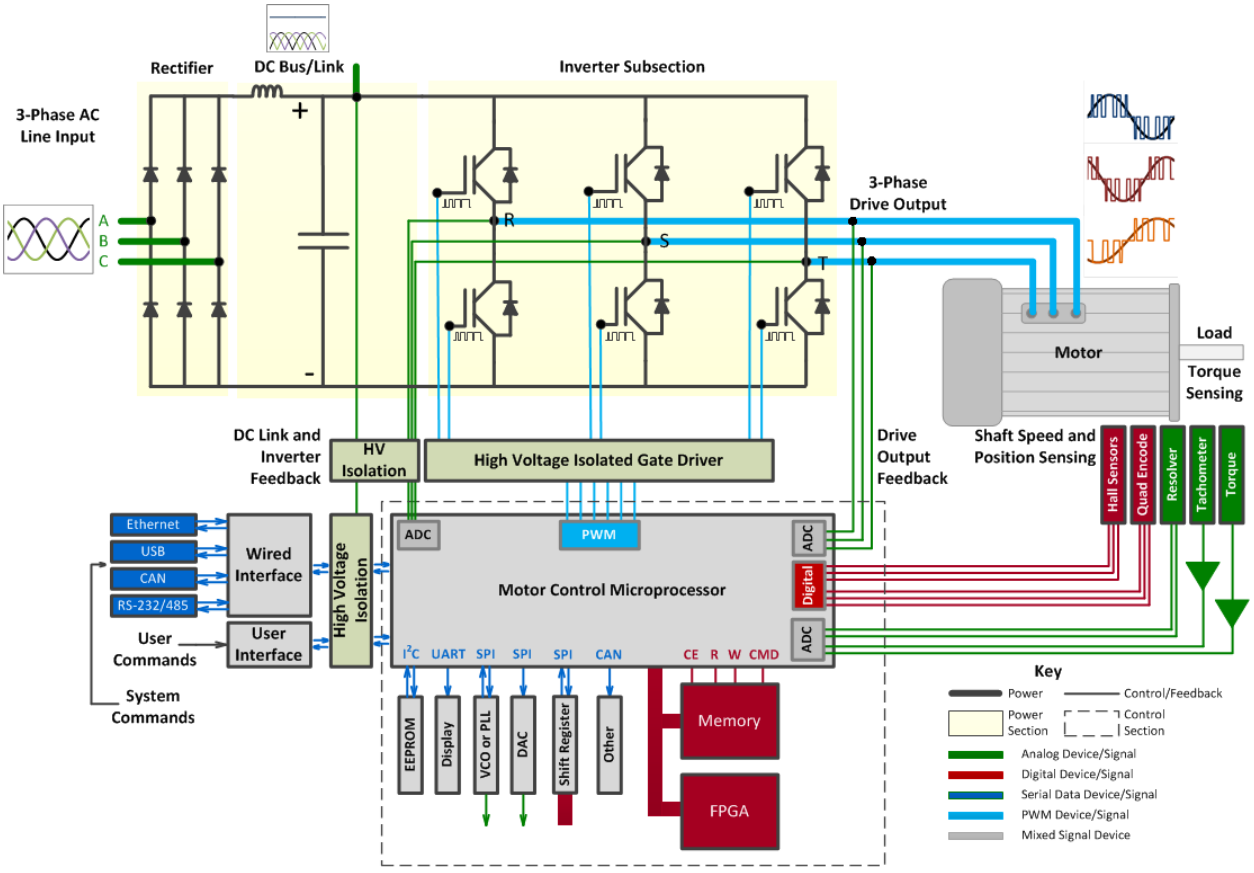


Figure 126: A complete AC-AC three-phase drive system.

## VFD Architecture and Topologies

All VFDs have much in common. The essential elements that describe the VFD power conversion section are:

- Input-output voltage ratings
- DC bus (link) topology
- Power semiconductor components used in the inverter subsection
- Inverter subsection topology

The essential elements that describe a VFD control and software section are:

- (Gate-drive) pulse-width modulation (PWM) techniques
- Motor drive control architecture and algorithms

 

### Input-Output Voltage Rating

The input to the VFD can be either single- or three-phase AC, or DC (e.g., from a battery). In the case of a DC input, the DC bus topology could change slightly because filtering is not required on a rectified AC input, and some load limiting might be necessary to prevent too much current being drawn from the battery too quickly.

The output of the VFD is nearly always three-phase, even with a single-phase input. The three-phase input to ACIM, PMSM, or BLDC motors makes control simpler and efficiency higher, which overrides any additional up-front cost for a three-phase motor winding compared to a single-phase winding. The exception would be very simple loads (e.g., fans and blowers) that run at low power levels, do not require much speed control, and/or have simple speed control requirements, and serve highly cost-sensitive applications.

### DC Bus (Link) Topologies

The DC bus stores energy for input to the inverter subsection. Enough energy should be stored so that the DC bus is "stiff" (i.e., stable) and does not change voltage appreciably under load. Ideally, the DC bus is free of ripple and well isolated from changes or perturbations in the line input. Ripple on the bus may indicate inadequate mains (line) supply, poor inverter design, or problems with the inverter operation, and engineers often monitor the DC bus ripple to correlate it with other VFD behaviors. We supply DC bus voltage data to the motor drive as a feedback signal. For instance, knowledge of the DC bus voltage and the switching times of the inverter drive circuit facilitate calculations regarding the AC output voltage, which is critical feedback for more complex drive-control systems.

If the input comes from a battery or step-down AC power supply, the DC bus voltage may be relatively low (≤50 V). From 240 $V_{AC}$ single-phase inputs, it may be as high as 340 $V_{DC}$, or 690 $V_{DC}$ (using three-phase 480 $V_{AC}$ rectified outputs). Vehicle propulsion systems commonly use DC buses (batteries) in the range of 300-500 $V_{DC}$. The maximum DC bus voltage for a 600 V class device is 976 $V_{DC}$ (based on 600 $V_{AC}$ +15% overvoltage rating, three-phase). The DC bus voltage is the highest possible (common-mode) voltage present in the circuit, and voltage probes or cables connected to the DC bus or inverter subsection must be properly isolated with a common-mode voltage safety rating equal to or greater than the DC bus voltage.

The three main topologies for the DC bus are:

- Voltage-sourced inverter (VSI)
- Current-sourced inverter (CSI)
- Load-commuted inverter (LCI)
- Matrix converter (MC) or cycloconverter

#### *Voltage-Sourced Inverter (VSI)*

In all VSIs, the DC bus stores energy as voltage in a capacitor in parallel with the inverter subsection. Typically, we place an inductor in series with the capacitor to perform harmonic filtering. VSI designs are the simplest and most cost-effective in motor drive applications. VSIs deliver higher-performance motor control (faster peak current deliveries and therefore better ability to dynamically control motor torque),

 

lower harmonics, and higher power factors on the mains input. All of these are important considerations for industrial power usage. Additionally, phase conversion (from one-phase to three-phase AC) is possible with a VSI drive, important for lower-power motor drive applications. Most VFDs are VSI-based, and all further discussions in this document will assume VSI architecture for the motor drive.

### *Current-Sourced Inverter (CSI)*

In a current-sourced inverter (CSI), the DC bus stores current in an inductor. CSI response times are slower due to the delay in delivery of current from the inductor to the inverter subsection input. CSIs also require a different PWM signal that contributes to higher harmonics on the mains. Lastly, the limitations of the CSI require a higher-cost design to mitigate the performance issues. We rarely see CSIs used in motor drive applications.

### *Load-Commutated Inverter (LCI)*

A Load-commutated inverter (LCI) uses thyristors (SCRs) and therefore cannot use PWM signaling for the output voltage. Historically, LCI applications were limited to soft starts of very large motors, and it is no longer widely used with the advent of IGBTs of higher power and voltage.

### *Matrix Converter (MC)*

A matrix converter (MC) or cycloconverter eliminates the DC bus and uses a direct connection from the AC rectified output to the inverter input. We find applications for MCs in HV power line switching or frequency conversion, or small-range control of relatively large motor loads (e.g., ship propulsion) where the efficiency or harmonics advantages of eliminating the DC bus are relatively high compared to the control drawbacks.

## Power Semiconductor Devices

As described in a prior section, motor drive inverter subsections use either MOSFETs or IGBTs. Both device types are widely used, with MOSFETs typically found in 240 $V_{AC}$ (and lower) input drives and IGBTs in 380 to 600 $V_{AC}$ input drives for cost, reliability, efficiency, and other reasons.

Devices incorporating wide-bandgap materials, such as SiC or GaN, have faster rise times; expect to see them used more often in drives for efficiency reasons. For semiconductor-device analysis of switching and conduction losses, engineers want higher-bandwidth voltage and current measurements. For measuring drive outputs, lower bandwidth works well enough because the fastest wide-bandgap materials are rarely deployed at their highest speeds due to reliability or EMI/RFI emissions issues.

## VFD Inverter Subsection Topology

We discussed basic power conversion topologies in a prior section. Single-phase VFDs use H-bridge topologies while three-phase VFDs use cascaded H-bridge topologies. Both topologies result in two-level output signals. Other topologies provide more than two levels, as described previously. Most VFDs paired with motors in the 600 V class and lower use two-level cascaded H-bridge topologies. Although additional levels add cost and complexity, they achieve lower output harmonics or better speed/torque control.

 

## Pulse-Width Modulation Techniques

Voltage output from the VFD is controlled with various modulation schemes, all of which result in simple one-level PWM gate-drive signals (one per power semiconductor device) and one-level (or sometimes more than one-level) signals at the output of each phase of the motor drive. When the output voltage is viewed line-line, these one-level line-reference signals are two-level line-line signals. The PWM drive's output signals vary in quality based on the control and modulation technique chosen for the drive. In general, customers refer to these different control techniques as one of many different "sine-modulated" techniques or a "six-step commutation" technique. A sine-modulated technique applies voltage to all three phases at once, whereas a six-step commutation technique applies voltage to only two of the three windings at any given time.

The one-level PWM gate-drive signals are determined and generated through a simple carrier-based method or through a more algorithmically complex space vector (pulse-width) modulation (SVM or SVPWM) method. Carrier-based PWM methods are simpler to program and implement and cost less (because they require less processing to generate the PWM signal) but have higher harmonic content. SVM methods require more implementation skill, cost more (due to higher microprocessor speed and cost in the VFD's embedded control system) and lower harmonic content. SVM methods are a necessary component of the vector FOCs, which provide the most advanced control capabilities, and are also simpler to employ in a multi-level (>2-level) inverter.

### Carrier-Based PWM

Typically, in a carrier-based PWM implementation, the carrier (high) frequency is a triangle wave and the modulating (low-frequency speed control) signal a sinewave. This is a common approach in simple Scalar V/Hz (sine-modulated) and Six-Step Commutated controls. Sinusoidal intersective carrier-based PWM method is the most widely used in new designs.

Sinusoidal, intersective carrier-based PWM employs a constant-amplitude, high frequency (~1-100 kHz) carrier and a low-frequency control signal (~60 Hz, or whatever the desired VFD output frequency may be, with a fixed or varying amplitude). The intersection of the modulating sinewave with the carrier frequency creates the width-modulated signal. Figure 127 shows a simple example of PWM for a single power semiconductor device in which the PWM signal has a 50% duty cycle of the modulating signal at 0 V:

 

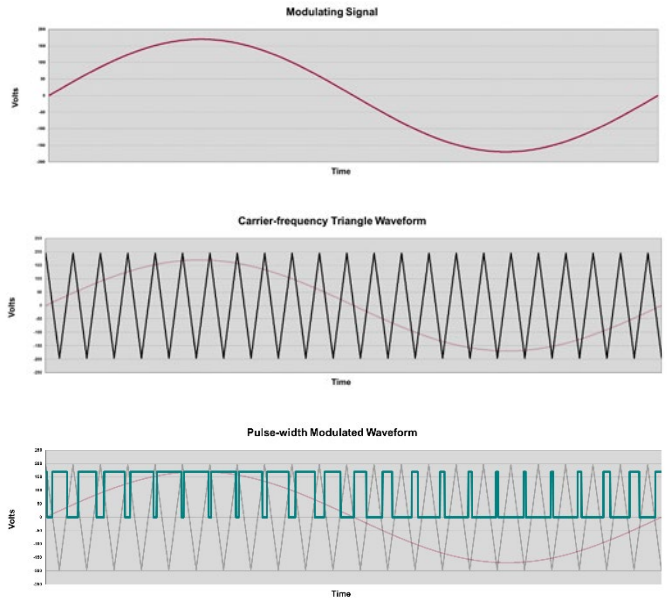


**Figure 127: In this example of sinusoidal, intersective carrier-based PWM, a low-frequency sinewave representing motor speed modulates a high-frequency triangle wave.**

The carrier frequency is either a triangle or a sawtooth waveform; the choice of waveform defines the intersection with the modulating waveform for purposes of width determination. The example shown above is for a triangle waveform, but the frequency used was <<1kHz (i.e., illustrative only) so that the signal could be more easily viewed with a lower-frequency modulating signal.

As described earlier, for half- or full-bridge power conversion systems, the upper and lower devices switch independently. Thus, the PWM waveforms for each device become slightly more complicated to "view" and understand how they relate to the power-conversion device or drive output, but the basic concept is the same. For example, for a half-bridge implementation, there is an upper and lower device, and the two devices switch in a complementary fashion to create the full output waveform. Figure 128 shows the upper device PWM waveform at the top, the lower device PWM waveform at center, and the total output (upper minus lower) PWM waveform and modulating waveform on the bottom (the carrier-frequency waveforms are omitted in this example, but they are the same as in the single-device example shown above):

 

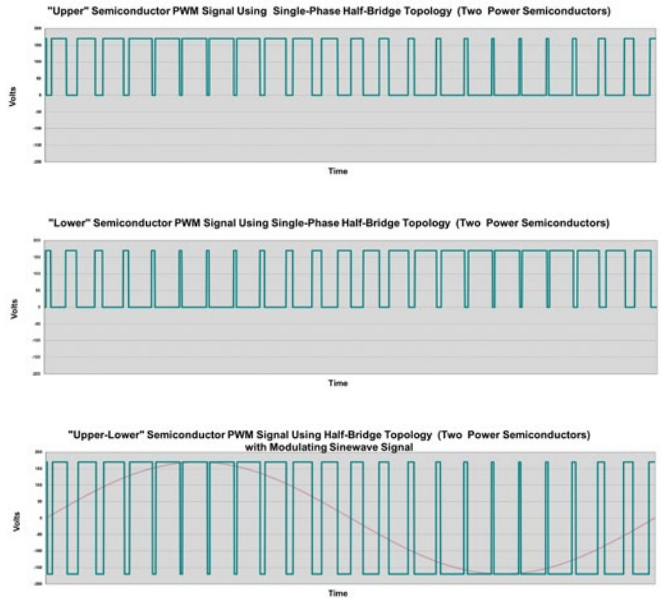


**Figure 128: PWM waveforms for a half-bridge implementation.**

Figure 129 shows the upper and lower device PWM waveforms and the total output PWM waveforms.

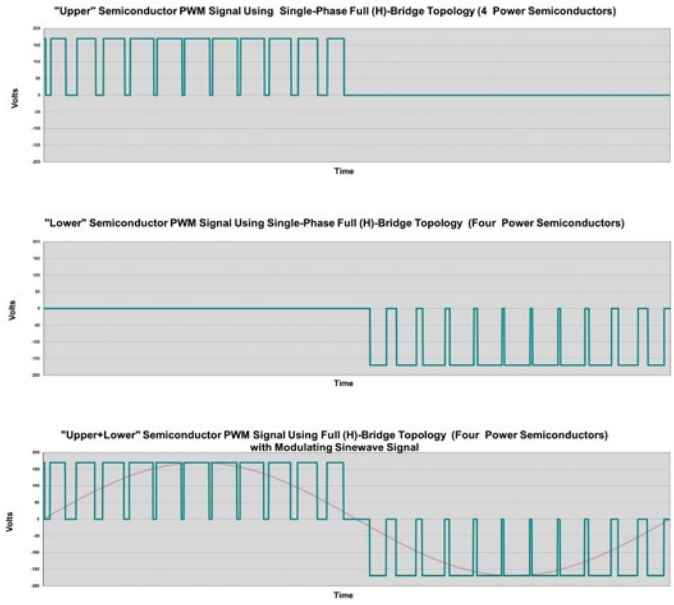


**Figure 129: PWM waveforms for a full-bridge (also known as H-bridge) implementation.**

Typically, for a three-phase (e.g., cascaded H-bridge) design, we create one modulating signal in the microcontroller and then phase-shift that signal by 120° and 240° to create the other two modulating signals for the other two phases. Therefore, there are three PWM waveforms sets in this case, as shown in an earlier example.

 

Note that both series power semiconductor devices in a half-bridge, full-bridge, or cascaded H-bridge topology cannot be switching ON at the same time, so some minimum "dead time" before and after switching is built in to the controls to avoid a "shoot through" short-circuit and subsequent device/system failure. The result of this dead-time can be seen in the lower waveform in Figure 129.

### Space Vector (Pulse-Width) Modulation (SVM, or SVPWM)

In SVM, we use a matrix transformation to transform a three-phase voltage signal corresponding to the rotating stator magnetic field into a single rotating "space vector" in a two-dimensional reference frame. This simplifies calculation of a single voltage magnitude and angle, which is then inverse-transformed back to a three-phase voltage signal from which we generate the gate-drive PWM signals.

This is an algorithmically more complex modulation scheme compared to a conventional carrier-based PWM, but it allows suppression of certain harmonics, improving the VFD's harmonic performance. SVM may be employed in either a scalar V/Hz control system (in place of a carrier-based PWM scheme) or in a vector (field-oriented or direct torque) control. It is required in the latter because vector controls require generation of a referenced space vector as part of their control system.

There are several variants of space vector modulation based on the alignment of the pulse widths within a defined "time slot." The alignment can be center-aligned, left-aligned, or right-aligned. The choice of alignment depends on available processing power and the importance of harmonic suppression (some alignment methods require less gate switching, and so create less harmonic content on the VFD output.

A more detailed explanation of how space vector modulation works is beyond the scope of this document. Regardless, the VFD PWM output signals look essentially the same as with carrier-based PWM modulation schemes.

 

# Motor Drive Control Architecture and Algorithms

## Introduction

There are three primary methods for achieving variable frequency motor control: scalar V/Hz, six-step commutation (also known as trapezoidal control), and vector control. One may implement all of these methods in an open loop (few or no sensor feedback signals from the motor) or closed loop (significant sensor feedback required from the motor) with various algorithms.

## Control Architecture and Algorithm Overview

Figure 130 shows the hierarchy for the various VFD control architectures and common algorithms.

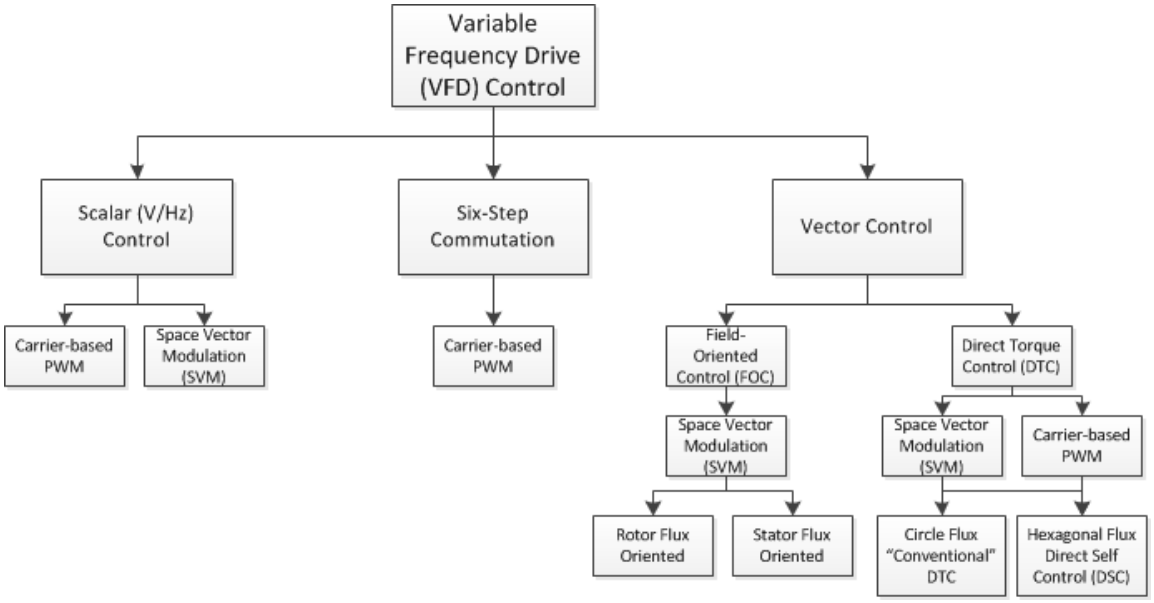


Figure 130: VFD control hierarchy

 

Figure 131 shows a “generic” control block diagram (note that not all control methodologies utilize all of the signal inputs to the control as shown below):

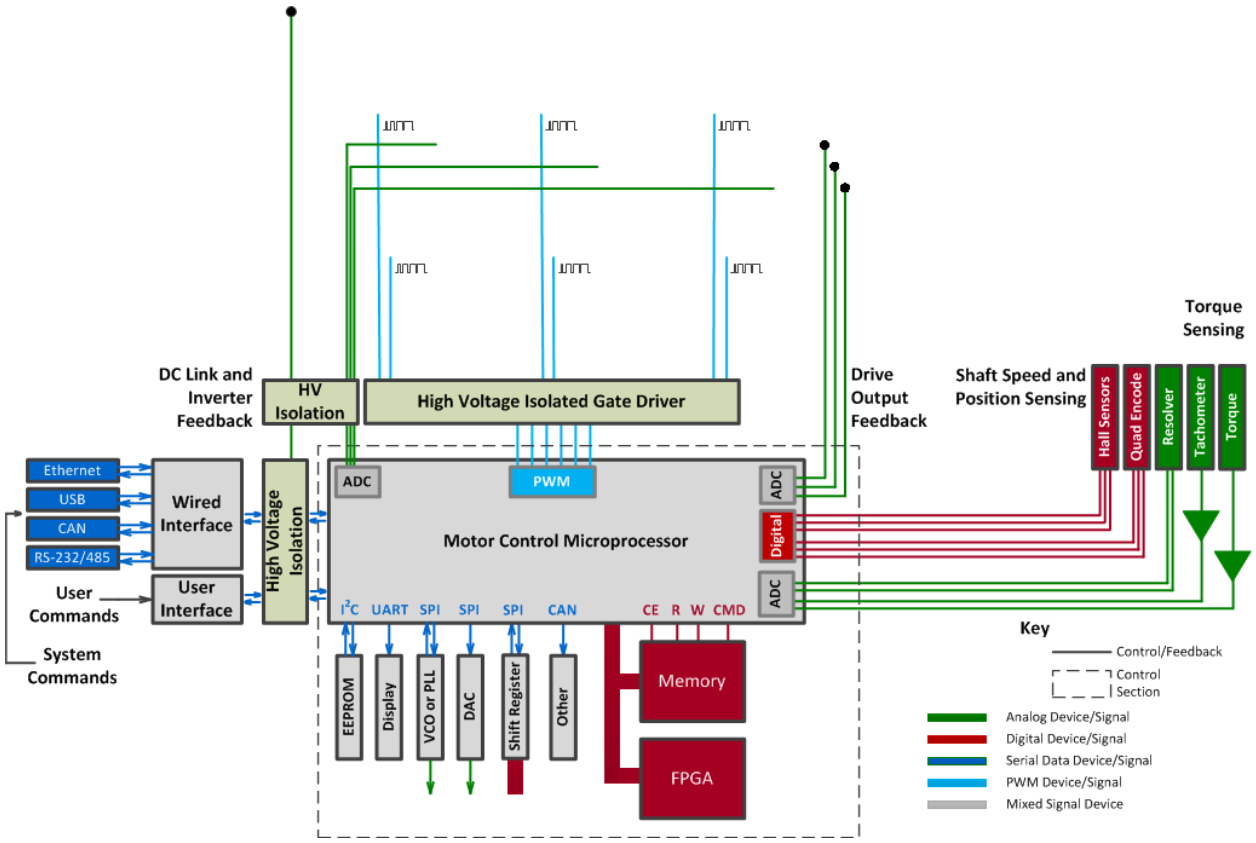


Figure 131: Generic control block diagram for variable-frequency motor drive.

The motor-control microprocessor system accepts inputs from the motor (speed, direction, position, and torque) and digitizes them for further processing. Drive feedback signals (output voltage or current, DC bus voltage and current, gate-drive signals, etc.) are likewise monitored and digitized. We combine knowledge of the motor and drive operational state with system or user (speed and torque) commands to permit calculation of the necessary gate-drive signals. Thousands of times per second, these signals switch the transistor devices in the inverter subsection to achieve the appropriate output voltage and frequency to the motor. Thus, a VFD control system is a very complex embedded control with a variety of analog, digital, serial data, and sensor feedback signals on the input/output, and it requires its own debug/validation separate from the inverter subsection before it can be debugged as part of the complete VFD.

The Teledyne LeCroy Motor Drive Analyzer with eight analog channels, 12-bit resolution, 16 digital inputs, and up to 2 GHz of bandwidth, is ideal given the large number of signals that must be monitored at one time for proper debug and characterization (Figure 132).

 

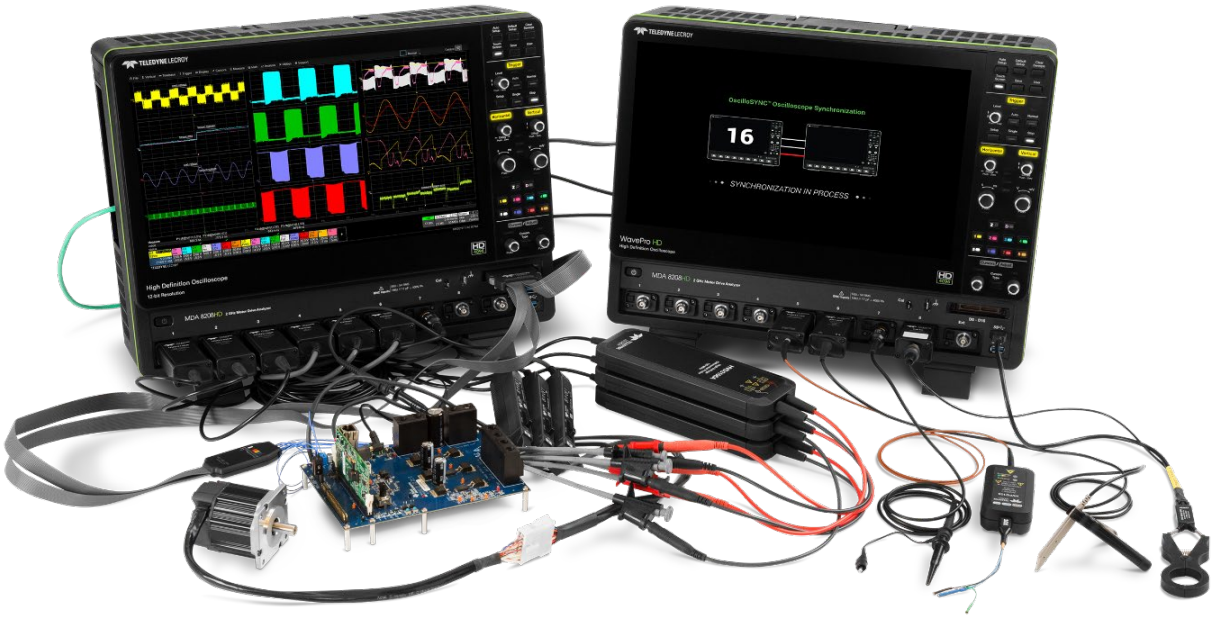


**Figure 132: Featuring eight analog channels (16 when connected with OscilloSYNC™) and 16 digital inputs, Teledyne LeCroy's MDA 8000HD series is optimized for debug and characterization of VFD power sections and control systems.**

VFD controls differ in the types and quantity of sensor signals that are input to the control system, the complexity of the processing done by the control system, and when output signals are sent to the power-transistor gate drives in the inverter subsection.

Scalar (V/Hz) VFD control is the simplest type, providing control of voltage and frequency (motor speed) in a simple xV-per-yHz relationship with no possibility of direct torque control. Scalar V/Hz controls are ideal when high quality control is not required and/or where low cost is highly desirable, such as in fan controls and power tools. Scalar controls can use a carrier-based PWM or space vector modulation. Realistically, simple carrier-based PWM would predominate in this type of control.

Six-step commutation control is used exclusively with BLDC motors. They typically use rotor-position feedback from Hall-effect sensors mounted on the rotor shaft. Sensorless (back-EMF sensing) techniques can help lower costs (with some loss of control at lower speeds). In both implementations (sensored and sensorless), only two of the three windings have a voltage waveform applied at any given time. The result is a trapezoidal (as opposed to sinusoidal) back-EMF (BEMF) waveform that is distinctly non-sinusoidal. Such a control, while very simple and relatively inexpensive for the level of control it provides, results in more distorted output voltages and applied currents. It also produces high torque ripple and an audibly noisier motor operation. It has the advantage of low implementation cost.

Vector field- or flux-oriented control (FOC) provides instantaneous and simultaneous control of speed and torque. Best known simply as vector controls, they are ideal in complex applications such as pumps, milling machines, elevators, or electric propulsion motors. However, implementation comes at a higher

 

cost due to increased control complexity and motor sensor requirements. Vector FOCs transform the three-phase AC voltage system of the motor into a two-coordinate vector system that represents the operation of the applied stator magnetic flux field from the perspective of the rotor (rotor flux-oriented) or stator (stator flux-oriented). They then use this simplified two-coordinate system for calculation of applied voltage before transformation back to a three-phase vector system for calculation of pulse-width modulated gate drive signals. Vector FOC controls always use a space vector modulation method for PWM.

As their name implies, vector direct torque controls (DTCs), control torque directly through precision motor-current sensing and a "lookup table" based on various torque hysteresis loop methods. Space vector modulation most often provides gate-drive signal generation. Vector DTC provides control and performance approaching that of vector FOC controls, but with (claimed) lower algorithmic complexity and cost due to the lack of mathematical transformations to the rotor reference frame. In short, they are "good enough" for many applications with potentially lower cost and higher reliability.

### Scalar V/Hz Controls

Scalar V/Hz controls, also known as V/f or variable-voltage, variable frequency controls, manage motor speed as a function of frequency using a simple lookup table. They do not directly control motor torque and have limited ability to control motors at low speeds or under highly dynamic conditions in which torque requirements change quickly. These controls can be either open loop (without sensors) or closed loop (with sensors), depending on the application, cost targets, and requisite control capabilities. Scalar controls can use either carrier-based PWM or SVM (both of which are sinewave-modulated methods) to control the gate-drive signals. A simple scalar V/Hz open- or closed-loop controller has inherent limitations on control of the motor's speed or torque, especially under dynamic conditions, but is low in cost.

Figure 133 shows a sample V/Hz voltage vs. speed (frequency) profile. We program an operating curve into the motor-control microcontroller to govern the operating profile ranging from maximum voltage and speed operation to low-voltage and low-speed cutoffs.

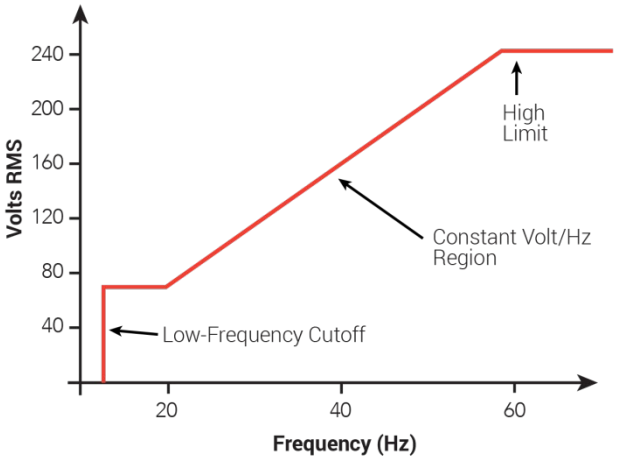


Figure 133: A voltage vs. speed (frequency) profile for scalar V/Hz control.

 

We most often find scalar V/Hz controls on smaller and/or lower voltage AC induction motors (ACIMs) or AC permanent magnet synchronous motors (PMSMs). The output voltage waveforms appear as previously described (reference the Vector FOC controls section for detailed screen captures). Each type of motor can use either open-loop or closed-loop control, depending on the application's needs.

### *Scalar V/Hz (Open-Loop) Control*

An open-loop scalar V/Hz control fits well when minute or fast changes in motor speed are not required, and when the accuracy requirements of speed changes are lax enough not to warrant the higher cost of a scalar V/Hz *closed-loop* control, which requires a speed sensor and a more complex and costly control system. With no feedback speed sensors on the motor, the PWM voltage signals are determined based on the desired speed and the assumption that the motor will roughly track the voltage vs. speed profile, with any errors in speed considered minor and acceptable. Torque control happens only under very specific and known conditions, so applications requiring constant or dynamic torque control do not use this method. Typical applications would be in heating, ventilation, and simple (and low-cost) air-conditioning (HVAC) motor applications (e.g., window air conditioners).

### *Scalar V/Hz (Closed-Loop) Control*

The closed-loop variant of the scalar V/Hz control is essentially the same as the open-loop version with the addition of a speed sensor input to the drive controller. Monitoring of this speed signal provides more accurate values for voltage and frequency, which in turn means better dynamic control and more accurate motor speeds. Torque control improves compared with open-loop controls but does not approach the performance of a vector control in this regard.

Figure 134 shows a detailed block diagram of a scalar V/Hz closed-loop control system. From it, one can see the isolation between the gate drive of the MOSFETs in the inverter, the six (three differential-pair) PWM output signals from the control to the VFD, and the speed feedback signal(s) from the motor to the control system.

 

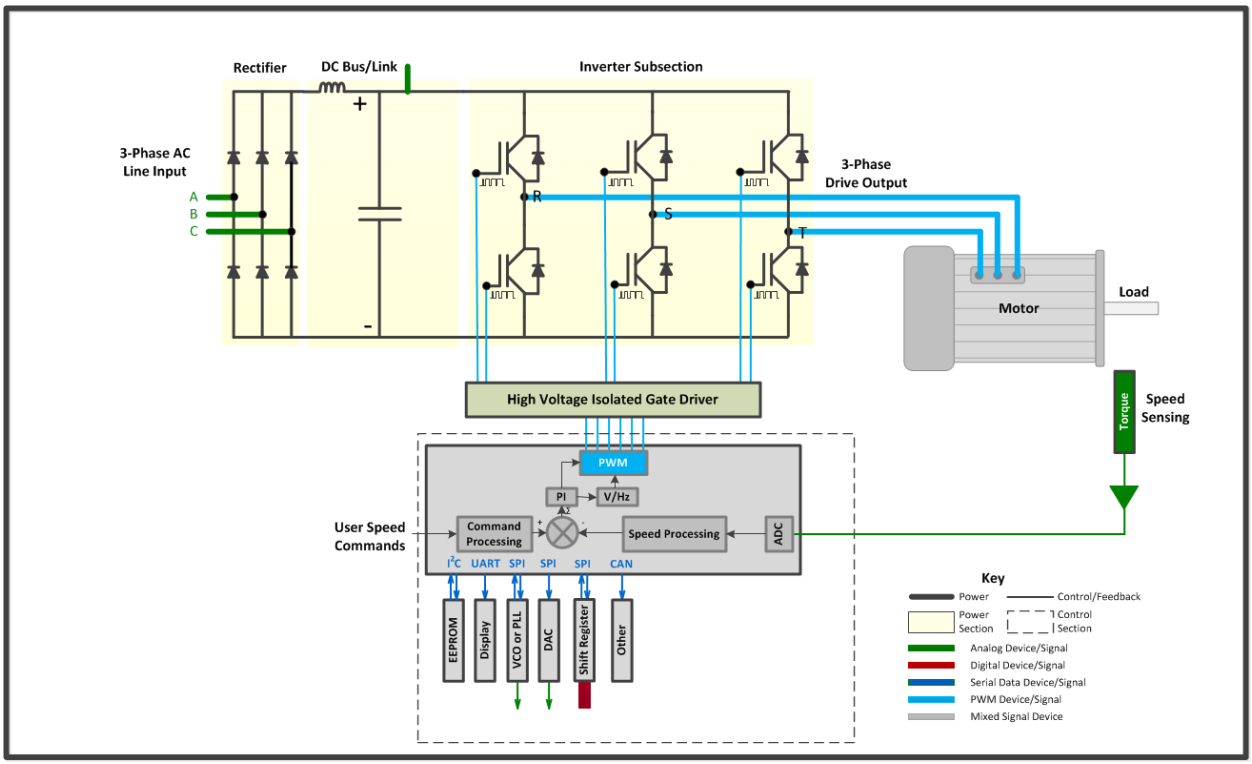


**Figure 134: A scalar V/Hz closed-loop control system employs isolation between the control circuitry and the gate driver and also between the control circuitry and the speed sensor.**

## Six-step Commutation (Trapezoidal) Control

Six-step commutation control finds use exclusively with BLDC motors. “Six-step” refers to the number of switching states in the electronic commutation circuit as one rotor magnetic pole rotates 360°. There are six steps because there are typically three Hall-effect sensors that can be either on or off, representing six rotor position steps that require specific stator commutations. What makes six-step commutation unique is that only two of the three stator motor phases are energized at any given time. Therefore, the back-EMF (voltage) in the stator winding appears trapezoidal when probed from line-reference, and for this reason is sometimes referred to as “trapezoidal control” or “trapezoidal modulation”.

Figure 135 shows a screen capture using Teledyne LeCroy’s Motor Drive Analyzer to capture a motor drive line-reference output voltage and current from a six-step commutated motor drive. Z1 (yellow), Z2 (magenta), and Z3 (blue) are the three line-reference voltage waveforms; Z4 (green), Z5 (gray), and Z6 (purple) are the three line currents. Note that there are six distinct “steps” on Z1, Z2 and Z3: two off steps, one step ramping up, two steps on, and one step ramping down. These represent the six different states in which PWM is not applied, partially applied, or fully applied to that stator coil. The back-EMF influence from a nearby (energized) phase on the adjacent (non-energized) phase results in the “ramp up” or “ramp down” of the peak voltage, and thus the trapezoidal shape.

 

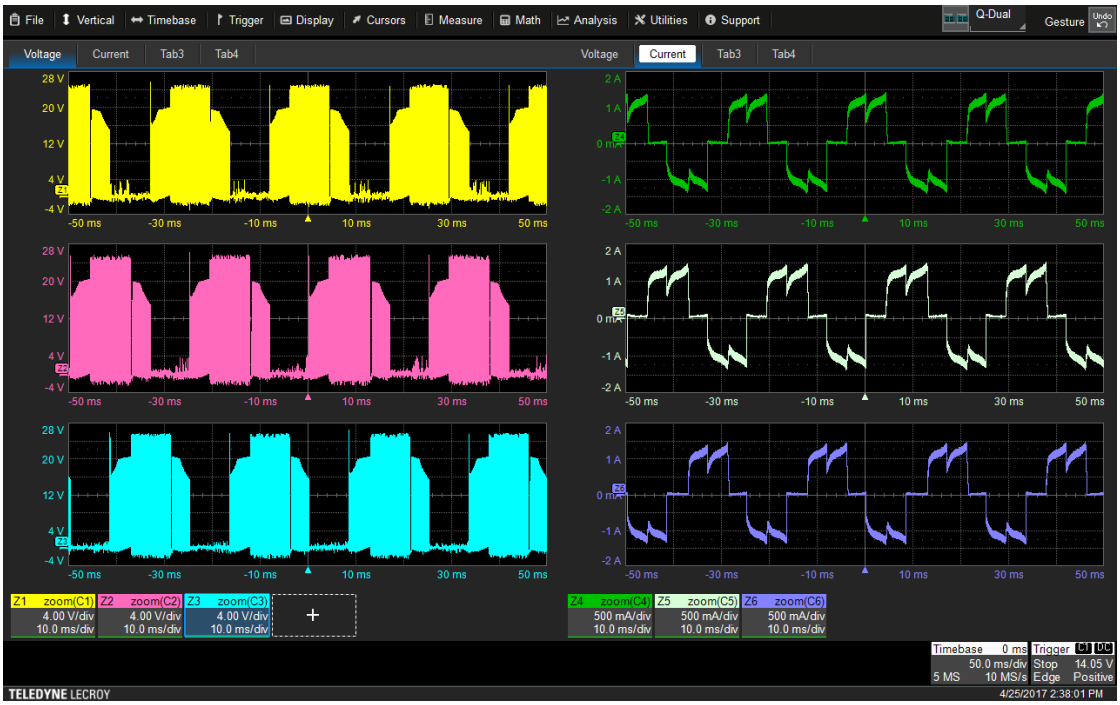


**Figure 135: Six-step commutation control produces the motor drive line-to-reference output voltages (waveforms on left) and currents (waveforms on right) shown here. The back-EMF influence from a nearby (energized) phase on the adjacent (non-energized) phase results in the "ramp up" or "ramp down" of the peak voltage, and thus the trapezoidal shape.**

Figure 136 shows a zoom of the complete trapezoid and the detail of the PWM waveforms.


**Figure 136: By zooming in on the trapezoidal waveforms, the underlying PWM signals become visible.**

 

The six-step commutation method reduces cost and complexity compared to the sinusoidally-modulated methods but results in higher torque ripple and more audible noise emanating from the motor.

BLDC VFDs may be closed-loop (sensored) or open-loop (sensorless) systems, with closed-loop systems more common. Hall-effect sensors (typically three) installed in the rotor perform closed-loop sensing to provide feedback to the VFD on both rotor position and direction. The Hall-sensors may be located either 60° or 120° apart. When the three sensors are spaced 60° apart, we place them on one side of the rotor. At 120° separation, they are equally spaced around the rotor. Figure 137 shows a screen capture of an acquisition of three line-reference six-step commutated voltages signals together with three Hall sensor signals captured using the digital logic (MSO) capability of the Motor Drive Analyzer. Note the time-correlation between the change in Hall sensor logic states and the three difference voltage waveforms.

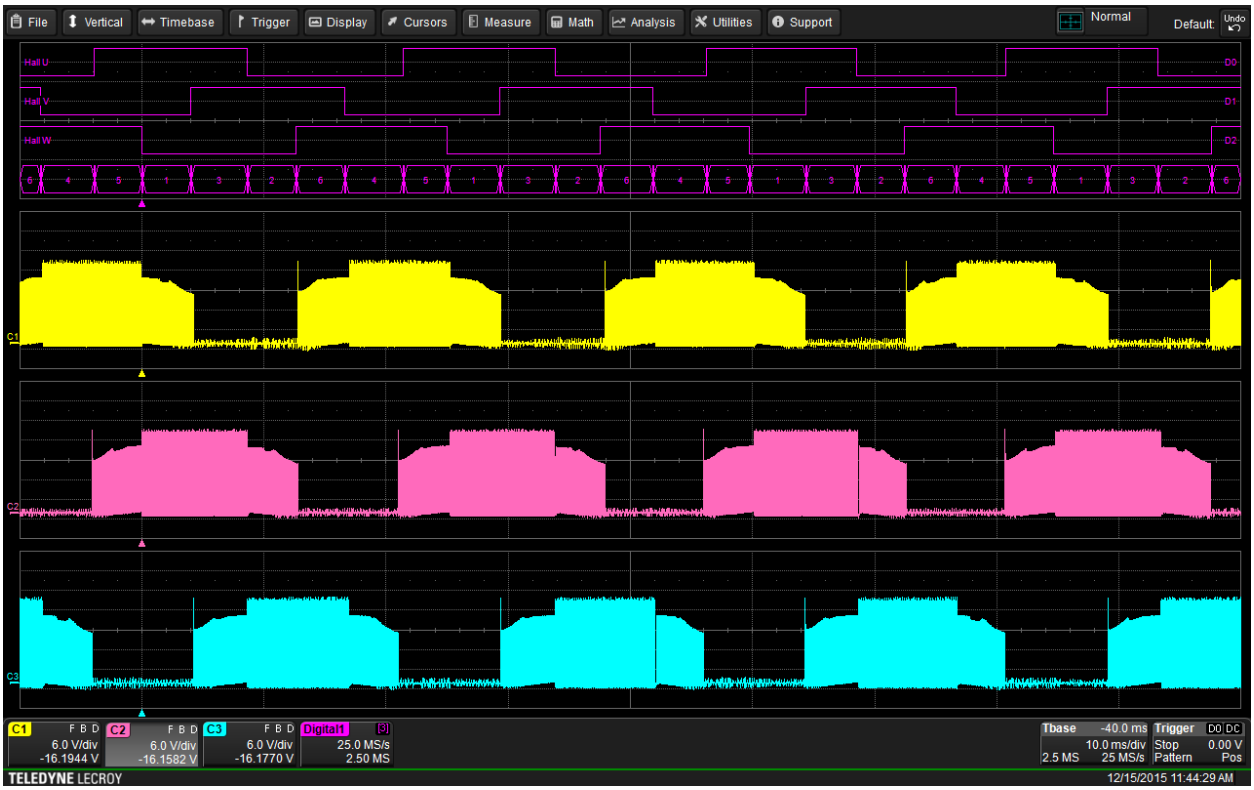


**Figure 137: Line-to-reference six-step commutated voltages signals together with their three Hall sensor signals.**

 

Note that a line-line voltage output always has some voltage present on it since no two lines ever both have a zero voltage level. Figure 138 shows these line-line voltage signals. Note that a differential voltage probe was used to probe the voltage signals in this case.


**Figure 138: Line-to-line six-step commutated voltages signals together with their three Hall sensor signals.**

Figure 139 shows an acquisition of two of three line-line drive output voltage signals (Z1, or yellow and Z2, or magenta) with two drive output motor line current signals (Z4, or gray and Z5, or green); the three digital Hall-sensor traces (Hall U, V, and W, yellow traces); and the torque sensor signals (Z7, or red). In this case, only two of the three voltage and current signals were acquired because a two-wattmeter method measured drive output power Note how the Hall-sensor signals overlap with the voltage switching, and the resultant torque ripple (high and low frequency).

 


**Figure 139: Two of three line-to-line drive output voltages (Z1, yellow and Z2, magenta) with drive output motor line-currents (Z4, gray and Z5, green); digital Hall-sensor signals (Hall U, V, and W, yellow traces); and torque sensor signals (Z7, red) are shown for a six-step commutated closed-loop (sensored) control system.**

Open-loop (sensorless) systems infer locations of Hall sensors based on back EMF sensing from the voltage signals. They provide reasonable control and have lower cost, but the motor must be spinning for back EMF to be developed. Therefore, sensorless systems are not well-suited to motors that operate at low speed or require control at startup.

Figure 140 shows a detailed block diagram of a six-step commutated (brushless DC) sensored control system. From it, one can see the isolation between the gate drive of the MOSFETs in the inverter (though on a low voltage drive, these would not be necessary), the six (three differential-pair) PWM output signals from the control to the VFD, and the Hall sensor speed/position feedback signal(s) from the motor rotor to the control system.

 

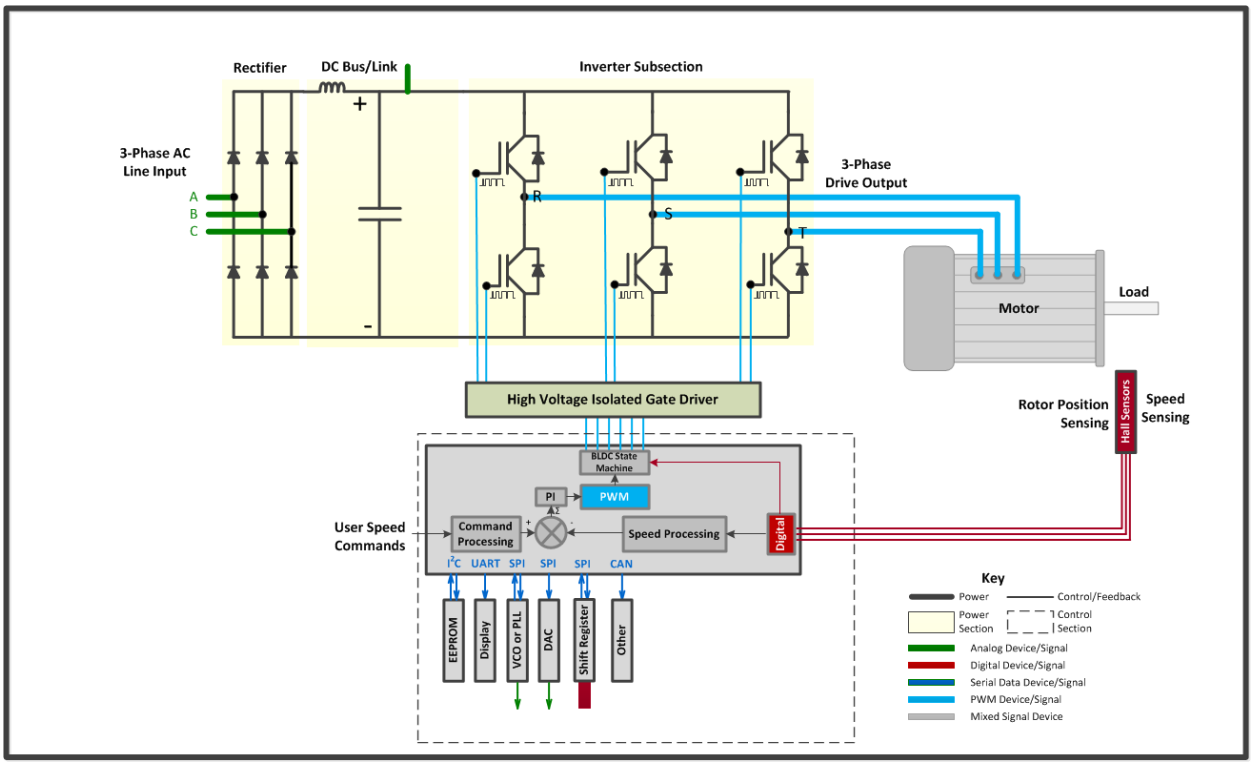


Figure 140: A six-step commutated (brushless DC) sensored control system.

## Vector Flux- (or Field-) Oriented (FOC) Control

Achieving more accurate dynamic speed control calls for use of a more complex control scheme with ACIMs or PMSMs. Vector FOCs simplify the three-phase rotating voltage and current vector system at the drive output to a stationary two-vector system that rotates under changing load, speed, or torque. This is very similar to the classic and simple method of controlling a brushed DC motor with separate field (stator) and armature (rotor) applied magnetic fields, except that one may use an AC motor that has more reliability and efficiency.

There are two methods of vector FOC control – stator flux-oriented or rotor flux-oriented. The difference is in the number of transformations performed on the three-phase rotating vector system. It is more intuitive to understand and apply algorithmic calculations from the perspective of the rotor, so this method is nearly universally used and will be the only method discussed. This method is referred to as a rotor flux-oriented vector FOC and is the more complex of the two methods.

In a rotor flux-oriented vector FOC control scheme, a mathematical matrix transformation decouples the magnetization (speed) producing (direct) currents in the stator from the torque-producing (quadrature) currents so that we may independently control speed and torque for the highest performance. We know this transformation as a dq0 transformation, or sometimes as a Park transformation.

 

The Vector FOC operates in this manner:

- The system either directly monitors or infers applied three-phase drive output signals and currents from known gate-drive switching behavior and DC bus voltage values.
- The system performs two matrix transformations (an αβ, or Clarke, and a dq0, or Park) of this data are performed to transform the rotating vector system in a stationary reference frame to a stationary vector system in a rotating reference frame (i.e., the rotor).
- The control system calculates the next required voltage values in the dq coordinate system (rotating reference frame).
- The calculated direct (d) and quadrature (q) values are then transformed back to a three-phase rotating voltage vector system in a stationary reference frame.
- Gate-drive signals are calculated and supplied to the power semiconductors in the bridge, which results in drive output PWM waveforms.

The calculated d and q values in the control system comprise a single motor stator voltage vector of d and q magnitudes ($V_D$ and $V_Q$) and a single motor stator current vector of d and q magnitudes ($I_D$ and $I_Q$). These are DC values in a steady-state situation (no changing load, speed, or torque), but they dynamically change over time as the load, torque, and speed of the motor change.

We show a summary of the signals at each stage of the transformation and inverse transformation in Figure 141.

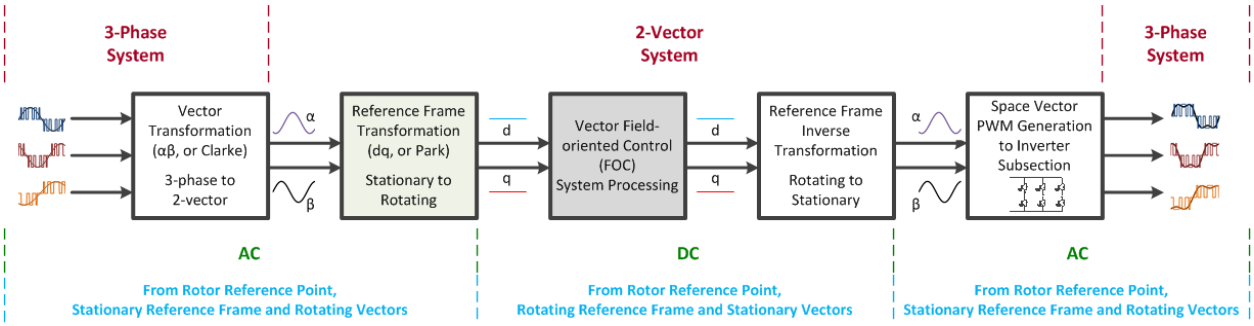


**Figure 141: In a rotor flux-oriented vector FOC control scheme, a mathematical matrix transformation decouples the magnetization (speed) producing (direct) currents in the stator from the torque-producing (quadrature) currents so that we may independently control speed and torque for the highest performance. We know this transformation as a dq0 transformation, or sometimes as a Park transformation.**

The $V_D$, $V_Q$, $I_D$, and $I_Q$ values provide important information to the vector FOC control engineer. For instance, the ripple of the $I_Q$ stator current correlates with torque ripple (lower torque ripple is better; engineers design for low torque ripple).

The calculations made by vector FOCs require high processing power, and therefore the microprocessor in the vector FOC control system is likely to run at speeds in the hundreds of megahertz. In turn, general-purpose control debugging calls for an oscilloscope with a bandwidth of at least 1 GHz. It also requires a measurement of speed, direction, and absolute rotor position using a quadrature encoder interface (QEI) or a resolver. The absolute rotor position provides the basis for calculation of the rotor

 

magnetic field position, which is a necessary step for proper calculation and application of the appropriate stator voltages.

Figure 142 shows the motor drive line-reference output voltage and current from a small, sensorless vector FOC drive output. Any “sine-modulated” drive output (including simple Scalar controls) would look very similar. The three line-reference voltage waveforms are Z1 (yellow), Z2 (magenta), and Z3 (blue) while the three line current waveforms are Z4 (green), Z5 (gray), and Z6 (purple).


**Figure 142: Motor drive line-to-reference output voltages and currents from a small, sensorless vector FOC drive output.**

 

Zooming in clearly reveals the PWM voltage waveform (Figure 143). Note the sawtooth shape to the output current waveforms - this can be clearly seen with the Motor Drive Analyzer's 12-bit resolution.

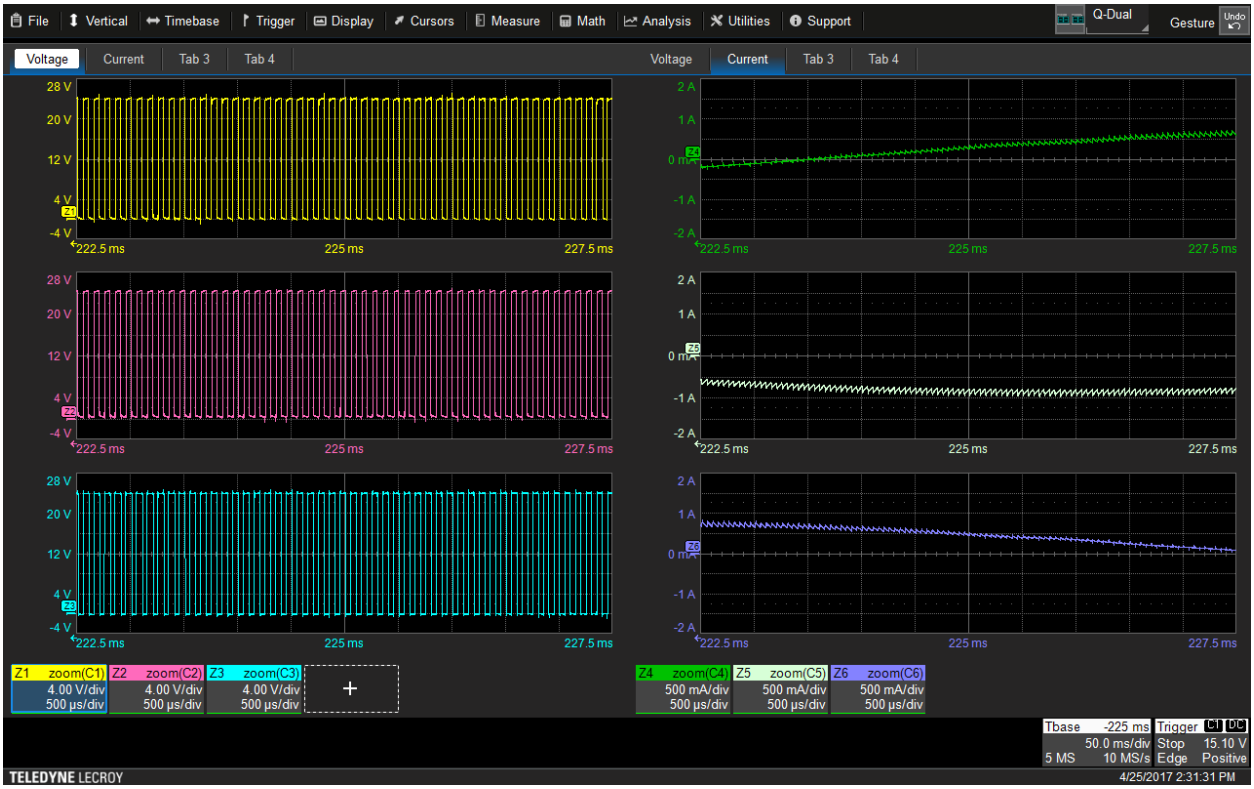


**Figure 143: Zooming in on the line-to-reference output voltages reveals the PWM voltage waveforms and the sawtooth shape of the output current waveforms.**

 

When the voltage is sensed line-line instead of line-reference, the output voltage appears as a two-level signal (Figure 144), with Z1 (yellow) the R-S voltage, Z2 (magenta) the S-T voltage, and Z3 (blue) the T-R voltage (R, S and T are abbreviations for the three-phase drive output).

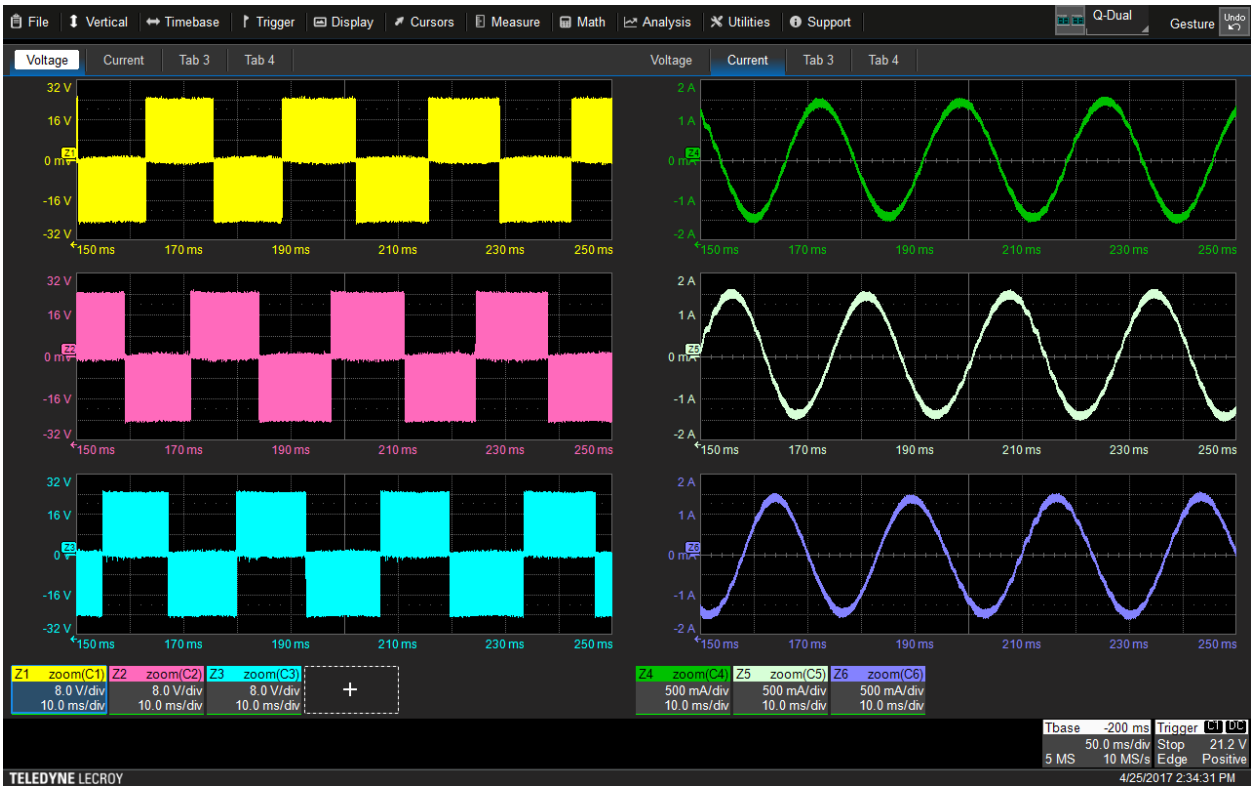


**Figure 144: Sensing the output voltages line-to-line in a sensorless vector FOC drive output causes the output voltages to appear as two-level signals.**

 

When zoomed in to a similar location as the line-reference example, the PWM voltage waveforms are clearly revealed (Figure 145).

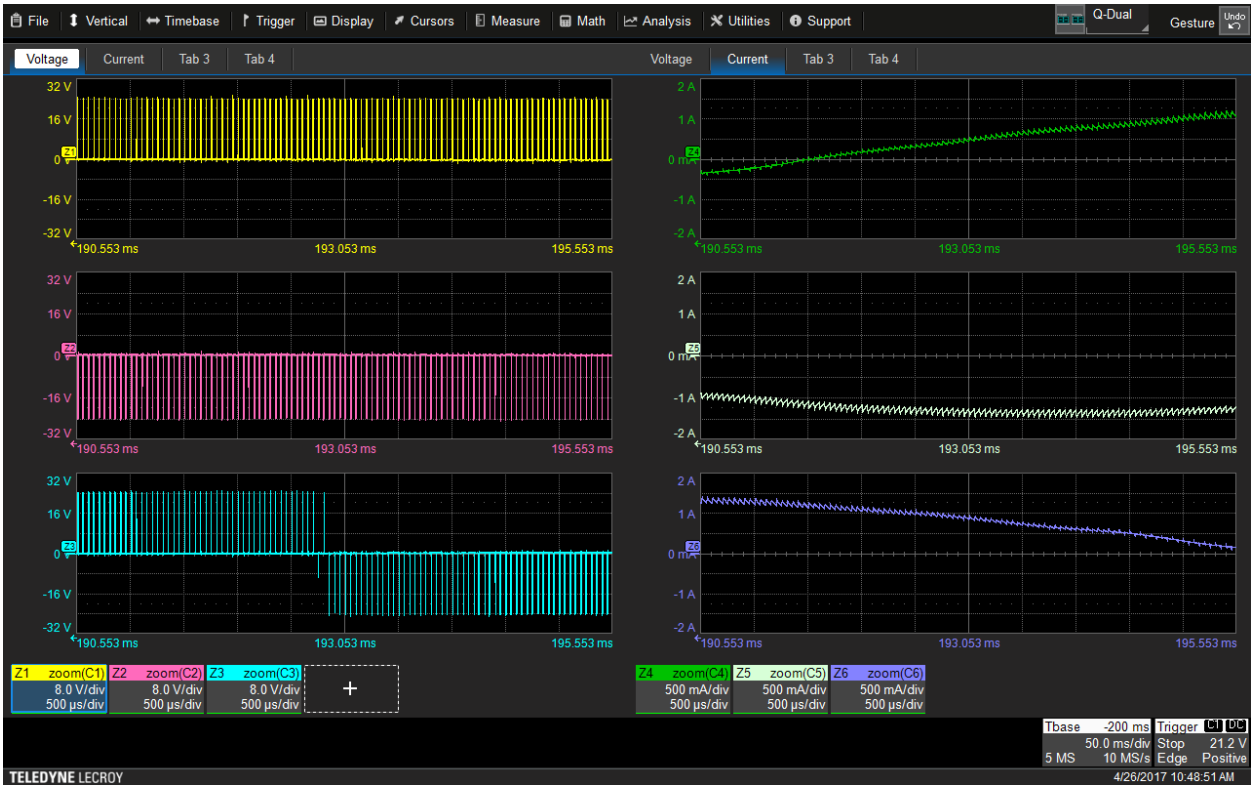


**Figure 145: Zooming in on the line-to-line output voltages reveals the pulse width modulation and two-level nature of the voltage waveforms and the sawtooth shape of the output current waveforms. Note that in this case, the voltage and current waveforms are 30° out-of-phase due to the line-line voltage probing method used.**

Figure 146 shows a typical block diagram for a vector FOC drive system. Note the quadrature encoder or resolver signals (either one may be used) for rotor position and speed that serves as input to the controller, and the DC bus voltage and current sensing.

 

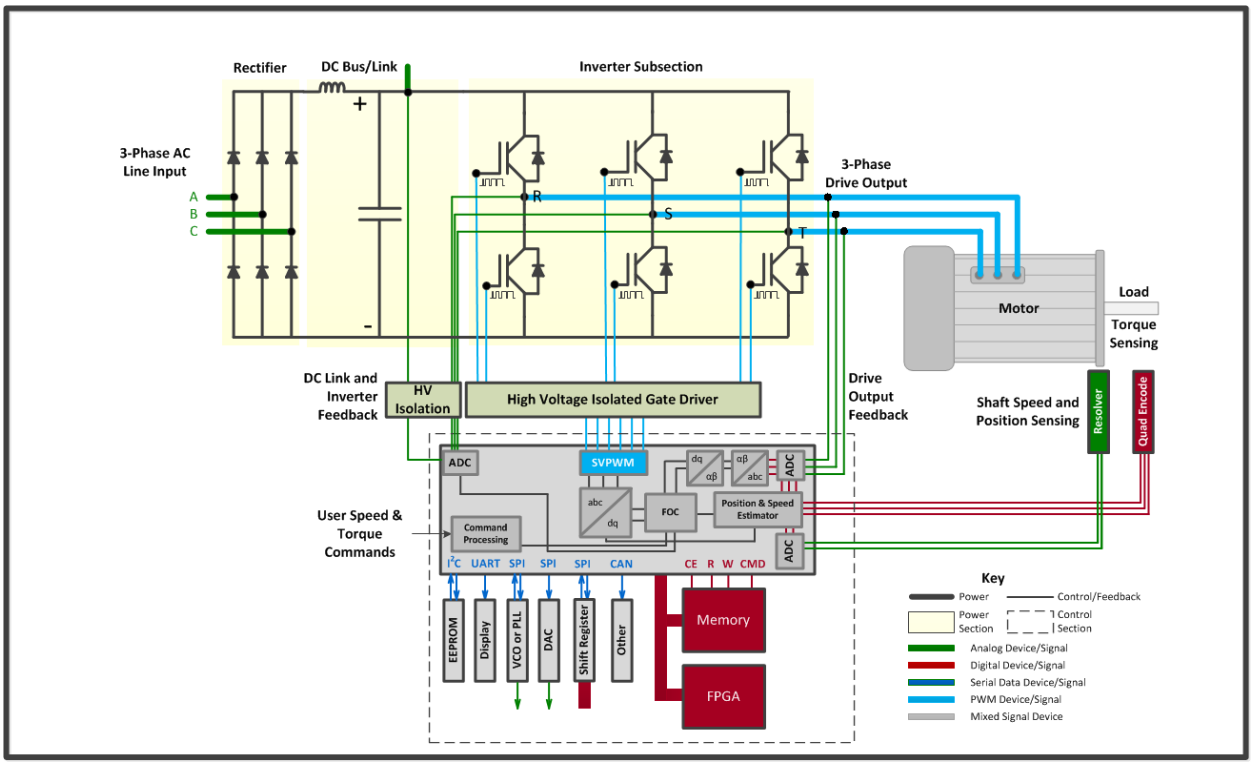


Figure 146: A vector FOC drive system with quadrature encoder or resolver signals and dc bus voltage and current sensing.

## Vector Direct Torque Control (DTC)

Direct torque control is also a vector-control technique, but it does not utilize real-time monitoring of rotor position and speed. Instead, it uses a look-up table to compare directly measured or derived values of motor torque and stator magnetic flux (via measured motor drive output stator currents) with control or user inputs and lookup tables. Then, it performs calculation of gate-drive PWM signals using a space vector modulation technique.

Vector DTC provides control and performance approaching that of vector FOC controls, but with (claimed) lower algorithmic complexity and cost due to the lack of mathematical transformations to the rotor reference frame. In short, they are “good enough” for many applications with potentially lower cost and higher reliability. In general, vector FOC controls are more common on PMSMs; direct torque control might be more common on large ACIMs.

All varieties of vector DTC utilize the same core principles for control—direct sensing detects two of the three drive output line currents with the third inferred. The system compares a torque estimate calculated from the sensed current values to the desired torque. If the estimated and desired torque values differ by more than an acceptable hysteresis value, the controller calculates a ΔTorque value used for subsequent calculation of stator voltages via a lookup table. The lookup table contains a pre-defined set of values for three-phase stator voltages depending on the input ΔTorque and calculated stator flux inputs, and the output values from the lookup table determine the gate-drive signals for the inverter subsection. Vector DTC has some advantages over vector FOC in that it may provide faster control of speed and torque, but also has disadvantages such as limited control at zero or low speeds.

 

# Power Measurements on Distorted Signals (e.g., PWM, Drive Output)

## Introduction

In an earlier section, single-and three-phase sinusoidal AC line systems were described as rotating vector systems with one set (single-phase) of voltage and current vectors or three sets (three-phase) of voltage and current vectors. However, power conversion systems and drives do not output sinusoidal signals – they are PWM signals and they have high harmonic content. This high harmonic content can be thought of as a multi-vector system, with one rotating voltage vector and one rotating current vector (for each phase) for "N" harmonics, with each voltage and current vector system associated with a given harmonic having a unique phase angle. As described earlier, we cannot directly measure the phase angle between distorted voltage and current waveforms. We must use a digitally sampled waveform technique, as described previously, for accurate calculation of the power values for these waveforms.

We will not repeat the previous description of the digitally sampled waveform technique. However, understanding of some additional considerations will aid in correct measurement of power on these types of signals. These considerations are:

- Advanced cyclic period detection and display
- Harmonic filtering of power measurements
- Impact of line-reference voltage probing

It is important to emphasize that *accurate per-cycle power calculations require accurate determination of the cyclic period during which power values are to be calculated*. Furthermore, distorted and dynamic waveforms introduce additional cyclic period calculation complications. If the cyclic period is visually confirmed to be correctly determined, you will gain confidence in your measurements. It will then also be possible to apply different harmonic filters and/or employ a line-reference probe technique (as necessary) when making power measurements.

## Advanced Cyclic Period Detection and Display

As described previously, we use a signal to determine the cyclic period for the measurement calculations. Ideally, the signal chosen (what Teledyne LeCroy refers to as the Sync signal) to determine the cyclic period is highly sinusoidal or could be made sinusoidal through low-pass filtering. When measuring power in distorted waveforms, proper selection of a suitable signal, understanding how to optimize settings for the desired results, and learning how to use viewable "feedback" of the settings is critical to ensuring accurate power measurements. With a thorough understanding of how to choose, filter, and set hysteresis for the Sync signal, one will obtain accurate measurements with Teledyne LeCroy's Motor Drive Analyzer or a power analyzer under most or all conditions.

Figure 147 shows the setup for the Sync signal in Motor Drive Analyzer. Power analyzer instruments have similar setups, though they usually do not allow a hysteresis band setting. Moreover, we cannot view the filtered signal, with cyclic period determination, on a power analyzer instrument as we can with the Motor Drive Analyzer.

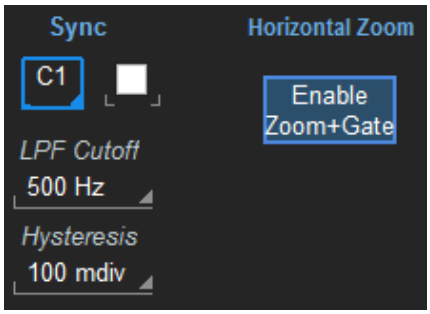


Figure 147: Setup for the Sync signal in the Teledyne LeCroy's Motor Drive Analyzer.

## Choosing a Sync Signal

The highest amplitude, least distorted signal is best for cyclic period determination. Use any acquired periodic signal with a period representing the interval for performing cyclic measurements. In general, the ideal Sync signal has these characteristics:

- Low or predictable distortion (e.g., a pure or nearly-pure sine wave, or a signal that could be made as such with low pass filtering)
- Constant amplitude (e.g., a constant-amplitude current signal during steady-state load, or constant-amplitude PWM drive voltage output)
- Low noise
- Variation around a zero crossing (e.g., line-line voltages, or sinusoidal current signals)

If a signal with the above characteristics is not naturally present in the acquisition, then adjust the low-pass filter (LPF) cutoff and hysteresis band (zero-crossing filter) settings to improve the 50% (zero) crossing determination and/or to reduce the noise and distortion on the signal. In the case of severely distorted waveforms (e.g., six-step commutated voltage or current waveforms), it may be necessary to adjust both. If no signal has the ideal characteristics described above, use a math function as the Sync signal. An example where this might be useful is if the voltage probing is line-reference (no variation around a zero crossing) and the current signals have a very wide dynamic range. In this case, one may define a math as the difference in two line-reference probed voltages to obtain a line-line voltage to use as a Sync source.

## LPF Cutoff Settings

The low-pass filter (LPF) applies a digital filter with a -3dB cutoff at the specified frequency. The default value in the Motor Drive Analyzer is 500 Hz. There is significant attenuation of Sync source signals with significant high-frequency content (e.g., a PWM voltage signal) when filtered to the default frequency, but they may still be suitable Sync signals if they are sinusoidal with low (post-filtered) distortion. Signals with very high harmonic content (e.g., six-step commutated voltage signals) will have significant attenuation when the low-pass filter is applied. Therefore, filtering may render such signals unsuitable for synchronizing unless care is taken in setting the hysteresis level. Signals that experience wide dynamic ranges, such as load current signals in acquisitions under highly dynamic loading conditions, may also be unsuitable. Be careful when setting the LPF filter value to a value that is lower than the default setting, and view the Sync signal to ensure that the chosen filter setting is providing the desired result.

 

The LPF cutoff may be set to a lower or higher frequency than the default 500 Hz to improve the quality of the Sync signal:

- Lower values improve the noise and distortion rejection, but may overly attenuate the signal, requiring undesirable hysteresis settings, or result in no cyclic detection at all.
- Higher values may improve the signal amplitude, but pass too much high-frequency content, leading to a distorted signal and incorrect 50% (zero) crossing determination.

### Hysteresis Band Settings

The hysteresis band setting defines an amplitude "band" above which the Sync signal must exceed before Sync signal slope is shown to be acceptable for use in the 50% (zero) crossing determination. The default value is 100 millidivisions (mdiv), with the unit "divisions" being equal to oscilloscope vertical grid divisions.

- Lower hysteresis values improve the ability to detect a 50% (zero) crossing on a smaller amplitude signal but with risk of detecting false 50% (zero) crossings.
- Higher hysteresis values improve the ability to reject the impact of signal distortion or noise in determination of the 50% (zero) crossing but with risk of reduced accuracy of 50% (zero) crossing detection.

Some non-zero hysteresis value is required to prevent false 50% (zero) crossing determination. However, this also means that the Sync signal must meet a minimum amplitude requirement and be relatively noise-free at lower amplitudes. Signals with very wide dynamic ranges and very high distortion (e.g., a six-step commutated current signal with very high dynamic range) likely require more care when setting the hysteresis band.

To understand how the hysteresis-band setting works, consider the example in Figure 148 of a perfect sinusoid. In this case, it is simple to detect the zero or 50% crossing level and determine the measurement intervals.

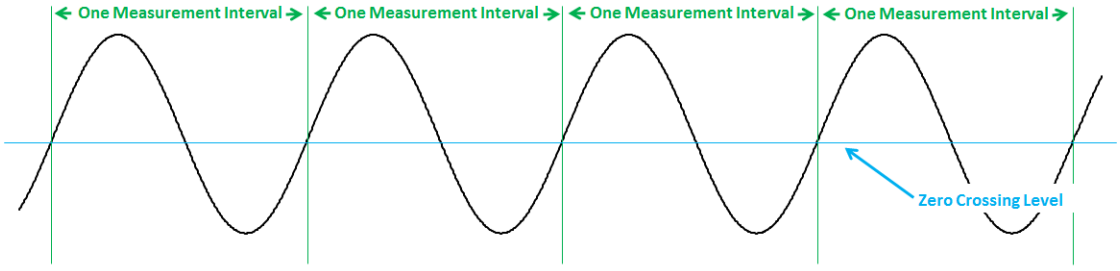


**Figure 148: Cyclic period measurement intervals on a sinewave signal. Determining the measurement interval is simple in this case.**

 

Now, consider the example in Figure 149 in which there is a non-monotonicity near the zero or 50% crossing level. The non-monotonicity results in an incorrect period determination because it is detected as a measurement interval, which results in incorrect calculations.

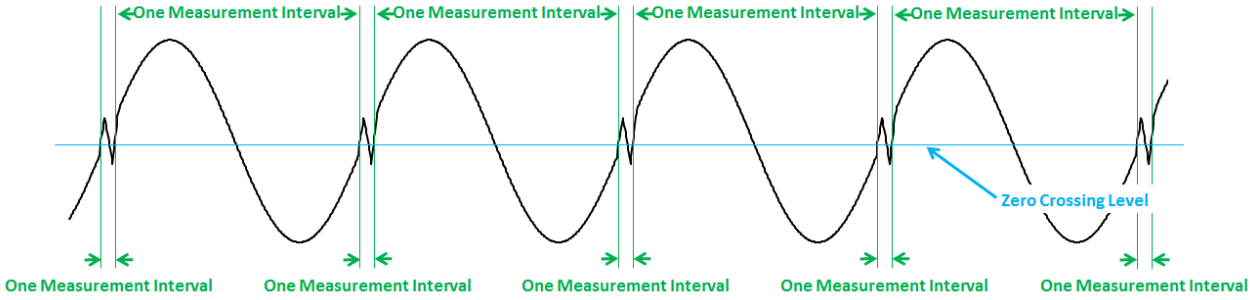


Figure 149: A non-monotonic signal produces "false" measurement intervals.

Using the hysteresis band controls, we set a hysteresis band level of greater than the amplitude of the non-monotonicity to avoid false measurement interval calculations. This is shown in Figure 150.

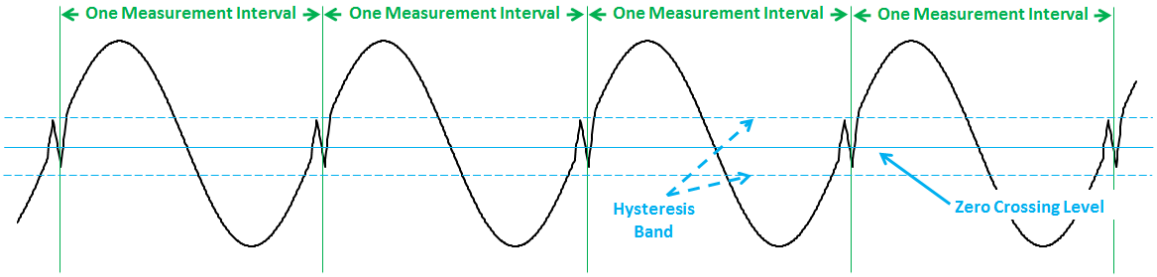


Figure 150: Setting a hysteresis band corrects for non-monotonicity when measuring intervals.

## Sync Signal Display + Zoom

Visual feedback on the Sync signal settings provides confidence that we have calculated a correct cyclic period. If the cyclic period calculation is wrong for some reason, all power values will be incorrect. Therefore, the Motor Drive Analyzer provides the ability to view the filtered Sync signal with a transparent, color-coded overlay to indicate the exact locations of measurement period (cyclic) determination. Figure 151 shows an example. We use this overlay to verify that the Sync signal is performing as would be expected. If the acquisition contains many Sync signal cycles, we zoom the display to see cyclic period details using the Motor Drive Analyzer's Zoom+Gate feature.

 

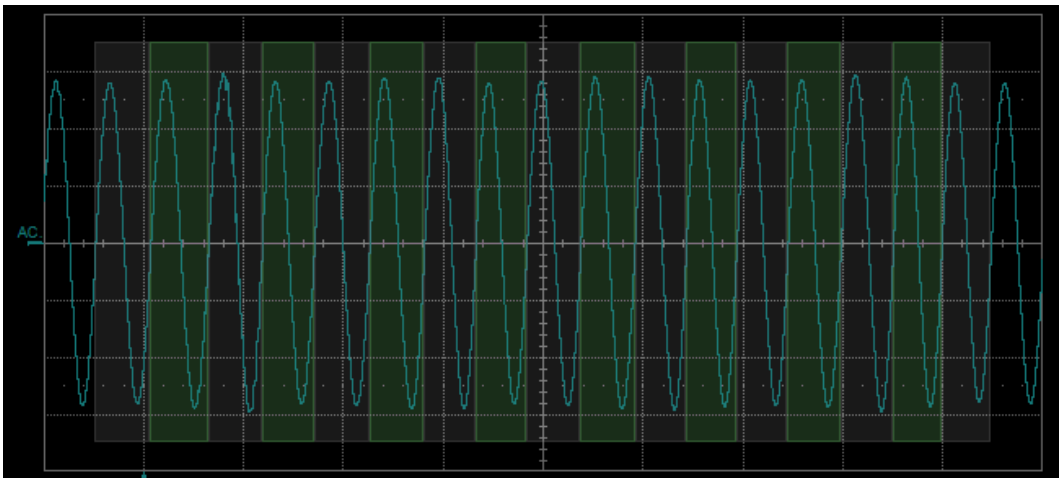


Figure 151: Transparent, colored overlays mark the measurement cycles on Sync signal.

## Simple Examples for Distorted Waveforms

To illustrate how to use a combination of the settings to obtain or verify an accurate cyclic period determination, we will show a number of examples. For simplicity, we show just a single phase of a three-phase system, but the examples are generic and apply to single- or three-phase systems.

Figure 152 shows a single line-line voltage (Z3, light blue, upper left) and line current output (Z6, purple, lower left) of a low-voltage vector FOC (sine-modulated PWM) drive. We have chosen the Sync as the line-line voltage signal and are using the default low-pass filter and hysteresis settings. The filtered Sync signal with cyclic period overlays appears as DrvOutSyncZ (green, upper right).


Figure 152: A single line-to-line voltage (Z3, light blue, upper left) and line-current output (Z6, purple, lower left) of a low-voltage vector FOC drive. The filtered Sync signal with cyclic period overlays appears as DrvOutSyncZ (green, upper right.)

 

While low in amplitude, the filtered line-line voltage signal is still of sufficient amplitude to determine the cyclic period, which is shown by the transparent overlays showing three cyclic periods.

If we choose the line current signal — a much more sinusoidal signal without filtering — as the Sync signal, Figure 153 shows that we can make the same cyclic period determination as when we used the line-line voltage signal as the Sync signal. Note that the same Sync filter settings were used in both cases, but the line current signal contains much less frequency content above the filter setting, so the filtered signal more closely resembles the acquired signal.

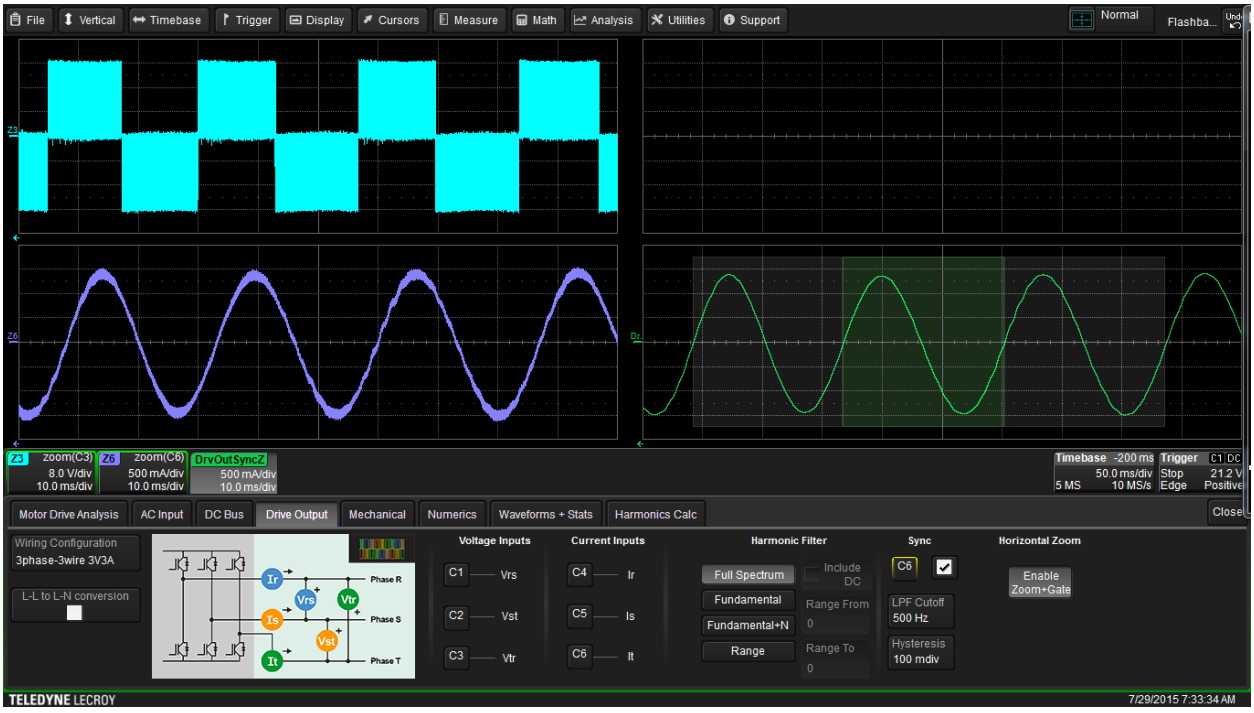


**Figure 153: Using the line current signal (Z6, purple, lower left) as the Sync signal, we can make the same cyclic period determination as when we used the line-to-line voltage signal, but less filtering is required. The Sync signal appears on the lower right.**

Figure 154 shows a single line-line voltage (Z3, light blue, upper left) and line current output (Z6, purple, lower left) of a low-voltage BLDC six-step commutated drive output. We have chosen the Sync signal as the line-line voltage signal and are using the default low-pass filter and hysteresis settings. The filtered Sync signal with cyclic period overlays appears as DrvOutSyncZ (green, upper right). While we might expect that this waveform would challenge the cyclic period detection algorithm, in fact, the default settings for low-pass filter and hysteresis band are acceptable, though this may not be the case with different but similar waveforms. Note that there are non-monotonicities present in the filtered signal, and some adjustment of the hysteresis band setting or low-pass filter may be necessary on similar waveforms.

 


**Figure 154: Even with the low-voltage BLDC six-step commutated drive output line-to-line voltage measured here, we can still obtain an accurate Sync signal from this line-to-line voltage signal using the default settings for the low-pass filter and hysteresis.**

Figure 155 shows a similar result when we choose the line current signals as the Sync. The same cautions apply as in the previous line-line voltage example.


**Figure 155: Choosing the line-current signals as the Sync signal for the low-voltage BLDC six-step commutated drive output produces similar results to those obtained in Fig 8.**

 

For instance, for the same example above, a waveform with a little more distortion or noise at the zero crossing (Figure 156) results in a false cyclic period determination with the default hysteresis band setting. In this case, the half period was determined instead, which would lead to incorrect power calculations. We identified this problem by viewing the Sync signal with the cyclic period overlays. Correcting it requires only a minor change in the hysteresis band setting.

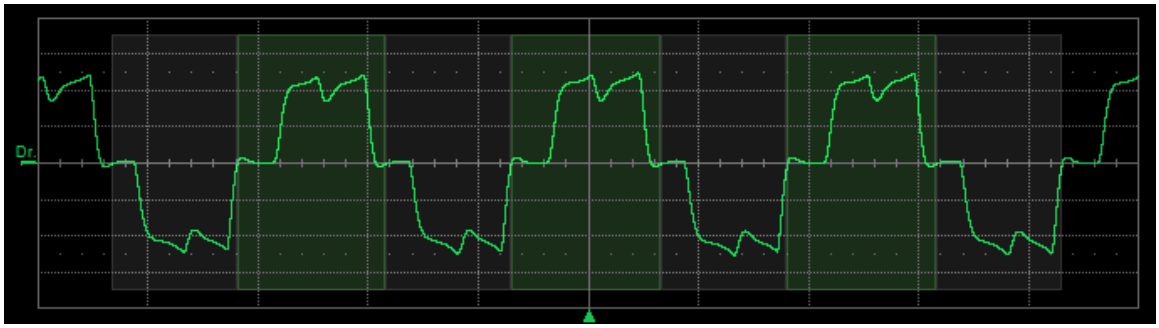

**Figure 156: This line current signal is essentially the same as in Fig 9, but the presence of slightly more noise causes the MDA to determine the cyclic period to be just half of the actual period as the overlays indicate when the default setting for hysteresis band is used.**

Figure 157 shows a single line-reference voltage (Z3, light blue, upper left) and line current output (Z6, purple, lower left) of a low-voltage, BLDC, six-step commutated drive output. We have chosen the Sync signal as the line-reference voltage signal and are using the default low-pass filter and hysteresis settings. The filtered Sync signal with cyclic period overlays appears as DrvOutSyncZ (green, upper right).


**Figure 157: A line-to-reference voltage (Z3, light blue, upper left) of a low-voltage, BLDC, six-step commutated drive output is chosen as the Sync signal, but the MDA software cannot accurate determine the cyclic period.**

 

In this case, the software algorithm cannot correctly determine the cyclic period. While not shown, it might be possible to adjust the filter or hysteresis settings and obtain a good Sync period. However, in this particular case, substituting the line current waveform creates a more suitable signal (Figure 158).


**Figure 158: When the line-current waveform is selected as the Sync signal, the MDA is able to correctly determine the cyclic period using default settings.**

 

Perhaps the best Sync signal is a Math waveform defined as the difference between two line-reference waveforms, or a line-line voltage. When done, we produce a result similar to that obtained with direct acquisition of the line-line voltage waveform (Figure 159).


**Figure 159: A Math function within the MDA takes the difference between the two line-to-reference waveforms shown on the left and uses this difference waveform as the Sync signal shown on the lower right.**

 

## Long Acquisitions with Distorted Signals

As previously described in this section, long acquisitions of signals with wide dynamic ranges and distortion require care in setting the Sync signal to achieve accurate results. Additionally, on longer acquisitions, especially those with dynamic load conditions, it may be necessary to zoom the Sync signal to verify a good cyclic period determination. This is where the Motor Drive Analyzer's Zoom+Gate capabilities shine.

Consider a two-second acquisition of a sine-modulated, three-phase drive that ultimately shuts down due to an overcurrent condition, incurring a substantial output-current change (i.e., wide dynamic current range) and significant signal distortion at the shutdown event. The three-phase, line-line voltage waveforms appear in the top grid of Figure 160, and the three-phase line currents appear in the bottom grid of the same figure.

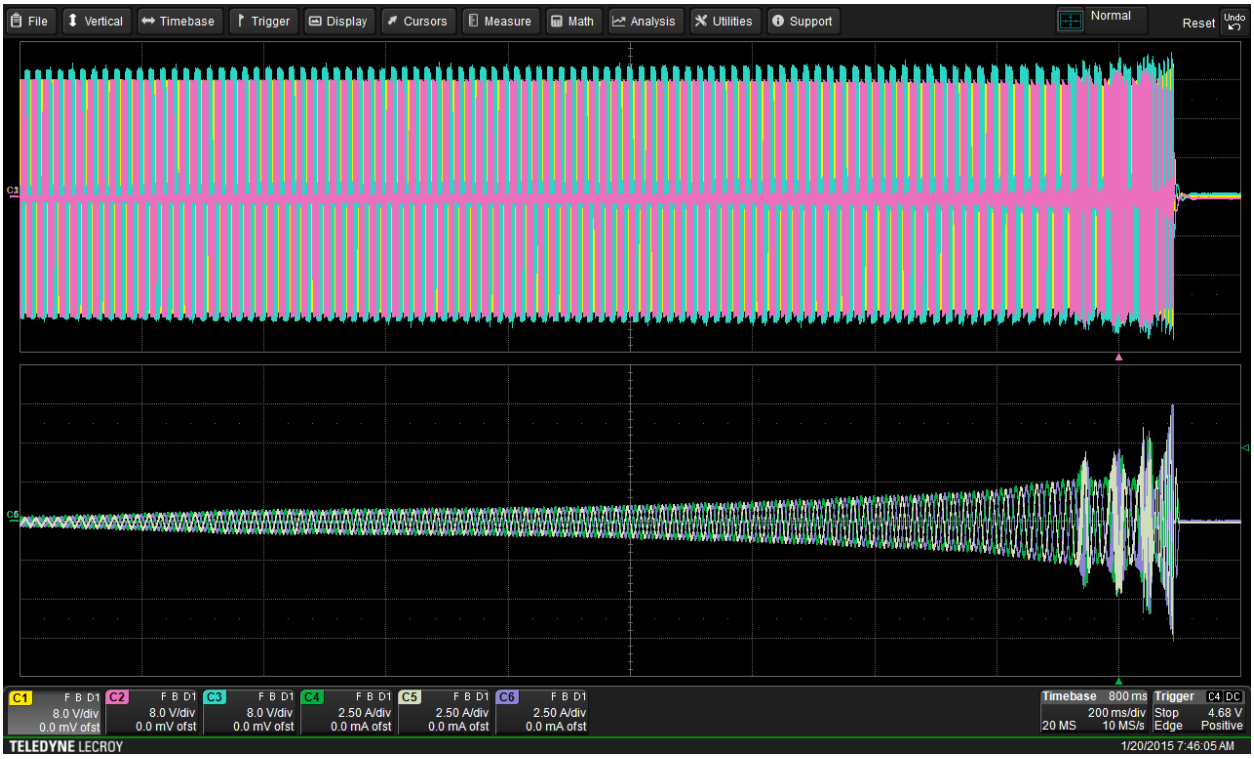


Figure 160: Initial display of input source waveforms for sine-modulated, three-phase drive.

 

In Figure 161 we enable Zoom+Gate for the same line-to-line voltage waveforms. The original, 2 S- long acquisitions appear on the left side of an octal grid with the zoomed waveforms on the right. Then, for illustrative purposes, C4 (a current signal on Channel 4) is assigned as the Drive Output Sync signal (named DrvOutSyncZ and shown as a green trace). C1 (a voltage signal on Channel 1) is assigned as the AC Input Sync signal (named ACInSyncZ and shown as a blue trace). We have retained the default LPF Cutoff (500 Hz) and Hysteresis (100 mdiv) settings.

Both signals display nearly the same amplitude. If we change the horizontal zoom ratio to encompass nearly half the waveform and change the zoom position location to the beginning of the acquisition, the transparent overlays show us that the Sync signal seems to have a well-defined period in both cases.

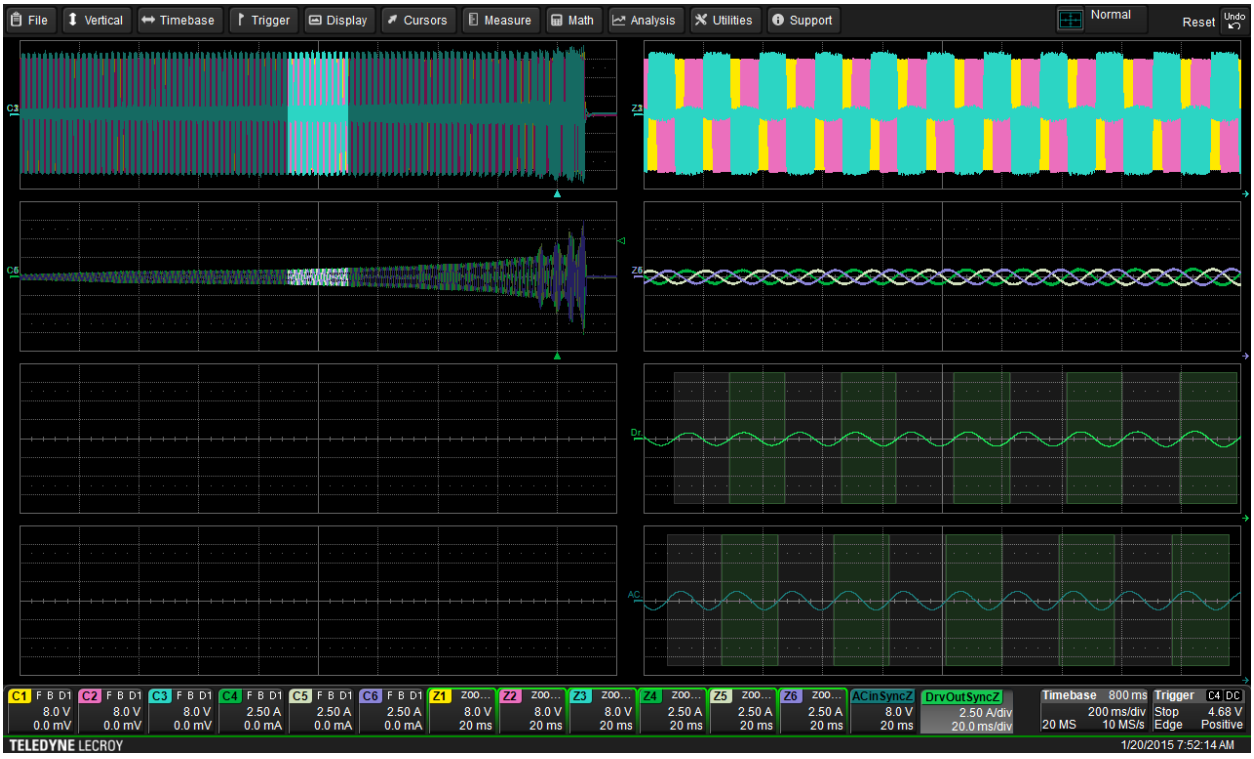


**Figure 161: Sync signal display after Zoom+Gate is enabled (lower right).**

 

In Figure 162 we change the zoom position to the end of the acquisition. The voltage and current signals display different behaviors near the end of the acquisition (where the overload condition is occurring). The voltage and current signals have different behaviors with identical LPF cutoff and hysteresis settings, but neither of them achieves a good period determination in this location.


**Figure 162: Changing zoom position changes display of all zoomed waveforms, including Sync signals.**

 

Zooming further to the end of the acquisition and adjusting LPF cutoff to 160 Hz and hysteresis to 20 mdiv on both Sync signals is done in Figure 163. This shows that the voltage source (green trace, used in DrvOutSyncZ) is the better source. With these changes, it would be wise to review the entire waveform (using the Zoom+Gate capabilities) to ensure that a good Sync period is found throughout the entire acquisition. This review (not shown in an image) shows that maintenance of proper period determination of the C1 line-line voltage signal reaches back to the beginning of the acquisition.


**Figure 163: Adjusting filters reveals DriveOutSyncZ (C4, second waveform from the bottom on the lower right) is the better choice Sync signal.**

## Low-Pass and Harmonic Filtering of Power Measurements

As described earlier, the Motor Drive Analyzers and most power analyzers utilize an analog-to-digital conversion system to digitize the voltage and current waveforms, and then perform power calculations on each acquired cycle. By default, the instrument's analog bandwidth and digital sample rate combine to determine the maximum (full-spectrum) frequency of the acquired voltage and current signals, and thus the number of harmonic orders present in the power calculations.

One may employ analog or digital low-pass filters, complex harmonic filters, or any combination of these, to achieve filtering of the acquired full-spectrum signals.

### Analog Low-Pass Filter

Analog low-pass filters limit the frequency content prior to the analog-to-digital conversion. This method requires no post-processing time, but it permanently removes frequency information from the acquired signals, and typically, there is little flexibility in the low-pass filter cutoff settings. Additionally, we base

 

filtering on a constant frequency limit, and thus may include more or less harmonic orders depending on the VFD's output frequency.

Figure 164 is an example from Teledyne LeCroy's Motor Drive Analyzer in which an analog filter may be set (in this case, to 20 MHz) in the Channel setup dialog:


Figure 164: Analog filter setting on Motor Drive Analyzer.

### Digital Low-Pass Filter

Application of a post-acquisition digital low-pass filter comes after the analog-to-digital conversion. This method requires post-processing time to apply the digital low-pass filter but retains the original data and provides much more flexibility in the low-pass filter cutoff settings. In some cases, this digital filter may be dependent on the digital sample rate, so if the digital sample rate is changed, the low-pass filter cutoff settings will change as well. Like the analog low-pass filter, this filter also may include more or less harmonic orders depending on the output frequency of the variable frequency drive.

Figure 165 from the Teledyne LeCroy Motor Drive Analyzer shows a simple (digital) noise filter that may be set (in this case, to improve noise by 1 bit, with a 3 dB cutoff at ~300 MHz) in the Channel setup dialog:

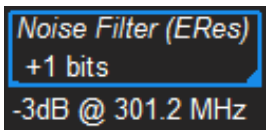


Figure 165: Digital filter settings on Motor Drive Analyzer.

Other types of digital filters are also available.

### Selective Hardware PLL-based Harmonic Filter

Power analyzer instruments often utilize a hardware PLL to recover the cyclic period in real time and dynamically adjust the sample rate to obtain a fixed number of samples per cyclic period upon which to perform an FFT for selective harmonic inclusion/exclusion from the power calculations. This method works well when the frequency is relatively stable and within the narrow loop bandwidth constraints of the PLL (i.e., a 50/60 Hz AC line input, or a variable frequency drive output under constant load, speed, and torque conditions). It will not perform properly under highly dynamic operating conditions.

### Selective Software-based FFT Digital Harmonic Filter

The Teledyne LeCroy Motor Drive Analyzer's fixed-frequency harmonics table calculation assumes a constant cyclic period (detected automatically or fixed by the operator). The calculation involves a fast-Fourier transform on the full acquisition length to selectively include the fundamental and a user-settable number of harmonics orders in the harmonics calculation table.

This method requires digital post-processing of the acquired data and takes longer to compute than a hardware-based PLL method. However, it provides the ability to set the frequency limit based on a per-

 

cycle harmonic order, and not a fixed bandwidth limit. In addition, because we perform digital filtering as a post-processing operation, one may change the settings to obtain a different result without having to reacquire the voltage and current data. This method only works well with a 50/60 Hz AC line input, or a variable frequency drive output under constant load, speed, and torque conditions, because it requires a constant frequency for correct calculations.

### Selective Software-based DFT Digital Harmonic Filter

The Teledyne LeCroy Motor Drive Analyzer's harmonic filter utilizes a complex Fourier sum (term of a DFT) for each of the specified harmonic frequencies. The analyzer calculates Fourier sums on the acquired (sampled) voltage and current data over the cyclic period defined by each Sync period. For each cyclic period, it uses the resulting complex results to reconstruct the current and voltage waveforms composed of only the specified harmonics. Then, it makes power calculations only on the fundamental and the specified harmonic waveforms, with an option to include or exclude the DC component in the calculations. Thus, this method permits inclusion or exclusion of selective harmonics from the power calculations.

This filter requires digital post-processing of the acquired data and takes the longest time to compute. However, it provides the ability to set the frequency limit based on a per-cycle harmonic order and not a fixed bandwidth limit, and because the filtering operation takes place digitally with a software-recovered cyclic period, this type of filter provides accurate power calculations by harmonic order under widely varying drive output frequencies. These two capabilities are highly advantageous when the cyclic period changes constantly during the acquisition (as would normally be the case with a variable frequency drive). In addition, because we perform digital filtering as a post-processing operation, one may change the settings to obtain a different result without having to reacquire the voltage and current data. This brings a significant advantage if an operator wishes to compare a single acquisition with multiple different settings, e.g., power calculated on the fundamental only compared to fundamental through the 50$^{th}$ harmonic (to understand power lost to heat in the windings).

Figure 166 from the Teledyne LeCroy Motor Drive Analyzer shows a harmonic filter applied to power calculations made on the AC input or drive output signals, including the fundamental per-cycle frequency through the 50th harmonic.

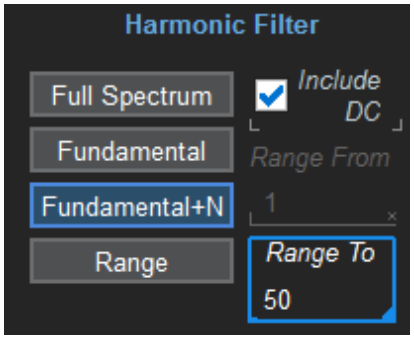


**Figure 166: Harmonic filter settings for a Motor Drive Analyzer configured to filter acquired motor drive waveforms up to the 50th harmonic.**

 

Figure 167 shows a similar selection in the harmonics table and spectral display setup in the Teledyne LeCroy Motor Drive Analyzer.

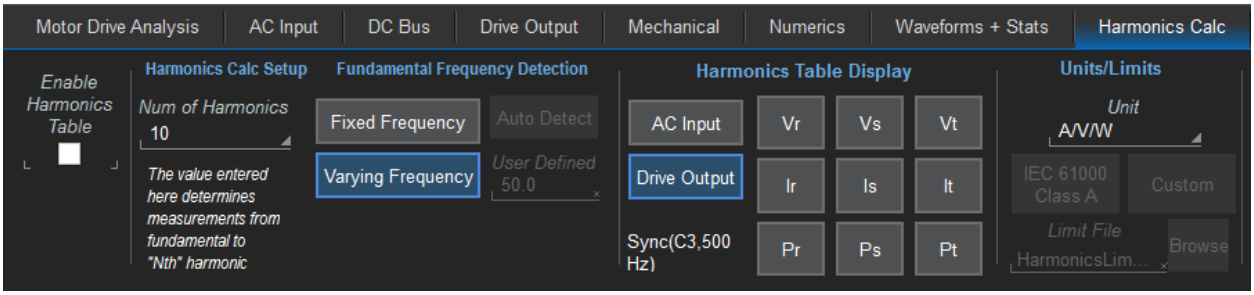


**Figure 167: The number of harmonics can also be specifics in the analyzer's harmonics table and spectral display setup.**

## Examples Using a Selective Software-based DFT Digital Harmonic Filter

Consider this example in Figure 168 of a three-phase, sine-modulated motor drive output. The acquisition is the three-phase, line-line voltage waveforms (all shown in the top grid) and the three-phase line currents (all shown in the bottom grid). The analyzer performs a Line-Line to Line-Neutral conversion. The Numerics table displays data for each of the three phases and the sum total of all three phases with the harmonic filter "off" (or set to Full Spectrum), which indicates that no harmonic filtering should be performed on the data reported in the Numerics table.


**Figure 168: Numerics data calculated for the Full Spectrum of the captured waveform.**

Note that the reported apparent power (S) and the reactive power (Q) values are very high. Therefore, the calculated power factor (PF) is very low and the phase angle value (φ) is correspondingly high.

 

Figure 169 shows that changing the Harmonics filter setting to Fundamental and unchecking the Include DC checkbox results in very different calculated data in the Numerics table.

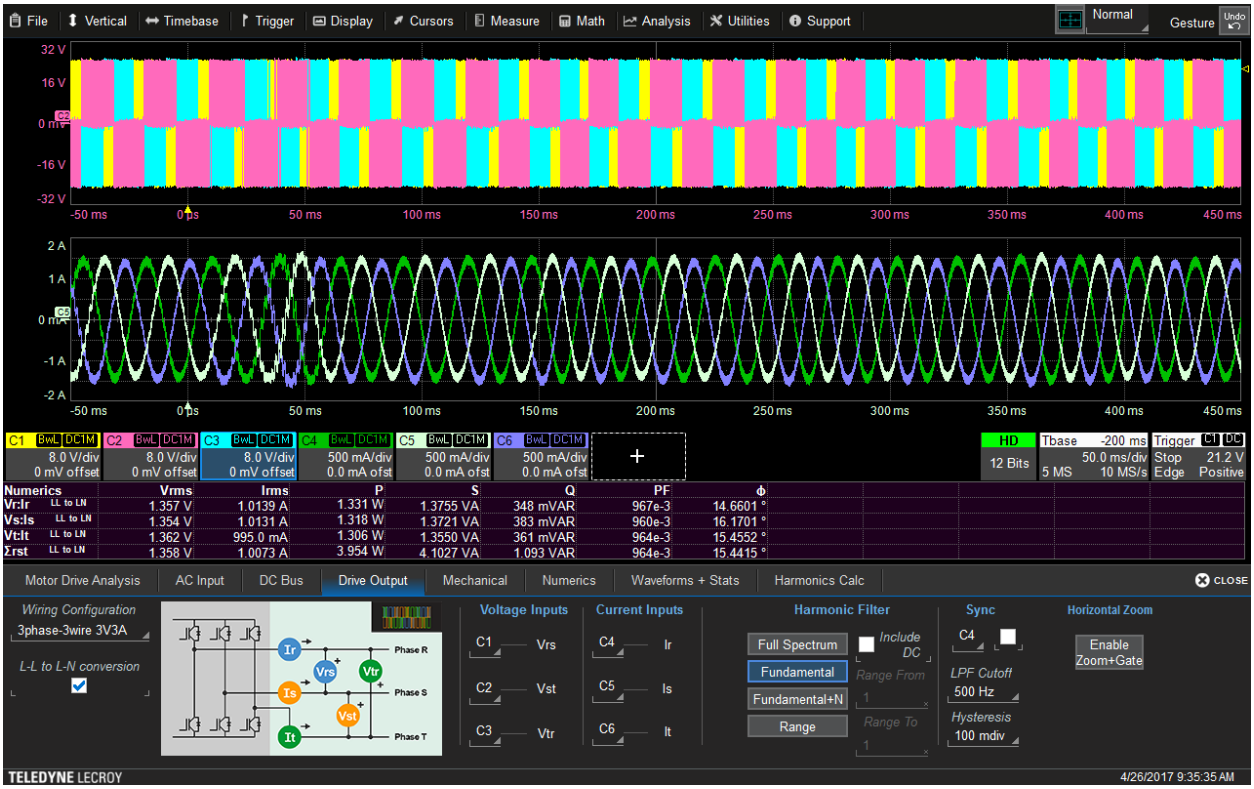


**Figure 169: Numerics data calculated for only the fundamental. Note that only the table changes.**

Notice that the displayed waveform data did not change — only the Numerics table values changed. With the Include DC checkbox checked, the calculation of Numerics data takes place on that basis, as shown in Figure 170.

| Numerics | | Vrms | Irms | P | S | Q | PF | Φ |
|---|---|---|---|---|---|---|---|---|
| Vr:Ir | LL to LN | 1.361 V | 1.0143 A | 1.331 W | 1.3804 VA | 364 mVAR | 965e-3 | 15.2965 ° |
| Vs:Is | LL to LN | 1.354 V | 1.0132 A | 1.318 W | 1.3724 VA | 382 mVAR | 960e-3 | 16.1618 ° |
| Vt:It | LL to LN | 1.365 V | 995.9 mA | 1.308 W | 1.3597 VA | 372 mVAR | 962e-3 | 15.8856 ° |
| Σrst | LL to LN | 1.360 V | 1.0078 A | 3.957 W | 4.1125 VA | 1.120 VAR | 962e-3 | 15.7873 ° |

**Figure 170: Numerics data calculated for fundamental including the dc component.**

Note that now in both cases, the calculated reactive power (Q) values are now much lower, and therefore, the calculated power factor (PF) is very high and the phase angle value (φ) is correspondingly low. This is expected. PWM waveforms will produce power calculations with very high levels of reactive power but when filtered to the fundamental only, the reactive power values are greatly reduced.

 

## Line-Reference Voltage Probing of PWM Signals on Drive Outputs

As described previously, the power electronics inverter subsection of any type of drive has no direct connection to earth ground or AC line input neutral. Therefore, voltage sensing typically is performed line-line, which requires one of the following:

- A high-voltage, isolated differential voltage probe
- A high-voltage isolated input (channel-channel and channel-ground) to the measurement instrument.

The Teledyne LeCroy Motor Driver Analyzer requires the former, while dedicated power analyzers generally provide the latter. Probes offer flexibility: one may use any input channel for multiple purposes while slightly reducing the accuracy of the measurement (the additional inaccuracy of the probe is additive to that of the channel) and increasing cost. Isolated inputs have the advantage of lower cost. However, at high input voltages or currents, additional step-down devices become necessary, which increases cost, and the non-shielded cable connections from the isolated input to the DUT can result in significant noise pickup.

However, some users also measure voltages from each line to a common “reference” plane, which could be a common reference location on a printed circuit board or simply three (single-ended) probe ground leads or (differential) probe negative leads connected together. While this is not the same as a line-neutral connection, it does eliminate the need to use a differential probe with the Motor Drive Analyzer. If the drive output voltage is less than ~400 V, inexpensive, single-ended passive probes suffice for the voltage measurements.

Figure 171 shows an example of a low-voltage, six-step commutated brushless DC drive output. Z1 (yellow) is the line R-reference voltage signal, Z2 (magenta) is the line S-reference voltage signal, and Z3 (blue) is the line T-reference voltage signal. The nature of the six-step voltage commutation clearly reveals the “reference” where no PWM activity is occurring.

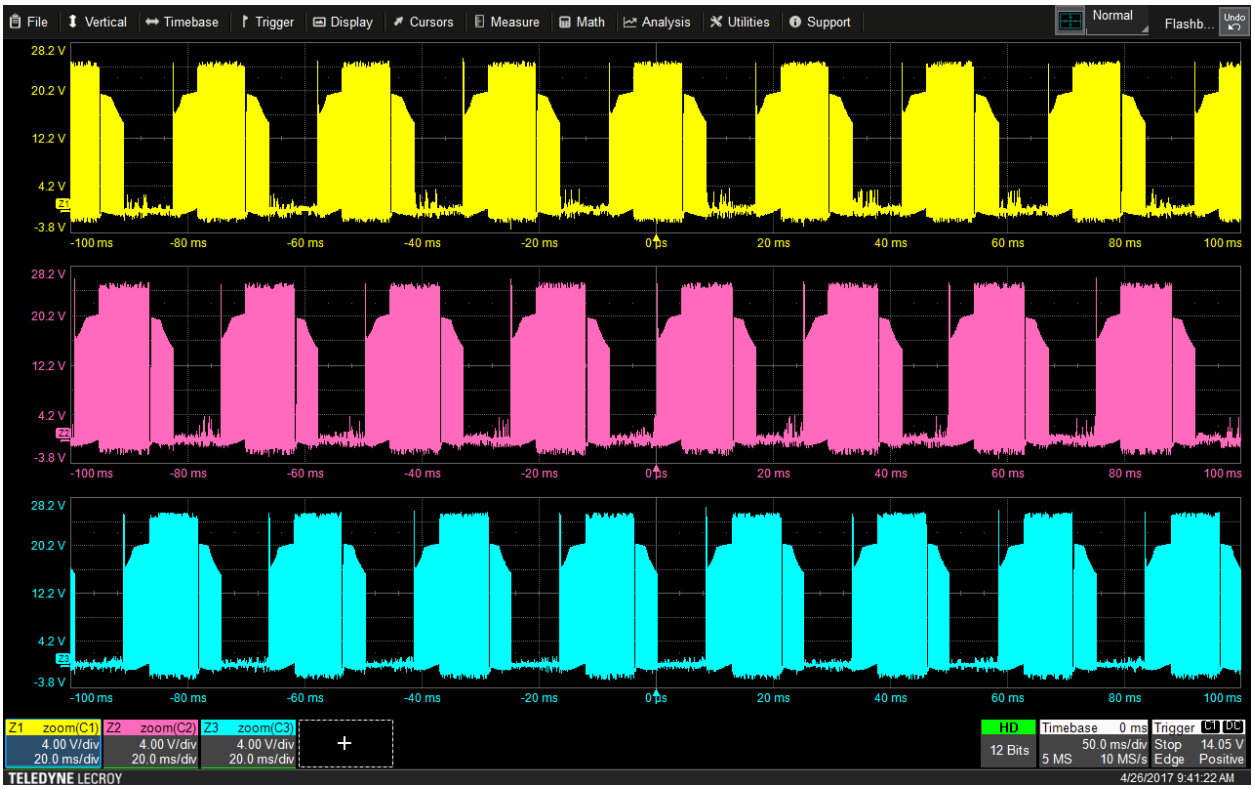


**Figure 171: Waveforms produced by a low-voltage, six-step commutated brushless dc drive output as measured by a Motor Drive Analyzer.**

Note that in the Motor Drive Analyzer Drive's output setup in Figure 172, we have used the three-phase, four-wire (3V3A) wiring configuration, which shows a connection to Neutral. This connection point can also be a "reference" and not true neutral connection point.

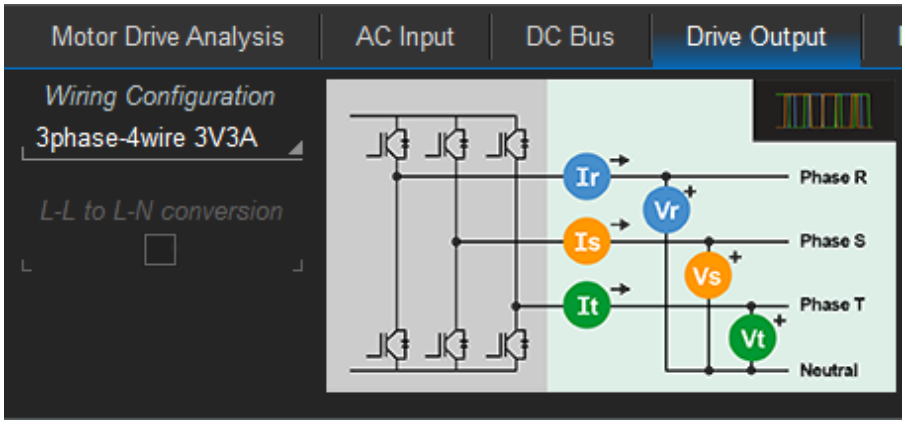


**Figure 172: Drive output setup in the Motor Drive Analyzer.**

The practical impact of using a line-reference probe connection instead of line to true neutral is that the Motor Drive Analyzer or power analyzer instrument measures the voltage signal as pulse-width modulated from 0 V to some positive voltage value, and therefore the PWM signal exhibits a very high overall common-mode (DC, or average) value. A line-line or true line-neutral measured voltage signal

 

alternates around 0 V, leaving the PWM signal's common-mode (DC, or average) value near 0 V. This high measured common-mode voltage will not have practical impact on the calculated real power (P), but does have two other impacts:

- The high common-mode RMS voltage increases the value of the apparent power (S), which then increases the value of the reactive power (Q) and phase angle (φ) and decreases the power factor (λ).
- The high common-mode RMS voltage increases the measurement error due to residual offsets in the RMS current measurement, due to either the current probe/sensor or the acquisition system. The $I_{DC}$ measurement can be used to measure the residual offset. If this is a significant portion of the $I_{RMS}$, then measurement errors will increase.

Consider the line-reference voltage acquisition in Figure 173 from a three-phase, six-step commutated brushless DC motor. C1 (yellow) is the R-reference voltage and C4 (green) is the R current. C2 and C5, and C3 and C6 are the corresponding S and T phase line-reference voltage and current pairs. The Numerics table with various voltage, current, and power calculations appears at the bottom. Note that we set the Harmonic Filter to Full Spectrum.


| Numerics | Vrms | Vdc | Irms | Idc | P | S | Q | PF | Φ |
|---|---|---|---|---|---|---|---|---|---|
| Vr:Ir | 6.3438 V | 1.8364 V | 892.8 mA | -4.1 mA | 1.177 W | 5.6638 VA | 5.540 VAR | 208e-3 | 78.0020 ° |
| Vs:Is | 6.5758 V | 1.8622 V | 911.4 mA | 70.2 mA | 1.337 W | 5.9934 VA | 5.842 VAR | 223e-3 | 77.1088 ° |
| Vt:It | 6.5244 V | 1.8660 V | 912.3 mA | 1.9 mA | 1.215 W | 5.9525 VA | 5.827 VAR | 204e-3 | 78.2244 ° |
| Σrst | 6.4813 V | 1.8549 V | 905.5 mA | 22.7 mA | 3.729 W | 17.610 VA | 17.210 VAR | 212e-3 | 77.7732 ° |

**Figure 173: Waveforms and Numerics calculations produced by a three-phase, six-step commutated brushless DC motor probed from line to reference with Harmonic Filter set to Full Spectrum.**

 

Visually the R, S, and T phase voltage and current pairs seem to be in-phase, so one would expect a very high calculated power factor (PF) and low calculated phase angle (ϕ). However, the opposite is true — the calculated power factor is very low, and phase angle is subsequently very high. This is a result of a very large calculated apparent power (S, refer to the earlier section regarding power calculations using a digital sampling technique for more details) due to the high common-mode voltage (observable in the large $V_{DC}$ measurement).

If we change the harmonic filter to fundamental (Figure 174) and uncheck the "Include DC" checkbox (excluding the DC value from the measurement), a change in calculated power values becomes evident (lower table in Figure 174). Note that no new set of acquisition data was required because this is a software post-process calculation.

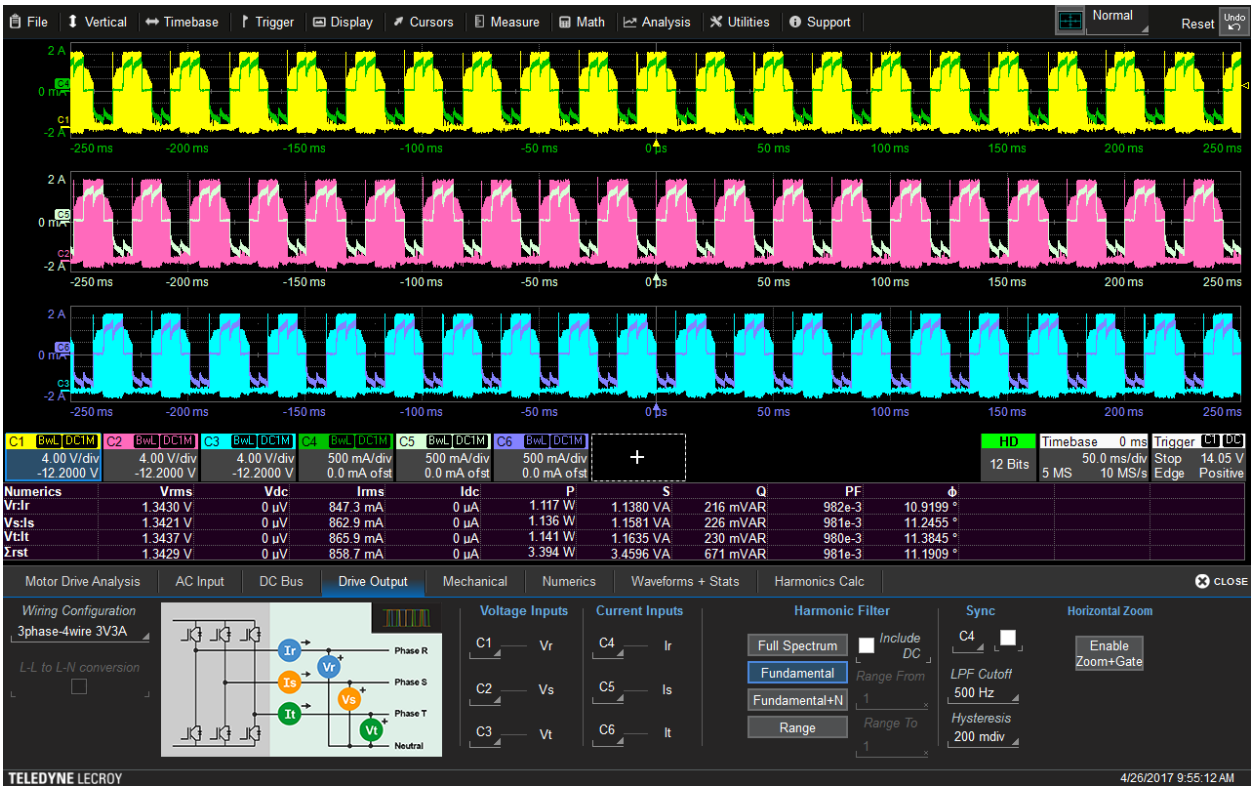


| Numerics | Vrms | Vdc | Irms | Idc | P | S | Q | PF | ϕ |
|---|---|---|---|---|---|---|---|---|---|
| Vr:Ir | 1.3430 V | 0 µV | 847.3 mA | 0 µA | 1.117 W | 1.1380 VA | 216 mVAR | 982e-3 | 10.9199 ° |
| Vs:Is | 1.3421 V | 0 µV | 862.9 mA | 0 µA | 1.136 W | 1.1581 VA | 226 mVAR | 981e-3 | 11.2455 ° |
| Vt:It | 1.3437 V | 0 µV | 865.9 mA | 0 µA | 1.141 W | 1.1635 VA | 230 mVAR | 980e-3 | 11.3845 ° |
| Σrst | 1.3429 V | 0 µV | 858.7 mA | 0 µA | 3.394 W | 3.4596 VA | 671 mVAR | 981e-3 | 11.1909 ° |

**Figure 174: Waveforms and Numerics calculations produced by a three-phase, six-step commutated brushless DC motor as in the previous figure, but with Harmonic Filter set to Fundamental.**

In this case, the $V_{DC}$ and $I_{DC}$ values are zero, as expected (DC was not included in the measurement). There is a great reduction in apparent power (S), which is now nearly equal to the real power (P). Therefore, the power factor (PF) is increased to nearly 1.0 (as would be expected from visual inspection of the voltage and current pairs for each phase), and the phase angle (ϕ) is much smaller.

 

Had we checked “Include DC” in the calculation of values with harmonic filter = fundamental, we would measure high $V_{DC}$ values, and the power factor and phase angle would fall from the expected values. However, they would not drop to the values in the harmonic filter = full spectrum case, because the $V_{RMS}$ value is lower due to the imposed harmonic filtering. Reference Figure 175.

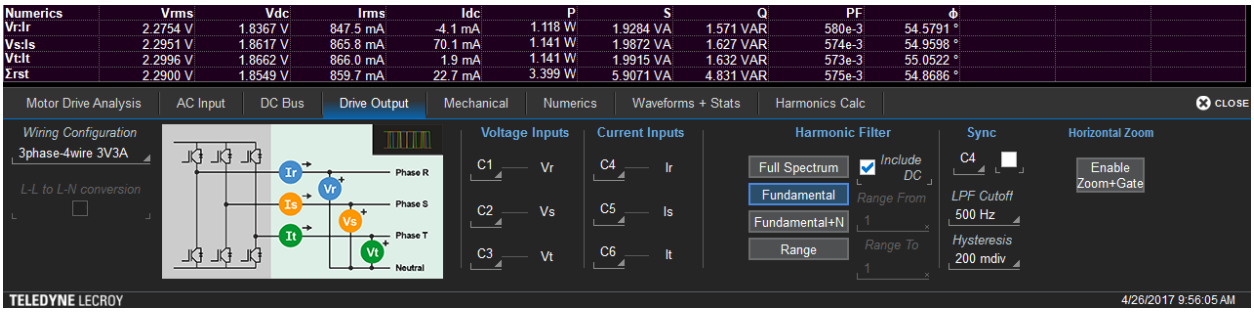


**Figure 175: Numerics table values for the three-phase, six-step commutated brushless DC motor with Harmonic Filter set to Fundamental and DC included.**

 

# Torque, Speed, Position, and Direction Sensing

## Introduction

Depending on the application and the required complexity of control, a motor may be instrumented with or without sensors for detection of rotor speed and position, and the control system may be a closed-loop or open-loop design, depending on the application. . In most cases, optimal operation of the motor by the variable frequency drive requires some direct sensing of the motor operation (sensored) or control system calculation of these quantities from other known data (sensorless). A motor running in a sensorless mode in normal operation would likely still be instrumented during design testing, or instrumented differently (e.g., one may use a quadrature encoder interface in an engineering debug and validation test, whereas the shippable product will use a resolver).

## Measurement and Sensor Types

Torque (usually specified as the symbol tau, or T) feedback sensors are nearly always analog devices with an analog output signal from a torque load cell corresponding to a specified torque value. The typical update rate of the output signal is very low as the load cell likely has on-board processing to convert sensed values into a torque reading (a "static" load cell). Therefore, it is hard to sense torque and report torque values under rapidly changing conditions. Therefore, most torque sensors are used in a final validation lab during static (steady-state) tests, and not included as part of a final motor or drive product.  More advanced control systems derive torque from other known data, as necessary for feedback. Torque is expressed in a variety of different units, such as Newton-meters (N·m) or pound-feet (lb·ft).

Speed (usually specified as the symbol ω) sensors may output analog, digital, or encoded serial data signals. Depending on the type, analog and digital speed sensors can collect speed only, speed and rotational direction, or speed, rotational direction and absolute rotor shaft position information. Absolute rotor shaft position is indicative of the rotor magnetic flux location, and knowledge of the latter is required in implementation of more complex motor control algorithms (e.g., vector FOCs). Speed, position, and direction sensors provide instantaneous information at the sensor output and are highly suitable for dynamic measurements. Speed is expressed in either radians/second (rad/s) or revolutions per minute (RPM). Note that there is no industry convention for what rotor direction of travel (clockwise or counter-clockwise as the motor is viewed looking down the shaft) indicates positive speed.

An angle tracking observer is commonly employed to filter the speed calculation and provide a better estimation of speed with better resolution than would otherwise be available.

Figure 176 shows a block diagram of the types of torque, speed, position, and direction sensors that one might attach to a motor:

 

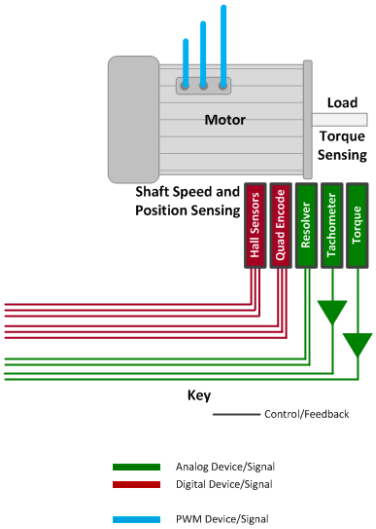


**Figure 176: Motors use a variety of sensor types to measure torque, speed, position, and rotational direction of the motor shaft.**

Mechanical power at the output of the motor shaft is simply calculated as Torque * Speed. Thus, if we input torque and speed signals from a sensor to the Motor Drive Analyzer (or calculate them from other known inputs), then we may also measure motor output power, in kW or hp.

## Torque Sensors (Load Cells, Transducers)

Torque sensors convert a torsional mechanical input (like that present on a motor shaft) into an electrical output signal. They most commonly provide an analog output signal corresponding to a measured torque value. There are two, basic types of analog output methodologies: 0-xVdc and mV/V. Additionally, analog output may be as a frequency-modulated signal or could be embedded in digital serial data. In all types, conditioning electronics are used to condition the sensed torque signal into an analog output signal to achieve higher accuracy and linearity. This means that the update rate of the torque sensor output may be less than the motor's rotation speed.

By definition, measurement of motor shaft torque requires a rotary torque sensor, which can fit over the motor shaft and transmit the signal to an output while the shaft is rotating.

### 0-xVdc Output

0-xVdc torque sensors output a linear, fixed DC voltage for a given torque input. An example would be 0-10 Vdc = 0-10 N·m (Newton-meters). Because their analog output signal is rather high, 0-xVdc torque sensors match up well with a Motor Drive Analyzer input channel.

### mV/V Output

The output of a mV/V torque sensor is proportional to an applied DC power supply voltage. An example would be 10mV/V for a 10N·m torque sensor. Applying a 5V DC voltage to the torque sensor would result in a full-scale output of 0-50mV = 0-10N·m.

Because the analog output signal of a mV/V torque sensor is typically small (in this case 50 mV or less, full scale), the accuracy of the torque measurement through a Motor Drive Analyzer channel will likely

 

not be as high as obtainable with 0-xVdc output torque sensors. An input of 50mV full scale = ~7 to 8 mV/div on the input channel, which means that the Motor Drive Analyzer introduces more noise on the signal.

### Analog Frequency

Some torque load cells provide a frequency modulated output signal that is proportional to a torque value, with the output frequency at torque equal to zero being the mid-span of the modulation range. This type of torque load cell is more immune from analog noise and interference.

### Other Torque Sensors and Sensing Methods

To reduce sensor costs, incorporate measured torque data into some other existing signal, or to permit the control system to calculate torque from other measured data, the following are often implemented in motor drive designs:

- Torque data can be embedded in digital form in a variety of different serial data signals for deliver to the control system. The control system then decodes the serial data information to extract the torque data.
- Torque can be inferred from either a simple torque constant proportional to current consumed by the motor (e.g., Torque = x N·m/A) or by use of a dq0 transformation $I_q$ value (assuming the control system is performing this transformation).

## Analog Speed, Direction, Position Sensing

### Analog Tachometer Signal

The simplest approach to measuring analog speed is an analog tachometer signal, with a tachometer output signal (0-xVdc) corresponding to some angular speed. In this case, there is no information regarding rotor shaft position, but signing the output voltage as either positive or negative indicates rotation direction.

### Resolver

A resolver outputs two analog sinewave signals 90° apart (sine and cosine signals) to convey mechanical rotation and direction information. It is essentially a rotary transformer with one primary winding and two secondary windings that are rotated 90 mechanical degrees with respect to each other. Figure 177 shows the mechanical winding construction of a resolver.

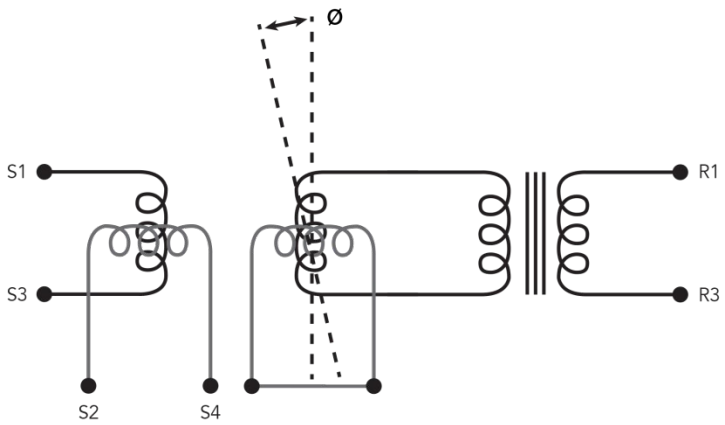


**Figure 177: A resolver generates two sine wave signals that are 90° apart. These signals can be used to determine shaft speed and angle.**

Figure 178 shows a basic resolver with two poles (one pole-pair). This is known as a single-pole resolver. The excitation signal is input across R1 and R2 (in the figure above), and the output signals are sensed across S1 and S3, and S2 and S4. These output signals appear as below for a single-pole (one pole-pair) resolver:

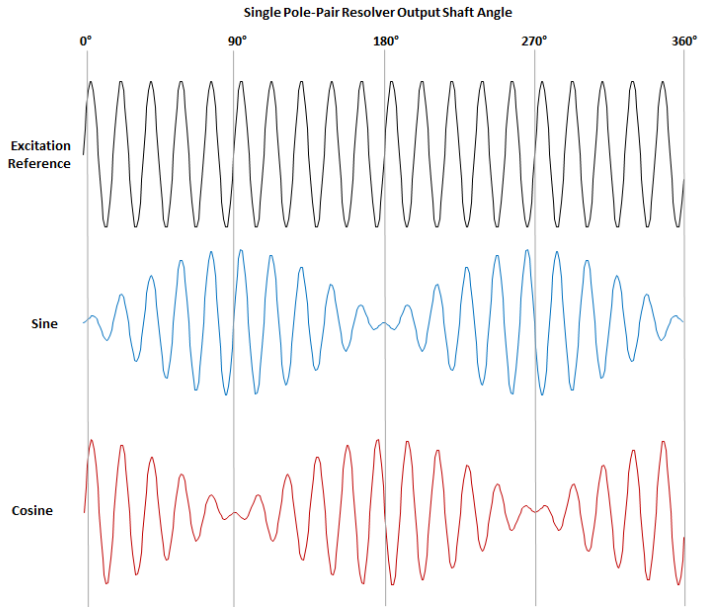


**Figure 178: A basic resolver with a single pole pair generates sine and co-sine outputs. One complete transition of the sine and co-sine waves represents a single rotation of the shaft.**

For a basic resolver with one pole-pair, one complex sine/cosine pair equals one revolution, and the arctangent of the ratio of the amplitude of the sine and cosine signals determines the angle. We can attain more accuracy for lower rotational speeds by providing more than a single pole-pair in the resolver.

By defining the offset angle from the resolver placement to the rotor magnetic field, we can calculate electrical rotor magnetic field angle, and then use this information to create measurements and waveforms of the rotor magnetic flux angle.

 

Figure 179 shows a resolver capture taken with the Motor Drive Analyzer. In this example, two seconds of time is captured. The excitation reference appears as C7 (red, bottom left grid), and the sine and cosine signals appear as C3 (blue, top left grid) and C4 (green, bottom left grid). The full acquisitions appear on the left, and the zooms of the full acquisitions appear on the right.

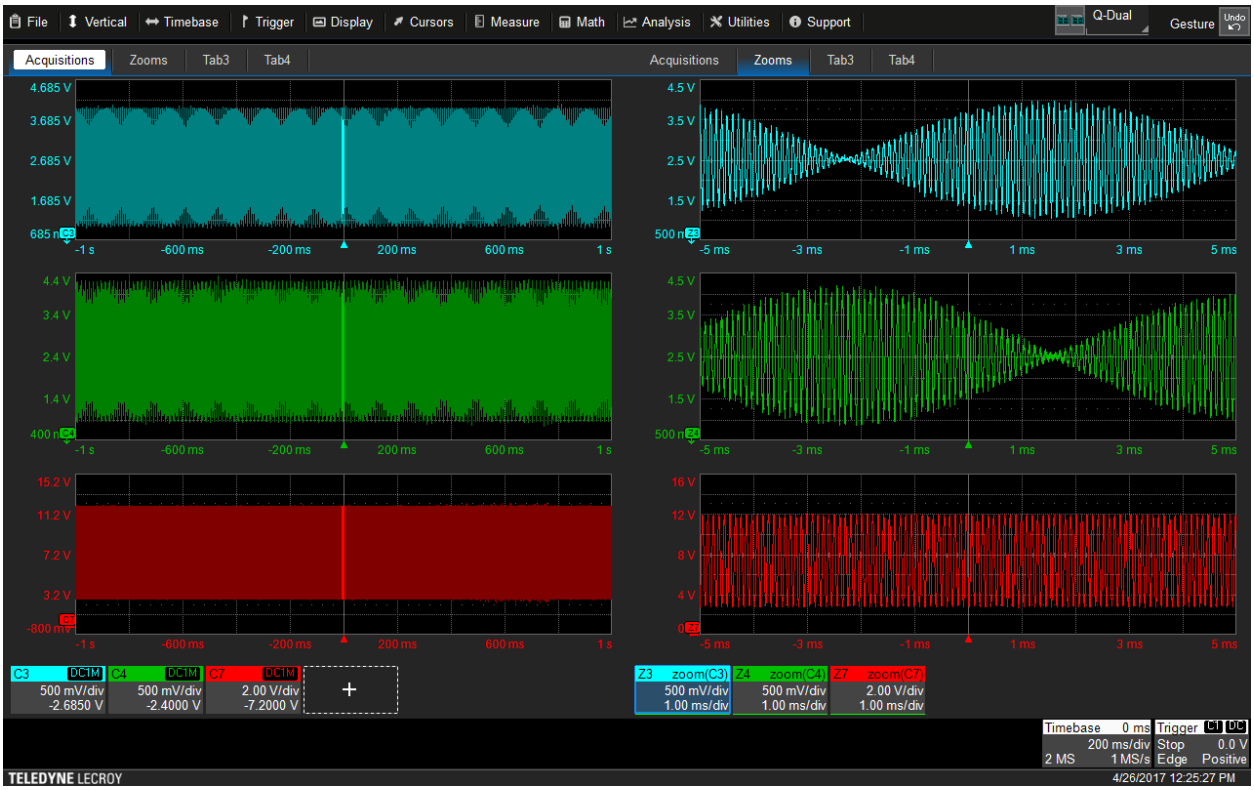


**Figure 179: Measurement of resolver signals using the Motor Drive Analyzer. On the left side of the display, we see full 2-s acquisitions of the excitation reference (C7, bottom left), the sine output (C3, top left) and cosine output (C4, middle left). Zooms of the full acquisitions appear on the right.**

Both speed and angle values can be calculated and displayed as Waveforms. Figure 180 shows these calculations and waveforms for the full acquisition. Note that the angle tracking observer (a type of filter that will be explained in a later section) is applied in this case to reduce the speed measurement variation to approximately ±5 RPM in a nominally 1000 RPM steady-state measurement.

 

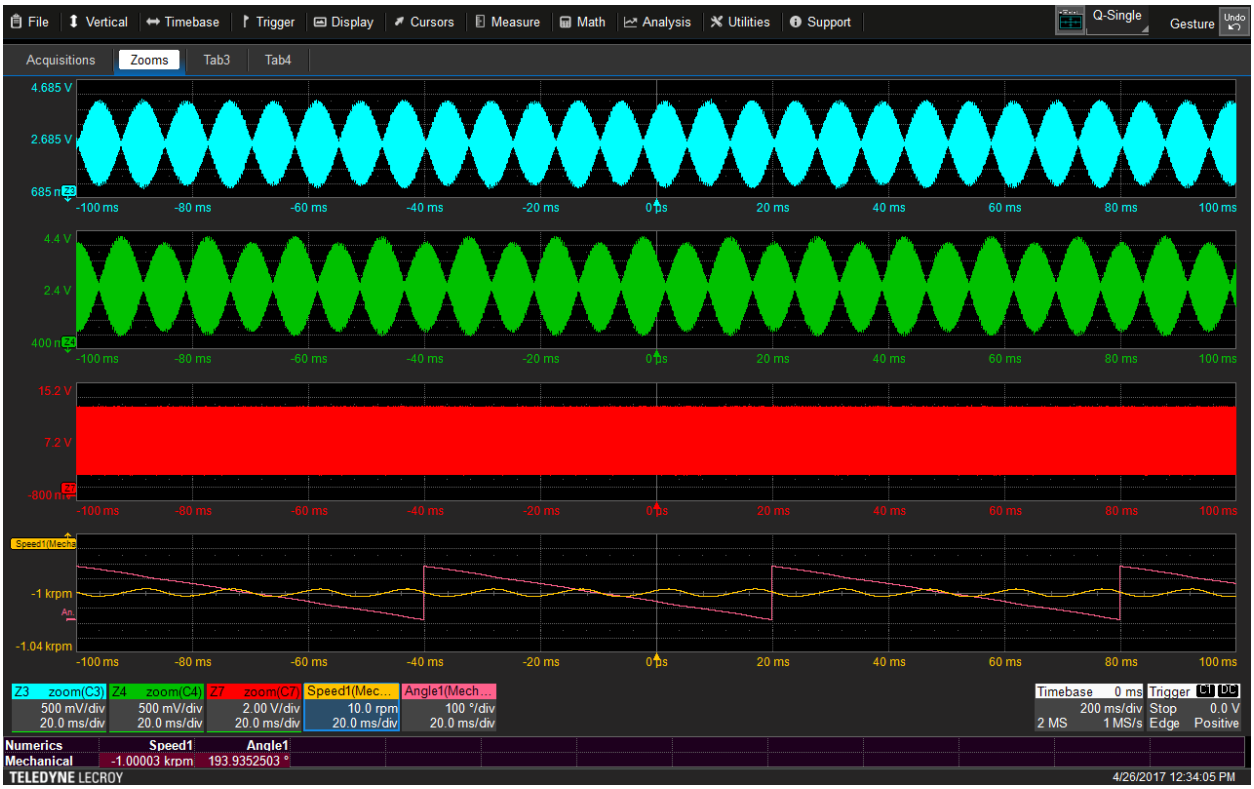


Figure 180: The MDA calculates speed and angle values from the captured resolver waveforms.

Figure 181 shows a larger view of the Numerics table with the calculated mean values of Speed and Angle.

| Numerics | Speed1 | Angle1 |
|---|---|---|
| Mechanical | -1.00003 krpm | 193.9352503 ° |

Figure 181: A larger view of the Numerics table from the previous figure shows the mean values of speed and angle for the captured resolver waveforms.

Figure 182 shows the detailed setup for converting the resolver acquisition data to a speed and angle value, including the use of the angle tracking observer filter.

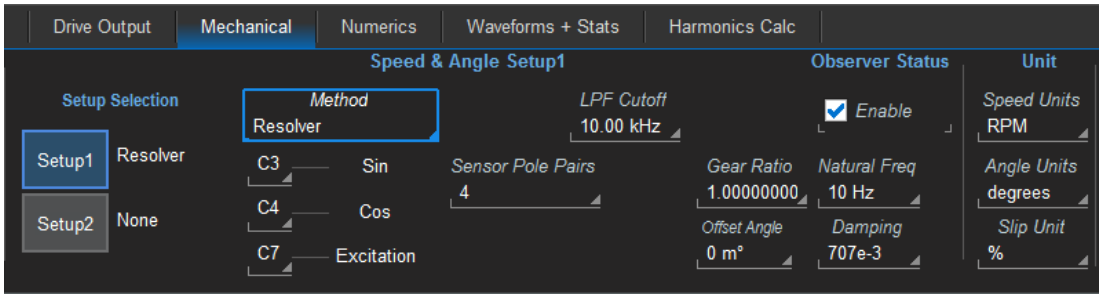


Figure 182: The MDA is configured for converting resolver data to speed and angle values with the angle tracking observer filter enabled.

 

Figure 183 displays a two second capture of resolver signals measuring the dynamic movement of a servo motor shaft. From these signals, calculations (using the angle tracking observer) of speed and angle are made and displayed as Waveforms. The resolver sine (M1, or yellow), cosine (M2, or magenta), and excitation frequency (M3, or light blue) along with speed and angle mean values are displayed.


**Figure 183: Capture of resolver signals measuring the dynamic movement of a servo motor shaft. Resolver sine (M1, yellow), cosine (M2, magenta), and excitation frequency (M3, or light blue) are shown along with speed and angle mean values and waveforms.**

## Digital Speed, Direction, Position Sensing

### Pulse (Digital) Tachometer Signal

A pulse (digital) tachometer outputs a TTL-level digital pulse that repeats N times per revolution, with N a known quantity. It provides speed data but not information on direction or position.

### Hall Sensors

Brushless DC (BLDC) motors using six-step commutation most often utilize Hall effect sensors embedded in and around the rotor to provide a non-contact signal output representing rotor position. A Hall effect sensor actually has two components—a magnet and the actual sensor, which may also be referred to as a pickup.

In BLDC motors, the Hall magnets are typically embedded in the rotor, while the Hall sensors are mounted within an assembly that surrounds the rotor. In some cases, sensors may be mounted in the stator, though in practice, this approach is often avoided because of requirements for manufacturability.

 

These sensors are used to sense rotor position and then directly control the electrical commutation of voltage in the stator. The Hall sensor signals can be used to indicate rotor speed, from which shaft speed can be calculated.

Figure 184 shows a cutaway transverse view of a BLDC with Hall-effect sensors.

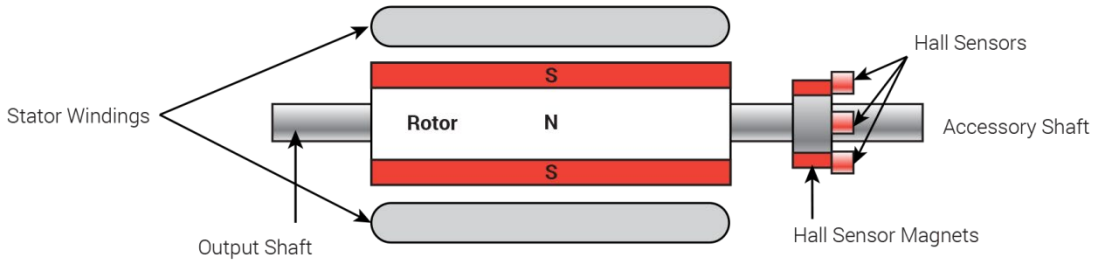


**Figure 184: Magnetic fields produced by Hall sensor magnets embedded in the rotor are sensed by Hall sensors mounted to an assemby surrounding the rotor. The electrical signals produced by the Hall sensors permit the control system to determine rotor location and speed.**

The three Hall sensors provide pulse outputs that, when read as a 3-bit binary string, provide six different values (values 000 and 111 being disallowed as they are not possible due to the mechanical configuration) that repeat in a defined order. One repetition of the six values corresponds to one rotation of the rotor for a motor with one rotor pole pair, or two repetitions corresponds to one rotation of the rotor for a two-pole-pair rotor. The sequence of the repetition indicates either clockwise (+RPM) or counter-clockwise (-RPM) rotation. Figure 185 shows Hall-effect sensor signals for a three Hall-effect sensor configuration with the sensors placed 120° apart on the stator (equally spaced) and one rotor pole pair. At every 120°, one of the Hall-effect sensors makes a positive transition (the figure shows 60°/horizontal division) and one electrical cycle completes in the same time as one mechanical shaft revolution.

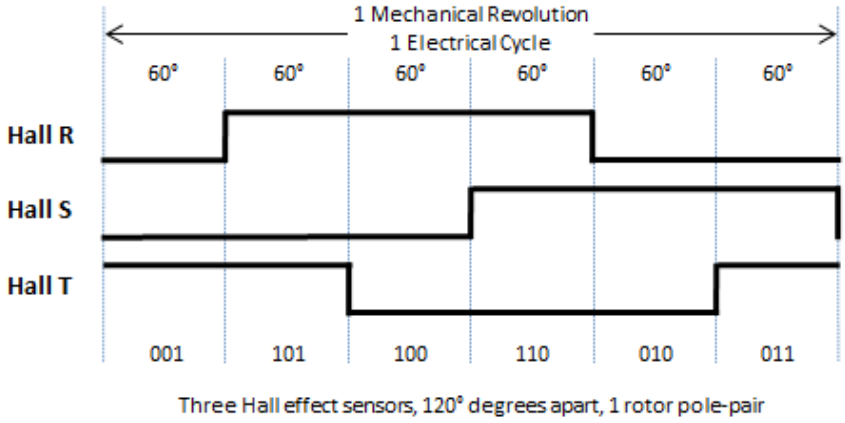


**Figure 185: In the BLDC motor of Fig. 9, one of the Hall-effect sensors makes a positive transition every 120°. In the case of a motor with a single rotor-pole pair, one electrical cycle completes in the same time as one mechanical shaft revolution.**

 

Based on the combination and sequence of these three Hall sensor signals, we may determine the exact sequence of electronic commutation and apply it to energize the stator windings for appropriate motor operation.

The screen image in Figure 186 shows the Hall-effect sensor signals captured using the digital logic inputs of the Motor Drive Analyzer. The waveforms on the left (Digital1, purple) are the full two second capture of the three Hall-effect sensor signals, and the images on the right (Zoom of Digital1, yellow) are the 10:1 zoom of these same signals.

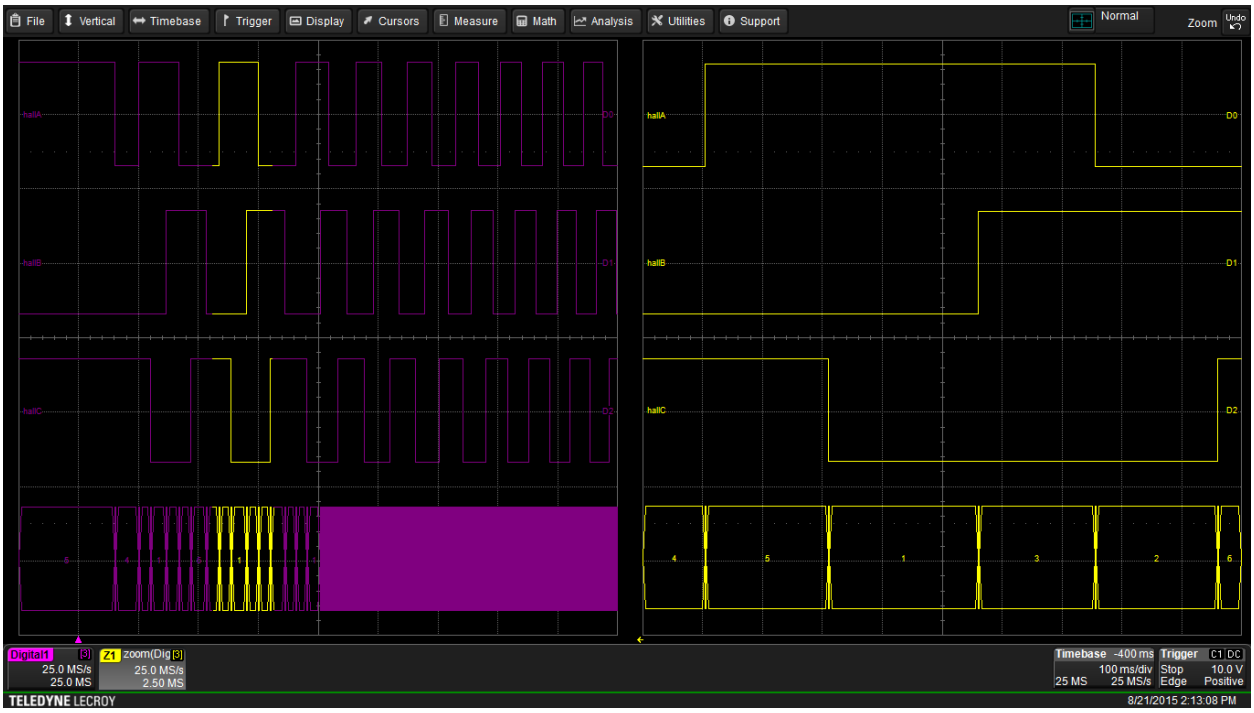


**Figure 186: Hall-effect sensor signals produced by a BLDC motor like that depicted in Fig 9 (one rotor-pole pair) are captured using the digital logic inputs of the Motor Drive Analyzer. The waveforms on the left (Digital1, purple) are the full 2-s captures of the three Hall-effect sensor signals, and the images on the right are zoomed versions of these signals.**

Note that the Hall sensor three-bit signal codes are different than those shown in the earlier diagram — this is simply a reflection of the order of the codes. Regardless, there are six states, and a six-step commutation control system simply needs to know which of the six states the rotor is in at any given time.

The screen image in Figure 187 shows Hall-effect sensor signals (indicated as Digital 1, or purple trace) and line-reference voltage output envelopes (indicated as Channel 1, or yellow trace, Channel 2, or magenta trace, and Channel 3, or blue trace). Note the correlation of the Hall-effect sensor transitions with the beginning or ending of PWM activity on a line-reference voltage waveform. Note also that any particular line-reference voltage waveform is only energized for four of the six different Hall logic states.

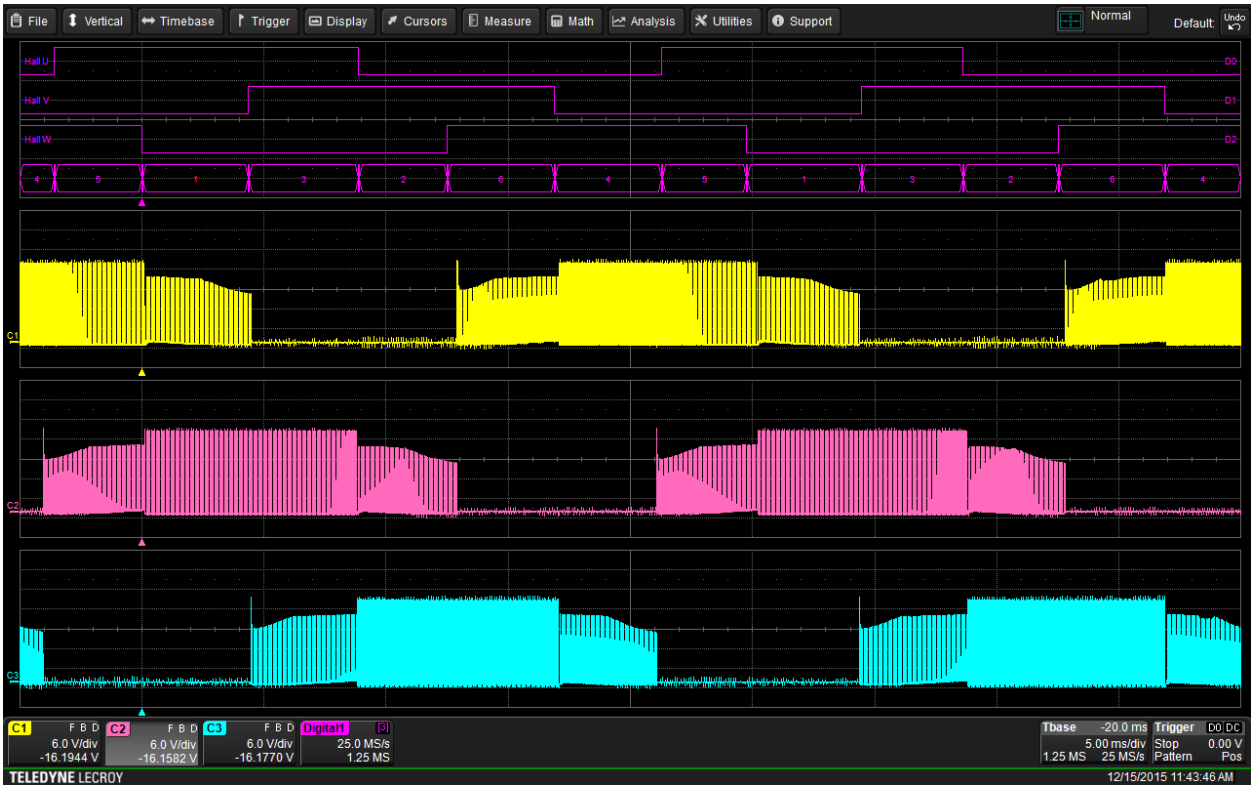


**Figure 187: Hall-effect sensor signals (Digital 1, purple trace) and line-to-reference voltage output envelopes (C1, or yellow trace, C2, or magenta trace, and C3, or blue trace) are shown for the BLDC motor measured in the figure above.**

 

Figure 188 is the same as Figure 187, but now showing voltage probed line-line:

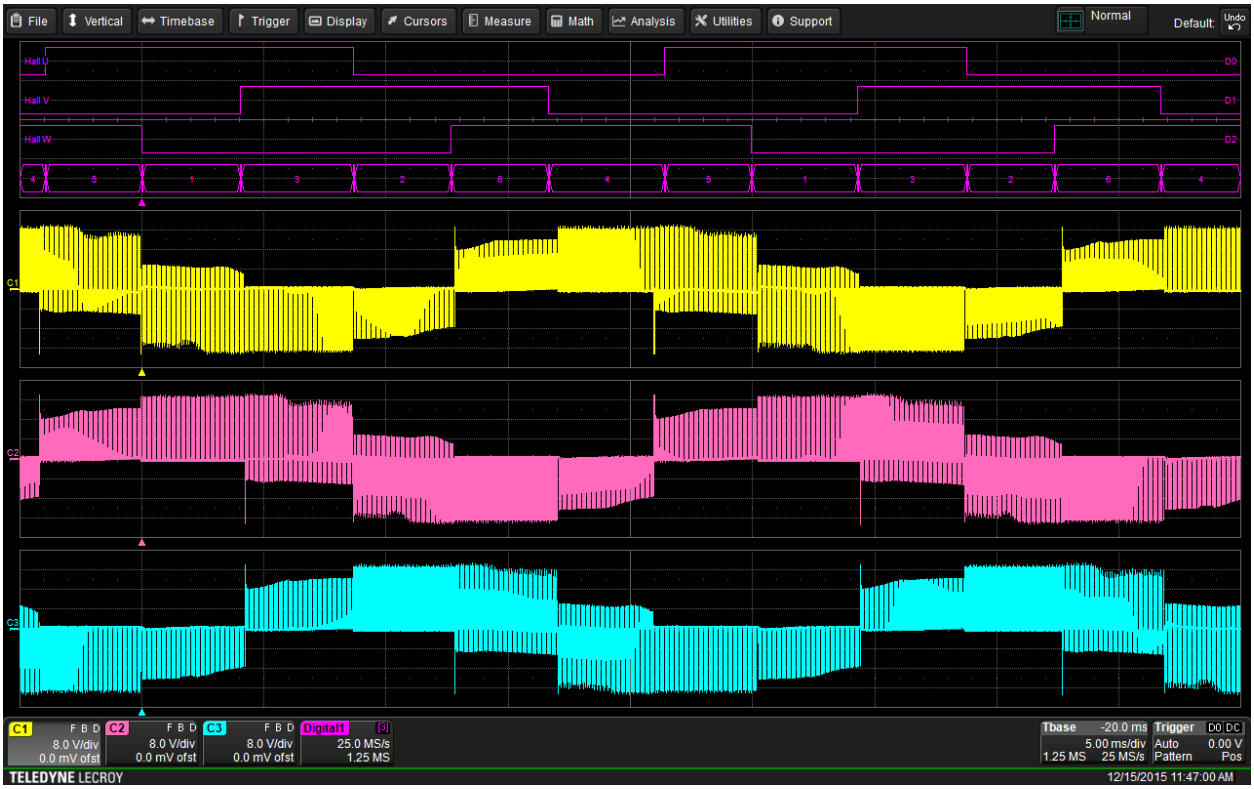


**Figure 188: Hall-effect sensor signals and voltage output envelopes are measured again, but with the voltage probed line-to-line.**

In the above examples, the Hall effect sensors were spaced 120° apart from each other. However, if the three sensors are mounted 60° apart from each other, then we have placed the three Hall sensors on one side of the stator. There are still six unique three-bit transitions, so the operation is essentially the same, but there is 60° separation of the rising edges of the Hall-sensor signals at the beginning of the Hall cycle. Figure 189 shows the resulting Hall sensor signals from this arrangement.

 

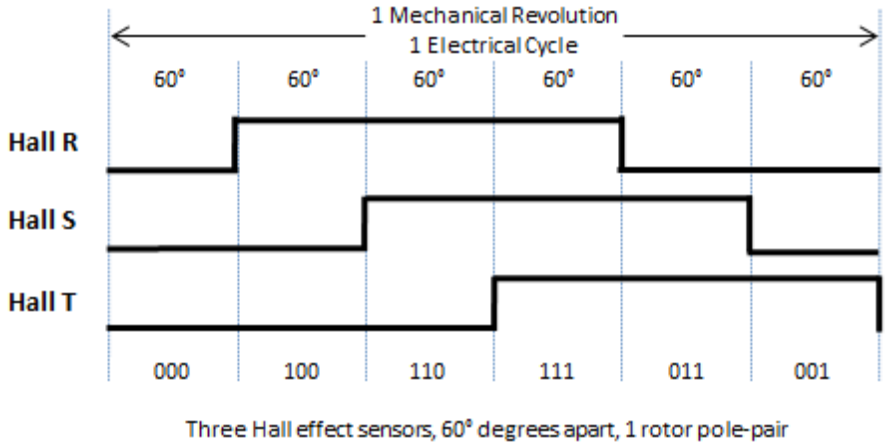


**Figure 189: Hall effect sensors may be placed 60 degrees apart. As was the case with the more widely spaced sensors, one electrical cycle is completed in the same time as one mechanical shaft revolution when there is a single rotor-pole pair.**

Figure 190 shows the Hall sensor signals when there are "N" rotor pole pairs. This results in "N" electrical cycles per mechanical shaft revolution.

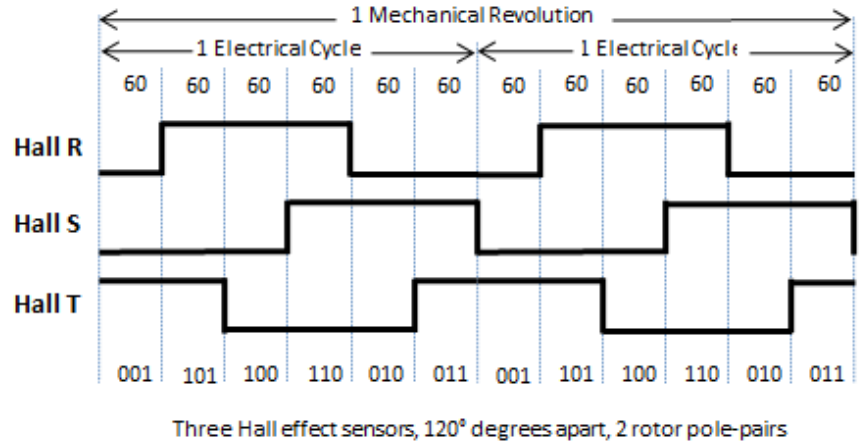


**Figure 190: With two rotor-pole pairs, two electrical cycles of the Hall effect signals will be completed in one revolution of the motor shaft.**

Speed can be calculated from the Hall-sensor signals. The screen image in Figure 191 shows the Hall-effect sensor signals captured using the digital logic inputs of the Motor Drive Analyzer, but in this case, a plot or rotor shaft speed is also shown. The waveforms on the left in the Mechanical tab (Digital1, purple) are again a full two-second capture of the three Hall-effect sensor signals. Immediately to the right are zooms of these signals (Z1, yellow). On the right in the Speed tab is a waveform plot of various values of speed over time as we start a BLDC motor and run it up to speed with an applied load. At the bottom of the Figure 191 screen image is the Numerics table that shows an average speed value for the full two-second acquisition. Figure 192 shows a larger view of the Numerics table shown at the bottom of Figure 191.

 

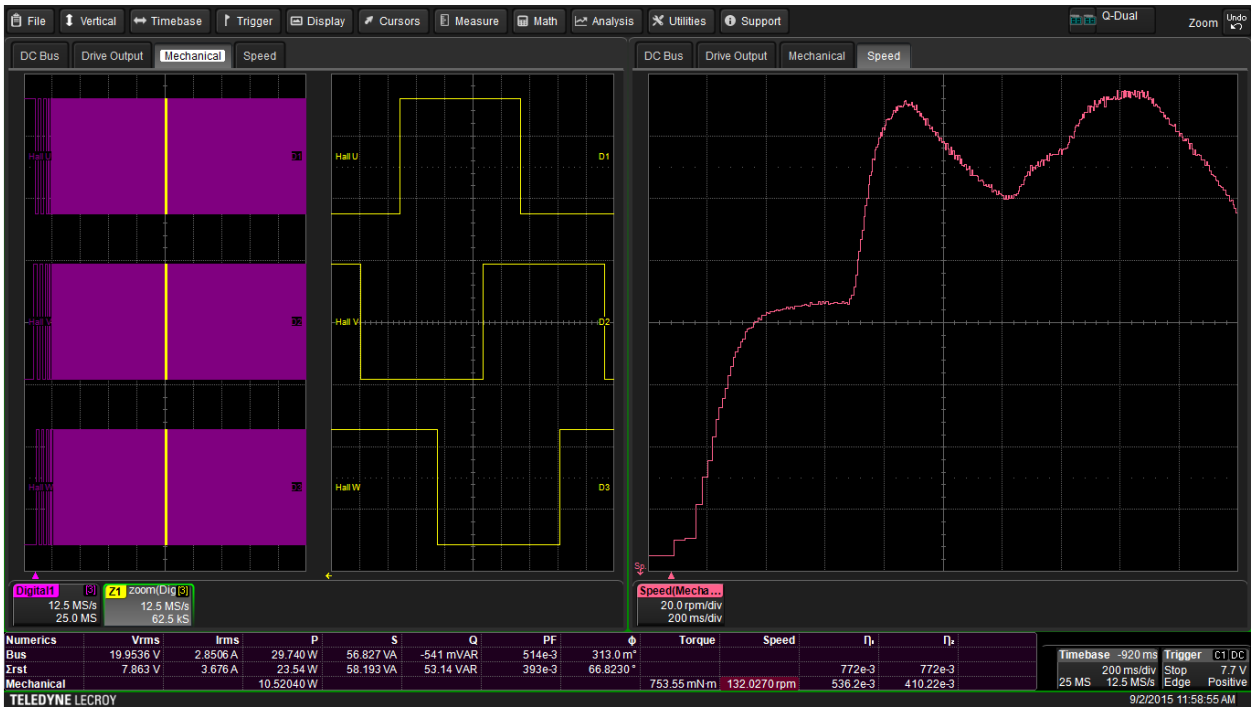


Figure 191: Hall effect sensor signals (shown on the left) captured by the MDA are used to calculate the speed of the rotor.

| Numerics | Vrms | Irms | P | S | Q | PF | Φ | Torque | Speed | η1 | η2 |
|---|---|---|---|---|---|---|---|---|---|---|---|
| Bus | 19.9536 V | 2.8506 A | 29.740 W | 56.827 VA | -541 mVAR | 514e-3 | 313.0 m° | | | | |
| Σrst | 7.863 V | 3.676 A | 23.54 W | 58.193 VA | 53.14 VAR | 393e-3 | 66.8230 ° | | | 772e-3 | 772e-3 |
| Mechanical | | | 10.52040 W | | | | | 753.55 mN·m | 132.0270 rpm | 536.2e-3 | 410.22e-3 |

Figure 192: A larger view of the Numerics table from the previous figure shows motor power measurements and calculations as well as the calculated values for motor speed and torque.

Figure 193 shows a detailed view of the Motor Drive Analyzer setup to convert the Hall-sensor data to a speed value, taking into account the gearing between the motor and the shaft.

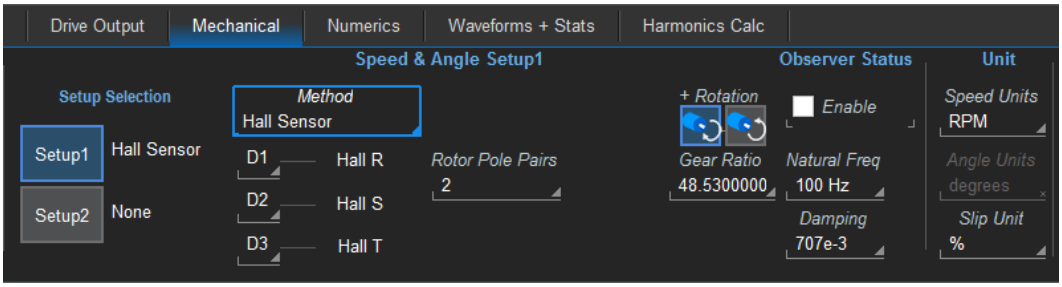


Figure 193: Configuration of MDA settings for calculating motor speed from Hall sensor data.

 

## Quadrature Encoder Interface (QEI)

QEIs are commonly used as a low-cost method to measure speed and angle, especially during the research and development phase as they are simple to connect to a shaft and implement in a control system. In this case, three digital pulses (A, B and Z, or the Index pulse) are used to define speed, direction and absolute position.

The QEI utilizes two digital signals (A and B) that are 90° out of phase to communicate a two-bit pulse sequence N times per shaft revolution. A third digital signal is used to communicate position information once per revolution. This third signal is the "Z" index pulse signal. This type of sensor is also referred to as an “incremental encoder” since it provides information on incremental, but not absolute, rotor shaft position.

The A and B signals together form four unique binary AB pulse patterns, and the sequence of pulse patterns is different for different rotation directions. The QEI can be constructed so that the “A” signal rising edge can lead the “B” signal, or vice-a-versa. Rotation direction can be conveyed based on the order of the digital AB sequence (for A leading B they are, in order, 00, 10, 11, 10 for a “positive” rotation direction). However, rotation direction is arbitrary, so the user must also define in the QEI setup interface which rotation direction represents positive.

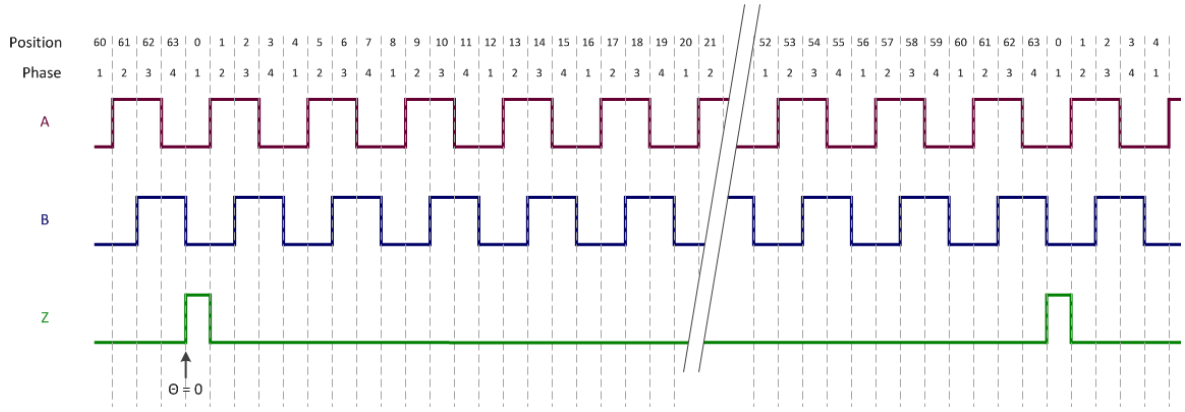


The unique two-bit (AB) pulse patterns are referred to as the QEI phases, which proceed through the binary sequence 00, 10, 11, 01 for positive shaft rotation. In this hypothetical encoder, there are a total of 16 repetitions of the phase sequences, or 64 pulses/revolution (ppr). There are multiple AB pulse pattern sequences per shaft rotation. The Z index pulse occurs once per revolution (once every 64 pulse transitions). While it could be used directly for speed measurements, it lacks enough resolution, especially at low speeds, to be useful.

Figure 194 shows a QEI signal captured with a Motor Drive Analyzer. The QEI A, B, and Z signals are digital, but in this case we have used analog channels to acquire them (digital inputs available with the Motor Drive Analyzer mixed-signal option can also be used, and normally would be used to conserve analog channels for other uses). Z4 (green) and Z7 (red) (both in the top left grid) shows a 100-ms capture of the QEI A and B signals. Z8 (orange, bottom left grid) shows the Z signal. To the right is a zoom of these signals so that more details are seen.

 

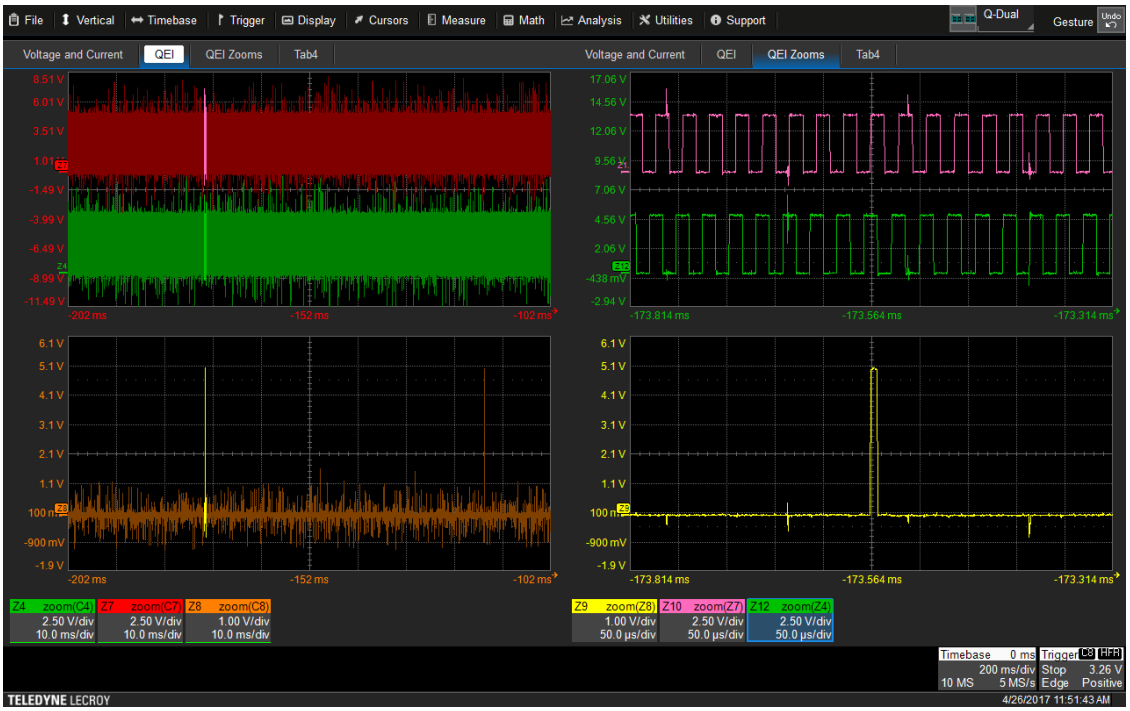


**Figure 194: A, B, and Z signals from a QEI acquired using the analog channels of an MDA. 100-ms acquisitions of these signals are shown on the left side of the display and zoomed versions (over 0.5 ms) are shown on the right side.**

The Motor Drive Analyzer calculates both speed and angle values from the QEI signals and displays them as Waveforms, shown at the bottom of Figure 195).


**Figure 195: The MDA calculates speed and angle values from QEI signals, displaying the results as waveforms and as well values in the Numerics table.**

 

Note that the angle tracking observer is applied in this case to reduce the speed measurement variation to approximately ±10 RPM in a nominally 1000 RPM steady-state measurement. Figure 196 shows a larger view of the measurement values at the bottom of Figure 195.

| Numerics | Speed1 | Angle1 |
|---|---|---|
| Mechanical | 1.037798 krpm | 187.2353111 ° |

**Figure 196: A larger view of the Numerics table from the previous figure shows the mean values of speed and angle for the captured waveforms.**

Figure 197 shows the setup for converting the QEI data to a speed and angle value, including the use of the angle tracking observer filter.

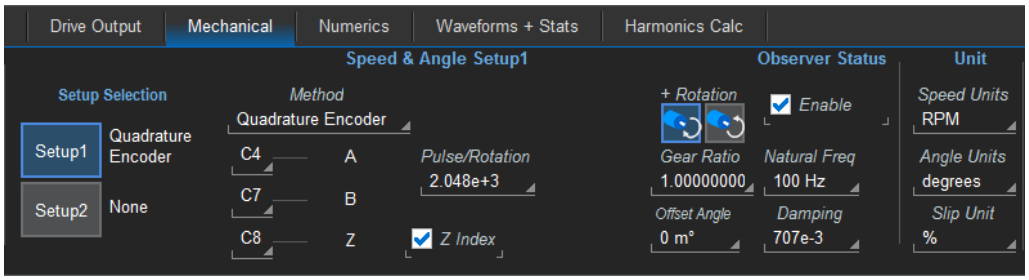


**Figure 197: Configuration of MDA settings for calculating motor speed and angle from QEI data.**

Note that we may convert the calculated QEI shaft angle to a rotor magnetic pole field electrical angle by entering a value for the offset angle (offset of the rotor magnetic pole field electrical angle compared to the QEI shaft angle). It is useful to know the rotor electrical field angle for analyzing advanced vector FOC control systems, but it is unnecessary for speed or direction sensing.

## Other Speed Sensors and Sensing Methods

To reduce sensor costs and/or provide more reliability, sensorless techniques or a variety of other sensors are often utilized, as described below.

- Voltage or current sensing on the drive output or the motor winding can be used to determine the period of the stator magnetic field. Shaft speed can be calculated if the number of stator pole pairs and rotor pole pairs is known. This is a fairly simple process for a permanent-magnet rotor motor but becomes more complicated for an AC induction motor given the slip between the rotor and the stator.
- Speed data can be embedded in digital form in a variety of different serial data signals for deliver to the control system. The control system then decodes the serial data information to extract the speed data.
- A variety of lower-cost Sine/Cosine analog sensors may be used. These sensors do not require an applied excitation frequency, and the Sine and Cosine signals are not amplitude modulated (as with the resolver). Speed, direction and position (angle) is calculated from an arctangent calculation from the Sine and Cosine signals. These are commonly referred to as SinCos encoders. NXP Semiconductors has released an encoder that uses a similar approach. It is named the KMZ60 and is specifically focused towards automotive applications.

 

## Angle Tracking Observers

Motor drive control systems engineers often use angle tracking observers to provide rotor speed estimations at a better resolution than would otherwise be achieved, and at far greater resolution than the excitation period (resolver), the Sin/Cos period (SinCos or KMZ60 encoders), or the digital switching frequency (QEI or Hall Sensor) can provide. Additionally, the angle tracking observer provides smoothing of the speed calculations through use of an integrator and proportional-integral (PI) controller. These capabilities are necessary in order to provide appropriate control capabilities for more complex control systems (e.g., Vector FOC).

Figure 198 shows a block diagram of an angle tracking observer filter. The angle tracking observer is essentially nothing more than a second-order PLL implemented as a software algorithm in the control system.

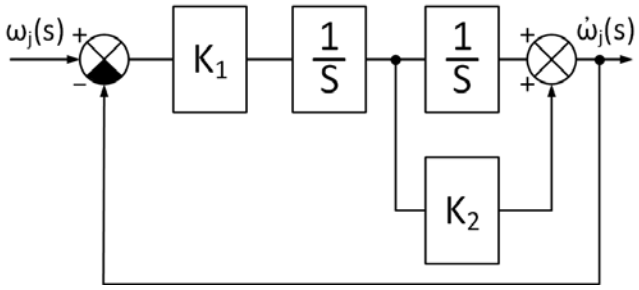


**Figure 198: An angle tracking observer implements the transfer function shown here in software.**

Here ωj(s) is the instantaneous angle value input to the angle tracking observer and ω̇j(s) is the instantaneous angle value output. The system shown above is a second-order system, and the transfer function T(s) of the system is expressed in the following equation:

$$T(s) = \frac{\dot{\omega}(s)}{\omega(s)} = \frac{K_1(1 + K_2 s)}{s^2 + K_1 K_2 s + K_1}$$

The transfer function of a general second-order system G(s) is expressed in the following equation:

$$G(s) = \frac{{\omega_n}^2}{s^2 + 2\zeta\omega_n s + {\omega_n}^2}$$

Where $\omega_n$ is the natural frequency in rad/s and ζ is the damping factor. Solving for K1 and K2 leads to the following:

$$K_1 = {\omega_n}^2$$

$$K_2 = \frac{2\zeta}{\omega_n}$$

The Teledyne LeCroy Motor Drive Analyzer includes this software algorithm, and it may be applied to Resolver, SinCos, KMZ60, Hall sensor, and QEI speed calculations. The setup is shown Figure 199 and we simply enter the Natural Freq(uency) and Damping factor:

 


Figure 199: Configuring the MDA for use of the Angle Tracking Observer algorithm.

These two values define the second-order system response that provides the filtering ("smoothing") to the speed calculations.

## Angle Tracking with Digital Encoders

Figure 200 shows an example of the angle tracking observer applied to a digital Hall Sensor method speed calculation. The Speed1 trace (yellow) has the angle tracking observer applied whereas the Speed2 trace (magenta) does not. There is more resolution in the speed trace with the angle tracking observer applied and less variation due to the filtering of the observer.


Figure 200: Angle tracking observer applied to Hall Sensor digital signals.

 

Figure 201 shows the angle tracking observer applied to a short record capture (a 200-µs zoom of a 100-ms capture) of a digital Quadrature Encoder Interface (QEI). The Speed1 trace (orange, top grid) has the angle tracking observer applied (Natural Frequency = 100 Hz, Damping Factor = 0.707) whereas the Speed2 trace (magenta, top grid) does not. Again, there is more resolution in the speed trace with the angle tracking observer applied and less variation due to the filtering of the observer.

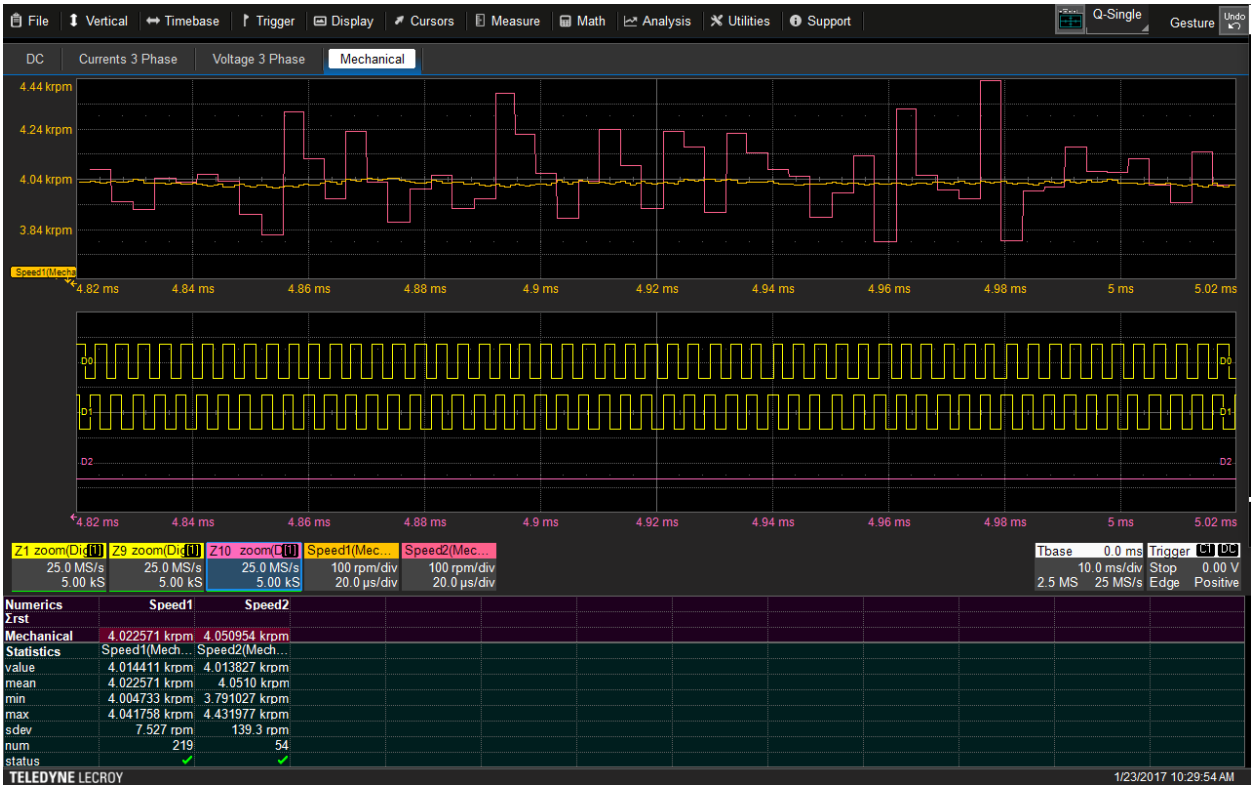


**Figure 201: Angle tracking observer applied to QEI digital signals.**

Figure 202 is the same calculation shown in Figure 201, but for the full acquisition of 100 ms. Note that the Speed2 calculation (without the angle tracking observer applied) has significantly more variation in the measurement than the Speed1 calculation (with the angle tracking observer applied), especially near the Z index (angle reset) pulse. Also, with the angle tracking observer settings described above, there is a startup filter time of ~20 ms. This would normally not be something seen in a motor drive control system since the filter is applied in real-time to acquired data, but it is present in the acquire and post-process approach used in the Motor Drive Analyzer. This startup filter time can be ignored in the Motor Drive Analyzer using a Zoom+Gate to a location after the angle tracking observer filter has settled.

 

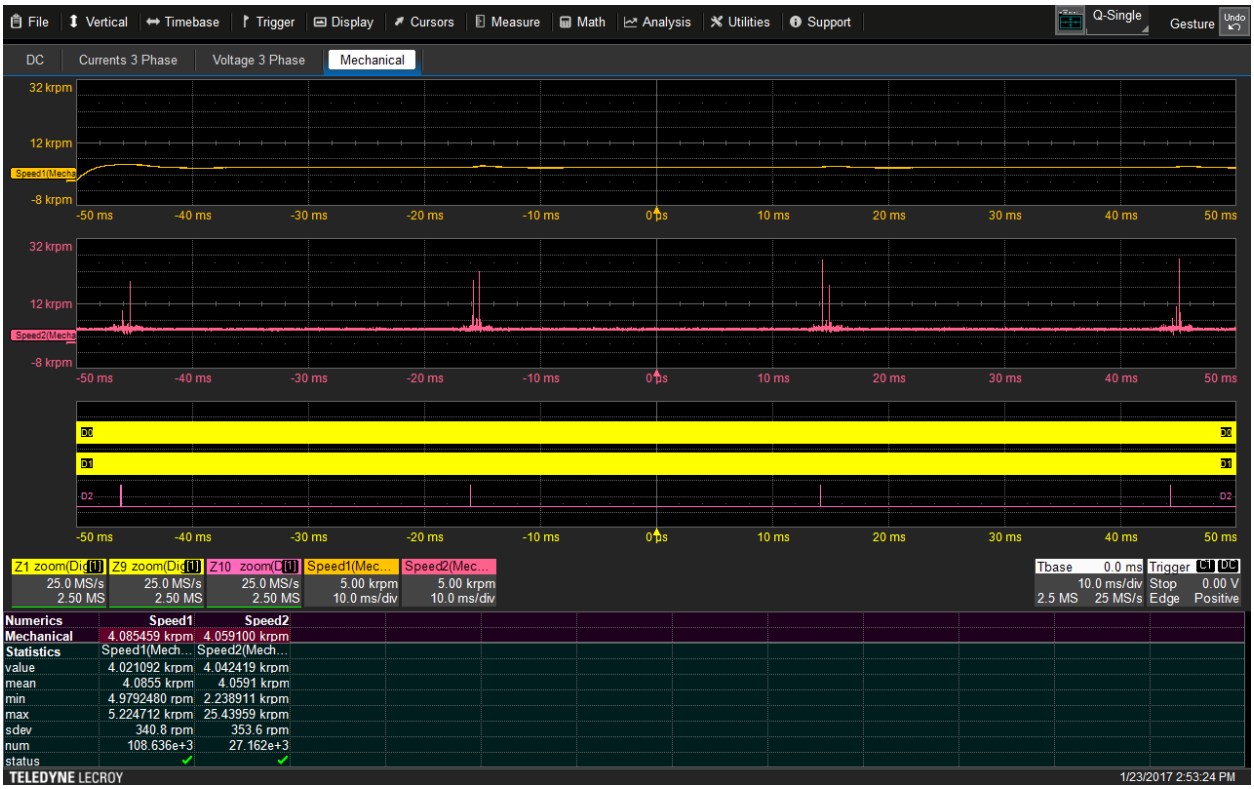


**Figure 202: Angle tracking observer applied to QEI digital signals for full 100 ms acquisition.**

 

## Angle Tracking Observer with Analog Encoders

Figure 203 shows the angle tracking observer applied to a short record capture (a 20-ms zoom of a 2-second capture) using an analog Resolver method speed calculation of a Resolver Sin (Z4), Cos (Z3), and Excitation Frequency (Z7). The Speed1 trace (orange, top grid) has the angle tracking observer applied (Natural Frequency = 25 Hz, Damping Factor = 0.707) whereas the Speed2 trace (magenta, top grid) does not.


**Figure 203: Angle tracking observer applied to Resolver signals for short (20-ms) acquisition.**

 

Figure 204 shows the full 2-second acquisition that was shorted in Figure 203. Note the filter startup time in this example on the orange Speed waveform in the top grid.

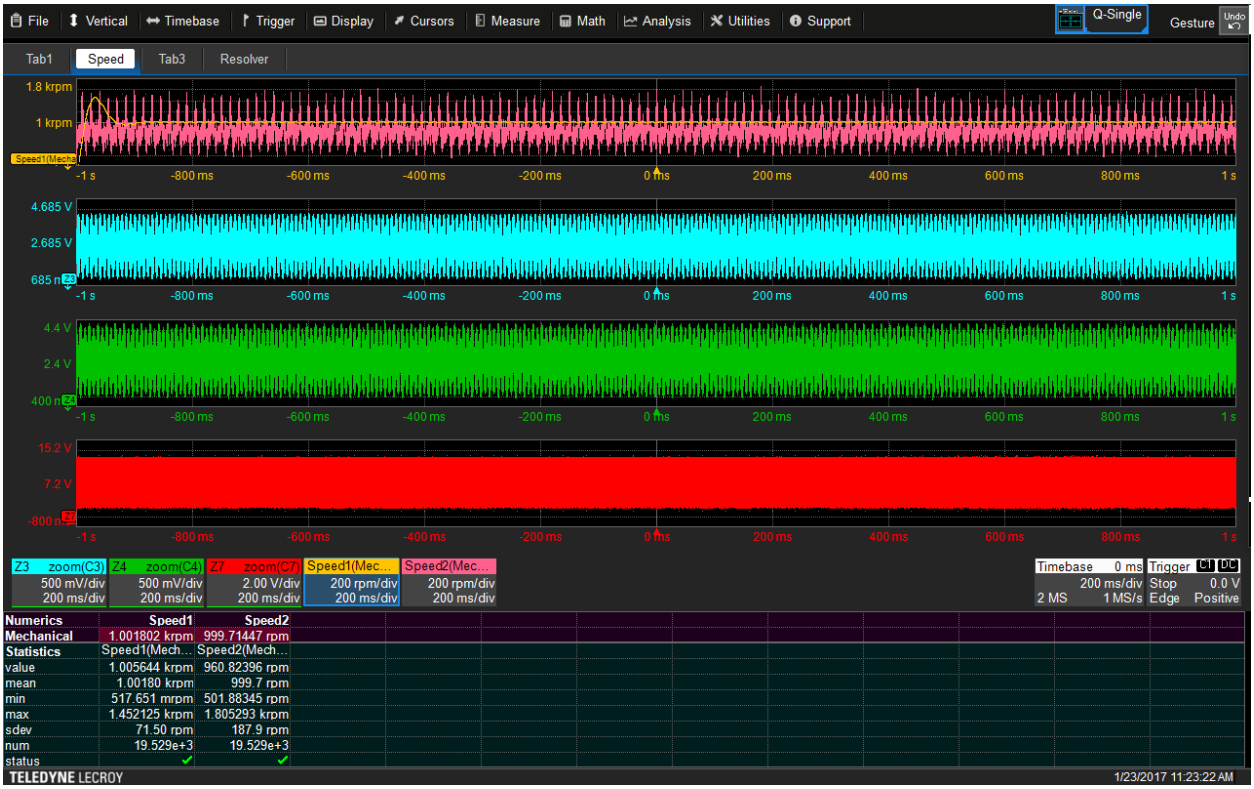


**Figure 204: Angle tracking observer applied to Resolver signals for full 2 S acquisition. This longer capture highlights the filter start-up time.**

 

## Glossary

AC – Alternating Current

ACAM – Alternating Current Asynchronous Motor

ACIM – Alternating Current Induction Motor

ACSM – Alternating Current Synchronous Motor

ANSI – American National Standards Institute

BLDC – Brushless DC Motor

C - Collector

CSI - Current-Sourced Inverter

DC – Direct Current

DTC - vector Direct Torque Control

E - Emitter

FOC – Flux or Field Oriented Control

G - Gate

GaN – Gallium Nitride

GFCI – Ground Fault Current Interrupter

GTO - Gate Turn-On Thyristor

IEC – International Electrotechnical Commission

IEEE – Institute of Electrical and Electronic Engineers

IGBT – Insulated-Gate Bipolar Transistor

IGCT- Insulated-Gate Commutated Thyristor

 

Lb-ft – Pound Feet

LCI – Load-Commuted Inverter

MC - Matrix Converter or Cycloconverter

MOSFET – Metal Oxide Semiconductor Field Effect Transistor

N-m – Newton-meter

NPC - Neutral Point Clamped topology

P – Real Power

PF – Power Factor

PMSM – AC Permanent Magnetic Synchronous Motor

PPR – Pulses per Rotation

PWM – Pulse Width Modulation

Q – Reactive Power

QEI – Quadrature Encoder Interface

Rad/s – radians per second

RMS – Root Mean Square

RPM – Revolutions per minute

S – Apparent Power

SCR – Silicon Controlled Rectifier

Si - Silicon

SiC – Silicon Carbide

SRM – Switched Reluctance Motor

 

SVM – Space Vector Modulation

SVPWM – Space Vector Pulse-Width Modulation

THD – Total Harmonic Distortion

VFD – Variable Frequency (motor) Drive

VSD – Variable Speed Drive

VSI - Voltage-Sourced Inverter

 